Electric Dipole Moments of Light Nuclei in Chiral Effective Field Theory

Dissertation
zur
Erlangung des Doktorgrades (Dr. rer. nat.)
der Mathematisch-Naturwissenschaftlichen Fakultät
der
Rheinischen Friedrich-Wilhelms-Universität Bonn

vorgelegt von

Jan Bsaisou

aus
Darmstadt

Bonn 2014

Angefertigt mit Genehmigung der Mathematisch-Naturwissenschaftlichen Fakultät
der Rheinischen Friedrich-Wilhelms-Universität Bonn

1. Gutachter: PD Dr. Andreas Wirzba

2. Gutachter: Prof. Dr. Ulf-G. Meißner

Tag der Promotion: 25.04.2014

Erscheinungsjahr: 2014

Summary:

Electric dipole moments (EDMs) break parity (P) and time-reversal (T) symmetry and thus, by the CPT theorem, CP-symmetry. Once measured, they will be unambiguous signs of new physics since CP violation from the complex phase of the Cabibbo-Kobayashi-Maskawa matrix in the Standard Model predicts EDMs that are experimentally inaccessible in the foreseeable future. The θ-term of Quantum Chromodynamics (QCD) and extensions of the Standard Model such as supersymmetry and multi-Higgs scenarios comprise P- and T-violating interactions which are capable of inducing significantly larger EDMs. The extensions of the Standard Model give rise to a set of effective non-renormalizable operators of canonical dimension six at energies $\Lambda_{\text{had}} \gtrsim 1$ GeV when the heavy degrees of freedom are integrated out. The effective dimension-six operators are known as the quark EDM, the quark-chromo EDM, four-quark left-right operator, the gluon-chromo EDM and the four-quark operator.

Starting from the QCD θ-term and this set of P- and T-violating effective dimension-six operators, we present a scheme to derive the induced effective Lagrangians at energies below $\Lambda_{\text{QCD}} \sim 200$ MeV within the framework of Chiral Perturbation Theory (ChPT) for two quark flavors in the formulation of Gasser and Leutwyler. The differences among the sources of P and T violation manifest themselves at energies below Λ_{QCD} in specific hierarchies of coupling constants of P- and T-violating vertices. We compute the relevant coupling constants of P- and T-violating hadronic vertices which are induced by the QCD θ-term with well-defined uncertainties as functions of the physical parameter $\bar{\theta}$. The relevant coupling constants induced by the effective dimension-six operators are given as functions of yet unknown Low Energy Constants (LECs) which can not be determined within the framework of ChPT itself. Since the required supplementary input from *e.g.* Lattice QCD is not yet available, we present Naive Dimensional Analysis (NDA) estimates of the coupling constants. These estimates prove to be sufficient to reveal certain hierarchies of coupling constants.

The different hierarchies of coupling constants translate into different hierarchies of the nuclear contributions to the EDMs of light nuclei. We calculate within the framework of ChPT the two-nucleon contributions to the EDM of the deuteron up to and including next-to-next-to leading order and the two-nucleon contributions to the EDMs of the helion (^{3}He nucleus) and the triton (^{3}H nucleus) up to and including next-to-leading order. These computations comprise thorough investigations of the uncertainties of the results from the P- and T-violating component as well as the P- and T-conserving component of the nuclear potential. We present quantitative predictions of the nuclear contributions to the EDMs of the deuteron, the helion and the triton induced by the QCD θ-term as functions of $\bar{\theta}$ with well-defined uncertainties. The EDM predictions for the effective dimension-six sources are given as function of the yet unknown LECs with NDA estimates.

We present several strategies to falsify the QCD θ-term as a relevant source of P and T violation by a suitable combination of measurements of several light nuclei and, if needed, supplementary lattice QCD input. If the QCD θ-term fails these tests, one or several of the effective dimension-six sources encoding physics beyond the Standard Model are most likely the source(s) of P and T violation. We demonstrate how particular effective dimension-six sources can be tested by EDM measurements of light nuclei with eventually supplementary Lattice QCD input.

Contents

Chapter 1

Introduction

1.1 Motivation

The Standard Model (SM) has proven to be a highly accurate theory of elementary particles and their interactions. However, there are some observations which are apparently irreconcilable with this otherwise successful theory. Among them is the significant excess of matter over antimatter in the universe. WMAP and COBE measured a baryon-antibaryon asymmetry parameter at the photon freeze-out point of [1]:

$$A_B = (n_B - n_{\bar{B}})/n_\gamma = (6.079 \pm 0.090) \cdot 10^{-10}\,, \tag{1.1}$$

where $n_{B,\bar{B}}$ denote the number densities of baryons and antibaryons, respectively, and n_γ the number density of photons in the cosmic background radiation. The SM prediction of the baryon-antibaryon asymmetry $A_B \sim 10^{-18}$ [2] on the other hand deviates from this measurement by approximately eight orders of magnitude. If one assumes that the baryon-antibaryon asymmetry was absent shortly after the origin of the universe (after the inflationary epoch), it had to be generated dynamically. This observation implies the existence of a mechanism which is responsible for profoundly different production rates of matter and antimatter. According to A. Sakharov [3], such a mechanism generating baryons has to simultaneously obey the following three conditions:

1. Any difference in the abundances of baryons and antibaryons implies the existence of interactions which violate baryon number conservation.

2. If the theory is invariant under charge conjugation C, each baryon number violating transition would be compensated for by its charge conjugated one. Therefore, different production rates of baryons and antibaryons require the violation of the charge conjugation symmetry. Furthermore, the theory can not be invariant under the combination of charge conjugation and the parity transformation P. As pointed out in [4], CP conservation yields – after

integration over phase space and summation over all spin configurations – equal transition rates of baryon-number violating transitions and their charge conjugated transitions. CP conservation would, therefore, also imply a vanishing dynamically generated baryon-antibaryon asymmetry.

3. According to the CPT theorem, all Lorentz invariant and local quantum field theories with a hermitian Hamiltonian are invariant under a simultaneous application of charge conjugation, the parity transformation and the time reversal transformation T. Since a physical system in thermal equilibrium is time independent, the CPT theorem requires the theory to be symmetric under CP, which contradicts the previous condition. The dynamical generation of the baryon-antibaryon asymmetry had to take place outside of thermal equilibrium.

Any theory describing physics beyond the Standard Model (BSM) has therefore to comprise CP-violating interactions which are capable of accounting for a significantly larger baryon-antibaryon asymmetry than the Standard Model prediction.

This conclusion has triggered the development of new low-energy experimental concepts to assess physics beyond the Standard Model [5]. Electric dipole moments (EDMs) of atoms, nucleons and nuclei are commonly regarded as some of the most promising signals of CP-violation and their upper bounds have gained remarkable accuracy since the null measurement of the neutron EDM by Purcell and Ramsey in 1957 [6]. This approach to assessing new physics constitutes a complimentary approach to high-energy collider experiments that is also likely to require significantly less financial means.

The EDM is defined as the displacement of positive and negative electric charges (ρ: distribution of electric charges):

$$\vec{d} = \int d^3r \rho(\vec{r})\vec{r}\,, \tag{1.2}$$

which is a polar three-vector. For an elementary non-degenerate massive spin-1/2 particle in its rest frame, the only three-vector is given by the particle spin $\vec{S}$ and the EDM has to be proportional to $\vec{S}$, which is an axial vector: $\vec{d} = d\,\vec{S}$. This is equally true for the magnetic dipole moment of the particle: $\vec{\mu} = \mu\,\vec{S}$. The Hamiltonian in the non-relativistic limit of a spin-1/2 particle in a electromagnetic field is then given by

$$H = -\mu\vec{B}\cdot\vec{S} - d\vec{E}\cdot\vec{S}\,, \tag{1.3}$$

where $\vec{B}$ is the magnetic field and $\vec{E}$ is the electric field. Whereas the magnetic field and the particle spin have both P eigenvalue $+1$, the electric field has P eigenvalue -1. The respective T eigenvalues are of opposite sign, which demonstrates that the EDM of an elementary particle violates parity and time-reversal invariance simultaneously[1]:

$$H = -\mu\vec{B}\cdot\vec{S} - d\vec{E}\cdot\vec{S} \quad \overset{P}{\to} \quad -\mu\vec{B}\cdot\vec{S} + d\vec{E}\cdot\vec{S}\,, \tag{1.4}$$

$$H = -\mu\vec{B}\cdot\vec{S} - d\vec{E}\cdot\vec{S} \quad \overset{T}{\to} \quad -\mu\vec{B}\cdot\vec{S} + d\vec{E}\cdot\vec{S}\,. \tag{1.5}$$

Utilizing the CPT theorem, the simultaneous violation of P and T invariance implies the simultaneous violation of CP and CT invariance. For a composite particle such as a nucleus, the elementary particle spin in the above equation has to be replaced by the total angular momentum $\vec{J}$ of the composite system.

The complex phase of the Cabibbo-Kobayashi-Maskawa (CKM) matrix is the conventional source of CP violation within the SM, which only starts to contribute to EDMs at the three-loop level and thus gives only very small EDMs [5]. The SM predictions for the EDMs induced by the complex phase of the CKM matrix of the neutron and the electron, for instance, amount to $d_n \sim 10^{-31}\,e$ cm and $d_e \sim 10^{-38}\,e$ cm, respectively [5][2]. The θ-term of quantum chromodynamics (QCD) [9] and extensions of the SM such as supersymmetry [10] and many-Higgs scenarios [11] (subsequently referred to as *new physics*) might yield profoundly larger values.

As emphasized in [5], there are three major[3] categories of intrinsic EDM measurements: the EDMs of paramagnetic atoms and molecules, the EDMs of diamagnetic atoms and the EDMs of hadrons and light ions. In paramagnetic atoms or molecules where the total electron angular momentum does not vanish because of an unpaired electron, the permanent EDM is due to the EDM of the valence electron and to P- and T-violating electron-nucleus interactions. The permanent EDM of a diamagnetic system with vanishing electron total angular momentum is caused by P- and T-violating nuclear interactions [13]. If the nucleus itself has non-vanishing angular momentum, the well-known Schiff theorem states that for non-relativistic systems composed of point-like, charged particles in an external electric field the shielding is complete. The violation of the Schiff theorem due to finite sizes of nuclei and relativistic effects gives rise to EDMs of diamagnetic atoms with non-zero nuclear spin.

Until now, there have not been any non-zero measurements of the EDMs of paramagnetic atoms, diamagnetic atoms, the electron or the neutron. The upper bound on the EDM of the neutron is currently at $d_n < 2.9\cdot 10^{-26}\,e$ cm [14]. The upper bound on the EDM of the proton, $d_p < 7.9\cdot 10^{-25}\,e$ cm, has been inferred from a measurement of the diamagnetic ^{199}Hg atom [15], and the one

[1]Since an induced EDM is proportional to the square of the electric field E^2 (quadratic Stark effect), it does not signal P and T violation.

[2]The nucleon EDMs from the loop-less SM mechanism of [7, 8] are estimated to be of comparable sizes.

[3]Since the current upper bound of the muon EDM $\sim 10^{-19}\,e$ cm [12] does not compete with the experimental upper bounds of the EDMs of the proton, neutron and electron (see below), this category of EDM measurements is disregarded in this thesis.

of the electron, $|d_e| < 1.05 \cdot 10^{-27}\, e$ cm, from a measurement of the dipolar YbF molecule [16, 17]. The ACME collaboration recently further reduced the upper bound on the electron EDM by a measurement of the EDM of ThO to $|d_e| < 8.7 \cdot 10^{-29}\, e$ cm [18]. These upper bounds have to be put into relation to the above SM model predictions. The EDMs of composite particles such as hadrons are expected to be intrinsically larger than the EDMs of elementary particles, *e.g.* the electron, due to their finite sizes. The current upper bound of the neutron EDM is therefore closer to its SM prediction than the current upper bound of the electron EDM to the SM electron EDM prediction. These null measurements already provide valuable insights into new physics since they impose strong constraints on parameters in BSM theories.

Another conceptual approach entails the high-precision measurements of the electric dipole moments of the proton and other light nuclei in storage rings [19–23]. Light nuclei are electrically charged systems that can not be stored in traps while exposed to an electric field. The Storage Ring EDM collaboration and the JEDI (*Jülich Electric Dipole moment Investigations*) collaboration propose direct measurements of the EDMs of the proton and of light nuclei in dedicated storage rings and aim to increase the sensitivity of EDM measurements to the region of $d_p \sim 10^{-29}$ e cm. The underlying principle of this kind of measurement is the following [24]: since the EDM of a particle is proportional to its spin (or total angular momentum for a composite particle as a nucleus), any exposure to an electric field results in a change of the spin with respect to the time t by

$$\frac{d\vec{S}}{dt} = \vec{d} \times \vec{E}^{*}\,, \tag{1.6}$$

where $\vec{E}^{*}$ is the electric field in the rest frame of the particle. In a storage ring with a radial electric field in the ring plane, the EDM of an initially longitudinally polarized particle causes a precession of the spin (or total angular momentum) around the beam axis out of the beam plane. Such a spin precession can be detected by using polarimeters. This class of proposed experiments is the primary motivation of this work.

1.2 Objective

In recent years various theoretical studies have focused on the calculation of EDMs of light nuclei [25–33]. These studies have largely been triggered by the above mentioned plans for experiments to measure EDMs of light nuclei in dedicated storage rings. These calculations revealed that different P- and T-violating mechanisms contribute to the EDMs of different probes at different strengths. A single successful measurement of an EDM of a nucleon would signal P and T violation beyond the CKM mechanism of the SM, but would not suffice to isolate the specific P- and T-violating mechanism. Therefore, non-zero measurements as

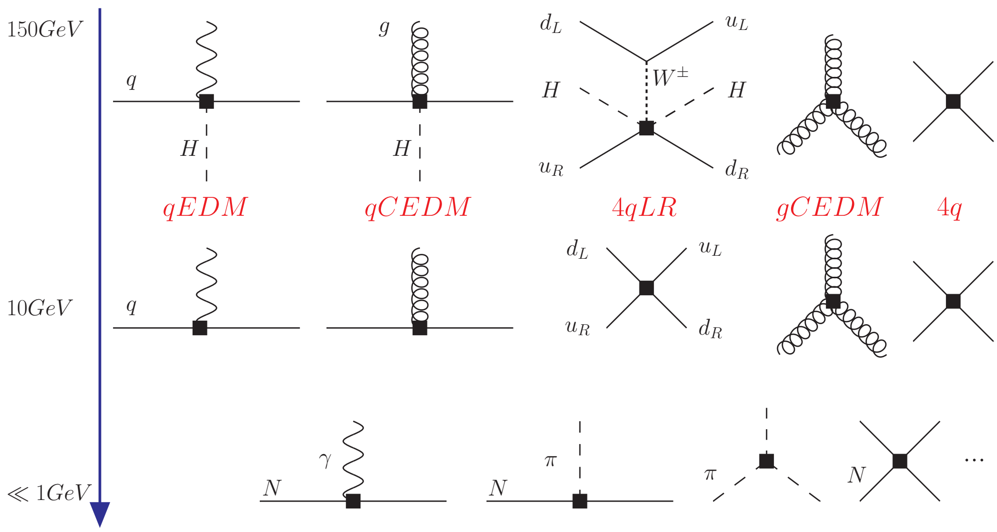

Figure 1.1: P- and T-violating dimension-six sources at different energy scales. A P- and T-violating vertex is depicted by a solid black box.

well as controlled calculations of the EDMs of nucleons and of light nuclei, *e.g.* of the deuteron (^{2}H nucleus), the helion (^{3}He nucleus) and the triton (^{3}H nucleus), are necessary to reveal additional information on new physics.

Within the SM, the source of P and T violation which is of interest for our analysis is the previously mentioned QCD θ-term. The topologically non-trivial structure of the QCD vacuum gives rise to a P- and T-violating term parameterized by the dimensionless constant θ which has to be added to the QCD Lagrangian. It can be rotated into a complex phase of the quark mass matrix by an axial $U(1)$ transformation which vanishes if one of the quarks is massless. However, there is no evidence of a vanishing quark mass for any quark flavor [34]. The QCD θ-term is then a P- and T-violating quark operator of canonical dimension four.

In order to establish the connection between the high-energy sector of BSM physics at an energy scale Λ_{BSM} and operators at the significantly lower hadronic energy scale $\Lambda_{\text{QCD}} \sim 200$ MeV, a two-step effective field theory approach is employed. The concept of effective field theories entails the following: when passing from high energies at a scale Λ_{high} to energies below a certain low-energy scale Λ_{low}, the heavy degrees of freedom with masses above Λ_{low} have to be systematically integrated out from the underlying theory to obtain the set of low-energy operators. The resulting theory with low-energy degrees of freedom at the energy scale Λ_{low}, the effective field theory, is then essentially an expansion in powers of $1/\Lambda_{\text{high}}$. The heavy degrees of freedom manifest themselves as $(1/\Lambda_{\text{high}})^n$ corrections (with n being a positive integer) to the leading terms composed of the remaining light degrees of freedom.

The first step entails the evolution of operators from extensions of the SM at a characteristic energy scale Λ_{BSM} to the energy scale $\Lambda_{\mathrm{had}} \gtrsim 1$ GeV, which has been performed in [5, 10, 35–40]. Since the SM successfully describes the physics at Λ_{had}, any extension of the SM has to exhibit the same gauge symmetry and contain the degrees of freedom of the SM. After integrating out all heavy degrees of freedom from extensions of the SM with mass of $\sim \Lambda_{\mathrm{BSM}}$ and also the heavy SM degrees of freedom ($W^{\pm}$, Z^0, Higgs), the set of effective operators at the energy scale Λ_{had} is obtained. These effective operators are composed of the light SM degrees of freedom, i.e. the up quark, the down quark, the gluons and the photon[4]. By compiling the list of all leading P- and T-violating operators at the energy scale Λ_{had}, any bias favoring one particular extension of the SM is avoided. This procedure gives rise to five non-renormalizable operators of canonical dimension six (subsequently referred to as effective dimension-six sources or operators) known as the quark-chromo EDM ($qCEDM$), the four-quark left-right operator ($4qLR$-op), the quark EDM ($qEDM$), the gluon-chromo EDM ($gCEDM$) and the four-quark operator ($4q$-op). These effective dimension-six operators and the corresponding operators with heavy SM degrees of freedom from which they originate are depicted in fig. 1.1. Since the $qEDM$ and the $qCEDM$ both have an isospin-conserving and an isospin-violating component and since the $4q$-op contains two components with different color structures, there are actually eight independent effective dimension-six sources which, together with the QCD θ-term, serve as the starting point of the analysis presented in this thesis.

The second step entails the transition from operators at the energy scale $\Lambda_{\mathrm{had}} \gtrsim 1$ GeV to operators at the energy scale $\Lambda_{\mathrm{QCD}} \sim 200$ GeV. The description of physics at and below Λ_{QCD} requires the employment of non-perturbative techniques. The analysis presented in this thesis is based on two-flavor *Chiral Perturbation Theory* (ChPT), which is the effective field theory of QCD and as such preserves its symmetries, but is formulated in the language of hadrons. It admits a consistent expansion of hadronic operators in the pion mass M_π over $\Lambda_\chi \sim 1$ GeV. Instead of quarks and gluons, the effective degrees of freedom are now hadrons, namely pions and nucleons.

P and T violation induced by the QCD θ-term and the effective dimension-six sources within the Weinberg formulation of ChPT (see *e.g.* chapter 19 of [41] and appendix C) have recently been studied in [39, 42]. The first objective of this thesis is to refine these studies within the Gasser-Leutwyler formulation of ChPT [43,44]. The link between operators at the energy scale Λ_{had} and operators at energies below Λ_{QCD} is mainly established by the transformation properties of operators under chiral $SU(2)_L \times SU(2)_R$ rotations. The study of the P- and T-violating hadronic operators at the energy scale Λ_{QCD} induced by particular P-

[4]Since the aim of this thesis is to investigate the EDMs of light nuclei in the ground state, strange quarks and all other heavier quarks can be neglected.

and T-violating operators requires a detailed investigation of the representation theory of the group of chiral transformations $SU(2)_L \times SU(2)_R$.

The QCD θ-term expressed as a complex phase of the quark mass matrix is part of the same isospin multiplet as the isospin-violating component of the quark mass matrix and can thus be treated within standard ChPT. Therefore, the leading P- and T-violating πNN vertices induced by the θ-term arise from terms in the effective Lagrangian whose low-energy constants (LECs) are related to quantitatively known observables such as the quark mass induced contribution to the neutron-proton mass difference, the πN sigma term and the quark mass induced component of the squared mass splitting between charged and neutral pions. This allows for a computation of the leading P- and T-violating coupling constants as functions of the physical parameter $\bar{\theta}$.

The effective dimension-six operators transform as elements of new and separate isospin multiplets, which requires an amendment of standard ChPT, that is accompanied by the introduction of new unknown LECs. The P- and T-conserving isospin multiplet partners of the effective dimension-six sources also yield minor contributions to previously mentioned P- and T-conserving observables, such as the quark mass induced contribution to the neutron-proton mass difference. It is therefore impossible to disentangle the different P- and T-conserving operators and to infer the sizes of the new LECs from hadronic observables.

This implies that there is no means available within the framework of effective field theory alone to assess the sizes of the coupling constants of leading P- and T-violating vertices which are induced by the effective dimension-six sources. Supplementary input from other non-perturbative techniques are required in order to obtain values for these coupling constants. Among these non-perturbative techniques, Lattice QCD has the most accurate predictive capacity. Since Lattice QCD is not expected to produce any results for the new LECs soon, one has at least for now to resort to Naive Dimensional Analysis (NDA) to obtain order of magnitude estimates for the coupling constants.

The computation of the EDM of a *single* nucleon has been the subject of various publications [45–51]. The θ-term starts to contribute at the one-loop level, at the same order as unknown counter terms which absorb the loop divergences. The predictive capacity of ChPT is therefore limited without any quantitative knowledge of the unknown counter terms. A quantitative assessment of the counter terms requires the employment of *e.g.* Lattice QCD. The currently available Lattice QCD data produced by several groups are still for large unphysical pion masses [52, 53]. An interpolation of the available Lattice QCD predictions for the EDMs of single nucleons to physical pion masses in order to quantify the counter terms (as done in [51]) yields still too large uncertainties[5]. As pointed

[5]More recent Lattice QCD predictions for the single-nucleon EDMs indicate that the uncertainties of the Lattice QCD input which underlies [51] is significantly understated. A revision

out in [25], the study of EDMs of light nuclei might evade this problem since the θ-term induces tree-level nuclear contributions to the EDMs of a light nuclei at leading order. This implies a potentially significant enhancement of nuclear contributions compared to the single-nucleon contributions.

Therefore, the second objective of this thesis is to compute the EDMs of the deuteron, the helion and the triton on the basis of the previously obtained sets of P- and T-violating hadronic operators within the framework of (amended) ChPT. The first nucleus under investigation is the two-nucleon (NN) system of the deuteron. The previous studies presented in [25, 27, 29, 30, 33] focused on the leading-order nuclear contribution to the deuteron EDM according to the power counting presented in this thesis. For a computation with controlled uncertainties, also subleading nuclear contributions have to be taken into consideration and the uncertainty originating from the P- and T-conserving component of the nuclear potential has to be investigated.

The computation is then extended to the significantly more complicated three-nucleon ($3N$) systems of the helion and the triton. The isospin selection rules of the deuteron channel impose strict constraints on P- and T-violating nuclear operators to yield non-vanishing contributions. Since these constraints are absent in the helion and triton channels, these $3N$ systems provide additional information on the underlying P- and T-violating mechanism. This thesis presents a more refined analysis of the nuclear contributions to the helion and triton EDMs than the previous ones published in [28, 30, 33]. In particular, it includes an assessment of the above mentioned uncertainties due to the different realizations of the P- and T-conserving component of the nuclear potential. The computation of the EDMs of the helion and triton required an extensive development of parallel software designed to run on the supercomputers *JUROPA* and *JUQUEEN* of the Forschungszentrum Jülich.

Several schemes to infer the source(s) of P and T violation from a combination of EDM measurements of light nuclei and (eventually) supplementary Lattice QCD input are presented as the main result of this thesis. The quantitative knowledge of the dominating coupling constants in the θ-term case translates into quantitative predictions with well-defined uncertainties for the nuclear EDM contributions. The NDA assessment of the coupling constants of leading P- and T-violating vertices induced by the effective dimension-six sources still allows for qualitative statements on the origin of P and T violation on the basis of larger experimental input (more measurements of nucleons and light nuclei EDMs compared to the θ-term case).

of the interpolation in [51] on the basis of [53] for still large but smaller unphysical pion masses is in the pipeline (private communication with the authors of [51]).

1.3 Outline

This thesis is organized as follows:

Chapter 2: in this chapter, the foundations of QCD needed in the subsequent analysis are briefly presented and the origin of the QCD θ-term in topologically non-trivial field configurations is explained.

Chapter 3: P and T violation from physics within and beyond the SM is discussed in chapter three, where the approach of refs. [10, 35–40] to describe the manifestation of high-energy BSM physics at significantly lower energy scales is presented. The evolution of P- and T-violating BSM operators to the energy scale $\Lambda_{\text{had}} \sim 1$ GeV itself proceeds in two substeps: the first step is to compile the list of all independent P- and T-violating operators composed of the SM degrees of freedom above the electroweak spontaneous symmetry breaking (SSB) scale. The second entails integrating out all SM degrees of freedom with masses above $\Lambda_\chi \sim$ GeV, i.e. the Higgs, $W^\pm$ bosons, the Z^0 boson and heavy quarks. The evolution of operators yields the previously mentioned P- and T-violating effective dimension-six operators ($qCEDM$, $4qLR$-op, $qEDM$, $gCEDM$, $4q$-op). The QCD θ-term and these effective dimension-six sources serve as the basis of the subsequent analysis of the EDMs of light nuclei.

Chapter 4: a brief introduction into *Chiral Perturbation Theory* (ChPT) is provided which contains all major aspects required for the computation of the EDMs of light nuclei. The set of P- and T-violating vertices induced by the θ-term and the hierarchy of their coupling constants (as well as their explicit calculation whenever possible) is derived within the framework of standard ChPT. The incorporation of the effective dimension-six operators into a chiral effective field theory framework (referred to as amended ChPT below) is presented, which also comprises a detailed study of the representation theory of the chiral group $SU(2)_L \times SU(2)_R$. A method to identify the altered ground state of QCD and likewise (amended) ChPT in the presence of P- and T-violating terms is explained and applied to the sets of P- and T-violating operators induced by the θ-term and the effective dimension-six sources. Technical details are explained and derived in the appendices A, B, D and I. The connection between the Gasser-Leutwyler formulation and the Weinberg formulation of $SU(2)$ ChPT is explained in appendix C.

Chapter 5: equipped with the results of chapter 4, the computation of the NN contributions to the EDM of the deuteron induced by the θ-term within standard ChPT is presented in two different ways: the first way entails a largely analytical calculation by utilizing a parametrization of the CD-Bonn [54] potential and the separable rank-two PEST potential [55] to take P- and T-conserving interactions in the intermediate state into account. Since not all realizations of the P- and T-conserving component of the nuclear potential are expressible in terms of separable potentials, the second way is a complementary numerical computation in which the phenomenological Argonne v_{18} potential [56] and ChPT potentials [57] are also considered. The discussion is subsequently extended to the deuteron EDM induced by the effective dimension-six sources. The solutions to some fundamental integrals which occurred during the analytic calculation are listed in appendix E. Some matrix elements of NN potential and transition current operators needed for the numerical computation are given in appendix F. Furthermore, a very efficient technique to calculate matrix elements of spin and isospin operators is briefly explained in appendix H.

Chapter 6: the complete numerical computation of the nuclear contributions to the EDMs of the helion and the triton induced by the θ-term is presented within the framework of ChPT. The CD-Bonn potential, the Argonne v_{18} potential and ChPT potentials are utilized for the P- and T-conserving component of the $3N$ potential. The discussion is then extended to the helion and triton EDMs induced by the effective dimension-six sources within the framework of amended ChPT. Several schemes of inferring the source(s) of P and T violation from a combination of measurements of light nuclei and (eventually) supplementary lattice QCD computations are presented as the main result of this thesis. The partial wave decompositions of some NN potential and transition current operators required by the numerical computation are listed in appendix F.

Chapter 7: the main conclusions of this thesis are briefly summarized and an outlook on pending work is given.

1.4 Conventions

- Electric charge of the electron[6] : $e < 0$
- Fine structure constant: $\alpha_{em} = e^2/(4\pi) \approx 1/137.036$ [34]
- Pion decay constant: $F_\pi = 92.2$ MeV [34]
- Pion mass: $M_\pi = (M_{\pi^0} + 2M_{\pi^\pm})/3 = 138.04$ MeV [34]
- Nucleon mass: $m_N = (m_n + m_p)/2 = 938.92$ MeV [34]
- Epsilon-tensor: $\epsilon^{123} = 1$
- Pauli matrices:

$$\sigma_1, \tau_1 = \begin{pmatrix} 0 & 1 \\ 1 & 0 \end{pmatrix}, \quad \sigma_2, \tau_2 = \begin{pmatrix} 0 & -i \\ i & 0 \end{pmatrix}, \quad \sigma_2, \tau_2 = \begin{pmatrix} 1 & 0 \\ 0 & -1 \end{pmatrix}$$

- Minkowski metric: $g^{\mu\nu} = \mathrm{diag}(1, -1, -1, -1)$
- Four-vector: $v^\mu = g^{\mu\nu} v_\nu$

[6] Convention consistent with appendix A of [58].

- Dirac matrices: $\{\gamma^\mu, \gamma^\nu\} = 2g^{\mu\nu}\mathbb{1}$, $\gamma_5 = i\gamma_0\gamma_1\gamma_2\gamma_3$
- Levi-Civita tensor: $\epsilon^{0123} = -\epsilon_{0123} = 1$
- Euclidean Levi-Civita tensor: $\epsilon_E^{1234} = 1$
- The Einstein summation convention is always assumed unless stated otherwise

Chapter 2

Quantum chromodynamics

Quantum chromodynamics (QCD) is the accepted quantum field theory of the strong interaction. It is a color $SU(3)$ Yang-Mills theory for N_f quark flavors. Since the focus of this thesis is on the two lightest quarks, the up quark and the down quark, all heavier quarks are neglected below. A quark field is therefore a spin-1/2 Dirac spinor, a color $SU(3)$ triplet and a quark flavor $SU(2)$ doublet. The flavor symmetric QCD Lagrangian for massless up and down quarks and gluons is given by:

$$\mathcal{L}^{\chi}_{\text{QCD}} = i \sum_{f,j,k} \bar{q}_{f,j}\, \gamma^{\mu}\, (D_{\mu})_{jk}\, q_{f,k} - \frac{1}{4} G^{a}_{\mu\nu} G^{a,\mu\nu} \,, \tag{2.1}$$

$(j, k = 1, 2, 3, 4,\ f = 1, 2,\ a = 1, ..., 8)$ with the $SU(3)$ covariant derivative:

$$(D_{\mu})_{ij} = \delta_{ij}\partial_{\mu} - i g_s (t^a_c)_{ij} A^a_{\mu} \,, \tag{2.2}$$

where g_s is the strong coupling constant, A^a_{μ} are the gluon fields and t^a_c are the generators of $SU(3)$ with $\text{Tr}(t^a_c t^b_c) = \delta^{ab}/2$. The gluon field strength tensor $G^a_{\mu\nu}$ is defined by $G^a_{\mu\nu} = \partial_{\mu} A^a_{\nu} - \partial_{\nu} A^a_{\mu} + g_s f^{abc} A^a_{\mu} A^b_{\nu}$, where f^{abc} are the structure constants of the Lie algebra of $SU(3)$.

The quark fields can be decomposed into their right- and left-handed components by utilizing the projection operator $P_{L,R} = (\mathbb{1} \pm \gamma^5)/2$:

$$q_R = \frac{1}{2}(\mathbb{1} + \gamma^5) q \,, \quad q_L = \frac{1}{2}(\mathbb{1} - \gamma^5) q \,. \tag{2.3}$$

The Lagrangian $\mathcal{L}^{\chi}_{\text{QCD}}$ is invariant under chiral $SU(2)_L{\times}SU(2)_R$ transformations:

$$q(x) \mapsto \exp(i\tau_k \alpha^k_R)\, P_R\, q(x) + \exp(i\tau_k \alpha^k_L)\, P_L\, q(x) \,, \tag{2.4}$$

where τ_k are the Pauli matrices which act on the flavor space. $\mathcal{L}^{\chi}_{\text{QCD}}$ is also invariant under the $U(1)_R{\times}U(1)_L$ transformations:

$$q(x) \mapsto \exp(i\alpha_R)\, P_R\, q(x) + \exp(i\alpha_L)\, P_L\, q(x) \,, \tag{2.5}$$

The chiral-symmetry-conserving QCD Lagrangian $\mathcal{L}^{\chi}_{\text{QCD}}$ is therefore invariant under the group of $SU(2)_L{\times}SU(2)_R{\times}U(1)_L{\times}U(1)_R \sim U(2)_L{\times}U(2)_R$ transformations.

2.1 Gauge anomalies in QCD

Although the group of axial $U(1)$ transformations, $U(1)_A$, is a symmetry group of $\mathcal{L}^{\chi}_{\rm QCD}$, it is not a symmetry group of the generating functional of QCD:

$$W_{\rm QCD} = \int \mathcal{D}\bar{q}\,\mathcal{D}q\,\mathcal{D}A^a_\mu \,\exp\left(i\int d^4x\,\mathcal{L}^{\chi}_{\rm QCD}\right)\,. \tag{2.6}$$

A continuos symmetry group of the classical action S is also a symmetry group of the quantum field theory if and only if the generating functional $W_{\rm QCD}$ is invariant under this group of transformations. The fermion measure $\mathcal{D}\bar{q}\,\mathcal{D}q$ of $W_{\rm QCD}$ transforms non-trivially under the group of axial transformations $U_A(1)$. The divergence of the Noether current associated with $U_A(1)$ does not vanish:

$$J^\mu_5(x) = \bar{q}(x)\gamma^\mu\gamma_5 q(x)\,,\quad \partial_\mu J^\mu_5(x) = \mathcal{A}(x)\,, \tag{2.7}$$

where $\mathcal{A}$ is the $U_A(1)$ gauge anomaly.

The anomaly $\mathcal{A}$ is most conveniently calculated in Euclidean space-time [41, 59]. The presentation below follows the lines of these two references. The transition from Minkowski space to Euclidean space-time is facilitated by the Wick rotation:

$$x_0 = -ix_4\,,\quad \partial_0 = i\partial_4\,,\quad A^k_0 = iA^k_4\,, \tag{2.8}$$

where A^k_μ are the color $SU(3)$ gauge fields. The euclidean gamma matrices are defined by

$$\tilde{\gamma}_4 := i\gamma^0,\quad \tilde{\gamma}_j := \gamma^j\,,\quad j\in\{1,2,3\}\,, \tag{2.9}$$

such that $\{\tilde{\gamma}^j,\tilde{\gamma}^k\} = -2\delta^{jk}\mathbb{1}$ for $j,k\in\{1,2,3,4\}$. The tilde is omitted for convenience below. The hermitian Dirac operator in Euclidean space-time is given by

$$\not{D} = (\partial_4 - ig_s A^k_4 t^k_c)\,\gamma_4 + (\partial_j - ig_s A^k_j t^k_c)\,\gamma_j\,,\quad j=1,2,3\,, \tag{2.10}$$

where t^k_c are the generators of the color $SU(3)$ gauge group with normalization $\mathrm{Tr}(t^k_c t^l_c) = \delta^{kl}/2$. The Euclidean Dirac operator $\not{D}$ then has a complete set of orthonormal spinor eigenfunctions:

$$\not{D}\,\phi_n(x) = \lambda_n\,\phi_n(x)\,, \tag{2.11}$$

with $\lambda_n\in\mathbb{R}$ which obey

$$\int d^4x_E\,\phi_n(x)^\dagger\phi_{n'}(x) = \delta_{nn'},\quad \sum_n \phi_n(x)\phi^\dagger_n(y) = \delta^{(4)}(x-y)\mathbb{1}\,. \tag{2.12}$$

This enables us to express the fermion fields q and $\bar{q}$ in terms of these eigenfunctions:

$$q(x) = \sum_n a_n\phi_n(x)\,,\quad \bar{q}(x) = \sum_n \phi_n(x)^\dagger\,\bar{b}_n\,, \tag{2.13}$$

where a_n and b_n are Grassmann variables. The fermion measure is then given by

$$\mathcal{D}\bar{q}(x)\,\mathcal{D}q(x) = \Pi_{n,m}\, d\bar{b}_n\, da_m\,. \tag{2.14}$$

For a general local transformation in flavor space

$$U(x) = \exp(i\gamma_5\, t^k\, \alpha^k(x)) = \mathbb{1} + i\gamma^5\, t^k\, \alpha^k(x) + \cdots\,, \tag{2.15}$$

with $t^k = (\mathbb{1}, \tau_1, \tau_2, \tau_3)$ and $k = 0, 1, 2, 3$, the quark fields transform according to

$$q(x) = \sum_n a_n\, \phi_n(x) \mapsto \sum_{n,m} \int d^4y_E\, \phi_n(y)^\dagger\, U(y)\, \phi_m(y)\, a_m\, \phi_n(x)\,. \tag{2.16}$$

Let the Jacobian J be defined by

$$J_{mn} = \int d^4x_E\, \phi_m^\dagger(x) U(x) \phi_n(x) = \int d^4x_E\, \phi_m^\dagger(x)[\mathbb{1} + i\gamma^5 t^k \alpha^k(x) + \cdots]\phi_n(x)\,, \tag{2.17}$$

For the Grassmann variables a_n, the change of the integration measure is then given by $\Pi_n\, da'_n = \det(J)^{-1}\, \Pi_n\, da_n$ and for the complete functional measure of eq. (2.14) by

$$\Pi_{m,n} d\bar{b}_m da_n \mapsto \Pi_{m,n} \det(J)^{-2} d\bar{b}_m da_n\,. \tag{2.18}$$

Utilizing $\det(J) = \exp(\mathrm{Tr}(\ln(J)))$ and $\ln(1+\epsilon) = \epsilon + \mathcal{O}(\epsilon^2)$, the complete Jacobian can be rewritten as

$$\det(J)^{-2} = \exp\left[-2i\, \mathrm{Tr}_{\mathrm{c,f}} \left(\int d^4x_E \sum_m \phi_m^\dagger(x) \gamma^5 t^k \alpha^k(x) \phi_m(x)\right)\right] + \cdots\,, \tag{2.19}$$

where the subindices c and f indicate that the trace is to be taken over the color and the flavor space. The integrand in the argument of the exponential,

$$\mathcal{A}^k(x) := -2\, \mathrm{Tr}_{c,f} \left(\sum_m \phi_m^\dagger(x) \gamma^5 t^k \phi_m(x)\right)\,, \tag{2.20}$$

is singular and has to be regularized by a monotonically decreasing smooth regulator function g (*e.g.* $g(s) = \exp(-s^2)$):

$$g : \mathbb{R}_0^+ \to [0, 1], \quad g(0) = 1,\, \lim_{s\to 0} g'(s)\, s = 0,\, \lim_{s\to\infty} g(s) = \lim_{s\to\infty} g'(s)\, s = 0\,. \tag{2.21}$$

By exploiting eq. (2.11) and eq. (2.12), the anomalous term $\mathcal{A}^k(x)$ then becomes

$$\begin{aligned} \mathcal{A}^k(x) &= -2 \lim_{M\to\infty} \mathrm{Tr}_{c,f} \left(\sum_m \phi_m^\dagger(x) \gamma^5 t^k g\left(\frac{\lambda_m^2}{M^2}\right) \phi_m(x)\right) \\ &= -2 \lim_{M\to\infty} \lim_{y\to x} \mathrm{Tr}_{c,f} \left(\gamma^5 t^k g\left(\frac{\not{D}_x^2}{M^2}\right) \delta^{(4)}(x-y)\right)\,, \end{aligned} \tag{2.22}$$

with $|\lambda_n| \ll M\, \forall n$ for some scale M. The Fourier transformation of the δ-function leads to

$$\begin{aligned}\mathcal{A}^k(x) &= -2 \lim_{M\to\infty} \lim_{x\to y} \int \frac{d^4k_E}{(2\pi)^4} \mathrm{Tr}_{c,f}\left(\gamma^5 t^k g\left(\frac{\not{D}_x^2}{M^2}\right)\right) \exp(ik\cdot(x-y)) \\ &= -2 \lim_{M\to\infty} M^4 \int \frac{d^4k_E}{(2\pi)^4} \mathrm{Tr}_{c,f}\left(\gamma^5 t^k g\left([i\not{k} + \not{D}_x/M]^2\right)\right)\,, \qquad (2.23)\end{aligned}$$

where the substitution $k \to k\,M$ has been made.In the limit $M \to \infty$, a non-vanishing term in the expansion of g has to be at most of order $1/M^4$. It also has to be the product of at least four gamma matrices in order to survive the Dirac trace. $\mathcal{A}^k(x)$ therefore equals:

$$\mathcal{A}^k(x) = -\int \frac{d^4k_E}{(2\pi)^4} \mathrm{Tr}_{c,f}\left(\gamma^5 t^k \not{D}_x^4\right) \frac{\partial^2 g(k^2)}{(\partial k^2)^2}\,. \qquad (2.24)$$

Due to the above stated properties of the regulator function g, the integral reduces to

$$\int \frac{d^4k_E}{(2\pi)^4} \frac{\partial^2 g(k^2)}{(\partial k^2)^2} = \frac{1}{16\pi^2} \int_0^\infty dk^2\, k^2 \frac{\partial^2 g(k^2)}{(\partial k^2)^2} = \frac{1}{16\pi^2}\,. \qquad (2.25)$$

By utilizing

$$\not{D}_x^2 = -D_x^2 - \frac{1}{4}[\gamma_i,\gamma_j] i g_s t_c^l\, G_{ij}^l(x) \quad \text{and} \quad \mathrm{Tr}(\gamma^5[\gamma_i,\gamma_j][\gamma_r,\gamma_s]) = 16\,\epsilon_{ijrs}^E\,, \quad (2.26)$$

the anomalous term $\mathcal{A}^k(x)$ becomes:

$$\mathcal{A}^k(x) = \frac{g_s^2}{32\pi^2} \epsilon_{ijrs}^E G_{ij}^l(x) G_{rs}^l(x) \mathrm{Tr}_f(t^k)\,, \qquad (2.27)$$

since $\mathrm{Tr}_c(t_c^l t_c^m) = (1/2)\,\delta^{lm}$. The analogous expression in Minkowski space is of opposite sign, i.e.

$$\mathcal{A}^k(x) = -\frac{g_s^2}{32\pi^2} \epsilon^{\mu\nu\rho\sigma} G_{\mu\nu}^l(x) G_{\rho\sigma}^l(x) \mathrm{Tr}_f(t^k)\,. \qquad (2.28)$$

When $t^k \to \mathbb{1}$, $\mathcal{A}(x)$ is called the *Chern-Pontryagin density.*

An infinitesimal local transformation thus shifts the fermion measure in eq. (2.6) by

$$\mathcal{D}\bar{q}\,\mathcal{D}q \mapsto \mathcal{D}\bar{q}\,\mathcal{D}q \,\exp\left(i\int d^4x\, \alpha^k(x)\, \mathcal{A}^k(x)\right) + \mathcal{O}((\alpha^k(x))^2)\,. \qquad (2.29)$$

Although $\mathcal{A}^k(x)$ can be expressed as a divergence,

$$\frac{1}{2}\epsilon^{\mu\nu\rho\sigma} G_{\mu\nu}^l(x) G_{\rho\sigma}^l(x) = \partial_\mu 2\,\epsilon^{\mu\nu\rho\sigma}\left(A_\nu^a \partial_\rho A_\sigma^a + \frac{g_s}{3} f^{abc} A_\nu^a A_\rho^b A_\sigma^c\right) \equiv \partial_\mu K^\mu\,, \quad (2.30)$$

the integral over $\mathcal{A}^k(x)$ in eq. (2.29) does not vanish due to topologically non-trivial solutions for A^k_μ as demonstrated below. The above calculation proves that the fermion measure is not invariant under transformations with generators that have a non vanishing trace. This gives rise to the $U(1)_A$ anomaly:

$$\partial_\mu J^\mu_5 = -\frac{g_s^2}{16\pi^2}\epsilon^{\mu\nu\rho\sigma}G^l_{\mu\nu}(x)G^l_{\rho\sigma}(x)\,. \tag{2.31}$$

The conserved current associated with $U(1)_A$ of the classical action is not a conserved current of the quantum field theory.

The $SU(2)_L \times SU(2)_R$ symmetry is explicitly broken by the non-zero masses of the up and the down quark and by the different electric charges of the quarks. The complete QCD Lagrangian is thus given by

$$\begin{aligned} \mathcal{L}_{\mathrm{QCD}} &= \mathcal{L}^{\chi}_{\mathrm{QCD}} + \mathcal{L}^{\not\chi}_{\mathrm{QCD}}\,, && (2.32)\\ \mathcal{L}^{\not\chi}_{\mathrm{QCD}} &= \bar{q}\gamma^\mu e\mathcal{Q}A_\mu q - \bar{q}\mathcal{M}q\,, && (2.33) \end{aligned}$$

where $\mathcal{Q}$ is the two-flavor quark electric charge matrix, $\mathcal{M}$ is the two-flavor quark mass matrix, A_μ is the electromagnetic field and $e < 0$ is the electric charge of the electron. The matrices $\mathcal{Q}$ and $\mathcal{M}$ are defined by

$$\mathcal{Q} = \frac{1}{6}\mathbb{1} + \frac{1}{2}\tau_3\,, \quad \mathcal{M} = \frac{m_u + m_d}{2}\mathbb{1} + \frac{m_u - m_d}{2}\tau_3\,, \tag{2.34}$$

where m_u, m_d are the masses of the up and the down quark, respectively.

As pointed out by Gasser and Leutyler [43, 44, 60], a quantum field theory is not completely determined by the global chiral $SU(2)_L \times SU(2)_R$ symmetries of the classical action. In the absence of anomalies, the set of all Green functions and chiral Ward identities can be incorporated into a generating functional by rendering it invariant under local chiral transformations. The Green functions and Ward identities of particular (composite) operators can then be studied by regarding these operators as additional currents $J^{j,\mu}(x)$ in the Lagrangian which couple to external fields $f^j_\mu(x)$. This method is briefly explained in appendix A. Therefore, the Lagrangian is amended by the sum over the products of these currents and source fields,

$$S \to \int d^4x \left(\mathcal{L}^{\chi}_{\mathrm{QCD}} + \sum_j f^j_\mu(x)\, J^{j,\mu}(x)\right)\,, \tag{2.35}$$

where

$$\begin{aligned} \sum_j f^j_\mu\, J^{j,\mu} = {} & \bar{q}\,\gamma_\mu(v^\mu_j\tau_j + a^\mu_j\tau_j\gamma^5)\,q + \bar{q}\,\gamma^\mu v^{(s)}_\mu\,q \\ & -\bar{q}\,(s_0\mathbb{1} + s_j\tau_j - i\gamma^5 p_0\mathbb{1} - i\gamma^5 p_j\tau_j)\,q\,. && (2.36) \end{aligned}$$

The source fields a_j^μ, v_j^μ, $v_\mu^{(s)}$, s_j, s_0, p_j, p_0 transform as basis states of particular irreducible representations of $O(4)$ (of which $SU(2)_L \times SU(2)_R$ is a double covering group as explained in appendix B) complementary to their associated quark bilinears, such that all terms $f_\mu^j\, J^{j,\mu}$ are locally $SU(2)_L \times SU_R(2)$ invariant. The two-flavor QCD Lagrangian is thus amended by

$$\begin{aligned}\mathcal{L}_{\rm QCD} = \mathcal{L}^{\chi}_{\rm QCD} + \mathcal{L}^{\not\chi}_{\rm QCD} &= \mathcal{L}^{\chi}_{\rm QCD} + \bar{q}\,\gamma_\mu(v_i^\mu \tau_i + a_i^\mu \tau_i \gamma^5)\,q + \bar{q}\,\gamma^\mu v_\mu^{(s)}\,q \\ &\quad - \bar{q}\,(s_0 \mathbb{1} + s_i\tau_i - i\gamma^5 p_0 \mathbb{1} - i\gamma^5 p_i \tau_i\,)\,q\,, \qquad (2.37)\end{aligned}$$

where the source fields ($a_j^\mu = r_j^\mu - l_j^\mu$, $v_j^\mu = r_j^\mu + l_j^\mu$, $v_\mu^{(s)} = r_\mu^{(s)} + l_\mu^{(s)}$) are transformed under local $SU(2)_L \times SU(2)_R \times U(1)_V$ transformations by (see eq. (2.3),eq. (2.4) and eq. (2.5)):

$$\begin{aligned} r_i^\mu \tau_i &\mapsto R\, r_i^\mu \tau_i R^\dagger + iR\,\partial^\mu R^\dagger\,, && (2.38)\\ l_i^\mu \tau_i &\mapsto L\, l_i^\mu \tau_i L^\dagger + iL\,\partial^\mu L^\dagger\,, && (2.39)\\ r_\mu^{(s)} &\mapsto R\, r_\mu^{(s)} R^\dagger + iR\,\partial_\mu R^\dagger\,, && (2.40)\\ l_\mu^{(s)} &\mapsto L\, l_\mu^{(s)} L^\dagger + iL\,\partial_\mu L^\dagger\,, && (2.41)\\ (s_i\tau_i + ip_i\tau_i) &\mapsto R\,(s_i\tau_i + ip_i\tau_i)L^\dagger\,, && (2.42)\\ (s_i\tau_i - ip_i\tau_i) &\mapsto R\,(s_i\tau_i - ip_i\tau_i)L^\dagger\,, && (2.43)\\ (s_0 + ip_0) &\mapsto R\,(s_0 + ip_0)\,L^\dagger\,, && (2.44)\\ (s_0 - ip_0) &\mapsto R\,(s_0 - ip_0)\,L^\dagger\,. && (2.45)\end{aligned}$$

The complete generating functional of QCD is then given by

$$W_{\rm QCD} = \int \mathcal{D}\bar{q}\,\mathcal{D}q\,\mathcal{D}A_\mu^k\ \exp\left(i\int d^4x\,\mathcal{L}^{\chi}_{\rm QCD} + \mathcal{L}^{\not\chi}_{\rm QCD}(s_0, s_i, p_0, p_i, v^{(s),\mu}, v_i^\mu, a_i^\mu)\right)\,, \qquad (2.46)$$

and Green functions involving products of currents are obtained by differentiating the generating functional with respect to the corresponding source field:

$$\begin{aligned}&\langle 0|J^{j_1}_{\mu_1}(x_1)\cdots J^{j_n}_{\mu_n}(x_n)|0\rangle \\ = \quad & \frac{1}{W_{\rm QCD}[0]}\,\frac{1}{i}\,\frac{\delta}{\delta f^{j_1}_{\mu_1}(x_1)}\cdots\frac{1}{i}\,\frac{\delta}{\delta f^{j_n}_{\mu_n}(x_n)} W_{\rm QCD}\left[f^{j_1}_{\mu_1},\cdots,f^{j_n}_{\mu_n}\right]\Bigg|_{\{f^{j_k}_{\mu_k}\}=0}\,. \qquad (2.47)\end{aligned}$$

We will resort to the following notation for the source fields in the subsequent discussion:

$$v^\mu := v_i^\mu \tau_i\,, \quad a^\mu := a_i^\mu \tau_i\,, \quad s := s_0 \mathbb{1} + s_i\tau_i\,, \quad p := p_0\mathbb{1} + p_i\tau_i\,. \qquad (2.48)$$

2.2 The QCD θ-term

As mentioned in section 2.1, the $U(1)_A$ anomaly eq. (2.31) does not vanish although it can be expressed as a divergence due to the existence of topologically non-trivial field configurations of the gauge fields associated with a particular gauge group $SU(N)$. These field configurations are known as instantons [61]. This section provides a brief explanation of instantons along the lines of references [41, 61].

Consider a map of the three-sphere $\mathbb{S}^3$ into the simple Lie group $SU(N)$. As shown in [62], the third homotopy group of $SU(N)$ is $\pi_3(SU(N)) = \mathbb{Z}$ and all such maps are homotopic to a map of $\mathbb{S}^3$ into a particular $SU(2)$ subgroup of $SU(N)$:

$$f : \mathbb{S}^3 \to SU(2) \subset SU(N) , \quad \phi = (\phi_1, \phi_2, \phi_3) \mapsto f(\phi_1, \phi_2, \phi_3) . \tag{2.49}$$

If $\{b_1, \cdots , b_n\}$ is the basis of the fundamental representation of $SU(N)$, this subgroup is taken to be the one which acts on the subspace spanned by $\{b_1, b_2\}$. Since f maps into a matrix group, the Maurer-Cartan form is given by $f^{-1}df$. The integration of the Maurer-Cartan form gives the functional

$$\omega\big[f\big] = \int d\phi_1\, d\phi_2\, d\phi_3\, \epsilon^{ijk}\, \mathrm{Tr}\left(f^{-1}(\phi) \frac{\partial f(\phi)}{\partial \phi_i} f^{-1}(\phi) \frac{\partial f(\phi)}{\partial \phi_j} f^{-1}(\phi) \frac{\partial f(\phi)}{\partial \phi_k} \right) , \tag{2.50}$$

which is independent of the parametrization of the manifold $\mathbb{S}^3$ and, in particular, homotopy invariant. Therefore, eq. (2.50) is a function on the homotopy classes $[f]$ of maps $f : \mathbb{S}^3 \to SU(N)$, i.e. on $\pi_3(SU(N)) = \mathbb{Z}$. Furthermore, the functional ω has the following property under the product of homotopy classes induced by concatenation of homotopies, $[f_1] * [f_2]$:

$$\omega\big[[f_1] * [f_2]\big] = \omega\big[[f_1]\big] + \omega\big[[f_2]\big] \quad \to \quad \omega\big[[f]^\nu\big] = \nu\, \omega\big[[f]\big] . \tag{2.51}$$

ν is called the winding number (the Brower degree of the map f). When $[g]$ is the generator of $\pi_3(SU(N))$, a straight forward calculation shows:

$$\omega\big[[g]\big] = 24\pi^2, \quad \Rightarrow \quad \omega\big[[g]^\nu\big] = 24\pi^2\nu . \tag{2.52}$$

The Euclidean space-time can be regarded as bounded by $\mathbb{S}^3$ in the limit of large $r = \sqrt{x_1^2 + x_2^2 + x_3^2 + x_4^2} \to \infty$. Consider an $SU(3)$ gauge theory and let G^k_{ij} denote the Euclidean field strength tensor with Euclidean gauge fields A^k_i, structure constants f^{klm} and $g_s = 1$:

$$G^k_{ij} = \partial_i A^k_j - \partial_j A^k_i + f^{klm} A^l_i A^m_j . \tag{2.53}$$

Consider a gauge field which is a pure gauge at large r, i.e. on $\mathbb{S}^3$:

$$t^k A^k_i(\hat{r}) \equiv \tilde{A}_i(\hat{r}) \to -i\partial_i f(\hat{r}) f(\hat{r})^{-1} , \tag{2.54}$$

where t^k are the generators the gauge group $SU(3)$ with $\mathrm{Tr}(t^i t^j) = \delta_{ij}/2$. The field strength tensor eq. (2.53) then vanishes on $\mathbb{S}^3$ and eq. (2.50) becomes (with $\vec{r} = r\,\hat{r}$, $\hat{r} = \hat{r}(\phi_1, \phi_2, \phi_3)$)

$$\omega[[f]] = -i \lim_{r\to\infty} r^3 \int d\phi_1 d\phi_2 d\phi_3\, \epsilon^{ijk} \frac{\partial \hat{r}_a}{\partial \phi_i} \frac{\partial \hat{r}_b}{\partial \phi_j} \frac{\partial \hat{r}_c}{\partial \phi_k} \mathrm{Tr}(\tilde{A}_a \tilde{A}_b \tilde{A}_c) . \tag{2.55}$$

The current K_μ (see eq. (2.30)) in Euclidean space-time obeys:

$$K_i = 2\,\epsilon_E^{ijkl}\,\mathrm{Tr}\left(\tilde{A}_j\partial_k\tilde{A}_l + i\frac{2}{3}\tilde{A}_j\tilde{A}_k\tilde{A}_l\right)\,, \quad \partial_i K_i = \frac{1}{2}\epsilon_E^{ijkl}G^a_{ij}G^a_{kl}\,. \tag{2.56}$$

In the limit $r \to \infty$ where $A_i^k(x)$ becomes a pure gauge ($G^a_{ij} = 0$), the current K_i is given by

$$K_i \to i\,\frac{4}{3}\,\epsilon_E^{ijkl}\,\mathrm{Tr}(\tilde{A}_j\tilde{A}_k\tilde{A}_l)\,. \tag{2.57}$$

Applying Gauss's theorem and inserting eq. (2.57), the functional of eq. (2.50) reads

$$\omega[[f]] = -\frac{3}{4}\int d^4x_E\,\partial_i K_i = -\frac{3}{8}\epsilon_E^{ijkl}\int d^4x_E\,G^a_{ij}G^a_{kl} = 24\pi^2\,\nu\,. \tag{2.58}$$

Eq. (2.58) demonstrates that $\epsilon_E^{ijkl}G^a_{ij}G^a_{kl}$ does not vanish if topologically non-trivial field configurations for $\tilde{A}_i$ exist. Such field configurations are called instantons. An element h of the homotopy class of the generator of $\pi_3(SU(3))$ (i.e. with winding number $\nu = 1$) is given by

$$h(\hat{r}) = \left(\frac{x_4 + ix^k\tau^k}{r}\right) \in SU(2) \subset SU(3)\,, \tag{2.59}$$

where τ^k are the generators of an $SU(2)$ subgroup of $SU(3)$. A field configuration with winding number $\nu = 1$ is then given by [61]

$$iA_i(x) = \frac{r^2}{r^2+\Lambda^2}h^{-1}(\hat{r})\partial_i h(\hat{r})\,, \tag{2.60}$$

where $\Lambda \in \mathbb{R}-\{0\}$. This field configuration is clearly a pure gauge on $\mathbb{S}^3$. ν-fold concantenation of g yields the general instanton solution of winding number ν.

This result confirms that the $U(1)_A$ anomaly does in general not vanish although it can be expressed as a divergence. The violation of the $U(1)_A$ symmetry in QCD by the functional measure is therefore an inherent property of QCD. In order to avoid violating the cluster decomposition theorem [41], the only way of including the instanton solutions into the generating functional of QCD is by a factor $\exp(i\theta\nu)$, which is parameterized by the so called θ-angle. This amounts to an amendment of the QCD Lagrangian by the term (in Minkowski space)

$$\mathcal{L}_\theta = -\theta\frac{g_s^2}{64\pi^2}\epsilon^{\mu\nu\sigma\rho}\,G^a_{\mu\nu}G^a_{\rho\sigma}\,, \tag{2.61}$$

which breaks parity as well as time-reversal invariance. The fermion measure of the generating functional of QCD generates terms which only differ by some real number from eq. (2.61) under $U_A(1)$ transformations. The parameter θ instead of the functional measure can therefore be regarded to transform non-trivially under $U(1)_A$ transformations (see eq. (2.31), N_f: number of flavors):

$$\theta \mapsto \theta + 2\,N_f\,\alpha_A\,. \tag{2.62}$$

The full QCD Lagrangian for up and down quarks and gluons is then given by

$$\mathcal{L}_{\text{QCD}} = \bar{q}[i\not{D} - \exp(i\phi)\mathcal{M}]q - \frac{1}{4}G^a_{\mu\nu}G^{a,\mu\nu} - \theta\frac{g_s^2}{64\pi^2}\epsilon^{\mu\nu\sigma\rho}G^a_{\mu\nu}G^a_{\rho\sigma}\,, \tag{2.63}$$

where ϕ is just an arbitrary complex phase of the quark mass matrix. The QCD θ-term can be removed by a $U(1)_A$ transformation with $\alpha_A = -\theta/4$ at the price of modifying the complex phase of the quark-mass matrix [42, 63]:

$$U(1)_A: \quad \exp(i\phi)\mathcal{M} \mapsto \exp(i\bar{\theta})\mathcal{M}\,, \tag{2.64}$$

where $\bar{\theta} = 2\phi - \theta$. Assuming $\bar{\theta} \ll 1$, the quark mass term in the QCD Lagrangian after the $U(1)_A$ transformation with $\alpha_A = \theta/4$ can be decomposed into [42]

$$\begin{aligned}\mathcal{L}_{\text{QCD}} &= -\bar{m}\,\bar{q}q + (\phi + 2\alpha_A)\bar{m}\,i\bar{q}\gamma_5 q - \epsilon\bar{m}\,\bar{q}\tau_3 q + (\phi + 2\alpha_A)\epsilon\bar{m}i\bar{q}\gamma_5\tau_3 q + \cdots \\ &= -\bar{m}\,\bar{q}q + \frac{\bar{\theta}}{2}\bar{m}\,i\bar{q}\gamma_5 q - \epsilon\bar{m}\,\bar{q}\tau_3 q + \frac{\bar{\theta}}{2}\epsilon\bar{m}\,i\bar{q}\gamma_5\tau_3 q + \cdots\,,\end{aligned} \tag{2.65}$$

with

$$\bar{m} := \frac{m_u + m_d}{2}\,, \quad \epsilon := \frac{m_u - m_d}{m_u + m_d}\,. \tag{2.66}$$

The quark mass matrix of in eq. (2.65) serves as the starting point of the investigation of the hadronic operators induced by the θ-term in chapter 4.

2.3 Summary

The classical action of QCD is invariant under local $SU(2)_L \times SU(2)_R \times U(1)_V \times U_A(1)$ transformation. The fermion measure of the generating functional of QCD which is not invariant under local $U(1)_A$ transformations gives rise to an anomalous term consisting of gluon fields. Although this anomalous term can be expressed as a divergence of another term, it can not be removed by an application of Gauss' theorem due to topologically non-trivial solutions for the gluon fields. These topologically non-trivial gluon field configurations give rise to a P- and T-violating term in the QCD Lagrangian parametrized by a dimensionless constant θ, which is referred to as the QCD θ-term. The anomalous term generated by the fermion measure of the generating functional of QCD under $U(1)_A$ transformations is identical to the QCD θ-term up to a real constant and can be regarded to define the transformation law of the QCD θ-term under $U(1)_A$ transformations.

The QCD θ-term can be removed from the QCD Lagrangian by an $U(1)_A$ rotation at the price of generating a complex phase of the quark mass matrix. The QCD θ-term expressed as a complex phase of the quark mass matrix is given by

$$\mathcal{L}_{\rm QCD} = \cdots + \frac{\bar{\theta}}{2}\frac{(m_u + m_d)}{2}\, i\bar{q}\gamma_5 q + \frac{\bar{\theta}}{2}\frac{(m_u - m_d)}{2}\, i\bar{q}\gamma_5\tau_3 q + \cdots\,, \tag{2.67}$$

where $\bar{\theta} = 2\phi - \theta$ with a general initial complex phase ϕ of the quark mass matrix. The QCD θ-term can be removed completely if one of the quark masses vanishes: the quark mass matrix is then equivalent to a real matrix by an axial $SU(2)_L \times SU(2)_R$ rotation as demonstrated in section 4.3 (see eq. (4.148)).

Chapter 3

Sources of P and T violation

Extensions of the SM manifest themselves as effective operators to the energy scale $\Lambda_{\text{had}} \sim 1$ GeV. The aim of this chapter is to present the complete set of leading non-leptonic P- and T-violating operators at the hadronic energy scale Λ_{had}. The content of this chapter is a brief summary of the results published in refs. [35–38], which have been utilized and extended in the recent publications [39, 40]. It is intended to serve as the starting point of our analysis of the EDMs of light nuclei which are induced by BSM physics.

The SM is an $SU(3)_C \times SU(2)_L \times U(1)_Y$ (C: color, L: left, Y: weak hypercharge) gauge theory and its Lagrangian for three generations before the spontaneous symmetry breakdown $SU(2)_L \times U(1)_Y \to U(1)_{em}$ is given by (see *e.g.* [39, 64][1])

$$\begin{aligned}
\mathcal{L}_{\text{SM}} = \; & i\bar{q}_L^\alpha \not{D} q_L^\alpha + i\bar{u}_R^\alpha \not{D} u_R^\alpha + i\bar{d}_R^\alpha \not{D} d_R^\alpha + i\bar{l}_L^\alpha \not{D} l_L^\alpha + i\bar{e}_R^\alpha \not{D} e_R^\alpha \\
& - \bar{l}_L^\alpha f^e e_R^\alpha \phi - \bar{q}_L^\alpha f^u u_R^\alpha \tilde{\phi} - \bar{q}_L^\alpha f^d d_R^\alpha \phi + h.c. \\
& + (D_\mu \phi)^\dagger (D^\mu \phi) + \mu^2 \phi^\dagger \phi - \frac{\lambda}{2} (\phi^\dagger \phi)^2 \\
& - \frac{1}{4} G_{\mu\nu}^a G^{a,\mu\nu} - \frac{1}{4} W_{\mu\nu}^i W^{i,\mu\nu} - \frac{1}{4} B_{\mu\nu} B^{\mu\nu} \\
& - \theta \frac{g_s^2}{64\pi^2} \epsilon^{\mu\nu\rho\sigma} G_{\mu\nu}^a G_{\rho\sigma}^a \, .
\end{aligned} \tag{3.1}$$

The quantities q_L and l_L in eq. (3.1) denote the $SU(2)_L$ doublets of left-handed quarks and leptons for all three generations with implied summation over the generation index α:

$$q_L^\alpha := \left(\begin{pmatrix} u \\ d \end{pmatrix}_L , \begin{pmatrix} c \\ s \end{pmatrix}_L , \begin{pmatrix} t \\ b \end{pmatrix}_L \right) , \quad l_L^\alpha = \left(\begin{pmatrix} \nu_e \\ e \end{pmatrix}_L , \begin{pmatrix} \nu_\mu \\ \mu \end{pmatrix}_L , \begin{pmatrix} \nu_\tau \\ \tau \end{pmatrix}_L \right) . \tag{3.2}$$

The right-handed quark and lepton singlets in eq. (3.1) are also understood to be vectors in generation space:

$$u_R^\alpha = (u_R, c_R, t_R) \, , \quad d_R^\alpha = (d_R, s_R, b_R)_R \, , \quad e_R^\alpha = (e_R, \mu_R, \tau_R) \, . \tag{3.3}$$

[1]The notation and conventions of [64] are adopted in this chapter. The brief explanation of the SM Lagrangian follows [64].

The complex scalar $SU(2)_L$ doublet field ϕ in eq. (3.1) is defined in polar coordinates $\vec{\alpha}$ by

$$\phi(x) = \begin{pmatrix} \phi^+ \\ \phi^0 \end{pmatrix} = \frac{U^{-1}(\vec{\alpha})}{\sqrt{2}} \begin{pmatrix} 0 \\ v + h(x) \end{pmatrix}, \quad U(\vec{\alpha}) = \exp\left(\frac{i}{v}\vec{\alpha}(x) \cdot \tau\right). \tag{3.4}$$

The complex scalar $SU(2)_L$ doublet field $\tilde{\phi}$ is defined by $\tilde{\phi} = i\tau_2\phi^*$. The terms proportional to μ^2 and to λ in the third line of eq. (3.1) constitute the potential of the scalar ϕ. For $\mu^2 > 0$, the scalar $SU(2)_L$ doublet develops a vacuum expectation value (VEV):

$$\langle 0|\phi|0\rangle = \frac{v}{\sqrt{2}} \begin{pmatrix} 0 \\ 1 \end{pmatrix}, \quad \langle 0|\alpha_i|0\rangle = \langle 0|h|0\rangle = 0\,. \tag{3.5}$$

By the gauge transformation $U(\vec{\alpha})$ as defined in eq. (3.4), the field ϕ can be re-expressed (in the unitary gauge) as

$$\phi(x) \to \phi'(x) = U(\vec{\alpha}(x))\phi(x) = \frac{v}{\sqrt{2}} \begin{pmatrix} 0 \\ 1 + h(x)/v \end{pmatrix}. \tag{3.6}$$

The Higgs boson field h is an excitation of the ground state. All primes denoting fields in the unitary gauge are subsequently omitted for convenience.

The covariant derivative of a general matter field ψ with hypercharge Y is given by:

$$D_\mu\psi(x) = \left(\partial_\mu - \frac{i}{2}g_s A^a_\mu \lambda^a - \frac{i}{2}g\tau_i W^i_\mu - \frac{i}{2}Yg' B_\mu\right)\psi(x)\,, \tag{3.7}$$

where W^i_μ and B_μ are the $SU(2)_L \times U(1)_Y$ gauge bosons, respectively, and A^a_μ are the $SU(3)_C$ gauge fields (gluons) with Gell-Mann matrices λ^a. g_s is the $SU(3)_C$ coupling constant and g and g' are the $SU(2)_L$ and $U(1)_Y$ coupling constants, respectively. The term involving gluons is absent from the covariant derivative for leptonic fields and the scalar doublet field ϕ. The hypercharges Y of the particles in eq. (3.1) are given by:

$$\begin{aligned} &Y(q_L) = \frac{1}{3}, Y(u_R) = \frac{4}{3}, \;\; Y(d_R) = -\frac{2}{3}, Y(l_L) = -1, Y(e_R) = -2, \\ &Y(\phi) = 1, \quad Y(\tilde{\phi}) = -1\,. \end{aligned} \tag{3.8}$$

The matrices in generation space f^e, f^u and f^d in the second line of eq (3.1) are the Yukawa couplings between fermions and the scalar doublet field ϕ.

The $SU(2)_L$ and $U(1)_Y$ field-strength tensors in eq (3.1) are given by

$$W^i_{\mu\nu} = \partial_\mu W^i_\nu - \partial_\nu W^i_\mu + g\epsilon^{ijk} W^j_\mu W^k_\nu\,, \tag{3.9}$$

$$B_{\mu\nu} = \partial_\mu B_\nu - \partial_\nu B_\mu\,. \tag{3.10}$$

The physical states of the $SU_L(2)$ and $U_Y(1)$ gauge fields are the $W^\pm$ bosons,

$$W^\pm_\mu = \frac{1}{\sqrt{2}}(W^1_\mu \mp iW^2_\mu)\,, \tag{3.11}$$

the Z boson and the photon field A_μ,

$$\begin{aligned} Z_\mu &= \cos(\theta_\omega)W^3_\mu - \sin(\theta_\omega)B_\mu\,, && (3.12)\\ A_\mu &= \sin(\theta_\omega)W^3_\mu + \cos(\theta_\omega)B_\mu\,, && (3.13)\\ & && (3.14) \end{aligned}$$

where θ_ω is the Weinberg-angle. The coupling constants g and g' obey

$$\frac{g'}{g} = \tan(\theta_\omega)\,. \tag{3.15}$$

Eigenstates of the fermion mass matrices are in general linear combinations of gauge eigenstates, which implies the existence of couplings of fermions from different generations. The quark mass matrix can be diagonalized by a biunitary transformation. For three generations, the resulting diagonal 3×3 matrix has one overall complex phase. The left-handed $SU(2)_L$ quark doublet has therefore to be redefined by

$$q^\alpha_L \to \left(\begin{pmatrix} u \\ d' \end{pmatrix}_L, \begin{pmatrix} c \\ s' \end{pmatrix}_L, \begin{pmatrix} t \\ b' \end{pmatrix}_L\right)\,, \quad \begin{pmatrix} d' \\ s' \\ b' \end{pmatrix} = V \begin{pmatrix} d \\ s \\ b \end{pmatrix}\,, \tag{3.16}$$

where V is the Cabibbo-Kobayashi-Maskawa (CKM) matrix.

3.1 P and T violation in the Standard Model

There are two different sources of P and T violation within the SM. The CKM matrix (for three generations) has one P- and T-violating complex phase. As pointed out in [5], any diagram in the SM inducing a P- and T-violating quark-photon coupling has to involve four electroweak vertices and is thus at least a two-loop diagram. Furthermore, the authors of [65] demonstrated that all diagrams potentially contributing to quark EDMs with two loops vanish and the leading non-vanishing contributions emerge only at the three loop level [66, 67]. Due to this significant suppression, the computation of the d-quark EDM, for instance, yielded a numerical estimate of [5, 66] $d_d \approx 10^{-34}\,e$ cm. The only other source of P and T violation within the SM is the above mentioned QCD θ-term which is parametrized by the physical parameter $\bar\theta$. Depending on the size of $\bar\theta$, the θ-term is capable of inducing significantly larger EDMs than the complex phase of the CKM matrix. The current bound on the parameter $\bar\theta$ is $|\bar\theta| \lesssim 10^{-10}$ [45, 48, 51], which has been inferred from the current upper bound on the neutron EDM [14].

3.2 P and T violation from BSM physics

Extensions of the SM involve heavy particles with masses of the order of the energy scale $\Lambda_{\rm BSM} > \Lambda_{\rm SM} \sim 250$ GeV (which is significantly larger than the electroweak symmetry-breaking scale). Since the SM successfully describes physical phenomena up to the energy scale $\Lambda_{\rm SM}$, any BSM theory should obey the following principles [5, 35–37]: it must exhibit at least an $SU(3)_C \times SU(2)_L \times U(1)_Y$ gauge symmetry, it has to contain the degrees of freedom of the SM (either as fundamental fields or composite fields) and it has to reduce to the SM at energies well below $\Lambda_{\rm SM}$ if no still undiscovered light, weakly coupled fields exist. Therefore, the SM itself can be regarded as an effective field theory for all possible extensions of the SM. At the energy scale $\Lambda_{\rm SM}$, all heavy degrees of freedom from extension of the SM have to be systematically integrated out in the generating functional, which leads to an amendment of the standard SM Lagrangian by an infinite set of terms. These effective terms are of canonical dimension larger than four, are not renormalizable and admit an ordering by their dimension:

$$\mathcal{L}_{\rm eff}^{\rm BSM} = \mathcal{L}_{\rm SM} + \frac{1}{\Lambda_{\rm BSM}}\mathcal{L}_5 + \frac{1}{\Lambda_{\rm BSM}^2}\mathcal{L}_6 + \frac{1}{\Lambda_{\rm BSM}^3}\mathcal{L}_7 + \cdots . \tag{3.17}$$

The effective Lagrangian is therefore an expansion in powers of $\Lambda_{\rm SM}/\Lambda_{\rm BSM}$. The higher the dimension of an effective term, the larger is its suppression by powers of $\Lambda_{\rm SM}/\Lambda_{\rm BSM}$.

The analysis in the remaining paragraphs of this section focuses on the leading effective terms of dimension five and six since contributions from higher-order effective terms to the EDMs of light nuclei can be assumed to be numerically irrelevant. In this sense, the most general effective Lagrangian accounting for all possible extensions of the SM is obtained by identifying the complete set of independent operators of dimension five and six. Only the subset of non-leptonic P- and T-violating effective operators is of relevance for the investigation of EDMs of light nuclei. Since the ultimate goal is to compile the list of P- and T-violating effective operators at the energy scale $\Lambda_{\rm had} \sim 1$ GeV, the derivation proceeds in two substeps: after identifying the effective operators at the energy scale $\Lambda_{\rm SM}$, the heavy SM degrees of freedom ($W^\pm$, Z, Higgs and heavy quarks) are systematically integrated out.

The list of independent dimension five and six operators at $\Lambda_{\rm SM}$ is presented in [35–39]. The P- and T-violating operators relevant for our analysis either involve dual field strength tensors or emerge as complex phases of P- and T-conserving operators. Since effective leptonic operators yield only irrelevant subleading contributions to the EDMs of light nuclei, only the non-leptonic effective operators in this list are retained. The leading effective operators then prove to be of dimension six. With the subscript q denoting a quark field, A a $SU(3)_C \times SU(2)_L \times U(1)_Y$ gauge boson field and ϕ the Higgs field, the list of independent effective dimension-six operators relevant for EDMs of light nuclei reads [37, 39]

$$\begin{aligned}\mathcal{L}^{(6)}_{qqA\phi} = {} & \delta^u_G\, i\bar{q}_L\sigma^{\mu\nu}\lambda_a\tilde{\phi}u_R G^a_{\mu\nu} + \delta^u_W\, i\bar{q}_L\sigma^{\mu\nu}\tau_i\tilde{\phi}u_R W^i_{\mu\nu} + \delta^u_B\, i\bar{q}_L\sigma^{\mu\nu}\tilde{\phi}u_R B_{\mu\nu} + h.c. \\ & + \delta^d_G\, i\bar{q}_L\sigma^{\mu\nu}\lambda_a\phi d_R G^a_{\mu\nu} + \delta^d_W\, i\bar{q}_L\sigma^{\mu\nu}\tau_i\phi d_R W^i_{\mu\nu} + \delta^d_B\, i\bar{q}_L\sigma^{\mu\nu}\phi d_R B_{\mu\nu} + h.c.\,,\end{aligned} \tag{3.18}$$

$$\mathcal{L}^{(6)}_{AAA} = \beta_G\, f^{abc}\epsilon^{\mu\nu\alpha\beta}G^a_{\alpha\beta}G^b_{\mu\rho}G^{c,\rho}_{\nu} + \beta_W\,\epsilon^{ijk}\epsilon^{\mu\nu\alpha\beta}W^i_{\alpha\beta}W^j_{\mu\rho}W^{k,\rho}_{\nu}\,, \tag{3.19}$$

$$\begin{aligned}\mathcal{L}^{(6)}_{AA\phi\phi} = {} & \alpha_G\,\phi^\dagger\phi\epsilon^{\mu\nu\alpha\beta}G^a_{\alpha\beta}G^a_{\mu\nu} + \alpha_W\,\phi^\dagger\phi\epsilon^{\mu\nu\alpha\beta}W^i_{\alpha\beta}W^i_{\mu\nu} + \alpha_B\,\phi^\dagger\phi\epsilon^{\mu\nu\alpha\beta}B_{\alpha\beta}B_{\mu\nu} \\ & + \alpha_{WA}\phi^\dagger\tau_i\phi\epsilon^{\mu\nu\alpha\beta}W^i_{\alpha\beta}B_{\mu\nu}\,,\end{aligned} \tag{3.20}$$

$$\mathcal{L}^{(6)}_{qq\phi\phi\phi} = \gamma^u\, i(\phi^\dagger\phi)\bar{q}_L\tilde{\phi}u_R + \gamma^d\, i(\phi^\dagger\phi)\bar{q}_L\tilde{\phi}d_R + h.c.\,, \tag{3.21}$$

$$\mathcal{L}^{(6)}_{qqqq} = \mu_1\, i\epsilon^{ij}(\bar{q}^i_L u_R)(\bar{q}^j_L d_R) + \mu_8\, i\epsilon^{ij}(\bar{q}^i_L\lambda^a u_R)(\bar{q}^j_L\lambda^a d_R)\,, \tag{3.22}$$

$$\mathcal{L}^{(6)}_{qq\phi\phi} = \nu_1\, i(\tilde{\phi}^\dagger iD_\mu\phi)\bar{u}_R\gamma^\mu d_R + h.c.\,, \tag{3.23}$$

where $\delta^{u,d}_{G,W,B}$, α_G, α_W, α_B, α_{WB}, $\beta_{G,W}$, $\gamma^{u,d}$, $\mu_{1,8}$ and ν_1 are the effective coupling constants $\sim 1/\Lambda^2_{\rm BSM}$. Below the electroweak symmetry-breaking scale (of the breakdown $SU(2)_L\times U(1)_Y\to U(1)_{em}$), $\mathcal{L}^{(6)}_{qqA\phi}$ in eq. (3.18) becomes

$$\begin{aligned}\mathcal{L}^{(6)}_{qqA\phi} = \Big(& i\tilde{\delta}^0_G\,\bar{q}\sigma^{\mu\nu}\gamma_5\lambda_a q\, G^a_{\mu\nu} + i\tilde{\delta}^3_G\,\bar{q}\sigma^{\mu\nu}\gamma_5\lambda_a\tau_3 q\, G^a_{\mu\nu} \\ & + i\tilde{\delta}^0_F\,\bar{q}\sigma^{\mu\nu}\gamma_5 q\, F_{\mu\nu} + i\tilde{\delta}^3_F\,\bar{q}\sigma^{\mu\nu}\gamma_5\tau_3 q\, F_{\mu\nu} \\ & + i\tilde{\delta}^0_Z\,\bar{q}\sigma^{\mu\nu}\gamma_5 q\, Z_{\mu\nu} + i\tilde{\delta}^3_Z\,\bar{q}\sigma^{\mu\nu}\gamma_5\tau_3 q\, Z_{\mu\nu} \\ & + i\tilde{\delta}^0_W\,\bar{q}i\sigma^{\mu\nu}\gamma_5 q\, W^+_\mu W^-_\nu + i\tilde{\delta}^3_W\,\bar{q}i\sigma^{\mu\nu}\gamma_5\tau_3 q\, W^+_\mu W^-_\nu + h.c. \\ & + i\tilde{\delta}^u_W\,\bar{d}_L\sigma^{\mu\nu}u_R\, W^-_{\mu\nu} + i\tilde{\delta}^d_W\,\bar{u}_L\sigma^{\mu\nu}d_R\, W^+_{\mu\nu} + h.c.\Big)\big(1+h/v\big)\,,\end{aligned} \tag{3.24}$$

where $q=(u,d)$ is the (isospin) doublet of up and down quarks. The most important operators in $\mathcal{L}^{(6)}_{qqA\phi}$ are the quark-chromo electric dipole moment ($qCEDM$) and the quark electric dipole moment ($qEDM$):

$$qCEDM\ :\quad i\bar{q}(\,\tilde{\delta}^0_G\,\mathbb{1} + \tilde{\delta}^3_G\,\tau_3)\sigma^{\mu\nu}\gamma_5\lambda^a q\, G^a_{\mu\nu}\,, \tag{3.25}$$

$$qEDM\ :\quad i\bar{q}(\,\tilde{\delta}^0_F\,\mathbb{1} + \tilde{\delta}^3_F\,\tau_3)\sigma^{\mu\nu}\gamma_5 q\, F_{\mu\nu}\,, \tag{3.26}$$

with $\tilde{\delta}^{0,3}_{G,F} = v(\,\delta^u_{G,F}\pm\delta^d_{G,F})/\sqrt{2}$. These operators count naively as dimension five, but are in fact dimension-six operators due to the original couplings to the Higgs field. The $qCEDM$ and $qEDM$ are chirality-changing quark operators as the quark-Higgs Yukawa couplings in eq. (3.1) and hence as the quark mass terms. The coupling constants of the remaining dimension-six operators in eq. (3.24), $\tilde{\delta}^{0,3}_{Z,W}$ and $\tilde{\delta}^{u,d}_W$, are linear combinations of the coupling constants $\delta^{u,d}_{W,B}$ in eq. (3.18). The effective operators in the third, fourth and fifth line of eq. (3.24) are referred to as weak dipole moments, which either contribute to the $qEDM$ and $qCEDM$ via loop diagrams or give rise to four-quark operators with one derivative of dimension seven [39]. This profound suppression renders the weak dipole moments irrelevant for our analysis.

The first and the second term in eq. (3.19) are known as the gluon-chromo electric dipole moment ($gCEDM$) and the electric dipole moment of the W boson. The electric dipole moment of the W boson yields interactions of at least two heavy gauge bosons below the electroweak symmetry-breaking scale and gives only numerically insignificant contributions to the $qEDM$ and $qCEDM$ [39].

Below the electroweak symmetry breaking scale, eq. (3.20) generates numerous effective operators involving gauge bosons:

$$\begin{aligned}\mathcal{L}^{(6)}_{AA\phi\phi} =\Big(&\alpha_G g_s^2 \epsilon^{\mu\nu\alpha\beta} G^a_{\alpha\beta} G^a_{\mu\nu} + \alpha_W g^2 \epsilon^{\mu\nu\alpha\beta} W^i_{\alpha\beta} W^i_{\mu\nu} + \alpha_B g'^2 \epsilon^{\mu\nu\alpha\beta} B_{\alpha\beta} B_{\mu\nu} \\ &+ \alpha_{WB} g g' \epsilon^{\mu\nu\alpha\beta} W^3_{\mu\nu} B_{\alpha\beta} \Big) \frac{v^2}{2} (1 + h/v)^2 \,, \end{aligned} \tag{3.27}$$

The first term on the right-hand side of eq. (3.27) without Higgs fields constitutes a correction to the QCD θ-term eq. (2.61). The second term on the right-hand side of eq. (3.27) without Higgs fields is a correction to the $SU(2)_L$ θ-term which is not displayed in eq. (3.1). The $SU(2)_L$ θ-term can be derived in the same manner as the QCD θ-term, but is not discussed in this thesis. It is suppressed since the weak couplings g is small at low energies in contrast to the strong coupling g_s. The integral over space-time of the third term on the right-hand side of eq. (3.27) vanishes. The fourth term on the right-hand side of eq. (3.27) without Higgs fields contributes to the weak dipole moments and the magnetic quadrupole moments of the $W^\pm$ bosons [39, 68]. By integrating out the Higgs fields from those terms in eq. (3.27) with a least one Higgs field, suppressed loop contributions to the $qEDM$, the $qCEDM$ and the weak dipole moments are obtained [39].

Those terms in eq. (3.21) which do not include any Higgs fields yield minor corrections to the Yukawa couplings in eq. (3.1). i.e. they constitute a small shift of the CKM matrix. Those terms with at least one Higgs field give suppressed loop corrections to the $qEDM$, $qCEDM$ and $gCEDM$ (see [39]).

The terms in eq. (3.22) are chiral symmetry conserving P- and T-violating four-quark operators (quark quardrilinears) which are referred to as $4q$-operators below. Eq. (3.22) can be rewritten into:

$$\begin{aligned}\mathcal{L}^{(6)}_{qqqq} &= i\mu_1(\bar{u}u\bar{d}\gamma_5 d + \bar{u}\gamma_5 u\bar{d}d - \bar{d}\gamma_5 u\bar{u}d - \bar{d}u\bar{u}\gamma_5 d) \\ &\quad + i\mu_8(\bar{u}\lambda^a u\bar{d}\gamma_5\lambda^a d + \bar{u}\gamma_5\lambda^a u\bar{d}\lambda^a d - \bar{d}\gamma_5\lambda^a u\bar{u}\lambda^a d - \bar{d}\lambda^a u\bar{u}\gamma_5\lambda^a d)\,. \end{aligned} \tag{3.28}$$

Due to the covariant derivative in eq. (3.23), the only terms without Higgs fields below the electroweak symmetry-breaking scale are flavor-changing couplings to $W^\pm$ bosons [38, 39]:

$$\begin{aligned}\mathcal{L}^{(6)}_{\phi\phi qq} &= i\nu_1(\tilde{\phi}^\dagger iD_\mu\phi)\,\bar{u}_R\gamma^\mu d_R + i\nu_1(\tilde{\phi}^\dagger iD_\mu\phi)\,\bar{d}_R\gamma^\mu u_R \\ &= i\nu_1\frac{gv^2}{2\sqrt{2}}(\bar{u}_R\gamma^\mu d_R W^+_\mu + \bar{d}_R\gamma^\mu u_R W^-_\mu) + \cdots\,. \end{aligned} \tag{3.29}$$

In order to obtain the effective operators at the energy scale Λ_{had}, the $W^{\pm}$ bosons have to be integrated out. These P- and T-violating vertices combine with their P- and T-conserving counterparts to P- and T-violating effective four-quark terms at the energy scale Λ_{had} [38, 39],

$$\begin{aligned} & i\nu_1 \frac{g^2 v^2 V_{ud}}{M_W^2} (\bar{u}_R \gamma_\mu d_R \bar{d}_L \gamma^\mu u_L - \bar{d}_R \gamma_\mu u_R \bar{u}_L \gamma^\mu d_L) \\ = \; & i\nu_1 V_{ud} (\bar{u}_R \gamma_\mu d_R \bar{d}_L \gamma^\mu u_L - \bar{d}_R \gamma_\mu u_R \bar{u}_L \gamma^\mu d_L)\,, \end{aligned} \tag{3.30}$$

where $M_W = gv$ has been used and V_{ud} is an element of the CKM-matrix. Although it breaks chiral symmetry, this four-quark term does not exhibit an explicit dependence on quark masses and is therefore unsuppressed. This operator will be referred to as the $4qLR$-operator below.

The evolution of operators from the energy scale Λ_{SM} to Λ_{had} is in general accompanied by a mixing of different effective operators, since the effective dimension-six sources are composite operators whose renormalization can require counter terms which are proportional to other composite operators. The recent publication [40] is dedicated to this issue. In particular, the evolution of operators gives rise to another $4qLR$-op operator with a more complicated color structure and a coupling constant ν_8 which is not independent from ν_1:

$$i\nu_8 V_{ud} (\bar{u}_R \gamma_\mu \lambda^a d_R \bar{d}_L \gamma^\mu \lambda^a u_L - \bar{d}_R \gamma_\mu \lambda^a u_R \bar{u}_L \gamma^\mu \lambda^a d_L)\,. \tag{3.31}$$

.

3.3 Summary

Extensions of the SM manifest themselves as non-renormalizable effective operators of canonical dimension larger than five at the energy scale $\Lambda_{\text{had}} \gtrsim 1$ GeV. The effective P- and T-violating operators which are relevant for our analysis of EDMs of light nuclei are the dimension-six operators

$$qEDM \;:\; i\bar{q}\,(\tilde{\delta}_F^1 \mathbb{1} + \tilde{\delta}_F^3 \tau_3)\,\sigma^{\mu\nu}\gamma_5 q\, F_{\mu\nu}\,, \tag{3.32}$$

$$qCEDM \;:\; i\bar{q}\,(\tilde{\delta}_G^1 \mathbb{1} + \tilde{\delta}_G^3 \tau_3)\,\sigma^{\mu\nu}\gamma_5 \lambda_a q\, G^a_{\mu\nu}\,, \tag{3.33}$$

$$4qLR\text{-op} \;:\; i\nu_1 V_{ud}\,(\bar{u}_R \gamma_\mu d_R \bar{d}_L \gamma^\mu u_L - \bar{d}_R \gamma_\mu u_R \bar{u}_L \gamma^\mu d_L)\,, \tag{3.34}$$

$$i\nu_8 V_{ud}\,(\bar{u}_R \gamma_\mu \lambda^a d_R \bar{d}_L \gamma^\mu \lambda^a u_L - \bar{d}_R \gamma_\mu \lambda^a u_R \bar{u}_L \gamma^\mu \lambda^a d_L)\,, \tag{3.35}$$

$$4q\text{-op} \;:\; i\mu_1\,(\bar{u}u\bar{d}\gamma_5 d + \bar{u}\gamma_5 u\bar{d}d - \bar{d}\gamma_5 u\bar{u}d - \bar{d}u\bar{u}\gamma_5 d)\,, \tag{3.36}$$

$$i\mu_8\,(\bar{u}\lambda^a u\bar{d}\gamma_5\lambda^a d + \bar{u}\gamma_5\lambda^a u\bar{d}\lambda^a d - \bar{d}\gamma_5\lambda^a u\bar{u}\lambda^a d - \bar{d}\lambda^a u\bar{u}\gamma_5\lambda^a d)\,, \tag{3.37}$$

$$gCEDM \;:\; \beta_G\, f^{abc}\epsilon^{\mu\nu\alpha\beta}\, G^a_{\alpha\beta} G^b_{\mu\rho} G^{c,\rho}_{\nu}\,, \tag{3.38}$$

which are graphically depicted in fig. 1.1. This set of leading P- and T-violating dimension-six operators together with the QCD θ-term serve as the starting point of our analysis in this thesis. The effective dimension-six sources constitute an amendment of the standard QCD Lagrangian. The QCD Lagrangian amended by these dimension-six sources will be referred to as *amended QCD Lagrangian* below.

The $4qLR$ operators eq. (3.34) and eq. (3.35) transform identically under chiral $SU(2)_L \times SU(2)_R$ rotations and it is impossible to disentangle them within the framework of ChPT. Instead of repeating the same analysis for the operator eq. (3.35), only the operator eq. (3.34) is considered below. The $4q$ operators eq. (3.36) and eq. (3.37) also exhibit the same transformation properties under chiral transformations and are treated in the same manner, i.e. only the operator in eq. (3.36) is discussed below. Finally, it is impossible to separate the $gCEDM$ from the $4q$-op by chiral symmetry considerations, which leaves us with six independent BSM classes of P- and T-violating operators.

Chapter 4

P and T violation in ChPT

4.1 Chiral perturbation theory

The spectrum of strongly interacting particles at low energies exhibits a significant mass gap. The masses of the mesons of the pseudoscalar octet are much lighter than all other hadrons. This is particularly true for the triplet of pions (with masses $M_{\pi^\pm} = 138.57\,\mathrm{MeV}$, $M_{\pi^0} = 134.98\,\mathrm{MeV}$ [34]), whose masses are well below the masses of the vector-meson resonances and also well below the masses of the lightest mesons with strangeness content, i.e. the Kaons ($M_{K^0} = 497.61\,\mathrm{MeV}$ [34]) and the η ($M_\eta = 547.83\,\mathrm{MeV}$ [34]). If the $SU(2)_L \times SU(2)_R$ symmetry of massless QCD translated into a symmetry of the ground state or the particle spectrum, parity doubling would be observable and another triplet of bosons with even parity would exist, since axial rotations couple odd and even parity states. The absence of such degeneracy implies that the ground state is not invariant under axial rotations and $Q_A^k|0\rangle \neq 0$, where Q_A^k is the charge associated with an axial $SU(2)_L \times SU(2)_R$ transformation. The $SU(2)_L \times SU(2)_R$ symmetry is spontaneously broken down to an $SU(2)_V$ symmetry. According to Goldstone's theorem [69, 70], each broken charge Q_A^k implies the existence of a massless state with zero spin known as Goldstone boson. In our case, the three Goldstone bosons are identified with the triplet of states with the lowest masses, the pions π_i. The Goldstone bosons possess the same transformation properties as the broken charges Q_A^k, i.e. they are parity odd (pseudoscalars) and transform under $SU(2)_V$ rotations as a triplet:

$$[Q_V^k, \pi^l(x)] = i\epsilon^{klm}\pi^m \,. \tag{4.1}$$

In particular, the Goldstone bosons couple to the vacuum through the Noether currents $J_A^{i,\mu} = \bar{q}\gamma^\mu\gamma_5\tau^i q/2$,

$$\langle 0|J_A^{k,\mu}(0)|\pi^l(p)\rangle = i\delta^{kl}p^\mu F \,, \tag{4.2}$$

where $F \neq 0$ is the pion decay constant in the chiral limit. The current physical value $F_\pi = F(1 + \mathcal{O}(m_u + m_d))$ is 92.2 MeV [34]. Eq. (4.2) proves to be a sufficient and necessary condition for the spontaneous symmetry breakdown $SU(2)_L \times SU(2)_R \to SU(2)_V$.

An effective field theory with the lightest mesons as dynamical degrees of freedom is only defined for momenta below a certain scale, which is naturally defined by the lowest masses of the resonances outside the meson octet. The chiral symmetry breaking scale Λ_χ can also be identified as the one-loop scale

$$\Lambda_\chi \approx 4\pi F_\pi \approx 1.2\,\mathrm{GeV}\,. \tag{4.3}$$

4.1.1 The effective Lagrangian in the pion sector

The transformation properties of the Goldstone bosons are completely determined by the geometry of the groups $SU(2)_L \times SU(2)_R$ and $SU(2)_V$ [60, 71]: let G be a simple Lie group, $H \subset G$ a subgroup and $F : G \times \mathcal{B} \to \mathcal{B}$ be the action of the group G on the space of Goldstone boson fields $\mathcal{B}$ which obeys

$$F_{g_2}(F_{g_1}(\pi)) = F_{g_2 \cdot g_1}(\pi)\,. \tag{4.4}$$

Let the ground state $v_0 \in \mathcal{B}$ be invariant under the subgroup H:

$$F\colon H \subset G \times \mathcal{B} \to \mathcal{B},\ F_h(v_0) = v_0 \quad \forall h \in H\,. \tag{4.5}$$

Every pion field π can be obtained by a suitable $g \in G$ such that $F_g(v_0) = \pi$, which implies $g \in G - H$. Furthermore, $F_{g_1}(v_0) = F_{g_2}(v_0)$ if and only if $g_1 = g_2 \cdot h$ for all $g_1, g_2 \in G$ and suitable $h \in H$. This demonstrates that F factors through the left cosets G/H:

$$F : G \times \mathcal{B} \to G/H \times \mathcal{B} \to \mathcal{B}\,, \tag{4.6}$$

and there is a one-to-one correspondence between Goldstone boson fields π and the left cosets G/H. The most convenient parametrization of the left costs $G/H = SU(2)_L \times SU(2)_R / SU(2)_V$ is by normal coordinates:

$$\mathcal{B} \to G/H, \quad \pi_i(x) \mapsto U(x) := \exp\left(\frac{i}{F_\pi}\sum_i \tau_i \pi_i(x)\right)\,. \tag{4.7}$$

$SU(2)_V$ is the diagonal subgroup of $SU(2)_L \times SU(2)_R$:

$$SU(2)_V = \{(g_1, g_2) \in SU(2)_L \times SU(2)_R |\, g_1 = g_2\}\,. \tag{4.8}$$

A general element of G/H is then given by

$$(g_1, g_2)\cdot H = (g_1 \cdot g_2^{-1} \cdot g_2, g_2)\cdot H = (g_1 \cdot g_2^{-1}, e)\cdot(g_2, g_2)\cdot H = (g_1 \cdot g_2^{-1}, e)\cdot H\,, \tag{4.9}$$

and is transformed under G by

$$(g_1, g_2)\cdot H \mapsto (R \cdot g_1, L \cdot g_2)\cdot H = (R \cdot g_1 \cdot g_2^{-1} \cdot L^\dagger, e)\cdot H\,, \tag{4.10}$$

i.e.

$$U(x) \to R(x)U(x)L^\dagger(x)\,. \tag{4.11}$$

Note that although the matrix $U(x)$ transforms linearly, the pion fields $\pi_i(x)$ do not transform linearly.

A major accomplishment at the early stages of chiral perturbation theory was the proof that an effective field theory whose Lagrangian exhibits the same symmetries as the Lagrangian of the underlying theory yields transition amplitudes and low-energy theorems which are identical to the ones derived by current algebra and PCAC (see *e.g.* [72–75]). Therefore, the low-energy effective Lagrangian can be constructed by writing down all hermitian, Lorentz invariant and $SU(2)_L \times SU(2)_R$ invariant terms composed of the matrix U. As shown by Gasser and Leutwyler [43, 60], the effective field theory is not sufficiently determined by a Lagrangian which exhibits the same *global* symmetries as the one of the underlying theory. The low-energy analysis should rather be based on the Green functions of the underlying theory and the Ward identities they obey.

Ward identities are a consequence of the invariance of the generating functional under particular *local* transformations. The effective Lagrangian has to be constructed to yield exactly the same Ward identities as the underlying theory when inserted into the effective generating functional:

$$W_{\mathrm{QCD}}[s,p,a_\mu,v_\mu] = W_{\mathrm{eff}}[s,p,a_\mu,v_\mu]\,. \tag{4.12}$$

The effective Lagrangian is then to be invariant under *local* $SU(2)_L \times SU(2)_R$ transformations and a hermitian Lorentz scalar [43, 44],

$$\mathcal{L}_{\mathrm{eff}} = \mathcal{L}_{\mathrm{eff}}(U, D_\mu U, D^2 U, \cdots, s, p, a_\mu, v_\mu, \cdots)\,, \tag{4.13}$$

where D_μ is the covariant derivative

$$D_\mu U(x) = \partial_\mu U - i r_\mu(x) U(x) + i U(x) l_\mu(x)\,, \tag{4.14}$$

and the dots denote higher order derivative terms of U and potentially further source fields. The covariant derivative generates the right- and left-handed field strength tensors

$$R_{\mu\nu} := \partial_\mu r_\nu - \partial_\nu r_\mu - i[r_\mu, r_\nu]\,, \quad L_{\mu\nu} := \partial_\mu l_\nu - \partial_\nu l_\mu - i[l_\mu, l_\nu]\,, \tag{4.15}$$

which transform under $SU(2)_L \times SU(2)_R$ by

$$R_{\mu\nu} \mapsto R(x)\, R_{\mu\nu}\, R^\dagger(x)\,, \quad L_{\mu\nu} \mapsto L(x)\, L_{\mu\nu} L^\dagger(x)\,. \tag{4.16}$$

The source fields of the scalar and pseudo-scalar currents in eq. (2.37) can be combined into one object $\chi = 2B(s+ip)$ which transforms under $SU(2)_L \times SU(2)_R$ by

$$\chi = 2B(s+ip) \mapsto R(x) 2B(s+ip) L^\dagger(x)\,, \tag{4.17}$$

where B is a constant to be determined later. The generating functional of the low-energy effective field theory of QCD, called *Chiral Perturbation Theory* (ChPT), is then defined by [43]

$$W_{\text{eff}}[s,p,v^\mu,a^\mu] = \int \mathcal{D}U(x) \exp\left(i\int d^4x\,\mathcal{L}_{\text{eff}}[U,s,p,v^\mu,a^\mu]\right). \tag{4.18}$$

The low-energy effective Lagrangian is a sum of an infinite number of terms which admit an ordering by the number of covariant derivatives and pion masses each term contains:

$$\mathcal{L}_{\text{eff}} = \mathcal{L}_\pi^{(2)} + \mathcal{L}_\pi^{(4)} + \mathcal{L}_\pi^{(6)} + \cdots, \quad \mathcal{L}_\pi^{(2)} = \mathcal{O}(p^2),\, \mathcal{L}_\pi^{(4)} = \mathcal{O}(p^4), \cdots. \tag{4.19}$$

The leading order Lagrangian is given by [43] (with $\langle\cdots\rangle$ denoting the trace):

$$\mathcal{L}_\pi^{(2)} = \frac{F_\pi^2}{4}\langle D_\mu U (D^\mu U)^\dagger\rangle + \frac{F_\pi^2}{4}\langle \chi U^\dagger + U\chi^\dagger\rangle. \tag{4.20}$$

The building block χ is considered to be $\mathcal{O}(p^2)$, which can be inferred from the following observation: Green functions of QCD correspond to perturbative expansions in derivatives of pion fields. The scalar quark condensates are obtained from functional derivatives of the effective generating functional eq. (4.18) (note that s_0 is a matrix here):

$$\begin{aligned}
\langle 0|\bar{u}u|0\rangle &= \frac{1}{W_{\text{eff}}[0,\cdots,0]} i \frac{\delta}{\delta(s_0)_{11}(x)} W_{\text{eff}}[s_0,0,\cdots,0]\bigg|_{s_0=0} \\
&= -\frac{1}{W_{\text{eff}}[0,\cdots,0]}\frac{F_\pi^2 B}{2}\int \mathcal{D}U(x)\,(U^\dagger(x)+U(x))_{11} \exp\left(i\int d^4x\,\mathcal{L}_\pi^{(2)}\right) \\
&= -\frac{F_\pi^2 B}{W_{\text{eff}}[0,\cdots,0]}\int \mathcal{D}U(x)\left(\mathbb{1} - \frac{\pi(x)^2}{2F_\pi^2} + \cdots\right)\exp\left(i\int d^4x\,\mathcal{L}_\pi^{(2)}\right) \\
&= -F_\pi^2 B + \cdots.
\end{aligned} \tag{4.21}$$

The result demonstrates that the constant B is proportional to the scalar quark condensate and (by setting $s_0 = \mathcal{M}$) that the squared pion mass is proportional to the sum of quark masses at leading order:

$$M_\pi^2 = B(m_u + m_d) + \cdots. \tag{4.22}$$

This relation was already known before the advent of ChPT and is known as the Gell-Mann-Oakes-Renner relation [76]. The quark mass matrix $\mathcal{M}$ is therefore considered to be $\mathcal{O}(p^2)$. The vector and axial-vector source fields v^μ and a^μ are regarded as $\mathcal{O}(p)$ since they are contained in the covariant derivative D^μ.

The power counting scheme for diagrams devised by Weinberg [77] is based on a linear rescaling of the external momenta $p_i \to tp_i$ and a simultaneous quadratic rescaling of the Goldstone boson masses $M_\pi^2 \to t^2 M_\pi^2$. When L denotes the number of loops and N_k the number of vertices of $\mathcal{O}(p^k)$ in a particular diagram in the pion sector, the chiral dimension D of the diagram is given by [41, 77]

$$D = 2 + 2L + \sum_k (k-2) N_k \,, \tag{4.23}$$

The chiral dimension increases with the number of loops and insertions of higher order vertices, which demonstrates that the chiral expansion is also an expansion in the number of loops.

By utilizing the equations of motions of $\mathcal{L}_\pi^{(2)}$, the set of independent terms of $\mathcal{O}(p^4)$ can be obtained. The $\mathcal{O}(p^4)$ pion sector ChPT Lagrangian contains seven independent chiral structures with low-energy constants (LECs) and a number of chiral-singlet terms with so called high-energy constants. The next-to leading order effective Lagrangian in the pion sector can be cast in the form [43, 78]

$$\begin{aligned}
\mathcal{L}_\pi^{(4)} =& \frac{l_1}{4}\langle D_\mu U (D^\mu U)^\dagger\rangle^2 + \frac{l_2}{4}\langle D_\mu U (D_\nu U)^\dagger\rangle\langle D^\mu U (D^\nu U)^\dagger\rangle \\
&+ \frac{l_3}{16}\langle \chi U^\dagger + U\chi^\dagger\rangle^2 + \frac{l_4}{4}\langle D_\mu U (D^\mu \chi)^\dagger + D_\mu \chi (D^\mu U)^\dagger\rangle \\
&+ l_5\left[\langle R_{\mu\nu} U L^{\mu\nu} U^\dagger\rangle - \frac{1}{2}\langle L_{\mu\nu}L^{\mu\nu} + R_{\mu\nu}R^{\mu\nu}\rangle\right] \\
&+ i\frac{l_6}{2}\langle R_{\mu\nu} D^\mu U (D^\nu U)^\dagger + L_{\mu\nu}(D^\mu U)^\dagger D^\nu U\rangle \\
&- \frac{l_7}{16}\langle \chi U^\dagger - U\chi^\dagger\rangle^2 \\
&+ \frac{h_1 + h_3}{4}\langle \chi\chi^\dagger\rangle + \frac{h_1 - h_3}{16}\Big[\langle \chi U^\dagger + U\chi^\dagger\rangle^2 \\
&+ \langle \chi U^\dagger - U\chi^\dagger\rangle^2 - 2\langle \chi U^\dagger \chi U^\dagger + U\chi^\dagger U\chi^\dagger\rangle\Big] \\
&- 2h_2\langle L_{\mu\nu}L^{\mu\nu} + R_{\mu\nu}R^{\mu\nu}\rangle \,.
\end{aligned} \tag{4.24}$$

The LECs l_i are not constrained by any symmetry considerations and encode also physics of resonances which are not degrees of freedom of the effective field theory [79]. The LECs have to be determined from experimental data by relating them to measurable quantities or from Lattice QCD. The LEC l_7, for instance, is related to the square of the strong mass difference of charged and uncharged pions [43, 44],

$$(\delta M_\pi^2)^{str} = (M_{\pi^+}^2 - M_{\pi^0}^2)^{str} = (m_u - m_d)^2 \frac{2B^2}{F_\pi^2} l_7 (1 + \mathcal{O}(\mathcal{M})) \,, \tag{4.25}$$

which is driven by the η-meson due to $\eta-\pi$-mixing [44]. In $SU(3)$ ChPT the effective mass term contains a term $\propto \eta\pi_0$ [44] and the strong pion mass difference equals [43, 44] (Dashens theorem)

$$(\delta M_\pi^2)^{str} = \frac{((M_{K^+}^2 - M_{K^0}^2)^{str})^2}{3(M_\eta^2 - M_\pi^2)} + \cdots . \tag{4.26}$$

The so called high-energy constants h_i in eq. (4.24) do not appear in physical low-energy processes.

4.1.2 The Wess-Zumino-Witten action

The effective Lagrangian in the above presented form does not yet exhibit the full range of symmetry properties of the QCD Lagrangian. Whereas the patterns of spontaneous and explicit symmetry breaking are accounted for, any notion of anomalies is still absent from the effective generating functional W_{eff}. In order to incorporate the anomaly structure of QCD into the effective field theory, the effective Lagrangian has to be extended by a non-invariant term which generates the anomalous terms upon the corresponding transformations. Wess and Zumino explicitly constructed generating functionals that reproduce the anomalous Ward identities of QCD [80].

By exploiting a purely geometrical argument, Witten [81] provided an elegant derivation of this extension in $SU(3)_L \times SU(3)_R$ ChPT: the Euler-Lagrange equations of the leading order effective Lagrangian can be amended by a P- and T-violating term,

$$\partial_\mu \left(\frac{F_\pi^2}{2} U \partial^\mu U^\dagger \right) + \lambda \epsilon^{\mu\nu\rho\sigma} U^\dagger (\partial_\mu U) U^\dagger (\partial_\nu U) U^\dagger (\partial_\rho U) U^\dagger (\partial_\sigma U) = 0 \,, \tag{4.27}$$

where λ is a constant and the matrix U is – for now – the $SU(3)$ counter part of U in eq. (4.7). The procedure to construct the corresponding extension of the effective action is the following: let space-time be regarded as a large four-dimensional sphere $\mathbb{S}^4$. The matrix U constitutes a map from $\mathbb{S}^4$ into the $SU(3)$ manifold. Since the fourth homotopy group of $SU(3)$ is trivial, $\pi_4(SU(3)) = 0$, the image $\mathbb{S}^4$ can be considered the boundary of a five-dimensional disk $\mathbb{D}^5$. This disk is not uniquely determined and $\mathbb{S}^4$ can also be regarded as the boundary of another disk $(\mathbb{D}^5)'$, such that both disks combined are homeomorphic to the five-dimensional sphere $\mathbb{S}^5$. There is a unique antisymmetric rank-five tensor ω_{ijklm} which is invariant under $SU(3)_R \times SU(3)_L$ transformations. This tensor is stationary at the point $U = \mathbb{1}$ under $SU(3)_V$ transformations and is given by

$$\omega_{12345} = \sum_\sigma \text{sgn}(\sigma) \text{Tr}[t_{\sigma(1)} t_{\sigma(2)} t_{\sigma(3)} t_{\sigma(4)} t_{\sigma(5)}] \,, \tag{4.28}$$

where the sum is over all permutations of indices σ and t_i are five basis elements of the Lie algebra of $SU(3)$. The tensor at other points of the $SU(3)$ manifold is obtained by $SU(3)_L \times SU(3)_R$ transformations. The corresponding five form is closed and the integral of this five form is homotopy invariant. The extension of the action, S^0_{WZW}, which is called the *Wess-Zumino-Witten action*, may be expressed in different ways,

$$S^0_{WZW} = \int_{\mathbb{D}^5} d\Sigma^{ijklm}\,\omega_{ijklm}\,, \quad S^{0'}_{WZW} = -\int_{(\mathbb{D}^5)'} d\Sigma^{ijklm}\,\omega_{ijklm}\,, \tag{4.29}$$

which leads to the requirement $\exp(iS^0_{WZW}) = \exp(iS^{0'}_{WZW})$, or equivalently

$$\int_{\mathbb{S}^5} d\Sigma^{ijklm}\,\omega_{ijklm} = 2\pi N\,, \quad N \in \mathbb{N}\,. \tag{4.30}$$

Let $\pi_5(SU(3)) = \mathbb{Z}$ be generated by the map $\mathbb{S}^5 \to \mathbb{S}^5_0 \subset SU(3)$ and ω be normalized to

$$\int_{\mathbb{S}^5_0} d\Sigma^{ijklm}\,\omega_{ijklm} = 2\pi\,. \tag{4.31}$$

For local coordinates $\{y_i\}$ of $\mathbb{D}^5$, Witten arrived after identifying $\mathbb{S}^5_0$ and normalizing ω at (see [78, 81])

$$S^0_{WZW} = -n\frac{i}{240\pi^2}\int_{\mathbb{D}^5} d\Sigma^{ijklm}\,\mathrm{Tr}\left[\hat{U}_{L,i}\hat{U}_{L,j}\hat{U}_{L,k}\hat{U}_{L,l}\hat{U}_{L,m}\right]\,, \quad n \in \mathbb{N} \tag{4.32}$$

where

$$\hat{U}_{R,i} := \hat{U}^\dagger\frac{\partial\hat{U}}{\partial y^i}\,, \quad \hat{U}_{L,i} := \frac{\partial\hat{U}^\dagger}{\partial y^i}\hat{U}\,, \tag{4.33}$$

and $\hat{U}$ is the generalization of the standard map U to five dimensions which can be defined by $\hat{U} = U(y_1, y_2, y_3, y_4)^{y_5}$ with $y_5 \in [0,1]$. Expanding the matrix $\hat{U} = \exp(iy_5\phi(y_1, y_2, y_3, y_4)/F_\pi)$ and utilizing Stokes' theorem, eq. (4.32) becomes at leading order in powers of Goldstone boson fields [78, 81]

$$S^0_{WZW} = \frac{n}{240\pi^2 F_\pi^5}\int d^4x\,\epsilon^{\mu\nu\rho\sigma}\,\mathrm{Tr}[\phi\,\partial_\mu\phi\,\partial_\nu\phi\,\partial_\rho\phi\,\partial_\sigma\phi + \cdots]\,, \tag{4.34}$$

for $\phi = \lambda^1\phi^1 + \lambda^2\phi^2 + \cdots$ with the Gell-Mann matrices λ^i.

The Wess-Zumino-Witten action S^0_{WZW} has also to be extended if a particular subgroup of $SU(3)_L \times SU(3)_R$ is to be gauged. Let $t^a_{L,R}$ denote the generators of that particular subgroup. A gauge invariant additional extension can be constructed if these generators obey $\mathrm{Tr}[t^a_L]^3 = \mathrm{Tr}[t^a_R]^3$ [81] for all a in accordance with the usual cancellation condition for anomalies in QCD. The Wess-Zumino-Witten action in the presence of the external fields r_μ and l_μ (l_μ, r_μ: source fields of eqs. (2.38), (2.39)-(2.41) generalized to $SU(3)$) is given by [78, 82–85]

$$S_{WZW}[U, l_\mu, r_\mu] = S^0_{WZW}[U] - \frac{n}{96\pi^2}\int d^4x\epsilon^{\mu\nu\rho\sigma}\mathrm{Tr}[Z_{\mu\nu\rho\sigma}(U, l_\mu, r_\mu)]\,, \tag{4.35}$$

where $Z_{\mu\nu\rho\sigma}$ is defined by (with derivatives acting only on the next object on the right-hand side)

$$\begin{aligned}
Z_{\mu\nu\rho\sigma} \;=\;& U l_\mu U^\dagger r_\nu U l_\rho U^\dagger r_\sigma + 2U l_\mu l_\nu l_\rho U^\dagger r_\sigma - 2U^\dagger r_\mu r_\nu r_\rho U l_\sigma + 2iU\partial_\mu l_\nu l_\rho U^\dagger r_\sigma \\
& -2iU^\dagger\partial_\mu r_\nu r_\rho U l_\sigma + 2i\partial_\mu r_\nu U l_\rho U^\dagger r_\sigma - 2i\partial_\mu l_\nu U^\dagger r_\rho U l_\sigma \\
& -2iU^\dagger\partial_\mu U l_\nu U^\dagger r_\rho U l_\sigma + 2iU\partial_\mu U^\dagger r_\nu U l_\rho U^\dagger r_\sigma - 2iU^\dagger\partial_\mu U l_\nu l_\rho l_\sigma \\
& +2iU\partial_\mu U^\dagger r_\nu r_\rho r_\sigma + U^\dagger\partial_\mu U U^\dagger\partial_\nu r_\rho U l_\sigma - U\partial_\mu U^\dagger U\partial_\nu l_\rho U^\dagger r_\sigma \\
& +U^\dagger\partial_\mu U U^\dagger r_\nu U\partial_\rho l_\sigma - U\partial_\mu U^\dagger U l_\nu U^\dagger\partial_\rho r_\sigma - 2U^\dagger\partial_\mu U U^\dagger\partial_\nu U U^\dagger r_\rho U l_\sigma \\
& +2U\partial_\mu U^\dagger U\partial_\nu U^\dagger U l_\rho U^\dagger r_\sigma + 2U^\dagger\partial_\mu U l_\nu\partial_\rho l_\sigma - 2U\partial_\mu U^\dagger r_\nu\partial_\rho r_\sigma \\
& +2U^\dagger\partial_\mu U\partial_\nu l_\rho l_\sigma - 2U\partial_\mu U^\dagger\partial_\nu r_\rho r_\sigma + U^\dagger\partial_\mu U l_\nu U^\dagger\partial_\nu U l_\sigma \\
& -U\partial_\mu U^\dagger r_\nu U\partial_\rho U^\dagger r_\sigma - 2iU^\dagger\partial_\mu U U^\dagger\partial_\nu U U^\dagger\partial_\rho U l_\sigma \\
& +2iU\partial_\mu U^\dagger U\partial_\nu U^\dagger U\partial_\rho U^\dagger r_\sigma \,. \qquad (4.36)
\end{aligned}$$

By considering the coupling to electromagnetism, the integer n in eq. (4.32) and eq. (4.35) was identified as the number of colors, N_C [81].

4.1.3 The effective Lagrangian in the pion-nucleon sector

A detailed study of the effective Lagrangian in the pion-nucleon sector is contained in [86,87]. This section provides a brief summary of the main aspects which are of relevance for this thesis. In order to include pion-nucleon interactions into the effective field theory, an appropriate transformation law for the fermion fields of the proton and neutron has to be established [88–90]. The discussion below follows the lines of [86,90,91]. Let

$$N(x) := \begin{pmatrix} p(x) \\ n(x) \end{pmatrix} \qquad (4.37)$$

denote the isospin doublet of the proton and neutron fields. Consider the composition of two elements of $SU(2)_L \times SU(2)_R$, an axial and an arbitrary transformation:

$$(L,R)\cdot(u^\dagger,u) = (Lu^\dagger, Ru) = (Lu^\dagger K^\dagger, RuK^\dagger)\cdot(K,K)\,, \qquad (4.38)$$

Eq. (4.38) implies that the matrix u is transformed under $SU(2)_L \times SU(2)_R$ by

$$u \mapsto RuK^\dagger = KuL^\dagger\,, \quad u^2 \mapsto RuK^\dagger KuL^\dagger = RUL^\dagger\,. \qquad (4.39)$$

The square of the matrix u transforms identically to the U matrix, which allows for the identification $u^2 = U$. $K \in SU(2)$ is in general a function of U, R and L and is called the compensator field. Eq. (4.39) defines a linear operation of $SU(2)_L \times SU(2)_R$ on the pair (U,N) by

$$(U,N) \mapsto (RUL^\dagger, K(R,L,U)N)\,, \qquad (4.40)$$

since $K(e,e,U) = \mathbb{1}$ and

$$\begin{aligned}(U,N) &\mapsto (R_1 U L_1^\dagger, K(R_1,L_1,U)N)\\ &\mapsto (R_2 R_1 U L_1^\dagger L_2^\dagger, K(R_2,L_2,R_1 U L_1^\dagger)K(R_1,L_1,U)N)\\ &= ((R_2R_1)U(L_2L_1)^\dagger, K(R_2R_1,L_2L_1,U)N)\,. \end{aligned} \tag{4.41}$$

In analogy to the construction procedure of the effective Lagrangian in the pion sector, the effective pion-nucleon sector Lagrangian consists of all hermitian terms which are invariant under local $SU(2)_L \times SU(2)_R$ transformations and Lorentz scalars. The covariant derivative for the pion-nucleon sector is defined by

$$\mathcal{D}_\mu N := (\partial_\mu + \Gamma_\mu - i v_\mu^{(s)})N\,, \quad \mathcal{D}_\mu K N = K \mathcal{D}_\mu N\,, \tag{4.42}$$

where the connection Γ_μ is given by

$$\Gamma_\mu = \frac{1}{2}[u^\dagger(\partial_\mu - i r_\mu)u + u(\partial_\mu - i l_\mu)u^\dagger]\,. \tag{4.43}$$

Furthermore, the following fundamental building blocks are defined:

$$u_\mu = i[u^\dagger(\partial_\mu - i r_\mu)u - u(\partial_\mu - i l_\mu)u^\dagger]\,, \tag{4.44}$$

$$\chi_\pm = u^\dagger \chi u^\dagger \pm u \chi^\dagger u\,, \tag{4.45}$$

$$f_\pm^{\mu\nu} = u R^{\mu\nu} u^\dagger \pm u^\dagger L^{\mu\nu} u\,. \tag{4.46}$$

The chiral dimension of a digram in the one-nucleon sector can be obtained analogously to eq. (4.23) and is given by [79]:

$$D = 2L + 1 + \sum_k N_k^{\pi\pi}(k-2) + \sum_{k'} N_{k'}^{\pi N}(k'-1)\,, \tag{4.47}$$

where L denotes the number of loops, $N_k^{\pi\pi}$ the number of pion vertices of order k and $N_{k'}^{\pi N}$ the number of pion-nucleon vertices of order k' in the considered diagram.

The so called heavy-baryon chiral perturbation theory provides a consistent framework in the extreme non-relativistic limit by integrating out the light components of the nucleon fields in the generating functional of ChPT [92, 93]. The four-momentum of a nucleon in a nucleus p^μ can be decomposed into the on-shell component described by the four-velocity v^μ with $v^2 = 1$ and a small off-shell momentum k^μ (m_N: nucleon mass):

$$p^\mu = m_N v^\mu + k^\mu\,. \tag{4.48}$$

The nucleon field N can be split into a heavy component H and a light component h by employing the velocity projection operator $P_v := (\mathbb{1} + \not{v})/2$ [93]:

$$N(x) = e^{-i m_N v_\mu x^\mu}(H(x) + h(x))\,, \quad \not{v}H = H\,, \not{v}h = -h\,. \tag{4.49}$$

Any product of Dirac matrices can be expressed as a combination of the velocity v^μ and the Pauli-Lubanski spin operator $S^\mu = i\gamma^5\sigma^{\mu\nu}v_\nu/2$, which equal in the nucleon rest-frame $v = (1,0,0,0)$ and $S = (0,\vec{\sigma})/2$. After integrating out the heavy component h in the generating functional as done in [93], the pion-nucleon Lagrangian as a series in powers of $1/m_N$ and derivatives of H is obtained. The leading order and next-to leading order Lagrangians in the pion-nucleon sector are given by [87, 93][1]

$$\begin{aligned}
\mathcal{L}_{\pi N}^{(1)} &= H^\dagger\left(iv\cdot\mathcal{D} + g_A S\cdot u\right)H\,, \qquad (4.50)\\
\mathcal{L}_{\pi N}^{(2)} &= \frac{1}{2m_N}H^\dagger\left((v\cdot\mathcal{D})^2 - \mathcal{D}^2 - ig_A\{S\cdot\mathcal{D}, v\cdot u\}\right)\\
&\quad + H^\dagger\Bigg(c_1\langle\chi_+\rangle - \frac{c_2}{2}\langle(v\cdot u)^2\rangle + \frac{c_3}{2}\langle u\cdot u\rangle + \frac{c_4}{2}[S^\mu, S^\nu][u_\mu, u_\nu]\\
&\quad + c_5\hat{\chi}_+ - i\frac{c_6}{4m_N}[S^\mu,S^\nu]f^+_{\mu\nu} - i\frac{c_7}{4m_N}[S^\mu,S^\nu]\langle f^+_{\mu\nu}\rangle\Bigg)H\,, \qquad (4.51)
\end{aligned}$$

where the hat denotes the traceless component of a general chiral structure A (*e.g.* $\chi_\pm$),

$$\hat{A} := A - \frac{1}{2}\langle A\rangle\,, \qquad (4.52)$$

and the quantities c_i are LECs. g_A is related to the pion-nucleon coupling constant $g_{\pi NN} \approx m_N g_A/F_\pi$ at leading order. The LEC c_5 in eq. (4.51), for instance, is related to the quark mass induced contribution to the neutron-proton mass difference:

$$\delta M_{np}^{str} := (m_n - m_p)^{str} = 4B_0(m_u - m_d)\,c_5\,. \qquad (4.53)$$

The strong neutron-proton mass splitting is $\delta m_{np}^{str} = (2.6 \pm 0.5)\,\mathrm{MeV}$ [94][2] by current estimates. The LEC c_1 can be related to the πN-sigma term. Reference [95] provides a compilation of various extractions of c_1 [91, 96–98] and gives a value of

$$c_1 = (-1.0 \pm 0.3)\,\mathrm{GeV}^{-1}\,. \qquad (4.54)$$

[1]The hats over the LECs in the heavy baryon ChPT Lagrangians of [87] are omitted throughout this thesis.

[2]The error of δm_{np}^{str} in this reference is understated. The uncertainty has to be increased to at least 0.85 MeV to ensure consistence of δm_{np}^{str} with the prediction in [43].

4.2 The P- and T-violating effective Lagrangian

This section is concerned with the P- and T-violating terms in the chiral effective field theory Lagrangian which are induced by the QCD θ-term eq. (2.61) (its expression in terms of a complex phase of the quark mass matrix is contained in eq. (2.65)) and the effective dimension-six sources eqs. (3.32) - (3.38). The transition from (amended) QCD to (amended) ChPT involves the introduction of source fields. Those transformation properties under chiral $SU(2)_L \times SU(2)_R$ rotations are assigned to each source field which render the combination of a particular source field and the associated quark term invariant. This implies that an investigation of the $SU(2)_L \times SU(2)_R$ transformation properties of quark terms is required to establish the connection between the levels of QCD and ChPT. A P- and T-violating quark term induces in general an infinite set of P- and T-violating terms of different orders in the (amended) ChPT Lagrangian. This ordering of terms in the (amended) ChPT Lagrangian can be different for each source of P and T violation. The aim of the remaining sections of this chapter is to identify the hierarchies of coupling constants of the leading P- and T-violating vertices for each considered source of P and T violation.

4.2.1 Chiral transformation properties of quark bilinears and quark quadrilinears

As demonstrated in appendix B, quark multilinears transform as states of representations of $O(4)$ and can be decomposed into quark multilinears which transform as basis states of irreducible representation of $O(4)$. According to appendix B, an irreducible $O(4)$ representation can be labelled by a pair of half-integers or integers (j_1, j_2) with $j_1 + j_2 \in \mathbb{N}$. For each case of $j_1 = j_2 = j$, there are two different irreducible $O(4)$ representations which are labelled by the superscript $\pm$: $(j, j)^{\pm}$. The list of quark bilinears (two-quark terms) and the irreducible representations of $O(4)$ to which they belong is given by

$$\mathrm{dim} = 1 \quad (0,0)^+ \quad : \quad \bar{q}\gamma^\mu q \,, \tag{4.55}$$

$$\mathrm{dim} = 1 \quad (0,0)^- \quad : \quad i\bar{q}\gamma^\mu\gamma_5 q \,, \tag{4.56}$$

$$\mathrm{dim} = 4 \quad (1/2,1/2)^+ \quad : \quad (i\bar{q}\gamma_5\tau_i q, \bar{q}q), (i\bar{q}\sigma^{\mu\nu}\gamma_5\tau_i q, \bar{q}\sigma^{\mu\nu} q) \,, \tag{4.57}$$

$$\mathrm{dim} = 4 \quad (1/2,1/2)^- \quad : \quad (\bar{q}\tau_i q, i\bar{q}\gamma_5 q), (\bar{q}\sigma^{\mu\nu}\tau_i q, i\bar{q}\sigma^{\mu\nu}\gamma_5 q) \,, \tag{4.58}$$

$$\mathrm{dim} = 6 \quad (1,0) \oplus (0,1) : \quad (\bar{q}\gamma^\mu\tau_i q, \bar{q}\gamma^\mu\gamma_5\tau_i q) \,. \tag{4.59}$$

The Dirac vectors and tensors in this list are understood to combine with other fields to form Lorentz invariant objects.

Quark quadrilinears (four-quark terms) transform as states of *symmetric tensor products* of the irreducible representations of $O(4)$ in eqs. (4.55)-(4.59). An arbitrary quark quadrilinear decomposes in general into a sum of quark quadrilinears which transform as basis states of specific irreducible representations of $O(4)$.

For the details of the connection between quark quadrilinears and the representation theory of $O(4)$ the reader is again referred to appendix B. The complete list of Lorentz invariant quark quadrilinears which transform as basis states of one particular irreducible representation of $O(4)$ is derived in appendix B (see eq. (B.92)-(B.98)) and is given by

$$\begin{array}{llcll}
(0,0)^- & 1\,\not{P}\ \text{-state} & : & \bar{q}\gamma_\mu\tau_k q\bar{q}\gamma^\mu\gamma_5\tau_k q\,, & (4.60)\\
(1,1)^+ & 3\,\not{P}\not{T}\text{-states} & : & \epsilon^{kij}\bar{q}\gamma_\mu\tau_i q\bar{q}\gamma^\mu\gamma_5\tau_j q\,, & (4.61)\\
(2,0)\oplus(0,2) & 5\,\not{P}\ \text{-states} & : & (\delta_{ik}\delta_{jl}+\delta_{jk}\delta_{il}-2\delta_{ij}\delta_{kl})\bar{q}\gamma_\mu\tau_i q\bar{q}\gamma^\mu\gamma_5\tau_j q\,, & (4.62)\\
(0,0)^- & 1\,\not{P}\not{T}\text{-state} & : & \bar{q}q\bar{q}i\gamma_5 q-\bar{q}\tau_k q\bar{q}i\gamma_5\tau_k q\,, & (4.63)\\
(1,1)^+ & 3\,\not{P}\not{T}\text{-states} & : & \bar{q}q\bar{q}i\gamma_5\tau_i q\pm\bar{q}\tau_i q\bar{q}i\gamma_5 q\,, & (4.64)\\
(1,1)^- & 6\,\not{P}\not{T}\text{-states} & : & \bar{q}\tau_i q\bar{q}i\gamma_5\tau_j q\pm\bar{q}\tau_j q\bar{q}i\gamma_5\tau_i q\quad i\neq j\,, & (4.65)\\
 & & & \bar{q}\tau_{i'}q\bar{q}i\gamma_5\tau_{i'}q+\bar{q}q\bar{q}i\gamma_5 q\,. & (4.66)
\end{array}$$

The first column contains the (j_1, j_2) labels of the irreducible representation of $O(4)$ of dimensions $(2j_1+1)(2j_2+1)$. The second column shows the number of P-violating (and T-violating) quark quadrilinears in a particular irreducible representation which are listed in the third column. Summation over equal indices is implied except for the index i' in eq. (4.66). Note that the two different relative signs in eq. (4.64) (and also in eq. (4.65)) define two different sets of tensors which both transform as the same basis states of the $(1,1)^+$ (or the $(1,1)^-$) representation (as demonstrated in appendix B). This list of quark quadrilinears reveals Fierz identities between two quark quadrilinears: in order for a Fierz identity between two quark bilinears or two quark quadrilinears to exist, they have to transform as the same basis state of the same irreducible representation as identical tensors. This is the case for the quark quadrilinears in eq. (4.61) and the quark quadrilinears in eq. (4.64) with relative minus signs.

Other Lorentz invariant quark quadrilinears can emerge when external fields such as the photon field are taken into consideration. Since the photon field, for instance, has to be integrated out to obtain tree-level nuclear operators without photons later on, such quark quadrilinears are suppressed and are disregarded in this thesis.

Only the following two of the eight quark quadrilinears in eqs. (4.60)-(4.66) are of relevance for our analysis: the $4q$-op eq. (3.36) can be re-expressed in terms of quark flavor doublets by

$$\begin{aligned}
& i(\bar{u}u\bar{d}\gamma_5 d+\bar{u}\gamma_5 u\bar{d}d-\bar{d}u\bar{u}\gamma_5 d-\bar{d}\gamma_5 u\bar{u}d)\\
= \quad & i(\bar{q}\gamma_5 q\bar{q}q-\bar{q}\gamma_5\tau_3 q\bar{q}\tau_3 q-\bar{q}\gamma_5\tau_2 q\bar{q}\tau_2 q-\bar{q}\gamma_5\tau_1 q\bar{q}\tau_1 q)/2\,,
\end{aligned} \qquad (4.67)$$

which demonstrates that it transforms as a basis state of the $(0,0)^-$ representation of $O(4)$. The $4qLR$-op eq. (3.34) can equally be rewritten in terms of quark flavor doublets by

$$
\begin{aligned}
& i\bar{u}_R\gamma_\mu d_R\bar{d}_L\gamma^\mu u_L - i\bar{d}_R\gamma_\mu u_R\bar{u}_L\gamma^\mu d_L \\
= \quad & -\epsilon^{3ij}\bar{q}_R\gamma^\mu\tau_i q_R\bar{q}_L\gamma_\mu\tau_j q_L/2 \\
= \quad & \epsilon^{3ij}\bar{q}\gamma^\mu\tau_i q\bar{q}\gamma_\mu\gamma_5\tau_j q/4\,, \qquad (4.68)
\end{aligned}
$$

and thus exhibits the transformation properties of a basis state of the $(1,1)^+$ representation of $O(4)$. Although the above list contains further P- and T-violating quark quadrilinears, eq. (4.67) and eq. (4.68) are the only unsuppressed ones as established in chapter 3. The other quark quadrilinears can be neglected until a BSM mechanism can be identified which renders an additional quark quadrilinear unsuppressed.

4.2.2 Source fields and P- and T-violating terms in chiral effective Lagrangian

It has been explained in section 4.1.1 that the connection between standard QCD and ChPT is drawn by the introduction of source fields for each quark term in the standard QCD Lagrangian. We extend this method to QCD when it is amended by effective dimension-six terms, which requires the introduction of further source fields. In order to ensure that the effective field theory obeys the same chiral Ward identities as the underlying theory, the source fields are assigned transformation properties under local $SU(2)_L\times SU(2)_R$ transformations and the group $\mathbb{Z}_2$ of parity transformations which render the Lagrangian of the underlying theory – QCD or amended QCD – locally invariant. The effective Lagrangian is then obtained by compiling for each source of P and T violation the set of all possible combinations of these source fields with the fundamental building blocks of standard ChPT. The source fields for each source of P and T violation are defined and the resulting terms in the (amended) ChPT Lagrangian are subsequently discussed in this section.

θ-term

The θ-term eq. (2.61) is rotated into a complex phase of the quark mass matrix by an axial $U_A(1)$ transformation via the anomaly. The resulting P- and T-violating quark bilinears are given by eq. (2.65),

$$
i\bar{q}\gamma_5 q \quad \text{and} \quad i\bar{q}\tau_3\gamma_5 q\,, \qquad (4.69)
$$

which transform as basis states of the $(1/2,1/2)^-$ and $(1/2,1/2)^+$ irreducible representations of $O(4)$ according to eq. (4.58) and eq. (4.57), respectively. They are thus connected by $SU(2)_L\times SU(2)_R$ transformations either to the isospin-violating component of the quark mass matrix or to the isospin-conserving component of the quark mass matrix. This implies that their corresponding source fields are given by the well-known χ source fields $p_0\mathbb{1}$ and $p_3\tau_3$ of standard ChPT. Their assigned transformation properties under local $SU(2)_L\times SU(2)_R$ transformations are identical to their global transformation properties and naturally reflect those of the corresponding quark bilinears, i.e. the source fields transform as the same basis states of the same irreducible representations [43]:

$$(1/2,1/2)^- \quad : \quad (s_1\tau_1, s_2\tau_2, s_3\tau_3, ip_0)\,, \tag{4.70}$$

$$(1/2,1/2)^+ \quad : \quad (ip_1\tau_1, ip_2\tau_2, ip_3\tau_3, s_0)\,. \tag{4.71}$$

Therefore, the θ-term induced effective Lagrangian for two quark flavors is just the standard $SU(2)$ ChPT Lagrangian as provided by [44] for the pion sector and by *e.g.* [91] for the pion-nucleon sector. The terms which are induced by the θ-term are the p_0 and p_3 components of all terms with insertions of the building block χ.

Before discussing the P- and T-violating terms in the ChPT Lagrangian induced by the θ-term in detail, a few general remarks which apply to all sources of P and T violation are required. The decomposition of the fundamental building block χ_+ into a traceless component ($\hat{\chi}_+$) and a component with a non-vanishing trace ($\langle\chi_+\rangle$) corresponds to the decomposition of the eight dimensional representation of source fields combined in χ into the two irreducible representations $(1/2,1/2)^-$ and $(1/2,1/2)^+$. The same is true for the building block $f_\pm^{\mu\nu}$, which contains the source fields $v_i^\mu\tau_i$, $a_i^\mu\tau_i$ and $v^{(s),\mu}$ and constitutes a reducible seven dimensional representation. The decomposition of this building block into the components $\hat{f}_+^{\mu\nu}$ and $\langle f_+^{\mu\nu}\rangle$ corresponds to the decomposition into the irreducible representations $(1,0)\oplus(0,1)$ and $(0,0)^+$ (see eq. (4.55) and eq. (4.59)).

Combinations of these fundamental building blocks correspond to tensor products of the above mentioned irreducible representations of $O(4)$. Consider a building block containing a P- and T-violating source field denoted by $\tilde{A}_{\not{P}\not{T}}$ for which another P- and T-conserving counterpart A_{PT} exists that transforms identically under $SU(2)_L\times SU(2)_R$ transformations. Let this building block be combined with a P- and T-conserving building block B_{PT} that also has a P- and T-violating counter part $\tilde{B}_{\not{P}\not{T}}$. In the language of group theory, the combination $\tilde{A}_{\not{P}\not{T}}B_{PT}$ transforms identically to the combination of building blocks $A_{PT}\tilde{B}_{\not{P}\not{T}}$, in which the former building block is replaced by the building block associated with its P- and T-conserving partner source field and in which the latter building block is replaced by its P- and T-violating counter part. This is the justification for the definition of the building block χ_- in eq. (4.45), in which a particular source field is combined with the chiral structure of its partner source field. It is apparent that this building block can only occur in combination with other building blocks: there is no term such as $F_\pi^2\langle i\chi_-\rangle/4$ in the pure pion sector Lagrangian eq. (4.20), for instance, whereas the term $-l_7\langle\chi_-\rangle^2/16$ exists in eq. (4.24) (this is just reflection of the fact that the representation $(1/2,1/2)^+\otimes(1/2,1/2)^+$ is identical to the representation $(1/2,1/2)^- \otimes (1/2,1/2)^-$). This reasoning extends to the pion-nucleon sector where the property of P and T violation can also be absorbed by products of Dirac matrices which act on nucleons fields and are contracted with other quantities.

The terms of the ChPT Lagrangian which are induced by the θ-term are contained in the expressions that include insertions of the building blocks $\langle\chi_\pm\rangle$ and $\hat{\chi}_\pm$ with the replacements of the source fields p_0 and p_3 according to eq. (2.65):

$$p_0 \to \frac{\bar{\theta}}{2}\bar{m}\,, \quad p_3 \to \frac{\bar{\theta}}{2}\bar{m}\epsilon\,. \tag{4.72}$$

However, it will be demonstrated in the next section 4.3 that the presence of chiral symmetry breaking P- and T-violating terms in the QCD Lagrangian alters the ground state of the theory and requires a redefinition of the quark fields by an axial $SU(2)_L \times SU(2)_R$ rotation. As a result of this redefinition, for instance, all terms with a factor of p_3 vanish. The P- and T-violating Lagrangians discussed in this section are thus the *naive* P- and T-violating Lagrangians in (amended) ChPT induced by the θ- term (or by the effective dimension-six sources) before the correct ground state of the theory has been selected. Furthermore, It will be shown in the next section that the selection of the ground state procedure ensures parametrization invariant leading order terms in the pion sector Lagrangian. The induced terms in the naive P- and T-violating Lagrangian discussed in this section in an arbitrary parametrization are obtained by the replacement of the matrix U by the generalized U matrix of [99] with a parametrization function g,

$$U = \exp\left(i\frac{\vec{\pi}\cdot\vec{\tau}}{F_\pi}g\left(\frac{\pi^2}{F_\pi^2}\right)\right)\,, \quad g\left(\frac{\pi^2}{F_\pi^2}\right) = 1 + \left[\alpha + \frac{1}{6}\right]\frac{\pi^2}{F_\pi^2} + \cdots\,, \tag{4.73}$$

where α is a real constant defining the parametrization ($\alpha = 0$ corresponds to the so called σ-parametrization of $SU(2)$ ChPT). This replacement is equivalent to the following replacement of terms at leading order in powers of pion fields:

$$\left(1 - \frac{1}{6}\frac{\pi^2}{F_\pi^2}\right) \to \left(1 + \alpha\frac{\pi^2}{F_\pi^2}\right)\,. \tag{4.74}$$

The terms induced by the θ-term in the leading order pion sector Lagrangian of [44] are given by eq. (4.20)

$$\begin{aligned}\mathcal{L}_\pi^{(2)} &= \frac{F_\pi^2}{4}\langle\chi_+\rangle + \cdots \\ &= (2Bp_3)F_\pi\pi_3\left(1 - \frac{\pi^2}{6F_\pi^2}\right) + \cdots\,,\end{aligned} \tag{4.75}$$

where the dots denote – throughout this section – either terms which are P- and T-conserving and not induced by the θ-term or terms of higher orders in the pion-field expansion.

The fourth-order pion sector Lagrangian of [44] leads to the following naive P- and T-violating terms induced by the θ-term (see eq. (4.24)):

$$\begin{aligned}\mathcal{L}_{\pi}^{(4)} &= \frac{l_3}{16}\langle\chi_+\rangle^2 - \frac{l_7}{16}\langle\chi_-\rangle^2 + \cdots \\ &= 2l_3(2Bs_0)(2Bp_3)\frac{\pi_3}{F_\pi}\left(1-\frac{2\pi^2}{3F_\pi^2}\right) - 2l_7(2Bs_3)(2Bp_0)\frac{\pi_3}{F_\pi}\left(1-\frac{2\pi^2}{3F_\pi^2}\right) \\ &\quad + \cdots . \end{aligned} \tag{4.76}$$

The naive P- and T-violating terms induced by the θ-term in the second-order pion-nucleon sector Lagrangian eq. (4.51) read after the redefinition $H \to N$ (see also [91])

$$\begin{aligned}\mathcal{L}_{\pi N}^{(2)} &= c_1\langle\chi_+\rangle N^\dagger N + \cdots + c_5 N^\dagger \hat{\chi}_+ N + \cdots \\ &= 4c_1(2Bp_3)\frac{\pi_3}{F_\pi}\left(1-\frac{\pi^2}{6F_\pi^2}\right) + 2c_5(2Bp_0)N^\dagger\frac{\vec{\pi}\cdot\vec{\tau}}{F_\pi}\left(1-\frac{\pi^2}{6F_\pi^2}\right)N \\ &\quad + \cdots . \end{aligned} \tag{4.77}$$

The naive fourth-order pion-nucleon sector Lagrangian of [91] which is also given in appendix D.2 contains identical structures at leading order in the pion-field expansion:

$$\begin{aligned}\mathcal{L}_{\pi N}^{(4)} &= e_{38}\langle\chi_+\rangle^2 N^\dagger N + e_{40}\langle\hat{\chi}_+\hat{\chi}_+\rangle N^\dagger N + \cdots \\ &= e_{38}32(2Bs_0)(2Bp_3)\frac{\pi_3}{F_\pi}\left(1-\frac{2\pi^2}{3F_\pi^2}\right) + e_{40}16(2Bs_3)(2Bp_0)\frac{\pi_3}{F_\pi}\left(1-\frac{2\pi^2}{3F_\pi^2}\right) \\ &\quad + \cdots . \end{aligned} \tag{4.78}$$

These terms constitute corrections to the leading P- and T-violating πNN vertices of $\mathcal{L}_{\pi N}^{(2)}$ shown in eq. (4.77), but prove to be negligible as demonstrated in the next section. The leading order P- and T-violating γNN vertices also emerge from the forth-order pion-nucleon Lagrangian $\mathcal{L}_{\pi N}^{(4)}$ of [91] and read

$$\begin{aligned}\mathcal{L}_{\pi N}^{(4)} &= e_{110}i\langle\chi_-\rangle\langle f_+^{\mu\nu}\rangle N^\dagger S_\mu v_\nu N + e_{111}i\langle\chi_-\rangle N^\dagger \hat{f}_+^{\mu\nu} S_\mu v_\nu N \\ &\quad + e_{112}i\langle f_+^{\mu\nu}\rangle N^\dagger\hat{\chi}_- S_\mu v_\nu N + e_{113}i\langle f_+^{\mu\nu}\hat{\chi}_-\rangle N^\dagger S_\mu v_\nu N + \cdots \\ &= e_{110}8e(2Bp_0)N^\dagger S_\mu v_\nu N F^{\mu\nu} + e_{111}4e(2Bp_0)N^\dagger\tau_3 S_\mu v_\nu N F^{\mu\nu} \\ &\quad + e_{112}2e(2Bp_3)N^\dagger\tau_3 S_\mu v_\nu N F^{\mu\nu} + e_{113}4e(2Bp_3)N^\dagger S_\mu v_\nu N F^{\mu\nu} \\ &\quad + \cdots . \end{aligned} \tag{4.79}$$

The P- and T-violating terms above extracted from [91] have also been found recently by [42] in the Weinberg formulation of $SU(2)$ ChPT. The complete list of P- and T-violating terms which are naively induced by the θ-term is provided by appendix D.2.

There are numerous four-nucleon contact terms induced by the θ-term which lead to the following leading order naive four-nucleon Lagrangian induced by the θ-term:

$$
\begin{aligned}
\mathcal{L}_{4N} = \;& C_1\langle\chi_+\rangle N^\dagger N N^\dagger N + C_2\langle\chi_+\rangle N^\dagger S_\mu N N^\dagger S^\mu N \\
&+C_3 N^\dagger\hat{\chi}_+ N N^\dagger N + C_4 N^\dagger\hat{\chi}_+ S_\mu N N^\dagger S^\mu N \\
&+C_5 i\langle\chi_-\rangle N^\dagger N \mathcal{D}_\mu(N^\dagger S^\mu N) + C_6 i\langle\chi_-\rangle N^\dagger\vec{\tau}N\cdot\mathcal{D}_\mu(N^\dagger S^\mu\vec{\tau}N) \\
&+C_7 i N^\dagger\hat{\chi}_- N\mathcal{D}_\mu(N^\dagger S^\mu N) + C_8 i N^\dagger\{\hat{\chi}_-,\vec{\tau}\}N\cdot\mathcal{D}_\mu(N^\dagger S^\mu\vec{\tau}N)/2 \\
&+\cdots \\
= \;& C_1 4(2Bp_3)\pi_3 N^\dagger N N^\dagger N/F_\pi + C_2 4(2Bp_3)\pi_3 N^\dagger S_\mu N N^\dagger S^\mu N/F_\pi \\
&+C_3 2(2Bp_0)N^\dagger\vec{\pi}\cdot\vec{\tau}N N^\dagger N/F_\pi + C_4 2(2Bp_0)N^\dagger\vec{\pi}\cdot\vec{\tau}S_\mu N N^\dagger S^\mu N/F_\pi \\
&-C_5 4(2Bp_0)N^\dagger N\mathcal{D}_\mu(N^\dagger S^\mu N) - C_6 4(2Bp_0)N^\dagger\vec{\tau}N\cdot\mathcal{D}_\mu(N^\dagger\vec{\tau}S^\mu N) \\
&-C_7 2(2Bp_3)N^\dagger\tau_3 N\mathcal{D}_\mu(N^\dagger S^\mu N) - C_8 8(2Bp_3)N^\dagger\tau_3 N\cdot\mathcal{D}_\mu(N^\dagger S^\mu\tau_3 N) \\
&+\cdots
\end{aligned}
\tag{4.80}
$$

Eq. (4.80) is a re-derivation within the Gasser-Leutwyler formulation of ChPT of the results previously presented in [39, 42, 49] in the Weinberg formulation of $SU(2)$ ChPT. The naive set of P- and T-violating terms induced by θ-term presented here is in agreement with the one derived in the Weinberg formulation of $SU(2)$ ChPT in [42] at all relevant orders.

qCEDM

As pointed out in [39, 49], the isospin-conserving and the isospin-violating components of the $qCEDM$, eq. (3.33), transform identically to the corresponding components of the θ-term in eq. (2.66) as basis states of the $(1/2,1/2)^-$ and $(1/2,1/2)^+$ irreducible representations of $O(4)$ (see eq. (4.57) and eq. (4.58)):

$$(1/2,1/2)^- : \quad (i\bar{q}\vec{\tau}\sigma^{\mu\nu}\gamma_5 G^a_{\mu\nu}\lambda^a q, \bar{q}\sigma^{\mu\nu}G^a_{\mu\nu}\lambda^a q)\,, \tag{4.81}$$
$$(1/2,1/2)^+ : \quad (\bar{q}\vec{\tau}\sigma^{\mu\nu}G^a_{\mu\nu}\lambda^a q, i\bar{q}\sigma^{\mu\nu}\gamma_5 G^a_{\mu\nu}\lambda^a q)\,. \tag{4.82}$$

The components of the $qCEDM$ constitute additional, separate isospin multiplets which are not connected by $SU(2)_L\times SU(2)_R$ rotations to the corresponding isospin multiplets of the standard QCD Lagrangian which contain the components of the θ-term in eq. (2.65) (see eq (4.57) and eq. (4.58)). In the Gasser-Leutwyler formulation of ChPT, this observation requires the introduction of an additional set of source fields, which can be combined in the new object $\tilde{\chi}$ in analogy to the definition of χ in standard ChPT:

$$\chi = 2B(s_0 + s_1\tau_1 + s_2\tau_2 + s_3\tau_3 + ip_0 + ip_1\tau_1 + ip_2\tau_2 + ip_3\tau_3)\,, \tag{4.83}$$
$$\tilde{\chi} = 2C(\tilde{s}_0 + \tilde{s}_1\tau_1 + \tilde{s}_2\tau_2 + \tilde{s}_3\tau_3 + i\tilde{p}_0 + i\tilde{p}_1\tau_1 + i\tilde{p}_2\tau_2 + i\tilde{p}_3\tau_3)\,. \tag{4.84}$$

Whereas the quantity B of eq. (4.17) in standard ChPT is proportional to the scalar quark condensate, $\tilde{\chi}$ contains an additional corresponding quantity denoted by C which is defined by

$$\begin{aligned} \langle 0|\bar{u}u|0\rangle &= -F_\pi^2 B + \cdots\,, && (4.85)\\ \langle 0|\bar{u}\sigma^{\mu\nu}G^a_{\mu\nu}\lambda^a u|0\rangle &= -F_\pi^2 C + \cdots\,. && (4.86)\end{aligned}$$

Since the effective dimension-six sources of P and T violation constitute an amendment of standard QCD, their treatment within the effective field theory requires an analogous amendment of standard ChPT. This leads to the definition of further fundamental blocks $\tilde{\chi}_\pm$, in analogy to $\chi_\pm$, by

$$\begin{aligned} \chi_\pm &= u^\dagger \chi u^\dagger \pm u\chi^\dagger u\,, && (4.87)\\ \tilde{\chi}_\pm &= u^\dagger \tilde{\chi} u^\dagger \pm u\tilde{\chi}^\dagger u\,. && (4.88)\end{aligned}$$

For the $qCEDM$, the source fields $\tilde{p}_0$ and $\tilde{p}_3$ have to be subsequently replaced according to eq. (3.25) by

$$\tilde{p}_0 \to -\tilde{\delta}^0_G\,, \quad \tilde{p}_3 \to -\tilde{\delta}^3_G\,. \tag{4.89}$$

The existence of new source fields has serious implications for the naive (before the selection of the correct ground state) P- and T-violating Lagrangian which is induced by the $qCEDM$. Since the two additional isospin multiplets give rise to new LECs as emphasized in [39, 49], all observables originally related only to source fields in χ such as δM^{str}_{np} and $(\delta m^2_\pi)^{str}$, for instance, are now also related to the source fields in $\tilde{\chi}$. The new LECs encode BSM physics which is expected to yield only minor modification to the SM at the energy scale $\Lambda_{\rm had}$ and below. The contributions from the new LECs to P- and T-conserving observables can then safely be considered insignificant compared to the ones from the standard LECs. Therefore, it is in general impossible to infer the values of these new LECs from measurements of P- and T-conserving observables.

The leading P- and T-violating terms induced by the $qCEDM$ in the modified pion sector Lagrangians $\mathcal{L}^{(2)}_{\pi N}$ and $\mathcal{L}^{(4)}_{\pi N}$ are contained in the structures

$$\mathcal{L}^{(2)}_\pi = \frac{F_\pi^2}{4}\langle \chi_+ + \tilde{\chi}_+\rangle + \cdots\,, \tag{4.90}$$

and

$$\begin{aligned} \mathcal{L}^{(4)}_\pi = {} & \frac{l_3}{16}\langle\chi_+\rangle^2 + \frac{\tilde{l}_3}{16}\langle\tilde{\chi}_+\rangle^2 + \frac{l'_3}{16}\langle\chi_+\rangle\langle\tilde{\chi}_+\rangle \\ & -\frac{l_7}{16}\langle\chi_-\rangle^2 - \frac{\tilde{l}_7}{16}\langle\tilde{\chi}_-\rangle^2 - \frac{l'_7}{16}\langle\chi_-\rangle\langle\tilde{\chi}_-\rangle + \cdots\,. \end{aligned} \tag{4.91}$$

In the absence of the θ-term, only those terms in $\mathcal{L}^{(4)}_{\pi N}$ proportional to the LECs $\tilde{l}_3$, l'_3, $\tilde{l}_7$ and l'_7 contain P- and T-violating components which are induced by the

$qCEDM$. Due to the insignificance of the P- and T-conserving components of $\langle\tilde{\chi}_\pm\rangle$ compared to those of $\langle\chi_\pm\rangle$, the P- and T-violating terms from the structures proportional to the LECs l'_3 and l'_7 clearly dominate.

All these statements are transferable to the pion-nucleon sector: the leading P- and T-violating terms induced by the $qCEDM$ in the pion-nucleon Lagrangian are contained in

$$\begin{aligned}\mathcal{L}^{(2)}_{\pi N} &= c_1\langle\chi_+\rangle N^\dagger N + \tilde{c}_1\langle\tilde{\chi}_+\rangle N^\dagger N \\ &\quad + c_5 N^\dagger\hat{\chi}_+ N + \tilde{c}_5 N^\dagger\hat{\tilde{\chi}}_+ N + \cdots \,. \end{aligned} \tag{4.92}$$

If the $qCEDM$ is the sole source of P and T violation, only the structures proportional to the LECs $\tilde{c}_1$ and $\tilde{c}_5$ contain P- and T-violating terms. By the same procedure of duplicating structures with insertions of $\chi_\pm$, higher order P- and T-violating πNN-, γNN- and $4N$-terms are obtained from $\mathcal{L}^{(3)}_{\pi N}$, $\mathcal{L}^{(4)}_{\pi N}$ and $\mathcal{L}_{4N}$ as described above for the θ-term case. All P- and T-violating terms listed above for the θ-term case are also induced by the $qCEDM$ when the source fields and LECs are replaced by the ones for the $qCEDM$. The findings regarding the naive set of P- and T-violating terms induced by the $qCEDM$ presented here are in agreement with those of [39] derived in the Weinberg formulation of $SU(2)$ ChPT at relevant orders.

$4qLR$-op

The $4qLR$-op eq. (3.34) transforms as a basis state of the $(1,1)^+$ irreducible representation of $O(4)$ according to eq. (4.61). Expressing the positive parity basis states of the $(1,1)^+$ representation in eq. (B.58) in terms of symmetric tensor products of quark bilinears, one obtains the new and separate isospin multiplet

$$(1,1)^+ \;:\quad \left(\bar{q}\tau^i\gamma^\mu q\,\bar{q}\tau^j\gamma_\mu q - \bar{q}\tau^i\gamma^\mu\gamma_5 q\,\bar{q}\tau^j\gamma_\mu\gamma_5 q,\, \epsilon^{klm}\,\bar{q}\tau_l\gamma\mu q\,\bar{q}\tau_m\gamma_\mu\gamma_5 q\right), \tag{4.93}$$

where $i,j,k = 1,2,3$ and the summation only over the indices l,m in the three P- and T-violating terms is implied. The isospin multiplet eq. (4.93) consists of six P- and T-conserving (left part) and three P- and T-violating (right part, see eq. (4.64)) quark quadrilinears.

Due to the absence of source fields in standard ChPT which transform as basis states of the $(1,1)^+$, a genuinely new set of source fields has to be defined (by the symmetric tensor product form of eq. (B.57) and eq. (B.58))

$$q_{ij}\big((\tau_i)_R(\tau_j)_L + (\tau_i)_L(\tau_j)_R\big) + r_k\epsilon^{klm}(\tau_l)_R(\tau_m)_L\,, \tag{4.94}$$

with $i,j,k,l,m = 1,2,3$ and summation only over the indices l,m in the second term. The symmetric tensor q_{ij} and the vector r_k are the $(1,1)^+$ counter-parts of the quantities s_0, s_i and p_0, p_i associated with the $(1/2,1/2)^\pm$ representations in standard ChPT. Note that the implied product of τ-matrices in this formula is the symmetric tensor product of matrices (see eq. (B.86)), whose constituent τ-matrices transform under $SU(2)_L \times SU(2)_R$ as indicated by the subscripts L and R (see appendix B for details):

$$\begin{aligned} & q_{ij}\big((\tau_i)_R(\tau_j)_L + (\tau_i)_R(\tau_j)_L\big) + r_k\epsilon^{klm}(\tau_l)_R(\tau_m)_L \\ \mapsto\ & q_{ij}\big((R\tau_iR^\dagger)_R(L\tau_jL^\dagger)_L + (L\tau_iL^\dagger)_L(R\tau_jR^\dagger)_R\big) + r_k\epsilon^{klm}(R\tau_lR^\dagger)_R(L\tau_mL^\dagger)_L\,. \end{aligned} \tag{4.95}$$

According to eq. (B.75) and eq. (B.76) in appendix B, there is another basis of the $(1,1)^+$ representation which exhibits the chiral structure associated with the product of familiar source fields $p_3 s_0$:

$$\begin{aligned} & \frac{1}{2} i r_k \Big([(\tau_k)_4 - (\tau_k)_4^\dagger][(\mathbb{1})_4 + (\mathbb{1})_4^\dagger] - (\tau_k \leftrightarrow \mathbb{1})\Big) \\ \mapsto\ & \frac{1}{2} i r_k \Big([(L\tau_kR^\dagger)_4 - (L\tau_kR^\dagger)_4^\dagger][(L\mathbb{1}R^\dagger)_4 + (L\mathbb{1}R^\dagger)_4^\dagger] - (\tau_k \leftrightarrow \mathbb{1})\Big)\ , \end{aligned} \tag{4.96}$$

where the subscript in $(t)_4$, $t = \mathbb{1}, \tau_1, \tau_2, \tau_3$, and the dagger indicates the above defined $SU(2)_L \times SU(2)_R$ transformation behavior of τ_k and $\mathbb{1}$. The three source fields in eq. (4.96) correspond to the P- and T-violating basis states of the $(1,1)^+$ representation in decompositions of the symmetric tensor products of the irreducible representations $(1/2,1/2)^\pm \otimes (1/2,1/2)^\pm$ (see eq. (B.88)). As previously mentioned, the two expressions of the source fields associated with the P- and T-violating basis states of the $(1,1)^+$ representation in eq. (4.94) and eq. (4.96) are Fierz equivalent.

The $4qLR$-op induces then all terms in the amended ChPT Lagrangian with insertions of the new building block η_+, which is defined four the two expressions of the source fields eq. (4.94) and eq. (4.96) by

$$\eta_+ \ := \ (2Dr_k)\epsilon^{klm}(u^\dagger\tau_l u)(u\tau_m u^\dagger) + \cdots\ , \tag{4.97}$$

$$\begin{aligned} \eta_+ \ &:= \ i(Dr_k)\big((u^\dagger\tau_k u^\dagger - u\tau_k u)(u\mathbb{1}u + u^\dagger\mathbb{1}u^\dagger) - (\tau_k \leftrightarrow \mathbb{1})\big) + \cdots \\ &= \ i(2Dr_k)\big((u^\dagger\tau_k u^\dagger)(u\mathbb{1}u) - (u\tau_k u)(u^\dagger\mathbb{1}u^\dagger)\big) + \cdots\ ,, \end{aligned} \tag{4.98}$$

where the dots denote terms proportional to P- and T-conserving source fields and the product between the brackets (i.e. $(\cdots)(\cdots)$) is understood to be the symmetric tensor product of matrices. The quantity D is defined by

$$\langle 0|\bar{u}\gamma^\mu u\bar{u}\gamma_\mu u - \bar{u}\gamma^\mu\gamma_5 u\bar{u}\gamma_\mu\gamma_5 u|0\rangle = D + \cdots\ , \tag{4.99}$$

where the P- and T-conserving component of the building block η_+ obtained from eq. (4.94),

$$\eta_+ = (2Dq_{ij})((u\tau_i u^\dagger)(u^\dagger\tau_j u) + (u^\dagger\tau_i u)(u\tau_j u^\dagger)) + \cdots\ , \tag{4.100}$$

has been utilized.

In analogy to the definition of the building block $i\chi_-$ as a P- and T-violating counterpart of χ_+ in standard ChPT, the building block η_- (which corresponds to the $(1,1)^-$ representation) can be defined by (see eq. (B.77) and eq. (B.78))

$$\eta_- = (2Dr_k)\big((u^\dagger\tau_k u^\dagger)(u\mathbb{1}u) + (u\tau_k u)(u^\dagger\mathbb{1}u^\dagger)\big) + \cdots . \tag{4.101}$$

The terms induced by the $4qLR$-op in the effective Lagrangian are obtained by compiling the list of all chiral structures with insertions of $\eta_\pm$ and by subsequently replacing (see eq. (3.34))

$$r_3 \to \frac{\nu_1 V_{ud}}{2}, \quad r_1 = r_2 = q_{ij} = 0\,. \tag{4.102}$$

In the pion sector, the first expression of η_+ eq. (4.97) yields at leading order the P- and T-violating terms[3]

$$(2Dr_k)\epsilon^{klm}\langle\tau_l U\tau_m U^\dagger\rangle = (2Dr_k)8\frac{\pi_k}{F_\pi}\left(\mathbb{1} - \frac{2}{3}\frac{\pi^2}{F_\pi^2}\right) + \cdots , \tag{4.103}$$

whereas the second expression of η_+ eq. (4.98) gives a more familiar structure with identical P- and T-violating terms:

$$\begin{aligned} i(2Dr_k)(\langle\tau_k U^\dagger\rangle\langle U\rangle - \langle\tau_k U\rangle\langle U^\dagger\rangle) &= \frac{i(2Dr_k)}{2}\langle\tau_k U^\dagger - \tau_k U\rangle\langle U + U^\dagger\rangle \\ &= (2Dr_k)8\frac{\pi_k}{F_\pi}\left(\mathbb{1} - \frac{2}{3}\frac{\pi^2}{F_\pi^2}\right) + \cdots . \end{aligned} \tag{4.104}$$

The chiral structure in eq. (4.104) is resemblant of the P- and T-violating component of the familiar chiral structure $\langle\chi_+\rangle^2$ in $\mathcal{L}_\pi^{(4)}$ of eq. (4.24) with the product of conventional source fields $(2Bs_0)(2Bp_3)$ replaced by $(2Dr_3)$. In this sense, an insertion of η_+ is equivalent to two insertions of χ_+, for instance, with the replacement $(2Bp_3)(2Bs_0) \to (2Dr_3)$. In the pion sector, the leading term is thus given by

$$\langle\chi_+\rangle^2 \rightsquigarrow (2Dr_k)8\frac{\pi_3}{F_\pi}\left(\mathbb{1} - \frac{2}{3}\frac{\pi^2}{F_\pi^2}\right) + \cdots . \tag{4.105}$$

The next pion tadpole term arises from a chiral structure with a simultaneous insertion of η_+ and χ_+:

$$\frac{l_{4qLR}}{16}(2Dr_3)(2Bs_0)\epsilon^{3lm}\langle\tau_l U\tau_m U^\dagger\rangle\langle U^\dagger + U\rangle = l_{4qLR}8Dr_3Bs_0\frac{\pi_3}{F_\pi} + \cdots . \tag{4.106}$$

[3] Note that the selection of the ground state procedure discussed in the next section ensures parametrization invariant 3π vertices. The naive 3π vertex in eq. (4.97) is not the same for all parametrizations.

The leading order P- and T-violating πNN vertices induced by the $4qLR$-op can be extracted from the fourth-order Lagrangian $\mathcal{L}_{\pi N}^{(4)}$ by the above described replacement of the source fields $(2Bs_3)(2Bp_3)$ and of the LEC[4]:

$$\langle\chi_+\rangle^2 N^\dagger N \rightsquigarrow c_{4qLR}(2Dr_k)8\frac{\pi_3}{F_\pi}\left(\mathbb{1}-\frac{2}{3}\frac{\pi^2}{F_\pi^2}\right)N^\dagger N+\cdots\,. \tag{4.108}$$

The $4qLR$-op also induces all isospin-violating terms in the Lagrangian $\mathcal{L}_{4N}$ in eq. (4.80) at leading order in the expansion of pion fields, i.e. those proportional to the LECs C_1, C_2, C_7, C_8. The corresponding terms induced by the $4qLR$-op are obtained by insertions of $\eta_\pm$. The remaining isospin-conserving terms in eq. (4.80) at leading order in the pion-field expansion are obtained by simultaneous insertions of $\eta_\pm$ and $\chi_\pm$ and are therefore suppressed. The γNN vertices in eq. (4.79) at leading order in the pion-field expansion are also induced by the $4qLR$-op. The isospin-conserving term in eq. (4.79) is in this case generated by a simultaneous insertion of η_- and $\hat{f}_+^{\mu\nu}$, whereas the isospin-violating term arises from an insertion of η_- and $\langle f_+^{\mu\nu}\rangle$. The naive set of P- and T-violating terms induced by the $4qLR$-op derived here is in agreement with the previous results of [39] derived in the Weinberg formulation of $SU(2)$ ChPT.

qEDM

The isospin-conserving and isospin-violating components of the $qEDM$ eq. (3.32) transform identically to the corresponding components of the $qCEDM$ as basis states of the $(1/2,1/2)^-$ and $(1/2,1/2)^+$ irreducible representations of $O(4)$. In contrast to the $qCEDM$, the $qEDM$ has an explicit insertion of the photon field. This requires the new source field to be identified with the photon field and to transform identically to the source fields $\tilde{p}_0$ and $\tilde{p}_3\tau_3$ in $\tilde{\chi}$. The set of all P- and T-violating terms in the amended ChPT Lagrangian is therefore obtained from all possible insertions of the building blocks $\tilde{\chi}_\pm$ and $F^{\mu\nu}$ by replacing the $qCEDM$ source fields $(2C\tilde{p}_3)$ and $(2C\tilde{p}_0)$ by the new defined $qEDM$ counterparts v_0 and w_3. All resulting terms contain at least one photon field, which has to be integrated out in order to generate P- and T-violating pion-, πNN- and $4N$ vertices at the price of picking up a loop factor of $\alpha_{em}/(4\pi)$. Therefore, all such vertices are heavily suppressed by a factor of at least $\alpha_{em}/(4\pi)$ with respect to vertices involving photons. The leading P- and T-violating γNN-terms are given

[4]Note that the $3\pi NN$ vertex in eq. (4.108) is not in a parametrization invariant form. To obtain this vertex in another parametrization, eq. (4.108) has to be replaced by

$$c_{4qLR}(2Dr_k)8\frac{\pi_3}{F_\pi}\left(\mathbb{1}-\frac{2}{3}\frac{\pi^2}{F_\pi^2}\right)N^\dagger N\to c_{4qLR}(2Dr_k)8\frac{\pi_3}{F_\pi}\left(\mathbb{1}-\frac{1}{2}\frac{\pi^2}{F_\pi}-\alpha\frac{\pi^2}{F_\pi^2}\right)N^\dagger N\,. \tag{4.107}$$

by

$$i\langle\tilde{\chi}_-\rangle N^\dagger S_\mu v_\nu N F^{\mu\nu} \rightsquigarrow 4v_0\left(1-\frac{\pi^2}{2F_\pi^2}\right)N^\dagger S_\mu v_\nu N F^{\mu\nu}+\cdots\,, \tag{4.109}$$

$$iN^\dagger\hat{\chi}_- S_\mu v_\nu N F^{\mu\nu} \rightsquigarrow 2w_3 N^\dagger\left(\tau_3-\frac{\vec{\pi}\cdot\vec{\tau}\pi_3}{2F_\pi^2}\right)S_\mu v_\nu N F^{\mu\nu}+\cdots\,. \tag{4.110}$$

These terms constitute the leading isoscalar and isovector contributions to the single-nucleon EDMs induced by the $qEDM$ and they are in agreement with the previous results derived in the Weinberg formulation of $SU(2)$ ChPT which are published in [39, 49].

$4q$-op and $gCEDM$

The $4q$-op and the $gCEDM$ are chiral singlets and thus transform as the basis state of the $(0,0)^-$ irreducible representation of $O(4)$. They are not connected to other terms in standard QCD by $SU(2)_L\times SU(2)_R$ or $U(1)_A$ transformations as the θ-term. In order to derive all terms in the amended ChPT Lagrangian which are induced by the $gCEDM$ and the $4q$-op, a new P- and T-violating source field has to be introduced that transforms as an $SU(2)_L\times SU(2)_R$ singlet. The leads to the definition of the new fundamental building block ς^- and its P- and T-conserving partner chiral-singlet building block ς^+ (analogous to the definition of $i\chi_-$ as a partner building block for χ_+). Since ς^- is a P- and T-violating source field, there are no non-vanishing chiral structures with insertions of ς^- (note that a P-violating counterpart to the standard source field $v_\mu^{(s)}$ would also not generate non-vanishing terms). The complete list of P- and T-violating terms in the amended ChPT Lagrangian induced by the $4q$-op and $gCEDM$ is thus obtained by all possible combinations of ς^+ with the fundamental building blocks of standard ChPT (and setting $p_0=p_3=0$ if $\bar{\theta}=0$). This procedure can be illustrated by the following example: let A_{PT} and B_{PT} be two conventional fundamental building blocks with P- and T-violating partner building blocks $\tilde{A}_{\not{P}\not{T}}$ and $\tilde{B}_{\not{P}\not{T}}$. Chiral structures induced by the $4q$-op and $gCEDM$ are then of the form:

$$\varsigma^+\tilde{A}_{\not{P}\not{T}}B_{PT},\quad \varsigma^+A_{PT}\tilde{B}_{\not{P}\not{T}}\,. \tag{4.111}$$

Some chiral structures induced by the $4q$-op and the $gCEDM$ obtained in the manner described above are given by

$$\begin{aligned}
\mathcal{L}_\pi &: \; i\varsigma^+\langle\chi_-\rangle,\, i\varsigma^+\langle\chi_-\rangle\langle\chi_+\rangle,\,\cdots\,,\\
\mathcal{L}_{\pi N} &: \; i\varsigma^+\langle\chi_-\rangle N^\dagger N,\, i\varsigma^+N^\dagger\hat{\chi}_- N,\, i\varsigma^+N^\dagger[S\cdot u, v\cdot u]N,\\
&\quad\; \varsigma^+\langle f_+^{\mu\nu}\rangle N^\dagger S_\mu v_\nu N,\, \varsigma^+N^\dagger\hat{f}_+^{\mu\nu}S_\mu v_\nu N,\,\cdots\,,\\
\mathcal{L}_{4N} &: \; \varsigma^+N^\dagger N\mathcal{D}_\mu(N^\dagger S^\mu N),\, \varsigma^+N^\dagger\vec{\tau}N\cdot\mathcal{D}_\mu(N^\dagger\vec{\tau}S^\mu N),\,\cdots\,.
\end{aligned} \tag{4.112}$$

Induced vertices involving pions emerge from terms with insertions of $\chi_\pm$ (or multiple derivatives (see the third term of $\mathcal{L}_{\pi N}$ in eq. (4.112))) and are thus suppressed by M_π^2/m_N^2. This observation is just a reflection of Goldstone's theorem. The leading P- and T-violating γNN and $4N$ vertices emerge from the third and fourth line of eq. (4.112), respectively. These results are in agreement with the findings of [39] derived in the Weinberg formulation of $SU(2)$ ChPT.

4.3 Selection of the ground state

If the ChPT action functional S is invariant under $SU(2)_L \times SU(2)_R$ transformation, the $SU(2)_V$ subgroup to which $SU(2)_L \times SU(2)_R$ breaks down is not unique. The presence of terms in the (amended) QCD Lagrangian or equivalently in $\mathcal{L}_\pi$ which explicitly violate the chiral $SU(2)_L \times SU(2)_R$ symmetry impose a constraint on the selection of the $SU(2)$ subgroup such that it is then in general well defined [63, 100]. The definition of this subgroup also implies the definition of the ground state of QCD and of (amended) ChPT around which the effective field theory is expanded. The selection of the ground state procedure is referred to as *vacuum alignment* in the Weinberg formulation of ChPT [41, 42]. The impact of an altered ground state due to effective dimension-six sources has been computed recently in the Weinberg formulation of ChPT in [39].

This section provides a thorough derivation of the ground state selection procedure and its impact on the effective Lagrangian in the Gasser-Leutwyler formulation of SU(2) *ChPT*[5]. This section is organized as follows: before computing the ground states of (amended) ChPT for all considered sources of P and T violation, the general selection procedure of the ground state in standard QCD and standard ChPT in the Gasser-Leutwyler formulation is discussed. The set of relevant P- and T-violating vertices for our analysis is given by

$$\begin{aligned} & \mathcal{L}_\pi^{(2)} + \mathcal{L}_\pi^{(4)} + \mathcal{L}_{\pi N}^{(2)} + \mathcal{L}_{\pi N}^{(4)} + \mathcal{L}_{4N} \\ = \quad & m_N \Delta_3 \pi_3 \pi^2 + g_0 N^\dagger \vec{\pi} \cdot \vec{\tau} N + g_1 N^\dagger \pi_3 N \\ & - 2 d_0 N^\dagger S^\mu v^\nu N F_{\mu\nu} - 2 d_1 N^\dagger \tau_3 S^\mu v^\nu N F_{\mu\nu} \\ & + C_1^0 N^\dagger N \mathcal{D}_\mu (N^\dagger S^\mu N) + C_2^0 N^\dagger \vec{\tau} N \cdot \mathcal{D}_\mu (N^\dagger S^\mu \vec{\tau} N) \\ & + C_1^3 N^\dagger \tau_3 N \mathcal{D}_\mu (N^\dagger S^\mu N) + C_2^3 N^\dagger N \mathcal{D}_\mu (N^\dagger \tau_3 S^\mu N) + \cdots . \end{aligned} \tag{4.113}$$

As the main result of this chapter, the coupling constants in eq. (4.113) are either calculated explicitly or estimated by the means of NDA and the relative ordering by their absolute values is identified for each source of P and T violation. By a detailed study, all other vertices which are not displayed in eq. (4.113) prove to yield negligible contributions to the EDMs of light nuclei and are not discussed in this section.

4.3.1 Selection of the ground state in standard QCD and ChPT

The correct $SU(2)_V$ subgroup of standard QCD is identified by minimizing the QCD potential

$$V = \int d^4x \, (s_0 \bar{q} q + s_3 \bar{q} \tau_3 q - i p_0 \bar{q} \gamma_5 q - i p_3 \bar{q} \gamma_5 \tau_3 q) \,. \tag{4.114}$$

[5] Parts of this section were published in [101].

Since explicit chiral symmetry breaking constitutes at most a small perturbation, the minimum can be identified by an infinitesimal variation of the quark fields defined by:

$$q \mapsto \exp(i\tau_3 \delta\,\alpha_V^3 + i\gamma_5\tau_3\,\delta\alpha_A^3)q\,, \tag{4.115}$$

i.e. the multiplication of q by a diagonal matrix (this corresponds to the procedure presented for $SU(3)$ ChPT in [102]). This variation yields the ground state condition

$$\delta V = 2\int d^4x\,\bar{q}(s_0 i\gamma_5\tau_3 + s_3 i\gamma_5 + p_0\tau_3 + p_3)q\,\delta\alpha_A^3 = 0\,. \tag{4.116}$$

The quark fields can be redefined by

$$q \mapsto \exp(i\gamma_5\tau_3\,\beta/2)q\,, \tag{4.117}$$

in order to obey the ground state condition eq. (4.116). However, the ground state condition is only fulfilled if $p_3/s_0 = p_0/s_3$ holds, which is in general not true. As argued in [42], the assumption that the ground state has to be P and T conserving as well as isospin conserving requires eq. (4.116) to be evaluated at

$$\bar{q}\tau_3 q = \bar{q}i\gamma_5 q = \bar{q}i\gamma_5\tau_3 q = 0\,, \tag{4.118}$$

which reduces the ground state condition eq. (4.116) to the requirement that the coefficient of $i\bar{q}\gamma_5\tau_3 q$ in eq. (4.114) has to vanish (i.e. $p_3' = 0$ of eq. (4.139)). This condition is obeyed if the angle β in the transformation eq. (4.117) applied to the quark fields in eq. (4.114) is chosen to be

$$\beta = \arctan\left(\frac{p_3}{s_0}\right)\,. \tag{4.119}$$

The ground state selection procedure can equivalently be carried out in ChPT. The ground state is identified by minimizing the leading order potential in the pion sector Lagrangian of ChPT which is given by

$$V = -\int d^4x \frac{F_\pi^2}{4}\langle \chi U^\dagger + U\chi^\dagger\rangle\,, \tag{4.120}$$

with

$$\chi = 2B(s_0\mathbb{1} + s_3\tau_3 + ip_0\mathbb{1} + ip_3\tau_3)\,, \tag{4.121}$$

as usual. The minimum of this functional is identified by a variation of $U = u^2$: since for each pair $g, g' \in SU(2)$ there is a $\tilde{g} \in SU(2)$ such that $g' = \tilde{g}g$, a variation of the field $U(x) \in SU(2)$ amounts to the multiplication by an element $G(x) \in SU(2)$:

$$U(x) \mapsto G(x)U(x) = \exp(i\vec{\tau}\cdot\vec{\alpha}(x))U(x)\,. \tag{4.122}$$

The minimization of V leads to

$$\delta V = i\frac{F_\pi^2}{4}\int d^4x\langle -\chi U^\dagger\tau_i + \tau_i U\chi^\dagger\rangle\alpha_i \;=\; 0\,, \tag{4.123}$$

which gives the ground state conditions

$$\langle\tau_i U\chi^\dagger - \chi U^\dagger\tau_i\rangle = 0\,, \quad i = 1,2,3\,. \tag{4.124}$$

For $p_0 = p_3 = 0$, these conditions reduce to the set of equations

$$\begin{aligned} i = 1,2,3: \qquad & s_0\langle\tau_i(U - U^\dagger)\rangle + s_3\langle\tau_3\tau_i U - \tau_i\tau_3 U^\dagger\rangle = 0\,,\\ \Leftrightarrow \quad & s_0\langle\tau_i(U - U^\dagger)\rangle - s_3\epsilon^{3ij}\langle\tau_j(U + U^\dagger)\rangle = 0\,,\\ \Leftrightarrow \quad & s_0\langle\tau_i(U - U^\dagger)\rangle = 0\,, \end{aligned} \tag{4.125}$$

which has the unique minimum solution $U = \mathbb{1}$. $p_0 \neq 0$ does not alter the ground state since the corresponding terms in the ground state conditions eq. (4.124),

$$-\,ip_0\langle\tau_i(U + U^\dagger)\rangle = 0\,, \tag{4.126}$$

vanish trivially for $i = 1,2,3$ (there is actually no term proportional to p_0 in $\mathcal{L}_\pi^{(2)}$ of eq. (4.20)). The situation is entirely different for $p_3 \neq 0$, which alters the ground state conditions eq. (4.124) to

$$i = 1,2: \quad s_0\langle\tau_i(U - U^\dagger)\rangle - ip_3\epsilon^{3ij}\langle\tau_j(U - U^\dagger)\rangle = 0\,, \tag{4.127}$$

$$i = 3: \quad s_0\langle\tau_3(U - U^\dagger)\rangle - ip_3\langle U + U^\dagger\rangle = 0\,. \tag{4.128}$$

Eq. (4.127) requires the U matrix to be of the form

$$U = \exp(i\tau_3\beta) = \cos(\beta) + i\tau_3\sin(\beta)\,. \tag{4.129}$$

The insertion of this expression for U into eq. (4.128) yields the familiar ground state condition eq. (4.119):

$$\beta = \arctan\left(\frac{p_3}{s_0}\right)\,. \tag{4.130}$$

This demonstrates that the U matrix has to be transformed in the presence of a non-vanishing P- and T-violating and isospin-violating source field p_3 by an axial rotation $A{=}R{=}L^\dagger{=}\exp(i\tau_3\beta/2)$:

$$U \mapsto AUA\,. \tag{4.131}$$

The ground state itself is then given by $U_0 = A^2 \approx \exp(i\,\tau_3\,p_3/s_0)$.

The ground state conditions eq. (4.128) in the presence of a non-vanishing source field p_3 is somehow obvious due to the following group theoretical argument: as demonstrated in the previous section and in particular in appendix B, the source fields transform inversely to their associated quark bilinears as basis states of the $(1/2, 1/2)^{\pm}$ irreducible representations of $O(4)$:

$$(1/2, 1/2)^{+} \quad : \quad (p_1\tau_1, p_2\tau_2, p_3\tau_3, s_0)\,, \tag{4.132}$$
$$(1/2, 1/2)^{-} \quad : \quad (s_1\tau_1, s_2\tau_2, s_3\tau_3, ip_0)\,. \tag{4.133}$$

Any $SU(2)_L\times SU(2)_R$ transformation of the quark fields or the matrix U, therefore, is equivalent to the inverse $SU(2)_L\times SU(2)_R$ transformation of the source fields:

$$(1/2, 1/2)^{+} : \quad (p_1\tau_1, p_2\tau_2, p_3\tau_3, s_0) \mapsto (p_1'\tau_1, p_2'\tau_2, p_3'\tau_3, s_0')\,, \tag{4.134}$$
$$(1/2, 1/2)^{-} : \quad (s_1\tau_1, s_2\tau_2, s_3\tau_3, ip_0) \mapsto (s_1'\tau_1, s_2'\tau_2', s_3'\tau_3, ip_0')\,. \tag{4.135}$$

The axial transformation of the source fields can then by chosen to yield $p_3' = 0$ and the ground state is again simply given by $U_0' = \mathbb{1}$. If this axial transformation is undone, the actual ground state for $p_3 \neq 0$ is on the path defined by the one-parameter subgroup $\exp(i\tau_3\beta)$. The infinitesimal axial $SU(2)_L\times SU(2)_R$ transformation of the quark bilinears or the U matrix to remove p_3 corresponds the following inverse axial $SU(2)_L\times SU(2)_R$ transformation of the source fields s_0, s_3, p_0 and p_3:

$$s_0' = s_0 + \beta p_3 + \cdots = s_0 + p_3^2/s_0 + \cdots\,, \tag{4.136}$$
$$s_3' = s_3 + \beta p_0 + \cdots = s_3 + p_3 p_0/s_0 + \cdots\,, \tag{4.137}$$
$$p_0' = p_0 - \beta s_3 + \cdots = p_0 - p_3 s_3/s_0 + \cdots\,, \tag{4.138}$$
$$p_3' = p_3 - \beta s_0 + \cdots = p_3 - p_3 + \cdots = 0 + \cdots\,. \tag{4.139}$$

As a result of the axial transformation, the original terms proportional p_3 are absent from the QCD Lagrangian and equivalently from the entire effective Lagrangian.

The ground state selection procedure ensures the absence of leading-order pion tadpole terms. However, a further pion tadpole term emerges in the pion sector Lagrangian $\mathcal{L}_\pi^{(4)}$ of eq. (4.24),

$$-\frac{l_7}{16}\langle \chi U^\dagger - U\chi^\dagger\rangle^2 = \cdots - 2l_7(2Bp_0)(2Bs_3)\frac{\pi_3}{F_\pi}\left(1 - \frac{2}{3}\frac{\pi^2}{F_\pi^2}\right) + \cdots\,, \tag{4.140}$$

which can be removed by another axial rotation $A' = \exp(i\tau_3\beta'/2)$. Pion tadpoles which occur at subleading orders cannot be rotated away within one specific order, since such a rotation would reintroduce the tadpole terms previously removed from lower orders, in this case the leading order. The axial rotation has to be chosen such that no tadpoles occur at all orders up-to-and-including the one from which the tadpole is to be removed. In the above case, this entails that the axial rotation has to generate terms in the leading order pion sector Lagrangian $\mathcal{L}_\pi^{(2)}$

(eq. (4.20)) which cancel the tadpole term in $\mathcal{L}_\pi^{(4)}$ (eq. (4.24)). This procedure may be iterated up to any desired order.

Before concluding the general discussion about the selection of the ground state, a few further issues have to be mentioned. The electromagnetic field A_μ is not contained in eq. (4.120) and does thus not affect the selection of the ground state. All terms apart from the l_3 and the l_7 term in $\mathcal{L}_\pi^{(4)}$ are invariant under the axial rotation A: the l_1 and the l_2 term are invariant since $[D_\mu, A] = 0$. In the sole presence of the electromagnetic field, the l_4 term vanishes due to

$$D_\mu \chi = ie[\chi, \mathcal{Q}] = 0\,, \tag{4.141}$$

where $\mathcal{Q}$ is the $SU(2)$ quark charge matrix of eq. (2.34). The l_5 and the l_6 term are invariant under A since

$$[R_{\mu\nu}, A] = [L_{\mu\nu}, A] = 0\,, \tag{4.142}$$

and the h_i-terms are designed to be chiral singlets which are also invariant under A. Therefore, the presence of an electromagnetic field A_μ does not affect the selection of the ground state.

The selection of the ground state also ensures parametrization invariant leading order terms in the pion sector. This statement can be illustrated by the following example: let the U matrix be the one defined in eq. (4.143) with a reparametrization function g,

$$U = \exp\left(i\frac{\vec{\pi}\cdot\vec{\tau}}{F_\pi} g\left(\frac{\pi^2}{F_\pi^2}\right)\right)\,, \quad g\left(\frac{\pi^2}{F_\pi^2}\right) = 1 + \left[\alpha + \frac{1}{6}\right]\frac{\pi^2}{F_\pi^2} + \cdots\,, \tag{4.143}$$

where α is a real number. Eq. (4.140) before the second axial rotation to remove the subleading tadpole term is then given by

$$-\frac{l_7}{16}\left(\chi U^\dagger - U\chi^\dagger\right)^2 = -2l_7(2Bp_0)(2Bs_3)\frac{\pi_3}{F_\pi}\left(1 - \frac{1}{2}\frac{\pi^2}{F_\pi^2} + \alpha\frac{\pi^2}{F_\pi^2}\right) + \cdots\,. \tag{4.144}$$

The second axial rotation $A' = \exp(i\tau_3\beta'/2)$ causes a shift of $\mathcal{L}_\pi^{(2)}$ of eq. (4.20) which cancels the pion tadpole term and the parametrization dependent component of the 3π vertex in eq. (4.144):

$$\frac{F_\pi^2}{4}\langle \chi U^\dagger + \chi^\dagger U\rangle \to -\beta'(2Bs_0)F_\pi \pi_3\left(1 + \alpha\frac{\pi^2}{F_\pi^2}\right) + \cdots\,. \tag{4.145}$$

Another issue is the role of $U(1)_A$ transformations. The $U(1)_A$ anomaly of QCD gives rise to the Wess-Zumino-Witten term in ChPT discussed in section 4.1.2, which is given by [46]:

$$\mathcal{L}_{WZW} = -\frac{F_\pi^2}{4}\frac{a}{N_c}\left[\frac{i}{2}(\ln(\det(U) - \ln(\det(U^\dagger))\right]^2\,, \tag{4.146}$$

(N_c: number of colors, a: constant related to the η, η' masses as mentioned below) and exhibits the same behavior under $U(1)_A$ transformations as the fermion measure in the generating functional of QCD eq. (2.46). This ensures the one-to-one correspondence with respect to axial $U(1)_A$ transformations between the QCD Lagrangian and ChPT. In standard $SU(2)_L \times SU(2)_R$ ChPT, the generator of $U(1)_A$ is not associated with an additional degree of freedom (the η or η') and is irrelevant for the selection of the ground state. If the $U(1)_A$ generator is regarded as an additional degree of freedom which might be called $\tilde{\eta}$ and which is an admixture of the physical η and η' mesons, the Wess-Zumino-Witten term constitutes a mass term with $M_{\tilde{\eta}}^2 = 2a/N_c$ for that additional degree of freedom. In the resulting $U(2)_L \times U(2)_L$ ChPT, the chiral symmetry breaking terms determine the $U(2)_V$ subgroup to which $U(2)_L \times U(2)_R$ breaks down. The ground state conditions are more complex due to the additional degree of freedom. In particular, also $\tilde{\eta}$ tadpoles emerge at leading order in the pion sector Lagrangian which have to be removed. Further subtleties of $U(2)_L \times U(2)_R$ ChPT have also to be taken into consideration: the low-energy constants, for instance, are in general not the same as their $SU(2)_L \times SU(2)_R$ counterparts, which is particularly true for l_7 in $\mathcal{L}_\pi^{(4)}$ since its size can largely be attributed to manifestations of the η and η' (see the paragraphs on $\eta - \pi^0$-mixing in [43, 44]).

4.3.2 Selection for the θ-term and the hierarchy of coupling constants

We will now focus on the selection of the ground state in the presence of the θ-term. We start from the expression of the θ-term as a complex phase of the quark mass matrix as in eq. (2.65). As explained in the previous section, the correct ground state is obtained by subjecting the quark fields in the QCD Lagrangian or likewise the matrix U to an axial rotation $A = \exp(i\tau_3\beta/2)$ with (see eq. (4.75) and eq. (4.119))

$$\beta = \arctan\left(\frac{p_3}{s_0}\right) = \frac{\bar{\theta}}{2}\epsilon + \mathcal{O}(\bar{\theta}^3)\,. \tag{4.147}$$

This implies a simultaneous shift of the parameter p_0 by (see eq. (4.72) and eq. (4.138))

$$p_0 = \frac{\bar{\theta}}{2}\bar{m} \to p_0' = \frac{\bar{\theta}}{2}\bar{m}\left(1-\epsilon^2\right) = \bar{\theta}\frac{m_u m_d}{m_u + m_d} \equiv \bar{\theta} m^*\,, \tag{4.148}$$

with $\bar{m} = (m_u + m_d)/2$, $\epsilon = (m_u - m_d)/(m_u + m_d) = -0.35 \pm 0.10$ [34] and the reduced quark mass m^*. The θ-term has thus been rotated into the isospin-conserving component of the quark mass matrix:

$$\bar{\theta} m^* \bar{q} i\gamma_5 q\,. \tag{4.149}$$

This redefinition of the quark fields also alters the naive set of P- and T-violating terms in the ChPT Lagrangian of section 4.2.2 by setting $p_0 = \bar{\theta} m^*$ and $p_3 = 0$ in eqs. (4.75)-(4.80). Furthermore, the subleading pion tadpole term in eq. (4.140) has to be canceled by a small shift of the leading order P- and T-conserving term proportional to s_0 in $F_\pi^2 \langle \chi_+ \rangle /4$ of eq. (4.75) that is induced by a second axial rotation of the ground state defined by the angle β' (see eq. (4.139)):

$$\beta'(\bar{\theta}) = -\frac{4Bl_7 s_3 p_0}{F_\pi^2 s_0} + \cdots = -l_7(1-\epsilon^2)\epsilon \frac{M_\pi^2}{F_\pi^2}\bar{\theta} + \mathcal{O}(\bar{\theta}^2)\,. \tag{4.150}$$

This shift of $F_\pi^2 \langle \chi_+ \rangle /4$ removes the tadpole term and modifies the term proportional to $\pi_3 \pi^2$ in $-l_7 \langle \chi_- \rangle^2/16$ (see eq. (4.76) and eq. (4.140)):

$$\frac{F_\pi^2}{4}\langle \chi_+ \rangle \to -\beta'(\bar{\theta})(2Bs_0)F_\pi \pi_3 \left(1 - \frac{\pi^2}{6F_\pi^2}\right) + \cdots\,, \tag{4.151}$$

The LEC l_7 included in β' is related to the strong-interaction component of the pion mass-square splitting $(\delta M_\pi^2)^{\rm str}$ mentioned in eq. (4.25) and given by [43]

$$\begin{aligned} (\delta M_\pi^2)^{\rm str} &:= \left(M_{\pi^+}^2 - M_{\pi^0}^2\right)\big|_{\rm strong} \\ &= 2(m_u - m_d)^2 B^2 l_7 / F_\pi^2 + \cdots \approx 2M_\pi \cdot 0.18\,\text{MeV}\,. \end{aligned} \tag{4.152}$$

The leading contribution to the 3π coupling constant Δ_3 in eq. (4.113) induced by the θ-term, Δ_3^θ, is obtained by adding the second term on the right-hand side of eq. (4.151) to the 3π term in eq. (4.76):

$$\begin{aligned} \Delta_3^\theta &= \frac{1}{m_N}\left(\frac{\beta'(\bar{\theta})(2Bs_0)}{6F_\pi} + \frac{4l_7(2Bs_3)(2Bp_0)}{3F_\pi^3}\right) = \frac{(\delta M_\pi^2)^{str}(1-\epsilon^2)}{4F_\pi m_N \epsilon}\bar{\theta} \\ &= (-0.0004 \pm 0.0002)\,\bar{\theta}\,. \end{aligned} \tag{4.153}$$

All additionally induced terms in the pion sector Lagrangian are of higher orders.

The redefinition of the ground state generates new structures in the pion-nucleon Lagrangian $\mathcal{L}_{\pi N}^{(2)}$ of eq. (4.77) as pointed out in [42]:

$$c_1 \langle \chi_+ \rangle N^\dagger N \;\to\; -4\beta'(\bar{\theta}) c_1 M_\pi^2 \frac{\pi_3}{F_\pi}\left(1 - \frac{\pi^2}{6\,F_\pi^2}\right) N^\dagger N + \cdots\,, \tag{4.154}$$

$$c_5 N^\dagger \hat{\chi}_+ N \;\to\; -2\beta'(\bar{\theta}) c_5 \epsilon M_\pi^2 N^\dagger \left(\frac{\vec{\pi}\cdot\vec{\tau}}{F_\pi} - \frac{(1-\epsilon^2)\bar{\theta}\,\tau_3}{2\epsilon}\right) N + \cdots\,. \tag{4.155}$$

The terms proportional to the LECs c_2, c_3, c_4, c_6 and c_7 in the pion-nucleon Lagrangian eq. (4.51) are invariant under the axial rotation A when the electromagnetic field is the sole external current. The second term on the right-hand side of eq. (4.155) is $\mathcal{O}(\bar{\theta}^2)$ and can be disregarded. The coupling constant of the P- and T-violating and isospin-conserving πNN vertex is then obtained by inserting eq. (4.148) into eq. (4.77) and adding eq. (4.155):

$$c_5\left(4Bm^*\bar{\theta} - 2\beta'(\bar{\theta})\epsilon M_\pi^2\right) N^\dagger \frac{\vec{\pi}\cdot\vec{\tau}}{F_\pi} N + \cdots . \tag{4.156}$$

These terms are proportional to the LEC c_5 and thus related to the to the quark mass induced part of the proton–neutron mass difference $\delta m_{np}^{\mathrm{str}}$ according to eq. (4.53). It can be quantified from three different sources: (i) the use of dispersion theory to quantify the electromagnetic part of the proton–neutron mass difference [94, 103–105], (ii) lattice QCD [106], or (iii) from charge-symmetry-breaking (CSB) studies of $pn \to d\pi^0$ [107]. All analyses lead to consistent results, where the most recent is given by [94][6]

$$4B(m_u - m_d)c_5 = \delta m_{np}^{\mathrm{str}} = (2.6 \pm 0.5)\,\mathrm{MeV}\,. \tag{4.157}$$

The first term in eq. (4.156) is the dominant contribution to the πNN coupling constant g_0 of eq. (4.113) induced by the θ-term, which is denoted by g_0^θ and equals

$$g_0^\theta = \frac{\delta m_{np}^{\mathrm{str}}(1-\epsilon^2)}{4F_\pi\epsilon}\,\bar{\theta} = (-0.018 \pm 0.007)\,\bar{\theta}\,. \tag{4.158}$$

This expression agrees with the prediction of ref. [50] when eq. (14) of ref. [50] is inserted into the corresponding eq. (8)[7]. It turns out that the value of g_0^θ is more than a factor of 10 smaller than the estimate from NDA given by $\bar{\theta}M_\pi^2/(m_N F_\pi)$. The second term in eq. (4.156) constitutes a small correction to g_0^θ which is given by

$$\delta g_0^\theta = \frac{\delta m_{np}^{\mathrm{str}}\,(1-\epsilon^2)}{4F_\pi\,\epsilon}\,\bar{\theta}\,\frac{(\delta M_\pi^2)^{\mathrm{str}}}{M_\pi^2} = g_0^\theta\,\frac{(\delta M_\pi^2)^{\mathrm{str}}}{M_\pi^2}\,, \tag{4.159}$$

reproducing the corresponding term in eq. (113) in [42].

The dominating contribution to the P- and T-violating and isospin-violating πNN coupling constant g_1 of eq. (4.113) induced by the θ-term, g_1^θ, is given by eq. (4.154), which includes the LEC c_1 and can thus be related to the πN sigma term. The value for this LEC is given in ref. [108], which contains a compilation of various extractions of c_1 [91, 98, 109, 110]:

$$c_1 = (-1.0 \pm 0.3)\,\mathrm{GeV}^{-1}\,. \tag{4.160}$$

[6]The error of δm_{np}^{str} in this reference is understated. The uncertainty has to be increased to at least 0.85 MeV to ensure consistence of δm_{np}^{str} with the prediction in [43]. The insertion of this larger uncertainty of δm_{np}^{str} into eq. (4.158) increases the uncertainty of g_0^θ from $0.007\,\bar{\theta}$ to $0.008\,\bar{\theta}$.

[7]The result of ref. [50] has the opposite sign to ours (which is compensated by the opposite sign of ϵ). Furthermore, F_π is defined twice as large there.

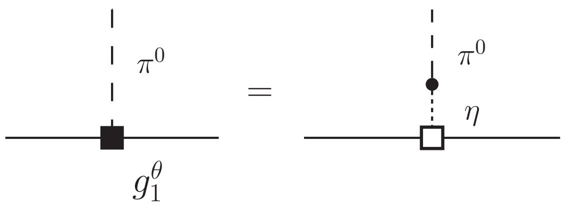

Figure 4.1: P- and T-violating $\pi^0 NN$ vertex g_1^θ (black square) induced by π^0–η-mixing and the P- and T-violating ηNN vertex (open square).

The coupling constant g_1^θ then equals:

$$g_1^\theta = \frac{2\,c_1\,(\delta M_\pi^2)^{\rm str}\,(1-\epsilon^2)}{F_\pi\,\epsilon}\bar\theta\,. \tag{4.161}$$

Inserting the relation [111]

$$(\delta M_\pi^2)^{\rm str} \approx \frac{B}{4}\frac{(m_u - m_d)^2}{m_s - (m_u + m_d)/2} \approx \frac{\epsilon^2}{4}\frac{M_\pi^4}{M_K^2 - M_\pi^2}\,, \tag{4.162}$$

into eq. (4.161) yields the result

$$g_1^\theta \approx \frac{c_1(1-\epsilon^2)\epsilon}{2F_\pi}\,\frac{M_\pi^4}{M_K^2 - M_\pi^2}\,\bar\theta = (0.003 \pm 0.001)\,\bar\theta\,, \tag{4.163}$$

where the uncertainty of this contribution to g_1^θ is dominated by the uncertainty of c_1. The expression given in (4.163) exactly agrees with the one presented in appendix G.1 which is derived from η–π^0 mixing, see ref. [26] and fig. 4.1, provided the strange-quark content of the nucleon is vanishingly small. An alternative derivation which uses SU(3) ChPT input instead of sigma-term estimates is presented in appendix G.2. Taking the rather large SU(3) errors into consideration, the SU(3) estimates for g_1^θ (and g_0^θ) are compatible with our final values.

In addition to the contribution eq. (4.154) to g_1^θ, there is an another linearly independent operator structure that contributes to g_1^θ (see ref. [42]). In our notation, it is given by eq. (4.78):

$$e_{40}\langle\hat\chi_+\hat\chi_+\rangle N^\dagger N = e_{40}16(2Bs_3)(2Bp_0)\frac{\pi_3}{F_\pi}\left(1 - \frac{2\pi^2}{3F_\pi^2}\right) + \cdots\;. \tag{4.164}$$

Unfortunately, this operator structure contributes to P- and T-conserving observables at such a high order that it cannot be constrained from a study of, say, πN scattering. We therefore need to estimate the value of e_{40} differently. The term in eq. (4.164) could have been replaced in eq. (4.78) by the term $N^\dagger\langle\chi_-\rangle^2 N$, which has the same P- and T-violating structure but does not explicitly appear in eq. (4.78) since it is not independent of $N^\dagger\langle\hat{\chi}_+\hat{\chi}_+\rangle N$. Therefore, the assessment of the contribution of the e_{40} term to g_1^θ can equally well be performed by considering $N^\dagger\langle\chi_-\rangle^2 N$.

While the operator χ_+ leads to terms that are even (odd) in the pion field for P- and T-conserving (violating) contributions, these relations are inverted for the operators χ_-: P- and T-conserving (violating) contributions are given by terms that are odd (even) in the pion field. Thus, a natural resonance saturation estimate for the operator of eq. (4.164) is given by a diagram, where one insertion of χ_- converts the even-parity nucleon into the lowest odd-parity nucleon-resonance, the $S_{11}(1535)$, which then decays via an isospin-violating decay into a neutral pion and a nucleon. The latter step may be modeled by a $S_{11}(1535)$ decaying into ηN which then converts into $\pi^0 N$ via $\eta - \pi$ mixing. This contribution is potentially important, since the coupling of this nucleon resonance to ηN is very significant [34]. However, an explicit calculation shows that the mentioned contribution does not exceed the value estimated from NDA: the magnitude of the unknown LEC can be assessed by the means of resonance saturation. According to ref. [34] the mass, width and $N\eta$ branching ratio of the $S_{11}(1535)$ odd-parity nucleon-resonance are $m_{N_{1535}} = (1535 \pm 10)\, MeV$, $\Gamma_{N_{1535}} = (150 \pm 25)\, MeV$ and $\mathcal{B}_{N_{1535}\to N\eta} = (42 \pm 10)\,\%$. Finally the CM-momentum is $p^\star = 186\, MeV$. The partial decay width $\Gamma_{N_{1535}\to N\eta}$ is then approximately $63\, MeV$, such that one finds for the effective coupling constant for the decay $N^* \to N\eta$

$$|g^\star| = \sqrt{\frac{8\pi\Gamma_{N_{1535}\to N\eta}}{p^\star}} \approx 2.9\,, \tag{4.165}$$

where we assumed an energy-independent decay vertex. By inserting

$$\tfrac{1}{2}\langle i\chi_-\rangle = -M_\pi^2(1-\epsilon^2)\bar{\theta}(1 - \tfrac{1}{2}\pi^2/F_\pi^2) + \epsilon 2M_\pi^2\pi_3/F_\pi + \ldots \tag{4.166}$$

into the effective interaction Lagrangian

$$\mathcal{L}_{N_{1535}N} = \tilde{h}N_{1535}^\dagger \tfrac{1}{2}\langle i\chi_-\rangle N + \text{h.c.} \tag{4.167}$$

we get

$$\mathcal{L}_{N_{1535}N} = \tilde{h}N_{1535}^\dagger\Big(-M_\pi^2(1-\epsilon^2)\bar{\theta} + \epsilon\frac{2M_\pi^2}{F_\pi} + \ldots\Big)N + \text{h.c.} \tag{4.168}$$

The first term provides the P- and T-violating transition of a nucleon into the N^*. As illustrated in fig. 4.2, we may model the second vertex by the decay of the resonance into an η and a nucleon, followed by η–π^0 mixing. Using the leading order ChPT expression for the mixing amplitude

$$\epsilon_{\pi^0\eta} \approx \sqrt{\tfrac{1}{3}}\,\frac{B(m_d - m_u)}{M_\eta^2 - M_\pi^2} \approx 1.37\,\%\,, \tag{4.169}$$

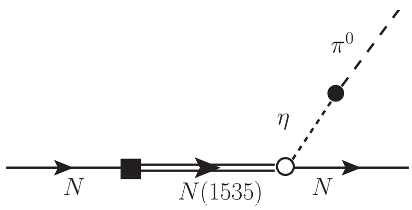

Figure 4.2: Effective P- and T-violating and isospin-violating $\pi_3 NN$ vertex estimated as P- and T-violating transition (black square) from the even-parity nucleon to the odd-parity $S_{11}(1535)$ nucleon-resonance (double line) which in turn decays into ηN (open circle) with subsequent isospin-breaking by $\eta - \pi^0$ mixing (black circle). The second topology of the diagram, where the pion emission comes first, is included in the calculation.

we can express $\tilde{h}$ by g^* and $\epsilon_{\pi^0\eta}$ as

$$\tilde{h} = \epsilon_{\pi^0\eta} \frac{F_\pi g^\star}{2\epsilon M_\pi^2} \,. \tag{4.170}$$

Thus the interaction Lagragian (4.168) can be rewritten as

$$\mathcal{L}_{N^\star N\chi_-} = g^\star \epsilon_{\pi^0\eta} \left(-\frac{F_\pi (1-\epsilon^2)\bar{\theta}}{2\epsilon} + \pi_3 \right) N^*_{1535} N + \text{h.c.} \tag{4.171}$$

In summary, we get the following estimate for the odd-parity contribution to the P- and T-violating isospin-breaking πNN coupling constant

$$\delta g_1^\theta = |g^\star|^2 (\epsilon_{\pi^0\tilde{\eta}})^2 \, \frac{\bar{\theta} F_\pi (1-\epsilon^2)/(-\epsilon)}{m_{N_{1535}} - m_N} \approx (0.6 \pm 0.3) \cdot 10^{-3} \, \bar{\theta} \,, \tag{4.172}$$

which is only one third of the NDA estimate

$$|\epsilon| \frac{M_\pi^4}{m_N^3 F_\pi} \, \bar{\theta} \sim 1.7 \cdot 10^{-3} \, \bar{\theta} \,.$$

Moreover, in order to get the proper SU(3) chiral limit of QCD, the η should be coupled with a derivative even to nucleon resonances — the resulting Lagrangian is given in ref. [112] — which leads to an additional suppression. We therefore consider it safe to estimate the additional g_1^θ-uncertainty due to our ignorance of e_{40} from an NDA estimate which is equal to $\epsilon M_\pi^4/(m_N^3 F_\pi) \sim 0.002$. In what follows we will therefore use

$$g_1^\theta = (0.003 \pm 0.002)\bar{\theta} \,, \tag{4.173}$$

which includes zero within two sigma. In particular, we find for the ratio

$$\frac{g_1^\theta}{g_0^\theta} = \frac{8c_1 (\delta M_\pi^2)^{\text{str}}}{\delta m_{np}^{\text{str}}} = -0.2 \pm 0.1 \,. \tag{4.174}$$

The value of g_1^θ/g_0^θ is numerically about a factor of 25 larger than the SU(2) estimate of order $\epsilon M_\pi^2/m_N^2$, which would follow from the first relation in eq. (4.174) if the scaling $\delta m_{np}^{\rm str} \sim \epsilon M_\pi^2/m_N$ were assumed. The main origin of this difference is that g_0^θ is unusually small — instead of two powers in the counting the relative suppression numerically is of the order of one power in the expansion parameter M_π/m_N. It is this observation that we will use in the power counting as outlined in the next chapter.

In order to summarize the results, the numerical or NDA estimates of the coupling constants defined in eq. (4.113) induced by the θ-term are listed:

$$
\begin{aligned}
g_0^\theta &= \frac{\delta m_{np}^{str}(1-\epsilon^2)}{4F_\pi\epsilon}\bar\theta = (-0.018\pm 0.007)\bar\theta \approx \bar\theta\frac{M_\pi^2}{m_N^2}\,, & (4.175)\\
g_1^\theta &= \frac{2c_1(\delta M_\pi^2)^{str}(1-\epsilon^2)}{F_\pi\epsilon}\bar\theta = (0.003\pm 0.002)\bar\theta \approx -\frac{M_\pi}{m_N}g_0^\theta\,, & (4.176)\\
\Delta_3^\theta &= \frac{(\delta M_\pi^2)^{str}(1-\epsilon^2)}{4F_\pi m_N\epsilon}\bar\theta = (-0.0004\pm 0.0002)\bar\theta \approx \frac{M_\pi^2}{m_N^2}g_0^\theta\,, & (4.177)\\
d_0^\theta &= 4e_{110}\,e\,M_\pi^2(1-\epsilon^2)\bar\theta = \mathcal{O}\left(\bar\theta e\frac{M_\pi^2}{m_N^3}\right)\,, & (4.178)\\
d_1^\theta &= 2e_{111}\,e\,M_\pi^2(1-\epsilon^2)\bar\theta = \mathcal{O}\left(\bar\theta e\frac{M_\pi^2}{m_N^3}\right)\,, & (4.179)\\
C_1^0 &= C_2^0 = \mathcal{O}\left(\bar\theta\frac{M_\pi^2}{F_\pi^2 m_N^3}\right)\,,\quad C_1^3 = C_2^3 = \mathcal{O}\left(\bar\theta\frac{\epsilon M_\pi^4}{F_\pi^2 m_N^5}\right)\,. & (4.180)
\end{aligned}
$$

The NDA estimate of the coupling constants $C_{1,2}^0$ have been obtained by the following reasoning: a P- and T-violating $4N$ vertex can be regarded as a P- and T- violating exchange of a heavy meson of mass m_N. Taking the NDA estimate of g_0^θ, $M_\pi^2/(m_N F_\pi)$, as a scale for the P- and T-violating meson-nucleon coupling, M_π/F_π as a scale for the P- and T-conserving meson-nucleon vertex, a factor of $1/m_N^2$ for the heavy meson propagator and removing one factor of M_π for the derivativs in the vertices belonging to $C_{1,2}^0$ (see eq. (4.113)), one obtains the order estimate $\bar\theta M_\pi^2/(F_\pi^2 m_N^2)$. The order estimates of the vertices $C_{1,2}^3$ involve another factor of $\epsilon M_\pi^2/m_N^2$ associated with an additional insertion of $(2Bs_3)$. The NDA estimates of $d_{0,1}^\theta$ and $C_{1,2}^{0,3}$ are in agreement with those in [42].

4.3.3 Selection for the $qCEDM$ and the hierarchy of coupling constants

In the presence of effective dimension-six sources, a few differences to the above discussed selection of the ground state for the θ-term occur which are due to the existence of additional LECs. Since the numerical values of these LECs are in general unknown, quantitative assessments of the pion-nucleon coupling constants are now impossible within the framework of ChPT alone. Until Lattice QCD might be able to provide numerical values for the new LECs, any estimates of the relevant coupling constants in eq. (4.113) induced by the effective dimension-six sources rely on NDA. As demonstrated in section 4.2.2, the source fields of the $qCEDM$ are $\tilde{p}_0 \neq p_0$ and $\tilde{p}_3 \neq p_3$. Due to the existence of new separate isospin multiplets, a simultaneous removal of p_3 and $\tilde{p}_3$ by an axial rotation $A = \exp(i\tau_3\beta/2)$ is impossible and only the leading pion tadpole is removed from the amended ChPT Lagrangian. Assuming a vanishing θ-term, one has $p_0 = p_3 = 0$.

The minimization of the potential eq. (4.120) with the generalized mass term of eq. (4.90) leads to the ground state conditions in the presence of the $qCEDM$, which are obeyed if $U_0 = \exp(i\tau_3\beta)$ with

$$\beta = \arctan\left(\frac{C\tilde{p}_3}{Bs_0 + C\tilde{s}_0}\right) = \frac{C\tilde{p}_3}{Bs_0 + C\tilde{s}_0} + \cdots . \tag{4.181}$$

A chiral rotation $A = \exp(i\tau_3\beta/2)$ of the quark fields or equivalently of the matrix $U = u^2$ in the effective Lagrangian results in corrections of all other terms in the amended QCD and the amended ChPT Lagrangians. Utilizing eqs. (4.136)-(4.139), χ and $\tilde{\chi}$ are shifted by

$$\tilde{\chi} \;\mapsto\; \tilde{\chi}' = 2C\big(\tilde{s}_0\mathbb{1} + \tilde{s}_3\tau_3 + i(\tilde{p}_0 - \beta\tilde{s}_3)\mathbb{1} + i(\tilde{p}_3 - \beta\tilde{s}_0)\tau_3\big) + \cdots , \tag{4.182}$$

$$\chi \;\mapsto\; \chi' = 2B\big(s_0\mathbb{1} + s_3\tau_3 - i\beta s_3\mathbb{1} - i\beta s_0\tau_3\big) + \cdots , \tag{4.183}$$

where the dots denote terms which are proportional to higher powers of $\tilde{p}_{0,3}$.

The axial rotation A profoundly affects the pion-sector Lagrangian $\mathcal{L}_\pi^{(4)}$ eq. (4.90) in the presence of the $qCEDM$ source fields. Utilizing eq. (4.182) and eq. (4.183), the next-to-leading order pion tadpole term after this axial rotation reads

$$\begin{aligned}\mathcal{L}_\pi^{(4)} = \; & \big[l_7(2B\beta s_3)(2Bs_3) - \tilde{l}_7(2C(\tilde{p}_0 - \beta\tilde{s}_3))(2C\tilde{s}_3) \\ & -l_7'(2C(\tilde{p}_0 - \beta\tilde{s}_3))(2Bs_3) + l_7'(2B\beta s_3)(2C\tilde{s}_3) \\ & +\tilde{l}_3(2C\tilde{s}_0)(2C(\tilde{p}_3 - \beta\tilde{s}_0) - l_3(2Bs_0)(2B\beta s_0) \\ & +l_3'(2C(\tilde{p}_3 - \beta\tilde{s}_0))(2Bs_0) - l_3'(2B\beta s_0)(2C\tilde{s}_0)\big] \\ & \times 2\frac{\pi_3}{F_\pi}\left(1 - \frac{2\pi^2}{3F_\pi^2}\right) + \cdots .\end{aligned} \tag{4.184}$$

Since $|\tilde{s}_0| \ll |s_0|$ and $|\tilde{s}_3| \ll |s_3|$, the tadpole term essentially reduces to

$$\begin{aligned}\mathcal{L}_\pi^{(4)} = \; & \big[l_7(2B\beta s_3)(2Bs_3) - l_7'(2C\tilde{p}_0)(2Bs_3) \\ & -l_3(2Bs_0)(2B\beta s_0) + l_3'(2C\tilde{p}_3)(2Bs_0)\big] \\ & \times 2\frac{\pi_3}{F_\pi}\left(1 - \frac{2\pi^2}{3F_\pi^2}\right) + \cdots .\end{aligned} \tag{4.185}$$

This next-to-leading order tadpole term is removed by subjecting the effective Lagrangian to another axial rotation $A' = \exp(i\tau_3\beta'/2)$ with

$$\beta' = 4\frac{l_7B^2\beta s_3^2 - l_7'BC\tilde{p}_0s_3 - l_3B^2\beta s_0^2 + l_3'BC\tilde{p}_3s_0}{F_\pi^2(Bs_0 + C\tilde{s}_0)} , \tag{4.186}$$

which causes a shift of the leading order mass terms $F_\pi^2\langle\chi_+\rangle/4$ and $F_\pi^2\langle\tilde{\chi}_+\rangle/4$ in eq. (4.90) in analogy to the θ-term case:

$$\frac{F_\pi^2}{4}(\langle\chi_+\rangle + \langle\tilde{\chi}_+\rangle) \to -F_\pi\beta'[(2Bs_0) + (2C\tilde{s}_0)]\pi_3\left(1 - \frac{\pi^2}{6F_\pi^2}\right) + \cdots . \tag{4.187}$$

This second axial rotation A' corresponds to a second axial rotation of the source fields in χ and $\tilde{\chi}$:

$$\chi \;\mapsto\; \chi' = 2B(s_0\mathbb{1} + s_3\tau_3 - i(\beta+\beta')s_3\mathbb{1} - i(\beta+\beta')s_0\tau_3) + \cdots , \tag{4.188}$$
$$\tilde{\chi} \;\mapsto\; \tilde{\chi}' = 2C(\tilde{s}_0\mathbb{1} + \tilde{s}_3\tau_3 + i(\tilde{p}_0 - (\beta+\beta')\tilde{s}_3)\mathbb{1} + i(\tilde{p}_3 - (\beta+\beta')\tilde{s_0})\tau_3) + \cdots . \tag{4.189}$$

The coupling constant Δ_3 of the P- and T-violating 3π vertex in eq.(4.113) is then obtained by adding the second term on the right-hand side of eq. (4.187) to the 3π-term in eq. (4.185):

$$\Delta_3 = -\frac{\beta'(Bs_0 + C\tilde{s}_0)}{F_\pi m_N} . \tag{4.190}$$

By inserting eq. (4.188) and eq. (4.189) into eq. (4.92), the leading P- and T-violating πNN coupling constants g_0 and g_1 of eq. (4.113) are obtained in analogy to the previous section ($\hat{\beta} := \beta + \beta'$):

$$g_0 = \frac{4\tilde{c}_5 C\tilde{p}_0 - 4Bc_5 s_3\hat{\beta}}{F_\pi} + \cdots , \quad g_1 = \frac{8\tilde{c}_1 C\tilde{p}_3 - 8Bc_1 s_0\hat{\beta}}{F_\pi} + \cdots , \tag{4.191}$$

Similar expression for the coupling constants $d_{0,1}$ and $C_{1,2}^{0,3}$ in eq. (4.113) involve further new LECs (corresponding to *e.g.* e_{110} and e_{111} in eq. (4.79) and to C_5-C_8 in eq. (4.80)) which are not discussed here since they are not required for NDA estimates.

All coupling constants of eq. (4.113) induced by the $qCEDM$ are proportional to the quark mass as in the case of the θ-term since the $qCEDM$ emerges from a coupling to the Higgs field at higher energies (see eq. (3.18)). Since the $qCEDM$ has an isospin-conserving as well as an isospin-violating component, the only difference to the hierarchy of coupling constants for the θ-term is that g_0 and g_1 are now induced at the same order and are thus expected to be numerically comparable. The same is true for the three pairs of coupling constants $d_{0,1}$, $C_1^{0,3}$ and $C_2^{0,3}$, respectively. Since the P- and T-violating 3π vertex arises from an additional insertion of the quark mass (i.e. and additional insertion of the building block $\chi_\pm$), the coupling constant Δ_3 is suppressed by a factor of M_π^2/m_N^2 with respect to g_0 and g_1. The NDA estimates of the coupling constants in eq. (4.113) is then given by

$$g_0 = g_1 = \mathcal{O}\left(c\frac{M_\pi^2}{F_\pi m_N}\right)\,,\ \Delta_3 = \mathcal{O}\left(c\frac{M_\pi^4}{F_\pi m_N^3}\right)\,, \tag{4.192}$$

$$d_0 = d_1 = \mathcal{O}\left(c\,e\frac{M_\pi^2}{m_N^3}\right)\,,\quad C_1^0 = C_1^3 = \mathcal{O}\left(c\frac{M_\pi^2}{F_\pi^2 m_N^3}\right)\,,$$
$$C_2^0 = C_2^3 = \mathcal{O}\left(c\frac{M_\pi^2}{F_\pi^2 m_N^3}\right)\,, \tag{4.193}$$

where c is a generic $\mathcal{O}(1)$ constant parametrizing BSM physics. The NDA estimates are in agreement with those in [39].

4.3.4 Selection for the $4qLR$-op and the hierarchy of coupling constants

In the case of the $4qLR$-op, the only non-vanishing P- and T-violating source field is the one given by eq. (4.94), i.e. $p_0 = p_3 = 0$ and $r_3 \neq 0$. The most convenient form of the leading order ChPT potential V is obtained by utilizing eq. (4.97) and eq. (4.100):

$$V = -\int d^4x \Bigg(\frac{F_\pi^2}{4}\langle 2B(s_0\mathbb{1} + s_3\tau_3)^\dagger U\rangle + \frac{F_\pi^2}{4}\langle 2B(s_0\mathbb{1} + s_3\tau_3)U^\dagger\rangle$$
$$+ (2Dq_{ij})\langle U\tau_i U^\dagger \tau_j + U^\dagger \tau_i U \tau_j\rangle + (2Dr_3)\epsilon^{3lm}\langle \tau_l U \tau_m U^\dagger\rangle \Bigg)\,. \tag{4.194}$$

By employing the variation of U,

$$U(x) \mapsto G(x)U(x) = \exp(i\vec{\tau}\cdot\vec{\alpha}(x))U(x)\,, \tag{4.195}$$

with $\alpha_1 = \alpha_2 = 0$ and $\alpha_3 \neq 0$, the ground state condition for a non-vanishing $4qLR$-op is obtained (neglecting terms proportional to $|2Dq_{ij}| \ll |2Bs_0|, |2Bs_3|$):

$$\frac{iF_\pi^2 Bs_0}{2}\langle \tau_3 U - \tau_3 U^\dagger\rangle + 4Dr_3\langle \tau_1 U \tau_1 U^\dagger + \tau_2 U \tau_2 U^\dagger\rangle = 0\,. \tag{4.196}$$

This ground state condition requires the ground state to be $U_0 = A^2 = \exp(i\tau_3\beta)$ with

$$\beta = \frac{8(2Dr_3)}{(2Bs_0)F_\pi^2} + \cdots\,. \tag{4.197}$$

The higher order tadpole term eq. (4.106) is removed by a second axial rotation $A' = \exp(i\tau_3\beta')$ with β' defined by

$$\beta' = \frac{4l_{4qLR}Dr_3}{F_\pi^2} + \cdots\,. \tag{4.198}$$

The matrix U in the amended ChPT Lagrangian has therefore to be subjected to an axial rotation $A'A = \exp(i\tau_3\hat{\beta}/2)$ with $\hat{\beta} = \beta + \beta'$ in order to adjust the amended ChPT Lagrangian to the altered ground state.

The leading order contribution to the coupling constant of the P- and T-violating 3π vertex in eq. (4.113), Δ, is given by the sum of the 3π term in eq. (4.105) and the shift of $F_\pi^2\langle\chi_+\rangle/4$ caused by the axial rotation A:

$$\Delta_3 = \frac{-32Dr_3 + Bs_0\beta F_\pi^2}{3F_\pi^3 m_N} + \cdots = -\frac{8Dr_3}{F_\pi^3 m_N} + \cdots . \tag{4.199}$$

The shift from other P- and T-conserving terms proportional to $2Dq_{ij} \ll 2Bs_0$ are heavily suppressed and have been neglected here. The second axial rotation A' generates further contributions to Δ_3, which are two orders suppressed with respect to the one displayed in eq. (4.106) due to the smallness of β'. The axial rotations also generate further P- and T-violating terms in the pion-nucleon Lagrangian $\mathcal{L}_{\pi N}^{(2)}$ from P- and T-conserving terms proportional to the LECs c_1 and c_5:

$$c_1\langle\chi_+\rangle N^\dagger N \quad\rightarrow\quad -4\hat{\beta}c_1 M_\pi^2 \frac{\pi_3}{F_\pi}\left(1 - \frac{\pi^2}{6F_\pi^2}\right) N^\dagger N + \cdots , \tag{4.200}$$

$$c_5 N^\dagger \hat{\chi}_+ N \quad\rightarrow\quad -\frac{2\hat{\beta}c_5\epsilon M_\pi^2}{F_\pi} N^\dagger \vec{\pi}\cdot\vec{\tau} N + \cdots . \tag{4.201}$$

The term on the right-hand side of eq. (4.200) constitutes a correction to the dominating contribution to the coupling constant g_1 of the P- and T-violating $\pi_3 NN$ vertex eq. (4.108):

$$g_1 = \frac{(16c_{4qLR}Dr_3 - 4\hat{\beta}c_1 M_\pi^2)}{F_\pi} + \cdots . \tag{4.202}$$

The term on the right-hand side of eq. (4.201) is the leading contribution to the coupling constant g_0:

$$g_0 = -\frac{2\hat{\beta}c_5\epsilon M_\pi^2}{F_\pi} + \cdots . \tag{4.203}$$

The first axial rotation A generates in principle leading order terms from leading order chiral structures, since $\beta = \mathcal{O}(1)$ in contrast to $\beta' = \mathcal{O}(M_\pi^2/m_N^2)$. One would naively expect g_0 and g_1 to be of the same order. Neglecting the first term on the right-hand side of eq. (4.202), the ratio of g_0 and g_1 is given by

$$\frac{g_0}{g_1} = -\frac{c_5}{2c_1} = \frac{\delta m_{np}^{str}}{8c_1 M_\pi^2} \approx \frac{(0.0026 \pm 0.0005)\,\mathrm{GeV}}{(-0.1524 \pm 0.0457)\,\mathrm{GeV}} \approx -0.017 \pm 0.006 \approx \frac{M_\pi^2}{m_N^2} , \tag{4.204}$$

which reveals a (potential) suppression of g_0 with respect to g_1 by at least two orders in magnitude.

The following hierarchy of the coupling constants defined in eq. (4.113) for the $4qLR$-op emerges: since the $4qLR$-op is not proportional to the quark mass, the NDA estimate of g_1 equals the one for the $qCEDM$ with the factor accounting for the quark mass suppression, M_π^2/m_N^2, removed. The coupling constant g_0 is suppressed by a factor of M_π^2/m_N^2 with respect to g_0 as revealed by eq. (4.204). In contrast to the $qCEDM$, the coupling constant Δ_3 does not arise from an additional insertion of the quark mass. Its NDA estimate therefore equals the one of the $gCEDM$ multiplied by a factor of m_N^4/M_π^4. The γNN coupling constants are generated by insertions of η_- and $f_+^{\mu\nu}$, which yields NDA estimates that equal the ones for the $qCEDM$ times a factor of m_N^2/M_π^2. $C_{1,2}^3$ vertices are obtained by insertions of the building block η_-, whereas the coupling constants $C_{1,2}^0$ are generated by the first axial rotation A in the same manner as the coupling constant g_0. Since there is no basis to assume that either $C_{1,2}^0$ or $C_{1,2}^3$ are unnaturally small or large, the NDA estimates for these coupling constants equal the respective ones for the $qCEDM$ without the suppression factor associated with the quark mass. The list of NDA estimates is then given by

$$
\begin{aligned}
g_0 &= \mathcal{O}\left(c\frac{M_\pi^2}{F_\pi m_N}\right), \quad & g_1 &= \mathcal{O}\left(c\frac{m_N}{F_\pi}\right), \quad & \Delta_3 &= \mathcal{O}\left(c\frac{m_N}{F_\pi}\right), \\
d_0 = d_1 &= \mathcal{O}\left(\frac{c\,e}{m_N}\right), \quad & C_1^0 = C_2^0 &= \mathcal{O}\left(\frac{c}{F_\pi^2 m_N}\right), \quad & C_1^3 = C_2^3 &= \mathcal{O}\left(\frac{c}{F_\pi^2 m_N}\right),
\end{aligned}
\tag{4.205}
$$

where c is again a generic parameter of BSM physics. The NDA estimates are in agreement with those in [39].

4.3.5 Selection for the $qEDM$, the $4q$-op and $gCEDM$ and the hierarchies of coupling constants

The selection of the correct ground states for the $qEDM$ and the chiral singlet sources $4q$-op and $gCEDM$ is performed in analogy to those of the previously considered sources of P and T violation. The effects of the ground state selection procedure on the coupling constants of leading P- and T-violating vertices induced by the $qEDM$ are twofold: the already heavily suppressed coupling constants of vertices without photon fields (by a loop factor of $\alpha_{em}/(4\pi)$) receive corrections of the same order. The same is true for the leading γNN coupling constants $d_{0,1}$. Since the $qEDM$ has both an isospin-conserving and an isospin-violating component, the effect of the ground state selection procedure is predominantly a mixing of the coupling constants of isospin-conserving vertices and of their isospin-violating counterparts. On the basis of NDA, the hierarchy among coupling constants of P- and T-violating operators is then the following: d_0 and d_1 are the leading coupling constants. g_0, g_1, Δ_3 and the $4N$ coupling constants $C_{1,2}^{0,3}$ are at least suppressed by a factor of $\alpha_{em}/(4\pi)$ with respect to $d_{0,1}$. Since the $qEDM$ arises from a coupling to the Higgs field at higher energies, the NDA estimates of all coupling constants of vertices induced by the $qEDM$ also include a factor of M_π^2/m_N^2.

The adjustment to the altered ground state in the presence of the $gCEDM$ and the $4q$-op removes the leading pion tadpole term and the leading 3π vertex and also causes a mixing of terms of equal order. The $C_{1,2}^0$ and $d_{0,1}$ coupling constants dominate whereas the coupling constants of vertices involving pions, g_0, g_1 and Δ_3, are suppressed by a factor M_π^2/m_N^2 since the are protected by Goldstone's theorem. The NDA estimates of the coupling constants of isospin-violating vertices $C_{1,2}^3$, g_1 and Δ_3 have an additional factor of ϵ. These findings are in agreement with the findings in [39].

4.4 Summary

In order to assess the manifestation of the various sources of P and T violation discussed in the previous chapter on the hadronic level, the employment of non-perturbative techniques is required. The analysis of hadronic operators has been presented within the framework of two-flavor ChPT, the low-energy effective field theory of QCD. Only the θ-term allows for a treatment within standard ChPT, since it can be considered as a regular term of the standard QCD Lagrangian.

The effective dimension-six terms are new non-renormalizable terms by which the standard QCD Lagrangian is amended. This implies that the treatment of their manifestations on the hadronic level are equally beyond the realm of standard ChPT as pointed out in [39,49]. A complete analysis of the manifestation of the sources of P and T violation in or as extensions of QCD has been presented within the Gasser-Leutwyler formulation of ChPT. The results previously published in the Weinberg formulation of $SU(2)$ ChPT in [39,49] are consistent with our results. Each source of P and T violation gives rise to a particular hierarchy of the coupling constants of P- and T-violating hadronic vertices defined by

$$\begin{aligned} & \mathcal{L}_\pi^{(2)} + \mathcal{L}_\pi^{(4)} + \mathcal{L}_{\pi N}^{(2)} + \mathcal{L}_{\pi N}^{(4)} + \mathcal{L}_{4N} \\ = \quad & m_N \Delta_3 \pi_3 \pi^2 + g_0 N^\dagger \vec{\pi}\cdot\vec{\tau} N + g_1 N^\dagger \pi_3 N \\ & - 2d_0 N^\dagger S^\mu v^\nu N F_{\mu\nu} - 2d_1 N^\dagger \tau_3 S^\mu v^\nu N F_{\mu\nu} \\ & + C_1^0 N^\dagger N \mathcal{D}_\mu (N^\dagger S^\mu N) + C_2^0 N^\dagger \vec{\tau} N \cdot \mathcal{D}_\mu (N^\dagger S^\mu \vec{\tau} N) \\ & + C_1^3 N^\dagger \tau_3 N \mathcal{D}_\mu (N^\dagger S^\mu N) + C_2^3 N^\dagger N \mathcal{D}_\mu (N^\dagger \tau_3 S^\mu N) + \cdots . \qquad (4.206) \end{aligned}$$

The hierarchies of these coupling constants are summarized in table 4.1. Those coupling constants in tab. 4.1 which can not be computed due to unknown LECs have been assessed by NDA. Tab. 4.1 underlies the assumption that for an effective dimension-six source with an isospin-conserving and an isospin-breaking component both respective BSM parameters are of comparable sizes. The quantitative assessments of the coupling constants can be refined by the means of

Table 4.1: Numerical or NDA estimates for the coupling constants of P- and T-violating vertices induced by the θ-term, $qCEDM$, $4qLR$-op, $qEDM$, $gCEDM$ and $4q$-op $\bar\theta$ is the physical θ parameter, the constant c is an $\mathcal{O}(1)$ parameter for BSM physics, e is the electric charge of the electron, F_π the pion decay constant, M_π the pion mass and m_N the nucleon mass. A factor of $\epsilon=(m_u-m_d)/(m_u+m_d)$ arises from insertions of the isospin-violating component of the quark mass matrix.

	g_0	g_1	Δ_3	$d_{0,1}$	$C_{1,2}^{0,3}$
θ-term	$\bar\theta\frac{M_\pi^2}{m_N^2}$	$\bar\theta\frac{M_\pi^3}{m_N^3}$	$\bar\theta\frac{M_\pi^4}{m_N^4}$	$e\,\bar\theta\frac{M_\pi^2}{m_N^3}$	$\bar\theta\frac{M_\pi^2}{F_\pi^2 m_N^3}$
$qCEDM$	$c\frac{M_\pi^2}{F_\pi m_N}$	$c\frac{M_\pi^2}{F_\pi m_N}$	$c\frac{M_\pi^4}{F_\pi m_N^3}$	$e\,c\frac{M_\pi^2}{m_N^3}$	$c\frac{M_\pi^2}{F_\pi^2 m_N^3}$
$4qLR$-op	$c\frac{M_\pi^2}{F_\pi m_N}$	$c\frac{m_N}{F_\pi}$	$c\frac{m_N}{F_\pi}$	$e\,c\frac{1}{m_N}$	$c\frac{1}{F_\pi^2 m_N}$
$qEDM$	$c\frac{\alpha_{em}}{4\pi}\frac{M_\pi^2}{F_\pi m_N}$	$c\frac{\alpha_{em}}{4\pi}\frac{M_\pi^2}{F_\pi m_N}$	$c\frac{\alpha_{em}}{4\pi}\frac{M_\pi^4}{F_\pi m_N}$	$e\,c\frac{M_\pi^2}{m_N^3}$	$c\frac{\alpha_{em}}{4\pi}\frac{M_\pi^2}{F_\pi^2 m_N^3}$
$gCEDM$	$c\frac{M_\pi^2}{F_\pi m_N}$	$c\frac{\epsilon M_\pi^2}{F_\pi m_N}$	$c\frac{\epsilon M_\pi^4}{F_\pi m_N^3}$	$e\,c\frac{1}{m_N}$	$c\frac{1}{F_\pi^2 m_N}$
$4q$-op	$c\frac{M_\pi^2}{F_\pi m_N}$	$c\frac{\epsilon M_\pi^2}{F_\pi m_N}$	$c\frac{\epsilon M_\pi^4}{F_\pi m_N^3}$	$e\,c\frac{1}{m_N}$	$c\frac{1}{F_\pi^2 m_N}$

Lattice QCD, which might be able to supply the yet unknown LECs and hence complete the connection between the energy scales of QCD and ChPT.

The existence of different hierarchies of coupling constants for different sources of P and T violation which are expected to translate into equally different nuclear EDM contributions provides the main incentive to investigate the EDMs of light nuclei.

Chapter 5

The EDM of the deuteron

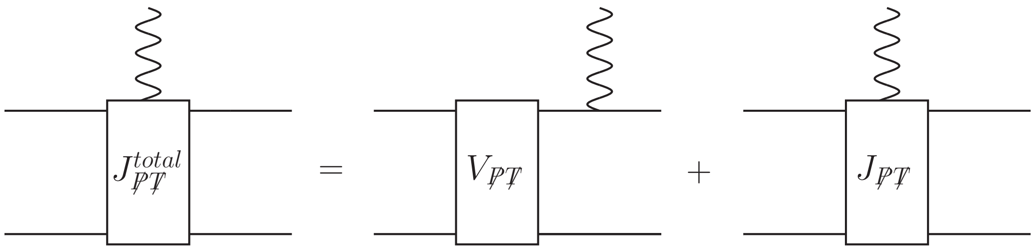

Figure 5.1: Total CP-violating transition current. The P and T violation stem from either P- and T-violating two-nucleon potentials or two-nucleon-irreducible P- and T-violating transition currents.

In this chapter[1], the two-nucleon contributions to the deuteron EDM up to next-to-next-to-leading order from the QCD θ-term are computed. The discussion is subsequently extended to the effective dimension-six sources. There are two types of contributions that are relevant for the present study, namely P- and T-violating NN interactions and P- and T-violating irreducible $NN \to NN\gamma$ transition currents — *c.f.* fig. 5.1. For the deuteron EDM, the latter kind of contributions contains at its leading non-vanishing order loop diagrams that are calculated in this chapter for the first time.

Two complementary computational approaches are employed in this chapter. The first approach is a largely analytical computation of the EDM contributions from the leading irreducible NN interactions and irreducible transition currents. The second numerical approach is employed for two reasons: (i) The analytic computation involves a parameterization of the NN potential in the intermediate state which is not available for most phenomenological and all ChPT potentials.

[1]Parts of the following sections of this chapter were published in [101]: introduction, section 5.1, section 5.2, summary.

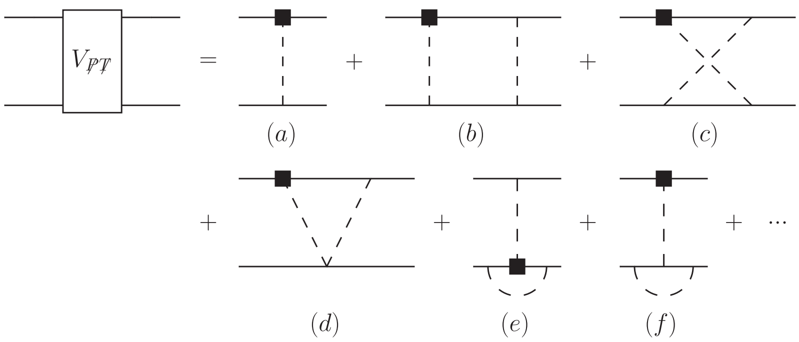

Figure 5.2: Contributions to the P- and T-violating two-nucleon potential: (a) LO contributions, (b)-(f) NLO and N^{2}LO contributions, where the former class contains the g_0^θ and the latter the g_1^θ coupling. Solid lines denote nucleons and dashed lines denote pions. The P- and T-violating vertex is depicted by a black box. For each class of diagrams only one representative is shown.

(ii) Since the number of relevant states in $3N$ systems is significantly larger compared to the NN system, an analytical computation is not a viable approach for ^{3}He and ^{3}H nuclei which are investigated in the next chapter. The parallel program developed to numerically compute the leading EDM contributions allows for a detailed study of the uncertainties attributed to the P- and T-conserving component of the nuclear potential.

The chapter is structured as follows: On the basis of the findings of chapter 4 where the hierarchies of the leading coupling constants have been derived, the power counting of P- and T-violating NN operators is presented in sect. 5.1. Section 5.2 contains the derivation of the two-nucleon contributions to the deuteron EDM induced by the θ-term. The contributions from NN interactions and transition currents are discussed in subsections 5.2.1 and 5.2.2, respectively. The discussion is extended to nuclear contributions induced by the effective dimension-six sources in section 5.4. Complementary to the largely analytical calculations of the nuclear contributions, the results of the numerical analysis are presented in section 5.3. Finally, a short summary of the presented results is given in sect. 5.5.

5.1 Power counting

It is crucial for this study to identify a power counting that allows for a comparison of the contributions to the nuclear EDMs from P- and T-violating transition currents to those from the P- and T-violating NN potential. The power counting originally proposed by Weinberg for nuclear matrix elements [113], in spite of its many successful applications [114], is not able to explain analogous ratios studied numerically in ref. [115] — we will therefore modify it slightly, as explained below. An alternative scheme is presented in ref. [30].

In Weinberg's counting, contributions to the deuteron EDM that come from a P- and T-violating potential (*c.f.* fig. 5.1) are regarded as reducible, while the transition currents are counted as irreducible. Thus, one needs to power-count the nuclear wave functions and the photon couplings separately, making it necessary to assign a scale to a disconnected nucleon line. For dimensional reasons the corresponding $\delta^{(3)}$ function is identified with $1/p^3$, where p denotes the typical momentum appearing in the evaluation of the integrals, identified with the pion mass, M_π. However, if indeed nucleon momenta are of order M_π, the two-nucleon intermediate state appearing between the photon coupling and the P- and T-violating NN potential is off-shell. Thus, also this contribution is to be regarded as irreducible with the two-nucleon propagator counted as $(p^2/m_N)^{-1}$, where m_N denotes the nucleon mass. Again p is identified with M_π. This power counting properly explains the numerical observations of ref. [115] and will be used in this work as well. For more details we refer to ref. [116].

5.1.1 Power counting for the contributions of the single-nucleon EDMs

In a world where P and T violation in the SM is driven by the θ-term, within the effective field theory the single-nucleon EDMs start at the one-loop level. At the same order there are two counter terms — the d_i terms in eq. (4.113). The isospin structure of the loops gives that the isoscalar component of the single-nucleon EDMs is suppressed by one order in the counting compared to the isovector one [45,63]. However, this suppression is not present for the counter terms [48, 117], and therefore for the power counting we may estimate both the contribution from the d_0 as well as the d_1 term from the estimate for the leading loop contribution given by ($E_\pi = M_\pi$)

$$g_0^\theta \times \frac{M_\pi}{F_\pi} \times eE_\pi \times \frac{1}{M_\pi^4} \times \frac{1}{E_\pi} \times \frac{M_\pi^4}{(4\pi)^2} = eg_0^\theta \frac{F_\pi M_\pi}{m_N^2} , \tag{5.1}$$

where the dimension-full factors in the first line come from the regular πNN vertex, the photon-pion vertex (with the electron charge $e < 0$), the propagators and the integration measure, respectively, and we identified $(4\pi F_\pi) \sim m_N$. In order to derive from this the total transition current we need to multiply the estimate with $(1/F_\pi^2) \times m_N/M_\pi^2$ from the NN potential and the two-nucleon propagator, respectively. We therefore find an estimate of the order of $eg_0^\theta/(F_\pi m_N M_\pi)$ from the single-nucleon EDM for the leading contribution to the total transition current. Thus, the single-nucleon EDMs start to contribute to the deuteron EDM at NLO, as we will outline in the next subsections — *c.f.* tab. 5.1.

Table 5.1: Power-counting scales of the P- and T-violating NN potentials (left) and (total) transition currents (right) relevant for the two-nucleon contribution to the θ-term-induced EDM of the deuteron, where the equivalence $4\pi F_\pi \sim m_N$ is assumed.

	NN potential	(total) transition current
LO	$g_0^\theta/(m_N F_\pi) \sim g_1^\theta/(M_\pi F_\pi)$	$g_0^\theta\, e/(M_\pi^2 F_\pi) \sim g_1^\theta\, e\, m_N/(M_\pi^3 F_\pi)$
NLO	$g_0^\theta M_\pi/(m_N^2 F_\pi) \sim g_1^\theta/(m_N F_\pi)$	$g_0^\theta\, e/(M_\pi m_N F_\pi) \sim g_1^\theta\, e/(M_\pi^2 F_\pi)$
N^{2}LO	$g_0^\theta M_\pi^2/(m_N^3 F_\pi) \sim g_1^\theta M_\pi/(m_N^2 F_\pi)$	$g_0^\theta\, e/(m_N^2 F_\pi) \sim g_1^\theta\, e/(M_\pi m_N F_\pi)$

5.1.2 Power counting of the irreducible P- and T-violating NN potential operators

The leading diagrams for the irreducible P- and T-violating NN potential are shown in fig. 5.2. The leading, isospin-conserving, P- and T-violating one-pion exchange can be estimated as

$$g_0^\theta \times \frac{1}{M_\pi^2} \times \frac{M_\pi}{F_\pi} = \frac{g_0^\theta}{M_\pi F_\pi} \,. \tag{5.2}$$

However, as will be discussed in the next section, this term does not contribute to the deuteron EDM due to selection rules. The first non-vanishing contribution comes from the subleading, isospin- and P- and T-violating coupling g_1^θ. It is estimated to contribute as $g_1^\theta/(M_\pi F_\pi) \sim g_0^\theta/(m_N F_\pi)$, where we used the empirical relation, presented in the previous section, $g_1^\theta/g_0^\theta \sim M_\pi/m_N$. This contribution will be called leading order (LO).

A P- and T-violating pion exchange potential from a g_0^θ coupling on one vertex and an isospin-violating, P- and T-conserving coupling on the other also leads to a non-vanishing contribution to the deuteron EDM [26, 30]. As long as we focus only on contributions to the deuteron EDM, the impact of the resulting potential is effectively a redefinition $g_1^\theta \to g_1^\theta[1+g_0^\theta\beta_1/(2g_A g_1^\theta)]$ [30], where β_1 is the strength parameter of the isospin-violating, P- and T-conserving πNN vertex and g_A is the axial-vector coupling constant of the nucleon. The Nijmegen partial-wave analysis provides $|\beta_1| \leq 10^{-2}$ [118], which is consistent with estimating its value from the same mechanism used in ref. [26] and appendix G.1, namely via η–π^0 mixing — see fig. 5.3. Thus the inclusion of β_1 shifts g_1^θ by a few percent at most and can therefore be neglected, given the significant uncertainty of g_1^θ.

The first relativistic correction is the recoil correction to the g_A vertex, given by $-g_A/(2m_N F_\pi) S\cdot(p_1+p_2) v\cdot k\tau^a$ where $p_{1,2}$ are the nucleon momenta and k is the outgoing pion momentum. The corresponding contribution is suppressed by three orders relative to the one of the g_A vertex due to the additional energy dependence (since $v=(1,\vec{0}\,)$ and $k=p_1-p_2$).

To one-loop order there are a couple of diagrams as shown in fig. 5.2. The power counting gives for these diagrams (*e.g.* diagram fig. 5.2 (d), $E_\pi = M_\pi$)

$$g_0^\theta \times \frac{1}{M_\pi^2} \times \frac{E_\pi}{F_\pi^2} \times \frac{1}{M_\pi^2} \times \frac{M_\pi}{F_\pi} \times \frac{1}{E_\pi} \times \frac{M_\pi^4}{(4\pi)^2} = \frac{g_0^\theta M_\pi}{m_N^2 F_\pi}\,, \tag{5.3}$$

where we identified $4\pi F_\pi \sim m_N$. Thus, the loop contributions with the P and T violation induced via the coupling g_0^θ are suppressed relative to the leading, non-vanishing contribution to the potential (proportional to g_1^θ) by one power of M_π/m_N and therefore contribute to NLO. However, as outlined below, the spin-isospin structure of all these diagrams is such that they do not contribute to the deuteron EDM. At N^{2}LO the same topologies appear, however, with g_0^θ replaced by g_1^θ. In addition, also triangle topologies of type (d) with the $\pi\pi NN$ vertex from $\mathcal{L}_{\pi N}^{(2)}$ [58] as well as vertex corrections (diagrams (e) and (f)) formally appear at this order. As shown below, besides the latter class none of the mentioned diagrams contributes to the deuteron EDM.

On dimensional grounds P- and T-violating four-nucleon operators start to contribute at order M_π/m_N relative to the leading term. Their largest θ-term-induced contributions are isospin conserving. Thus, as a consequence of the Pauli–principle, they change the two-nucleon spin. Therefore they do not contribute to the deuteron EDM. However, their isospin-violating counter parts contribute, but have a relative suppression of order $(M_\pi/m_N)^2$ and are therefore of N^{3}LO.

In summary, to the order we are working, the only contribution to the P- and T-violating NN potential that needs to be considered for the deuteron EDM is the isospin-violating tree-level contribution proportional to g_1^θ and its vertex corrections.

5.1.3 Power counting of the irreducible transition currents

We now turn to the transition currents. As explained in the beginning of this section, in order to compare the contribution from the P- and T-violating NN

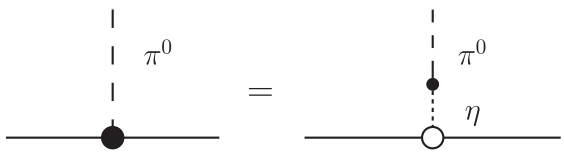

Figure 5.3: Isospin-violating P- and T-conserving πNN vertex (black circle) induced by π^0–η-mixing and the P- and T-conserving ηNN coupling (open circle).

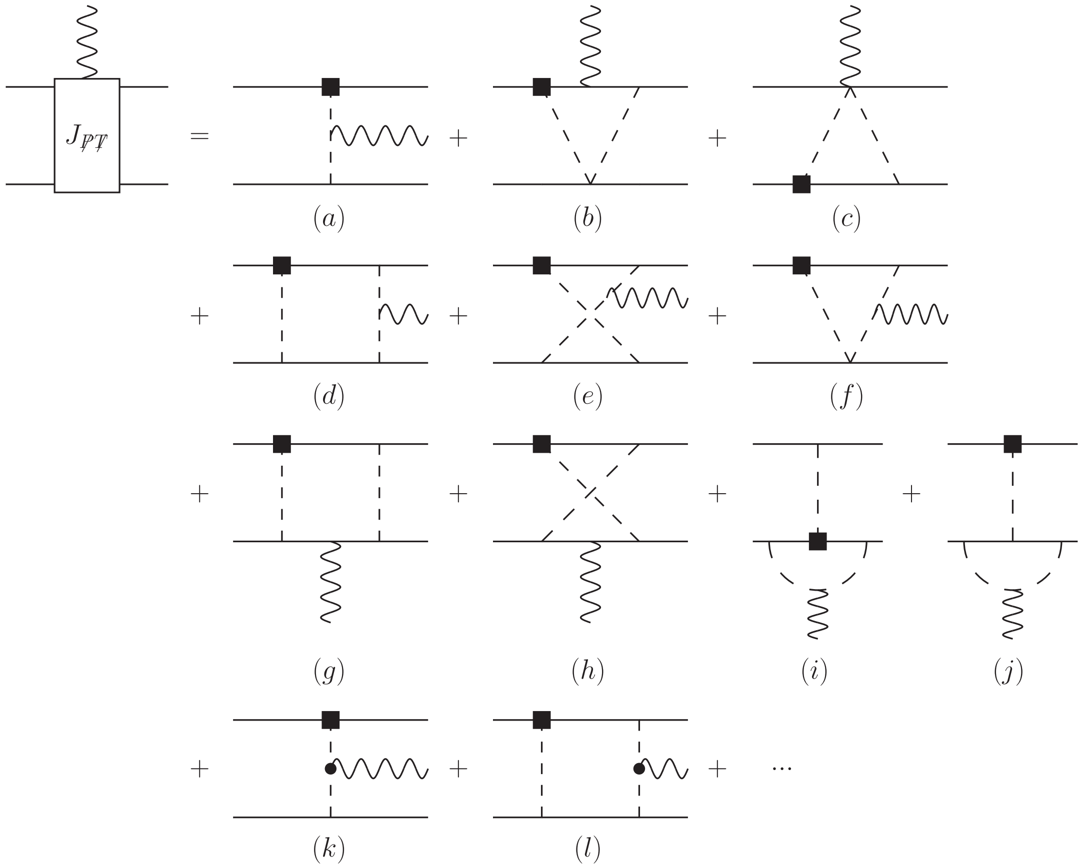

Figure 5.4: Contributions to the P- and T-violating transition current: (a) NLO contribution, (b)-(l) $\mathsf{N}^2\mathsf{LO}$ contributions. Solid lines denote nucleons and dashed line denote pions. The P- and T-violating vertex is depicted by a black box, a P- and T-conserving, but isospin-violating vertex by a filled circle. For each class of diagrams only one representative is shown.

potential to that of the P- and T-violating transition currents, the former needs to be multiplied by $e\, m_N/M_\pi^2$. Thus, the *leading order contribution* of the total transition current is estimated to scale as $g_1^\theta\, e\, m_N/(M_\pi^3 F_\pi) \sim g_0^\theta\, e/(M_\pi^2 F_\pi)$.

The tree-level contribution, shown in fig. 5.4, is formally of NLO, however, turns out to be of isovector character and thus does not contribute to the deuteron EDM.

The one-loop contributions to the irreducible transition current are estimated as (*e.g.* diagram fig. 5.4 (b), $E_\pi = M_\pi$)

$$g_0^\theta \times \frac{1}{M_\pi^2} \times \frac{E_\pi}{F_\pi^2} \times \frac{1}{M_\pi^2} \times \frac{M_\pi}{F_\pi} \times \frac{1}{E_\pi} \times e \times \frac{1}{E_\pi} \times \frac{M_\pi^4}{(4\pi)^2} = \frac{g_0^\theta\, e}{m_N^2 F_\pi}\,. \tag{5.4}$$

$g_0^\theta\, e/(m_N^2 F_\pi)$ and are therefore of $\mathsf{N}^2\mathsf{LO}$. The naive power counting of the diagram classes depicted in fig. 5.4 (d) and fig. 5.4 (e) is slightly more subtle due to the cancellation of one of the nucleon propagators by the energy dependence of the $\pi\pi\gamma$ vertex. Therefore these diagrams are part of the irreducible transition current and appear at $\mathsf{N^2LO}$.

Finally there are two additional structures — fig. 5.4 (k) and (l) — that appear since the zeroth component of the $\gamma\pi\pi$ vertex is proportional to the energy exchanged and thus gets sensitive to the total neutron–proton mass difference[2], δm_{np}. The contributions of the diagrams of fig. 5.4 (k) and (l) can be estimated as $g_0^\theta e\delta m_{np}/(M_\pi^3 F_\pi)$ and $g_0^\theta e\delta m_{np}/(m_N M_\pi^2 F_\pi)$, respectively. Thus the former (latter) appears to be suppressed by $\delta m_{np}/M_\pi$ ($\delta m_{np}/m_N$) compared to the leading order. Based on NDA one might asign $\delta m_{np} \sim \epsilon M_\pi^2/m_N$ such that diagram (k) would appear at NLO, while diagram (l) would appear at $\mathsf{N^2LO}$. However, as argued above the nucleon mass difference is significantly smaller that its NDA estimate — this observation made us asign $g_1^\theta/g_0^\theta \sim M_\pi/m_N$, and not $(M_\pi/m_N)^2$ as would follow from NDA. In full analogy we now asign diagram (k) and diagram (l) the orders $\mathsf{N^2LO}$ and $\mathsf{N^3LO}$, respectively. Therefore the former is included in our calculation while the latter can be neglected.

In tab. 5.1 the power-counting scales of the P- and T-violating irreducible NN potentials and those of the irreducible as well as of the total transition currents can be found. The power counting scales of specific P- and T-violating and P- and T-conserving vertices are listed in tab. 5.2. Since most of the vertices in tab. 5.2 are irrelevant for the deuteron system, their power counting scales are derived in section 6.2. This completes the discussion of the power counting. In the next section the various diagrams are discussed explicitly.

5.2 EDMs from the θ-term

The computation of the two-nucleon contributions to the deuteron EDM is most efficiently performed in the Breit frame defined by $q = P - P' = (0, \vec{P} - \vec{P}')$ where P and P' denote the total four-momenta of the incoming and outgoing deuteron states and q the momentum of the external 'Coulomb-like' photon. The electric dipole moment d of the deuteron nucleus of mass m_D is then defined (in analogy to the magnetic moment case) by

$$d = \lim_{\vec{q}\to 0} \frac{F_3(\vec{q}^{\,2})}{2m_D}\,, \tag{5.5}$$

[2]We would like to thank J. de Vries, U. van Kolck and R. G. E. Timmermans for drawing our attention to these currents. The same effect in a different context is discussed in detail in ref. [107].

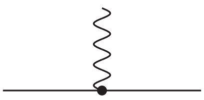	$\sim$	e	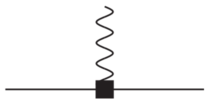	$\sim$	$e\dfrac{F_\pi M_\pi}{m_N^2} g_0^\theta$
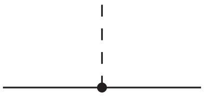	$\sim$	$\dfrac{M_\pi}{F_\pi}$	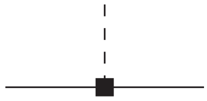	$\sim$	$g_0^\theta = \dfrac{m_N}{M_\pi} g_1^\theta$
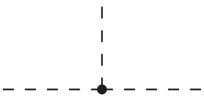	$\sim$	0	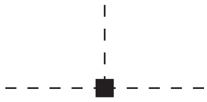	$\sim$	$\dfrac{M_\pi^2}{m_N} g_0^\theta$
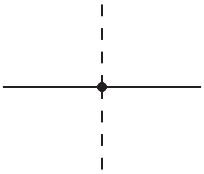	$\sim$	$\dfrac{E_\pi}{F_\pi^2}$	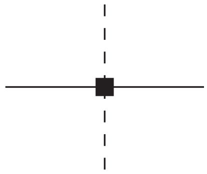	$\sim$	$\dfrac{M_\pi}{F_\pi m_N} g_0^\theta$
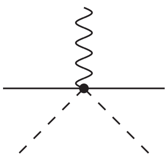	$\sim$	$e\dfrac{1}{F_\pi^2}$	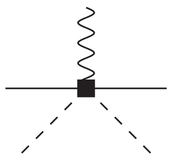	$\sim$	$e\dfrac{M_\pi}{F_\pi m_N^2} g_0^\theta$
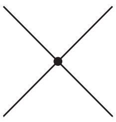	$\sim$	$\dfrac{M_\pi^2}{F_\pi^2 m_N^2}$	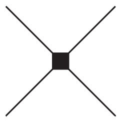	$\sim$	$\dfrac{M_\pi}{F_\pi m_N^2} g_0^\theta$

Table 5.2: Power counting scales of leading P- and T-conserving vertices (left column, see appendix A in [58]) and P- and T-violating vertices induced by the θ-term (right column, see section 6.2). A P- and T-violating vertex is depicted by a solid black box, whereas a P- and T-conserving vertex is depicted by a solid black dot in the figures in this table. Note that the appearance of M_π does not necessarily mean that the vertices vanish in the chiral limit. M_π is also used as a scaling for the 3-momentum here.

where the electric dipole form factor F_3 is related to the P- and T-violating transition current operator $(J^{\rm total}_{\not P \not T})^\mu$ by

$$\left\langle J = 1, J'_z = \pm 1; \vec{P}\,' \left| (J^{\rm total}_{\not P \not T})^0 \right| J = 1, J_z = \pm 1; \vec{P} \right\rangle$$
$$= \mp i q^3 \frac{F_3(\vec{q}^{\,2})}{2 m_D}\,, \tag{5.6}$$

where J is the total angular momentum of the deuteron and J_z and J'_z its z-components for the in- and out-state, respectively.

The total P- and T-violating transition current $J^{\text{total}}_{\not{P}\not{T}}$ can be separated into two contributions of different topology (see fig. 5.1): two-nucleon-reducible transition currents where the P- and T-violation is induced by a P- and T-violating two–nucleon potential on the one hand, and irreducible P- and T-violating transition currents on the other. These will now be discussed in detail.

5.2.1 Contributions from the P- and T-violating NN potential to the deuteron EDM

In order for a P- and T-violating two-nucleon potential to contribute in the deuteron channel, it must induce ${}^3S_1$-${}^3D_1 \to {}^3P_1$ transitions, *i.e.* isospin 0 to isospin 1 and spin 1 to spin 1 transitions since the photon-nucleon coupling is spin independent — it therefore must be antisymmetric in isospin space and symmetric in spin space.

Contributions to the P- and T-violating two-nucleon potential can be further separated into irreducible and reducible potentials. The latter class consists of a P- and T-violating potential and of multiple insertions of the NN potential in the ${}^3S_1$-${}^3D_1$ state and/or in the intermediate ${}^3P_1$ state, which can be either absorbed into the deuteron wave functions, or into the intermediate NN interactions in the ${}^3P_1$ state and therefore do not need to be considered separately.

The leading contribution to the P- and T-violating two-nucleon potential is the class of tree-level diagrams depicted in fig. 5.2 (a). The tree-level potential induced by the g_0^θ vertex is given by [25, 119]

$$V_{5.2(a)}(\vec{l}) = i\frac{g_0^\theta g_A}{2F_\pi}\frac{\vec{l}}{\vec{l}^2+M_\pi^2}\cdot(\vec{\sigma}_{(1)}-\vec{\sigma}_{(2)})\,\vec{\tau}_{(1)}\cdot\vec{\tau}_{(2)}\,, \tag{5.7}$$

where $\vec{l}$ denotes the pion momentum running from nucleon 1 to nucleon 2. It is spin antisymmetric and isospin symmetric and does not induce ${}^3S_1$-${}^3D_1 \to {}^3P_1$ transitions [25, 27, 119].

The potential induced by the g_1^θ vertex reads

$$V^{\theta\,\mathsf{LO}}_{5.2(a)}(\vec{l}) = i\frac{g_1^\theta g_A}{4F_\pi}\frac{\vec{l}}{\vec{l}^2+M_\pi^2}\cdot\Big[(\vec{\sigma}_{(1)}+\vec{\sigma}_{(2)})(\tau^3_{(1)}-\tau^3_{(2)})+(\vec{\sigma}_{(1)}-\vec{\sigma}_{(2)})(\tau^3_{(1)}+\tau^3_{(2)})\Big] \tag{5.8}$$

with $\vec{l}$ as above. It is the same as in [25, 27, 119] with g_1^θ replaced by g_1. This potential-operator has a spin-symmetric and isospin-antisymmetric component and thus contributes to the transition current in the deuteron channel. In order to evaluate its contribution to the EDM of the deuteron we resort to the parametrization of the deuteron wave function of [54] with a ${}^3D_1$-state probability of 4.8%. In order to include the NN interactions in the intermediate ${}^3P_1$-state we use the separable rank-2 representation of the Paris nucleon-nucleon potential of ref. [55] (PEST). The resulting contributions to the deuteron EDM listed in tab. 5.3 are in

Table 5.3: Leading order contributions to the deuteron EDM from the g_1^θ vertex without (d^θ_{PW}, PW: plane wave) and with (d^θ_{MS}, MS: multiple scattering) intermediate ${}^3P_1$-interactions and the total leading order contribution d^θ_{LO} in units of $(g_1^\theta/g_0^\theta)G_\pi^0\, e\,\mathrm{fm}$ with $G_\pi^0 = g_0^\theta g_A m_N/F_\pi$ – calculated in Zero-Range-Approximation (ZRA), with the Argonne v_{18} [56], Reid93 [120] and CD-Bonn [54] potentials.

	Potential	${}^3D_1$-adm.	d^θ_{PW}	d^θ_{MS}	d^θ_{LO}
[25, 29]	ZRA	—	$-1.8\cdot 10^{-2}$	—	$-1.8\cdot 10^{-2}$
[27, 33]	A v_{18}	5.76%			$-1.43\cdot 10^{-2}$
[27]	Reid93	5.7%			$-1.45\cdot 10^{-2}$
[31, 32]	Reid93	5.7%	$-1.93\cdot 10^{-2}$	$0.40\cdot 10^{-2}$	$-1.53\cdot 10^{-2}$
This work	CD-Bonn	4.8%	$-1.95\cdot 10^{-2}$	$0.44\cdot 10^{-2}$	$-1.52\cdot 10^{-2}$

agreement with the results for g_1 of refs. [27] using the Argonne v_{18} potential, of ref. [27, 31, 32] using the Reid93 potential, and of ref. [25, 29], where the deuteron wave function has been used in the Zero-Range-Approximation (ZRA). The ${}^3D_1$-admixture is found to enhance the deuteron EDM by about 20 %, whereas the interaction in the intermediate ${}^3P_1$-state reduces the contribution by about the same amount.

Loops formally start to contribute at NLO. The reducible component of the box potential of fig. 5.2 (b) constitutes a static one-pion exchange and is already accounted for either by the deuteron wave functions or by the interaction in the intermediate ${}^3P_1$-state. Its irreducible component may be obtained by shifting the pole of one of the nucleon propagators into the half plane of the pole of the other nucleon propagator, as outlined in [121–123]: $i/(-v\cdot p_i + i\epsilon) \to -i/(v\cdot p_i + i\epsilon)$. For the sum of the irreducible part of the box potential of fig. 5.2 (b) and the crossed-box potential of fig. 5.2 (c), one finds in dimensional regularization in d space–time dimensions

$$
\begin{aligned}
V^{\theta\,\mathsf{NLO}}_{5.2(b+c)}(\vec{l}) &= -i\frac{g_0^\theta g_A^3}{16\pi^2 F_\pi^3}\frac{1+\frac{3}{2}\xi}{\sqrt{\xi(1+\xi)}}\ln\left(\frac{\sqrt{1+\xi}+\sqrt{\xi}}{\sqrt{1+\xi}-\sqrt{\xi}}\right) \\
&\quad \times \vec{\tau}_{(1)}\cdot\vec{\tau}_{(2)}(\vec{\sigma}_{(1)}-\vec{\sigma}_{(2)})\cdot\vec{l}
\end{aligned}
\tag{5.9}
$$

with $\xi = \vec{l}^2/(4M_\pi^2)$. The divergence has been absorbed by a redefinition of the four-nucleon coupling constant C_2^0 (the scale μ is introduced in dimensional regularization)

$$
C_2^0 \to C_2^0 - \frac{g_0^\theta g_A^3}{F_\pi^3}\left[6L - \frac{3}{16\pi^2}\left(\ln\left(\frac{\mu^2}{M_\pi^2}\right) - 1\right) - \frac{2}{16\pi^2}\right] \tag{5.10}
$$

with

$$
L = \frac{\mu^{d-4}}{16\pi^2}\left\{\frac{1}{d-4} + \frac{1}{2}\left[\gamma_E - 1 - \ln(4\pi)\right]\right\} \tag{5.11}
$$

where $\gamma_E = 0.577215\cdots$ is the Euler–Mascheroni constant.

The triangular potential of fig. 5.2 (d) gives

$$\begin{aligned} V^{\theta\,\mathsf{NLO}}_{5.2(d)}(\vec{l}) &= i\frac{g_0^\theta g_A}{32\pi^2 F_\pi^3}\sqrt{\frac{1+\xi}{\xi}}\ln\left(\frac{\sqrt{1+\xi}+\sqrt{\xi}}{\sqrt{1+\xi}-\sqrt{\xi}}\right) \\ &\quad \times \vec{\tau}_{(1)}\cdot\vec{\tau}_{(2)}(\vec{\sigma}_{(1)}-\vec{\sigma}_{(2)})\cdot\vec{l} \end{aligned} \tag{5.12}$$

where the divergence has been absorbed by a further redefinition of C_2^0:

$$C_2^0 \to C_2^0 - \frac{g_0^\theta g_A}{F_\pi^3}\left[-2L + \frac{1}{16\pi^2}\left(\ln\left(\frac{\mu^2}{M_\pi^2}\right)-1\right) + \frac{2}{16\pi^2}\right]. \tag{5.13}$$

These results reproduce those of ref. [119]. Note that all g_0^θ potential-operators up to one loop as well as the four-nucleon vertex operators are isospin symmetric and spin antisymmetric and therefore vanish in the deuteron channel.

At $\mathsf{N^2LO}$ there are the same topologies as just discussed, however, with the g_0^θ vertex replaced by its isospin-violating counter part g_1^θ. The triangular-potential operator fig. 5.2 (d) vanishes at the considered order. The class of the crossed-box-potential diagrams of fig. 5.2 (c) gives

$$\begin{aligned} V^{\theta\,\mathsf{N^2LO}}_{5.2(c)}(\vec{l}) &= -i\frac{g_1^\theta g_A^3}{8F_\pi^3}\Bigg\{\frac{1}{16\pi^2}\frac{1+\frac{3}{2}\xi}{\sqrt{\xi(1+\xi)}}\ln\left(\frac{\sqrt{1+\xi}+\sqrt{\xi}}{\sqrt{1+\xi}-\sqrt{\xi}}\right) \\ &\quad + \left[3L - \frac{3}{2}\frac{1}{16\pi^2}\left(\ln\left(\frac{\mu^2}{M_\pi^2}\right)-1\right) - \frac{1}{16\pi^2}\right]\Bigg\} \\ &\quad \times \Big[(\tau^3_{(1)}-\tau^3_{(2)})(\vec{\sigma}_{(1)}+\vec{\sigma}_{(2)}) \\ &\qquad + (\tau^3_{(1)}+\tau^3_{(2)})(\vec{\sigma}_{(1)}-\vec{\sigma}_{(2)})\Big]\cdot\vec{l}. \end{aligned} \tag{5.14}$$

Resorting again to the method presented in [121–123] to isolate the irreducible component of the box potential-operator fig. 5.2 (b), the latter is found to be the negative of eq. (5.14) and to cancel the crossed-box-potential-operator fig. 5.2 (c). Therefore, contributions to the total P- and T-violating transition current induced by the P- and T-violating two-nucleon one-loop potential are absent to $\mathsf{N^2LO}$ — not only in the deuteron channel.

The only non-vanishing $\mathsf{N^2LO}$ contributions are thus the vertex corrections shown in diagrams 5.2 (e) and (f). The vertex correction on the P- and T-conserving vertex is readily accounted for, since we use the physical πNN coupling constant in our calculations. The situation is somewhat different for diagram 5.2 (e), where the physical value of the coupling constant is not known, but was calculated/estimated in sect. 4. Since g_0^θ only appears at the one-loop level in the case of the deuteron EDM, we only need to consider g_1^θ here. The quoted uncertainty for g_1^θ is of the order of 50%. On the other hand, the corresponding correction for the P- and T-conserving πNN coupling constant, the so called Goldberger–Treiman discrepancy, is very small [124], such that we may safely assume that the uncertainty given for g_1^θ is sufficiently large such that it includes vertex corrections.

Thus, the only piece of the NN potential that is P- and T-violating *and* contributes to the deuteron EDM is the tree-level diagram depicted in fig. 5.2 (a), with the g_1^θ coupling employed in the P- and T-violating πNN vertex: it is the LO potential.

5.2.2 Contributions from the P- and T-violating irreducible NN transition current

In order for an irreducible transition current not to vanish in the deuteron channel, it has to induce ${}^3S_1$-${}^3D_1 \to {}^3S_1$-${}^3D_1$ (isospin 0 to isospin 0 and spin 1 to spin 1) transitions. It therefore needs to be an isoscalar operator, symmetric in spin space. Therefore the tree-level transition currents — *c.f.* fig. 5.4 (a) — that are all isovector in character, do not contribute to the deuteron EDM. The relevant P- and T-violating irreducible one-loop NN current operators are listed in fig. 5.4 (b)-(j). Diagrams involving P- and T-conserving $NN\pi\gamma$ vertices have been neglected here since, to the order we are working, they do not yield EDM contributions: according to eq. (5.6) EDM contributions are extracted from the 0$^{\text{th}}$-component of matrix elements of transition currents. The leading order, P- and T-conserving $NN\pi\gamma$ vertex $ie(g_A/F_\pi)\,\varepsilon\cdot S\epsilon^{a3b}\tau^b$ (see appendix A of [58] where γ is the "Coulomb photon", $\varepsilon = (1,\vec{0})$) does not have a non-vanishing 0$^{\text{th}}$-component for $S = (0, \vec{\sigma}/2)$.

The diagram classes depicted in fig. 5.4 (g) and fig. 5.4 (h) are of order $g_0^\theta\, e/(m_N^2 F_\pi)$ and thus N^{2}LO. For a photon coupling to nucleon 2 the two-nucleon-irreducible component of diagram fig. 5.4 (g) and diagram fig. 5.4 (h) give

$$\left(J^{\theta\,\mathsf{N^2LO}}_{5.4(g+h)}\right)^\mu = i\frac{eg_0^\theta g_A^3}{128\pi F_\pi^3 M_\pi}\left[\frac{1}{1+\xi}+\frac{2}{\sqrt{\xi}}\arctan\sqrt{\xi}\right]v^\mu \\ \times(\vec{\tau}_{(1)}\cdot\vec{\tau}_{(2)}-\tau^3_{(2)})(\vec{\sigma}_{(1)}-\vec{\sigma}_{(2)})\cdot(\vec{p}_2^{\,\prime}-\vec{p}_2+\vec{q}) \tag{5.15}$$

with $\xi = |\vec{p}_2^{\,\prime}-\vec{p}_2+\vec{q}\,|^2/(4M_\pi^2)$ in terms of the initial (final) momentum $p_i(p_i')$ of nucleon i and the momentum of the out-going photon q. Although the operator (5.15) contains an isospin-symmetric component, it is spin-antisymmetric and vanishes in the deuteron channel.

The diagram classes depicted in fig. 5.4 (d) and (e) vanish in the deuteron channel, since they are isovectors.

In addition there are diagrams at N^{2}LO where the photon couples to a vertex correction (fig. 5.4 (i) and (j)); however, terms that contain the g_0^θ vertex turn out to be isovectors and thus do not contribute to the deuteron channel, and those that contain g_1^θ start to contribute only at $\mathsf{N^3LO}$.

The triangular diagrams depicted in fig. 5.4 (b), fig. 5.4 (c) and fig. 5.4 (f) are all of order $\mathsf{N^2LO}$. Diagrams of the types of fig. 5.4 (c) and fig. 5.4 (f) vanish in the deuteron channel which can be readily seen from their isospin components: diagram fig. 5.4 (c) is proportional to $\tau^3_{(2)}$ (photon coupling to nucleon 2) and diagram fig. 5.4 (f) is proportional to $2\tau_{(2)} + i(\vec{\tau}_{(1)} \times \vec{\tau}_{(2)})$. A class of currents that has a spin- and isospin-symmetric component is depicted in fig. 5.4 (b):

$$\begin{aligned} \left(J^{\theta\,\mathsf{N^2LO}}_{5.4(b)}\right)^\mu &= i\frac{eg_0^\theta g_A}{4F_\pi^3}\,v^\mu\,\left(\vec{\tau}_{(1)}\cdot\vec{\tau}_{(2)} - \tau^3_{(2)}\right) \\ &\times\;\left(I(p_1{-}p_1')\,(\vec{p}_1{}'{-}\vec{p}_1)\cdot\vec{\sigma}_{(2)} + (1\leftrightarrow 2)\right) \end{aligned} \tag{5.16}$$

with $I(l) = -\arctan(|\vec{l}|/(2M_\pi))/(8\pi|\vec{l}|)$ [58]. Resorting to the CD-Bonn wave function of the deuteron as used above, the resulting g_0^θ-contribution to the deuteron EDM for the ${}^3S_1$ state and ${}^3D_1$ admixture is found to be

$$d^\theta_{5.4(b)} = \underbrace{-2.00\cdot 10^{-4}\;\times G^0_\pi\, e\,\mathrm{fm}}_{{}^3S_1} - \underbrace{0.53\cdot 10^{-4}\;\times G^0_\pi\, e\,\mathrm{fm}}_{{}^3D_1\text{-adm.}} \tag{5.17}$$

where $G^0_\pi := g_0^\theta g_A m_N/F_\pi$.

The class of diagrams depicted in fig. 5.4 (k), see ref. [30], gives

$$\begin{aligned} \left(J^{\theta\,\mathsf{N^2LO}}_{5.4(k)}\right)^0 &= -i\frac{eg_0^\theta g_A \delta m_{np}}{F_\pi}(\vec{\tau}_{(1)}\cdot\vec{\tau}_{(2)} - \tau^3_{(1)}\tau^3_{(2)}) \\ \times\;& \frac{\vec{\sigma}_{(1)}\cdot(\vec{p}_1{-}\vec{p}_1{}') + \vec{\sigma}_{(2)}\cdot(\vec{p}_2 - \vec{p}_2{}')}{[(\vec{p}_1{-}\vec{p}_1{}')^2 + M_\pi^2]\,[(\vec{p}_2{-}\vec{p}_2{}')^2 + M_\pi^2]}\,. \end{aligned} \tag{5.18}$$

The explicit evaluation of the EDM contribution of fig. 5.4 (k) yields $0.31\cdot 10^{-4}\times G^0_\pi\, e\,\mathrm{fm}$, which justifies the classification as $\mathsf{N^2LO}$.

The absence of *both* — divergences and (undetermined) counter-terms up to $\mathsf{N^2LO}$— ensures the predictive power of the two-nucleon contributions to the deuteron EDM that is induced by the θ-term. Together with the g_1^θ contribution the total two-nucleon contribution to the EDM of the deuteron induced by the θ-term is then given by:

$$\begin{aligned} d^\theta_{^2\mathrm{H}} &= d^\theta_{\mathsf{LO}} + d^\theta_{\mathsf{N^2LO}} \\ &= \left[\left(-15.2\cdot\frac{g_1^\theta}{g_0^\theta} - 0.22\right) \pm 0.03\right]\times 10^{-3}\,G^0_\pi\, e\,\mathrm{fm}\,, \end{aligned} \tag{5.19}$$

where the uncertainty accounts for not considered higher order contributions according to the power counting. Alternatively we may express the result directly in terms of $\bar\theta$, the strength of the QCD θ-term, and write

$$\begin{aligned} d^\theta_{^2\mathrm{H}} &= d^\theta_{\mathsf{LO}} + d^\theta_{\mathsf{N^2LO}} \\ &= -\big((5.9\pm 3.9) - (0.5\pm 0.2)\big)\times 10^{-4}\,\bar\theta\, e\,\mathrm{fm}\,, \end{aligned} \tag{5.20}$$

where the uncertainties now contain, in addition to the one given in eq. (5.19), also the uncertainties in the coupling constants g_0^θ and g_1^θ. Therefore the final result is completely dominated by the contribution from the P- and T- and isospin-violating tree-level potential proportional to g_1^θ.

5.3 Numerical analysis

Additional to the largely analytical computation of the previous sections, the numerical analysis of the P- and T-violating form factor in the low-q regime and of the LO NN contribution to the deuteron EDM is presented in this section. Before turning to the results of the numerical computation, a brief explanation of applied numerical technique is given.

5.3.1 Numerical analysis technique

Let $|\psi_{^2\mathrm{H}}\rangle$ denote the deuteron state and $\mathcal{O}(q)$ the complete NN transition current operator which has in general a P- and T-conserving as well as a P- and T-violating component. If the Breit frame is chosen as the reference frame with the photon momentum $q = (0, \vec{q})$, the transition current operator $\mathcal{O}(\vec{q})$ only depends on the photon three-momentum $\vec{q}$. The operator $\mathcal{O}(\vec{q})$ acting on the deuteron state $|\psi_{^2\mathrm{H}}\rangle$ is considered to be the initial arrangement of particles (i.e. the starting seed in the iteration procedure described below).

The complete NN interaction Hamiltonian is comprised of three components,

$$\bar{H} := H_0 + V + V_{\not{P}\not{T}} \equiv H + V_{\not{P}\not{T}}\,, \tag{5.21}$$

where H_0 is the free NN Hamiltonian, V is the P- and T-conserving NN potential and $V_{\not{P}\not{T}}$ is the P- and T-violating NN potential. By utilizing the resolvent identity [125], the full NN propagator $\bar{G}$ can be re-expressed as

$$\begin{aligned}
\bar{G} \;&:=\; \frac{1}{E - H - V_{\not{P}\not{T}} + i\epsilon} \\
&=\; \frac{1}{E - H + i\epsilon} + \frac{1}{E - H + i\epsilon} V_{\not{P}\not{T}} \frac{1}{E - H - V_{\not{P}\not{T}} + i\epsilon} \\
&\equiv\; G + G\, V_{\not{P}\not{T}}\, \bar{G}\,.
\end{aligned} \tag{5.22}$$

Since $V_{\not{P}\not{T}}$ constitutes only a small perturbation of the P- and T-conserving NN potential V, all terms in $\bar{G}$ proportional to powers of $V_{\not{P}\not{T}}$ larger than one can be neglected and the above iteration terminates after one step. A viable approximation of $\bar{G}$ is thus given by

$$\bar{G} \approx G + G V_{\not{P}\not{T}} G\,. \tag{5.23}$$

The complete NN propagator eq. (5.23) has to be applied to the initial arrangement of particles $\mathcal{O}(\vec{q})|\psi_{^2\mathrm{H}}\rangle$ in order to construct the form factor of the deuteron.

The resulting state $|\Psi\rangle$ which describes an incoming photon coupling to the nucleus with multiple P- and T-conserving and P- and T-violating interactions of the nucleons in the nucleus is given by

$$\begin{aligned} |\Psi(\vec{q})\rangle &= \lim_{\epsilon\to 0} i\epsilon\,\bar{G}\,\mathcal{O}(\vec{q})|\psi_{^2\mathrm{H}}\rangle + \cdots \\ &= \lim_{\epsilon\to 0} \left(i\epsilon\,G + i\epsilon\,G\,V_{\not{P}\not{T}}\,G\right)\mathcal{O}(\vec{q})|\psi_{^2\mathrm{H}}\rangle + \cdots . \end{aligned} \tag{5.24}$$

For the bound state of the deuteron, the application of the P- and T-conserving operator G yields

$$G|\psi_{^2\mathrm{H}}\rangle = \lim_{\epsilon\to 0} \frac{i\epsilon}{E - H_0 - V + i\epsilon}|\psi_{^2\mathrm{H}}\rangle = |\psi_{^2\mathrm{H}}\rangle\,. \tag{5.25}$$

One then obtains for the matrix element $\langle\psi_{^2\mathrm{H}}|\Psi\rangle$:

$$\langle\psi_{^2\mathrm{H}}|\Psi(\vec{q})\rangle = \langle\psi_{^2\mathrm{H}}|\left(\mathbb{1} + \lim_{\epsilon\to 0} V_{\not{P}\not{T}} G\right)\mathcal{O}(\vec{q})|\psi_{^2\mathrm{H}}\rangle\,. \tag{5.26}$$

Eq. (5.26) is already sufficient as a starting point for the numerical analysis of the nuclear contributions to the deuteron EDM. However, as shown in chapter 6, the investigation of $3N$ systems requires the application of the resolvent identity for G, i.e.

$$G = G_0 + G_0\,V\,G\,, \tag{5.27}$$

with $G = (E - H_0 + i\epsilon)^{-1}$. The desired final expression of the form factor is then given by

$$\begin{aligned} \langle\psi_{^2\mathrm{H}}|\Psi(\vec{q})\rangle &= \langle\psi_{^2\mathrm{H}}|\mathcal{O}(\vec{q})|\psi_{^2\mathrm{H}}\rangle \\ &+ \lim_{\epsilon\to 0}\langle\psi_{^2\mathrm{H}}|\left(V_{\not{P}\not{T}}\,G_0 + V_{\not{P}\not{T}}\,G_0\,V\,G\right)\mathcal{O}(\vec{q})|\psi_{^2\mathrm{H}}\rangle + \cdots . \end{aligned} \tag{5.28}$$

Since the interest of this section is in the leading order contribution to the EDM of the deuteron, the transition current operator $\mathcal{O}(\vec{q})$ is identified with the leading order P- and T-conserving photon-nucleon coupling as depicted in fig. (5.5). The first term on the right-hand side of eq. (5.28) is then the P- and T-conserving form factor at leading order in ChPT which admits an expansion in even powers of $\vec{q}$. The second term and the third term on the right-hand side of eq. (5.28) constitute the leading P- and T-violating components of the form factor and admit expansions in odd powers of $\vec{q}$. Since only the second and the third term are relevant for the computation of the deuteron EDM, the first term on the right-hand side of eq. (5.28) is neglected from now on. One contribution of second term is diagrammatically depicted in fig. 5.5 (a), whereas one of the diagrams corresponding to the third term on the right-hand side of the above equation is depicted in fig 5.5 (b). The second term dominates the third term, which constitutes the correction to the second term due to multiple P- and T-conserving NN interactions in the intermediate state.

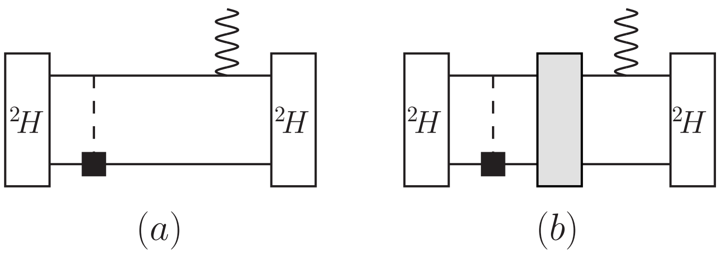

Figure 5.5: The P- and T-violating vertex is depicted by a black box. For each class of diagrams only one representative is shown. The shaded box in the center of diagram (b) denotes P- and T-conserving interactions in the intermediate $^3P_1$-state

The full P- and T-conserving propagator G can be rewritten for the NN-system in terms of the NN T-matrix t as $G = G_0 + G_0\, t\, G_0$ since

$$\begin{aligned} & G = G_0 + G_0\, t\, G_0 = G_0 + G_0\, V\, G_0 + G_0\, V\, G_0\, t\, G_0 \\ \Leftrightarrow \quad & G_0\, t\, G_0 = G_0(V + V\, G_0\, t)G_0 \\ \Leftrightarrow \quad & t = V + V\, G_0\, t\,. \end{aligned} \tag{5.29}$$

The second term on the right-hand side of eq (5.26) then becomes:

$$\lim_{\epsilon\to 0}\langle\psi_{^2\mathrm{H}}|V_{\not P \not T}\, G_0\, \mathcal{O}(\vec{q})|\psi_{^2\mathrm{H}}\rangle + \lim_{\epsilon\to 0}\langle\psi_{^2\mathrm{H}}|V_{\not P \not T}\, G_0\, t\, G_0\, \mathcal{O}(\vec{q})|\psi_{^2\mathrm{H}}\rangle\,. \tag{5.30}$$

As explained in section 5.2.1, the intermediate state is the $^3P_1$-state and P- and T-conserving NN interactions do not allow for transitions into other states since the total angular momentum, the total spin and the total isospin are conserved in NN interaction. The inversion of the operator $(\mathbb{1} - G_0\, V)$ required to obtain the T-matrix,

$$t = (1 - V\, G_0)^{-1} V\,, \tag{5.31}$$

is then particularly simple to compute in the absence of coupled channels.

The leading order photon-nucleon vertex in heavy baryon ChPT is given by $ie\,(\mathbb{1}+\tau^3)/2$. The effect of the operator $\mathcal{O}(\vec{q})$ is, apart from the potentially isospin-changing isospin operator component, a shift of the momentum of the nucleon to which the photon couples. The architecture of the developed program to compute the matrix elements of eq. (5.30) requires all operators to be decomposed into their partial wave components. The partial wave decomposition of $\mathcal{O}(\vec{q})|\psi_{^2\mathrm{H}}\rangle$ is given by F.20 in appendix F. The partial wave decomposition of the considered P- and T-violating NN potentials, the g_1 induced one-pion exchange potential, is given by eq. (F.10). The decompositions of the g_1 induced one-pion exchange potentials for η-, ρ- and ω-mesons, eqs. (F.16), (F.17), and (F.18), are obtained by slight modifications of eq. (F.10).

5.3.2 Numerical analysis of the deuteron EDM

Since the P- and T-violating form factor is included in the total form factor $\langle\psi_{^2\mathrm{H}}|\Psi\rangle$, the EDM of the deuteron $d^{tot}_{^2\mathrm{H}}$ is according to eq. (5.5) and eq. (5.6) in the Breit frame equal to

$$d^{tot}_{^2\mathrm{H}} = -i \lim_{|q|\to 0} \frac{1}{|q|} \langle\psi_{^2\mathrm{H}}; J'=1, J'_z=1, -\vec{q}/2|\Psi; J=1, J_z=1, \vec{q}/2\rangle\,. \tag{5.32}$$

The deuteron EDM has been computed by using the two phenomenological potentials Av_{18} and CD-Bonn as well as NLO, N^{2}LO and N^{3}LO ChPT potentials for the P- and T-conserving component of the nuclear potential. The numerical implementations of the phenomenological potentials have been provided by A. Nogga [126] and those of the ChPT potentials by E. Epelbaum [57]. The numerical routines used here which generate the deuteron wave functions for each of the considered potentials have also been developed by A. Nogga [127]. As explained in detail in [57], the regularizations of the P- and T-conserving ChPT potentials require two kinds of cutoffs: (i) for loop contributions to the potential, *e.g.* the two-pion exchange NN potential, the *Spectral Function Regularization* scheme is employed to render the expressions finite. Within this scheme, the potential obtained from dimensional regularization is re-expressed in its spectral representation, which reads for the central component [57]:

$$V_C(q) = \frac{2q^4}{\pi}\int_{2M_\pi}^{\infty} d\mu \frac{1}{\mu^3}\frac{\rho(\mu)}{\mu^2+q^2}\,, \quad \rho(\mu) = \mathrm{Im}(V_C(0^+ - i\mu))\,, \tag{5.33}$$

with the spectral function $\rho(\mu)$ and four-momentum transfer q. The dimensional regularization of the potential leads to the emergence of artificial and model-dependent large momentum (short-range) contributions. When the spectral function is subjected to the cutoff [57]:

$$\rho(\mu) \to \rho^{\tilde{\Lambda}}(\mu)\Theta(\tilde{\Lambda} - \mu)\,, \tag{5.34}$$

all large momentum components above $q > \tilde{\Lambda}$ are removed from the regularized expression. (ii) The fact that ChPT potential does not decrease with an growing momentum transfer renders the Lippmann-Schwinger equation for the ChPT potential ultraviolet divergent. Divergences of the Lippmann-Schwinger equation are removed by the application of an additional cutoff parameter Λ in the regulator function f^Λ which is applied to the potential V (p, p': incoming and outgoing relative momentum of the NN system) [57]:

$$V(p,p') \to \exp(-p^6/\Lambda^6)V(p,p')\exp(-p'^6/\Lambda^6)\,. \tag{5.35}$$

The results of the numerical analysis are presented in tab. 5.4. There are now two separate power countings when ChPT potentials for the P- and T-conserving component of the NN potential are considered: one for the P- and

Table 5.4: Leading order nuclear contributions to the deuteron EDM from the g_1 vertex without (d_{PW}, PW: plane wave) and with (d_{MS}, MS: multiple scattering) intermediate ${}^3P_1$-interactions and the total leading order nuclear contribution $d_{^2\mathrm{H}}$ in units of $10^{-2}\, G_\pi^1\, e\,\mathrm{fm}$ with $G_\pi^1 = g_1 g_A m_N / F_\pi$ – calculated with the Argonne v_{18} potential [56], the CD-Bonn potential [54] and chiral potentials up to $\mathsf{N^3LO}$ for several combinations of Lippmann-Schwinger cutoffs (LS) and Spectral Function Regularization cutoffs (SFR) [57].

Potential	LS [MeV]	SFR [MeV]	This work d_{PW}	This work d_{MS}	This work $d_{^2\mathrm{H}}$	[27] $d_{^2\mathrm{H}}$	[33] $d_{^2\mathrm{H}}$
Av_{18}	–	–	−1.93	0.48	−1.45	−1.43	−1.45
CD-Bonn	–	–	−1.95	0.51	−1.45	–	–
ChPT (NLO)	400	500	−1.86	0.21	−1.65	–	–
ChPT (NLO)	550	500	−1.88	0.23	−1.65	–	–
ChPT (NLO)	550	600	−1.87	0.24	−1.63	–	–
ChPT (NLO)	400	700	−1.86	0.22	−1.63	–	–
ChPT (NLO)	550	700	−1.86	0.25	−1.61	–	–
ChPT ($\mathsf{N^2LO}$)	450	500	−1.88	0.32	−1.56	–	–
ChPT ($\mathsf{N^2LO}$)	600	500	−1.92	0.43	−1.49	–	–
ChPT ($\mathsf{N^2LO}$)	550	600	−1.92	0.50	−1.43	–	–
ChPT ($\mathsf{N^2LO}$)	450	700	−1.89	0.42	−1.47	–	–
ChPT ($\mathsf{N^2LO}$)	600	700	−1.94	0.65	−1.29	–	–
ChPT ($\mathsf{N^3LO}$)	450	500	−1.65	0.25	−1.40	–	–
ChPT ($\mathsf{N^3LO}$)	600	600	−1.60	0.26	−1.34	–	–
ChPT ($\mathsf{N^3LO}$)	550	600	−1.62	0.26	−1.36	–	–
ChPT ($\mathsf{N^3LO}$)	450	700	−1.68	0.26	−1.42	–	–
ChPT ($\mathsf{N^3LO}$)	600	700	−1.62	0.27	−1.35	–	–

T-violating component of the NN potential which has been described in section 5.1 and one for the P- and T-conserving component of the NN potential. Only the leading order P- and T-violating NN operator which does not vanish in the deuteron channel, eq. (5.8), is considered in this section, whereas P- and T-conserving ChPT potentials up to $\mathsf{N^3LO}$ are utilized. The reason for the consideration of ChPT potentials up to $\mathsf{N^3LO}$ is to investigate the uncertainty of P- and T-conserving component of the nuclear potential. Since only the leading P- and T-violating potential operator is considered, the power counting mentioned below and in tab. 5.4 is exceptionally the one of the P- and T-conserving component of the nuclear potential. As pointed out in [57], the cutoff parameters Λ and $\tilde{\Lambda}$ of the ChPT potentials have to be chosen carefully in order to ensure that only the momentum regime where ChPT has full predictive capacity is considered. The numerical analysis of the leading order EDM contribution from ChPT potentials has been performed for various combinations of Lippmann-Schwinger cutoffs (LS) and Spectral Function Regularization cutoffs (SFR).

The results from the Av_{18} and CD-Bonn potentials are in agreement with the results obtained in section 5.2 and with those of [27, 33]. The phenomenological potentials do not allow for an assessment of the uncertainties attributed to the P- and T-conserving component of the nuclear potential. When ChPT potentials are employed, estimates of the inherent uncertainties can be obtained by considering different orders and by studying the cutoff dependence, i.e. different combinations of LS- and SFR-cutoff parameters. The ChPT potentials yield results which do not significantly deviate from the results based on the considered phenomenological potentials. In particular, the NLO ChPT potential gives plane-wave (PW) contributions which are very close to those obtained from the phenomenological potentials. This observation can be attributed to the fact that the dominating $^3S_1$ channel of the deuteron wave function is already quite accurately described by the LO one-pion exchange potential (see [57]). The inclusion of N^{2}LO nuclear interactions does not alter the plane-wave contributions significantly. Surprisingly, this order-independence of the plane-wave contributions does somehow not extend to N^{3}LO nuclear interactions: the plane-wave contributions from the N^{3}LO ChPT potential are well outside the bands defined by plane-wave contributions from the NLO and N^{2}LO ChPT potentials. By inspection of the plots of the radial component of the deuteron wave function in [128], unexpected oscillations in the large-distance part of the deuteron wave function ($\gtrsim 2$ fm) were revealed[3]. Due to this unexpected observation, the results from the N^{3}LO ChPT potential are disregarded in the assessment of the uncertainty of the deuteron EDM, but are still displayed for completeness.

The multiple-scattering (MS) contributions –the contributions from P- and T-conserving interactions in the intermediate $^3P_1$ state– do not exhibit any order independence: the band defined by the N^{2}LO multiple-scattering results is much broader and does not comprise the band defined by the NLO results. The N^{2}LO contributions to the nuclear ChPT potential include two-pion exchange diagram classes which cause a significant difference to the NLO ChPT potential [57]. The smaller cutoff dependence of the NLO results with respect to the N^{2}LO results has to be attributed to the following reason: since for the NLO ChPT potential the next higher-order contact interactions appear at N^{3}LO, the cutoff dependence is regarded as an N^{3}LO effect [57]. However, the cutoff dependence of N^{2}LO results reveals that this inferred uncertainty profoundly understates the actual uncertainty. The SFR regularization of the two-pion exchange diagrams enhanced by a factor of π is mainly responsible for the larger cutoff dependence of the total N^{2}LO results. Therefore, the difference between $d_{^2\mathrm{H}}$ from the NLO and from

[3]Private communication with the author of [57]: numerical implementation of the N^{3}LO ChPT potential is currently being revised.

Table 5.5: Nuclear contributions to the deuteron EDM from the g_1 induced one-meson exchange without (d_{PW}, PW: plane wave) and with (d_{MS}, MS: multiple scattering) intermediate ${}^3P_1$-interactions and the total nuclear contribution $d_{^2\mathrm{H}}$ for heavier mesons in units of $10^{-3}\,G^1_{\eta,\rho,\omega}\,e\,\mathrm{fm}$ with $G^1_{\eta,\rho,\omega} = g_1^{\eta,\rho,\omega} G_{\eta,\rho,\omega}$, where $G_{\eta,\rho,\omega}$ are the P- and T-conserving ηN, ρN, ωN coupling constants, respectively, and $g_1^{\eta,\rho,\omega}$ their P- and T-violating counterparts. The EDM contributions are calculated with the Argonne v_{18} [56] potential and the CD-Bonn potential [54].

Meson	Potential	This work			[27]	[33]
		d_{PW}	d_{MS}	$d_{^2\mathrm{H}}$	$d_{^2\mathrm{H}}$	$d_{^2\mathrm{H}}$
η	Av_{18}	-0.30	0.15	-0.16	-0.16	-0.16
η	CD-Bonn	-0.34	0.17	-0.17	–	–
ρ	Av_{18}	-0.14	0.08	-0.06	-0.06	-0.06
ρ	CD-Bonn	-0.17	0.10	-0.07	–	–
ω	Av_{18}	0.14	-0.08	0.06	0.06	0.06
ω	CD-Bonn	0.17	-0.10	0.07	–	–

the N^{2}LO ChPT potential is largely due to the d_{MS} contributions. The cutoff dependence of the N^{2}LO ChPT potential is therefore the most accurate one and the N^{2}LO ChPT potential is used to compute the nuclear contribution to the deuteron EDM and its uncertainty.

The center of the range of values defined by the results obtained from the two phenomenological potentials and the N^{2}LO ChPT potential is chosen to be the final result for the nuclear contribution to the deuteron EDM. The uncertainty is then determined by the maximum deviation of these values from the center. The leading order nuclear contribution to the deuteron EDM and its uncertainty are given by:

$$d^\theta_{^2\mathrm{H}} = (-1.43\,\pm\,0.14)\cdot 10^{-2}\,\frac{g_1^\theta}{g_0^\theta}\,G^0_\pi\cdot e\,\mathrm{fm}\,. \tag{5.36}$$

This result is consistent with the analytical result in tab. (5.3). The results for contributions from higher-order P- and T-violating diagrams obtained in section 5.2 can be exploited to refine the uncertainty, which yields:

$$\begin{aligned} d^\theta_{^2\mathrm{H}} &= (-1.43\,\pm\,0.18)\cdot 10^{-2}\,\frac{g_1^\theta}{g_0^\theta}\,G^0_\pi\cdot e\,\mathrm{fm} \\ &= -(0.55\pm 0.37)\cdot 10^{-16}\,\bar\theta\,e\,\mathrm{cm}\,. \end{aligned} \tag{5.37}$$

For completeness, the contributions to the deuteron EDM from P- and T-violating one-meson exchange potentials for the heavier η, ρ and ω mesons are listed in tab. 5.5, which provide an additional assessment of the short-range contributions encoded in the P- and T-violating $4N$ vertices of eq. (4.113). Due to

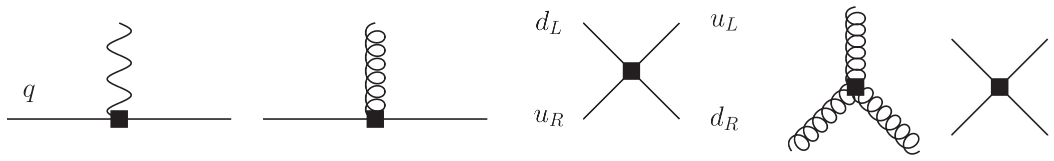

Figure 5.6: P- and T-violating dimension-six sources. The P- and T-violating vertex is depicted by a solid black box.

isospin selection rules, only the isospin violating $4N$ vertex is of relevance in the deuteron system, which is classified as $\mathsf{N^3LO}$. The one-meson exchange potentials are given by eqs. (F.16), (F.17) and (F.18), whereas their partial wave decompositions are easily obtained from the decomposition of the g_1 induced one-pion exchange potential operator eq. (F.9).

Taking into consideration that the P- and T-conserving ηNN, ρNN and ωNN coupling constants (for vector couplings) are numerically smaller than the P- and T-conserving πNN coupling constant [33] and assuming that the P- and T-violating ηNN, ρNN and ωNN coupling constants are in agreement with their NDA estimates, the power counting of the short-range $4N$ contribution to deuteron EDM is confirmed. Furthermore, the short-range sensitivity of the potentials are revealed: the larger the mass of the considered meson, the larger is the relative deviation of the result from the CD-Bonn potential to the one from the Av_{18} potential, for instance.

5.4 EDM from effective dimension-six sources

The different hierarchies of coupling constants of P- and T-violating vertices for the considered sources of P and T violation translate into different nuclear contributions to the deuteron EDM. The coupling constants of the P- and T-violating vertices from the effective dimension-six sources can not be computed within ChPT as established in section 4.2.2, which requires supplementary input from other non-perturbative techniques, *e.g.* Lattice QCD. Since such predictions for these coupling constants are not likely to be available soon, the only means at our disposal to assess their sizes is NDA. Section 4.3 provides NDA estimates of the leading coupling constants as defined in eq. (4.113) for each considered source of P and T violation. The NDA estimates and the hierarchies of coupling constants presented in section 4.3 allow for the following statements on nuclear contributions to the deuteron EDM from the effective dimension-six sources.

- $qCEDM$:
  As demonstrated in section 4.3, the $qCEDM$ which is graphically depicted in fig. 5.6 gives rise to an isospin-conserving g_0 πNN vertex and an isospin-

breaking g_1 πNN vertex at leading order. Therefore, the estimates of two P- and T-violating potential or current operators which only differ by the type of the P- and T-violating πNN vertex (g_0 or g_1 vertex) are identical. The leading-order contribution is again defined by the P- and T-violating one-pion exchange potential induced by the g_1 vertex. The contribution to the deuteron EDM from this potential is given in tab. 5.3 with g_1^θ replaced by g_1. Due to the absence of a suppression of g_1 with respect to g_0, the order estimates of operators for the $qCEDM$ is obtained from the one for the θ-term by multiplying the order estimates of g_1 induced operators for the θ-term by m_N/M_π.

Contributions from the one-loop potential operators depicted in figs. 5.2 (b)-(d) are now of order $\mathsf{N^2LO}$ with respect to the contribution from the leading g_0 and g_1 induced potential operator shown in fig. 5.2 (a). Contributions from the irreducible current operators figs. 5.4 (b)-(f) are counted as $\mathsf{N^3LO}$ — with a possible π-enhancement for triangular diagrams. Furthermore, the leading $4N$ vertex induced by the isospin-violating component of the $qCEDM$ which does not vanish in the deuteron channel appears at $\mathsf{N^2LO}$. It is thus sufficient to consider only those one-loop diagrams with the largest expected yield in order to ensure that no extraordinary enhancements occur and the uncertainty estimates are reliable.

The relevant contributions from the P- and T-violating potential operators were already discussed in the previous section. Additionaly, the share of the deuteron EDM generated by the class of diagrams depicted in fig. 5.4 (b) with g_1 vertices is found to be equal to the one generated by the class shown in fig. 5.4 (c) with g_1 vertices and non-vanishing. The contributions of the diagram classes depicted in fig. 5.4 (d) and fig. 5.4 (f) vanish, whereas the contribution of the diagram class pictured in fig. 5.4 (e) is equal to the sum of contributions of the diagrams shown in figs. 5.4 (b) and (c) times a factor of $-g_A^2$. All these diagram classes are enhanced by a factor of π that commonly appears for triangle topologies:

$$d_{5.4(b)+(c)} = -1.34 \cdot 10^{-4}\, g_1\, \frac{g_A m_N}{F_\pi}\, e\,\mathrm{fm} = d_{5.4(e)}/(-g_A^2) \tag{5.38}$$

These numerical results for each single diagram are in perfect agreement with their π-enhanced $\mathsf{N^3LO}$ power counting estimates, which demonstrates that no extraordinary enhancements of particular diagrams occur. The other diagram classes (fig. 5.4 (g), (h), (i) and (j)) are suppressed due to the absence of a π-enhancement and the smallness of δm_{np}^{str} as previously noted.

The leading order nuclear contribution to the EDM of the deuteron is given by

$$d_{^2\mathrm{H}} = (-1.43 \pm 0.18) \cdot 10^{-2}\, g_1\, \frac{g_A m_N}{F_\pi}\, e\,\mathrm{fm}\,. \tag{5.39}$$

- $4qLR$-op:
  According to eq. (4.205), the $4qLR$-op depicted in fig. 5.6 induces the g_1 πNN vertex as well the Δ_3 3π vertex at leading order. The leading order contribution to the deuteron EDM is again defined by the g_1 induced one-pion exchange potential, which is given in tab. 5.3 with g_1^θ replaced by g_1. The corresponding g_0 induced potential operator (which vanishes in the deuteron channel) is an N^{2}LO operator. The 3π Δ_3 vertex starts to contribute at the one-loop level and yields only suppressed EDM contributions. The leading order nuclear contribution to the deuteron EDM is thus given by eq. (5.39), where g_1 is induced by the $4qLR$-op.

- $qEDM$:
  All coupling constants of vertices which do not involve photon fields are suppressed by a factor of $\alpha_{em}/(4\pi)$. The deuteron EDM induced by the $qEDM$ therefore equals its single-nucleon contributions at leading order:

$$d_{^2\mathrm{H}}^{tot} = d_n + d_p + d_{^2\mathrm{H}} = d_n + d_p + \mathcal{O}(\alpha_{em}/(4\pi))\,. \tag{5.40}$$

- $4q$-op and $gCEDM$:
  The leading order contributions to the deuteron EDM for these two dimension-six sources (depicted in fig. 5.6) are induced by the P- and T-violating γNN coupling constants $d_{0,1}$ and $4N$ coupling constants $C_{1,2}^{0,3}$ of eq. (4.113). P- and T-violating πNN vertices are suppressed by at least two orders in magnitude. Since the leading coupling constants are not quantitatively known, the leading order contributions to the deuteron EDM are difficult to asses. The deuteron EDM from can tentatively be estimated to equal the sum of the single-nucleon contributions if the leading P- and T-violating γNN- and $4N$ vertices are indeed of the same order:

$$d_{^2\mathrm{H}}^{tot} \approx d_n + d_p\,. \tag{5.41}$$

These results confirm the conclusions presented in [30].

5.5 Summary

As already stated in the introduction, the established relation between the QCD θ-term and the P- and T-violating πNN coupling constant is not sufficient to predict the size of the electric dipole moment of a *single* nucleon (neutron or proton) within ChPT, since the calculable one-loop contributions are of the same order as undetermined counter terms, which could be estimated by resonance saturation. However, this unpleasant feature is not present for the two-nucleon contributions to the deuteron EDM and other light nuclei, which contribute already at tree-level order — unaffected by any counter terms — and which can be derived —

admittedly with a large uncertainty — up-to-and-including N^{2}LO, see eqs. (5.19) and (5.20) at the end of section 5.2.2. The N^{2}LO contributions of these results are (up to vertex corrections discussed in sect. 5.1) solely governed by the irreducible transition currents. The latter include loops which for the first time have been calculated in this chapter. Any contribution with unknown coefficients can only appear at N^{3}LO. All nuclear EDM contributions are in perfect agreement with their power counting estimates.

The dominant part of the deuteron's two-nucleon EDM from the QCD θ-term resulted from the isospin-violating and P- and T-violating πNN coupling constant g_1. The isospin violation of this coupling can be estimated from the strong contribution to the pion mass-square splitting $(\delta M_\pi^2)^{\rm str}/(M_\pi^2\epsilon)$. Although this ratio gives a small number, its contribution to g_1^θ gets enhanced by the relatively large pion-nucleon sigma term. Nominally, g_1^θ should be suppressed by two orders relative to its isospin-conserving counter part, g_0^θ. However, the latter is governed by the strong part of the neutron-proton mass splitting and therefore is found to be exceptionably small. Thus the isospin-violating coupling g_1^θ — as already observed by Lebedev *et al.* [26] — is effectively only suppressed by one power in the counting.

This is important since the one-pion exchange with one g_0^θ vertex cannot contribute to the two-nucleon part of the deuteron EDM because of isospin selection. This was summarized in the folklore that the deuteron would be blind to the two-nucleon contributions generated by the θ-term. This folklore, however, should be abandoned. A measurement of a non-vanishing neutron, a non-vanishing proton and a non-vanishing deuteron EDM would suffice to determine the strength of the QCD θ-term, $\bar\theta$, from data. In fact, the two-nucleon part of the deuteron EDM given in (5.20) is of the same magnitude and therefore comparable in size with the non-analytic isovector part of the nucleon EDM as calculated in ref. [48], which is, using as input the value of g_0^θ from eq. (4.158),

$$d_N^{\text{non-analyt.}} = -(21 \pm 9) \times 10^{-4}\,\bar\theta\, e\,\text{fm}\,, \tag{5.42}$$

where the uncertainty contains both the variation of the loop scale as proposed in ref. [48] as well as the uncertainty in g_0^θ. This number may presumably be taken as a scale which governs the single nucleon EDMs. However, the non-analytic contribution to the isoscalar part of the nucleon EDM is an order of magnitude smaller due to a suppression by a factor M_π/m_N as well as the absence of a chiral logarithm. Whether the proton or neutron EDM are really of the same magnitude as the two-nucleon part of the deuteron EDM is a question which *only* experiments might eventually be able to answer in the foreseeable future.

The computation of the leading order nuclear contribution to the deuteron EDM has been performed in two different ways. The first is a largely analytical computation up to N^{2}LO utilizing paramterizations of the CD-Bonn deuteron wave function [54] and of the PEST separable rank-two potential to account for interactions in the intermediate state [55]. Such parametrizations of the intermediate state wave function are not available for most potentials. In order to assess the uncertainty of the result from the P- and T-conserving component of the NN potential, the cutoff and order dependence of the result when using P- and T-conserving ChPT potentials have to be investigated. This has been done by the second computational approach, which entails a numeric calculation of the leading order nuclear EDM contribution by utilizing various phenomenological and ChPT potentials for the P- and T-conserving component of the NN potential. Out of all ChPT potentials considered, the $\mathsf{N^2LO}$ ChPT potential is identified to reflect the inherent uncertainties most accurately and is therefore chosen in combination with the Av_{18} and CD-Bonn phenomenological potentials to define the final result and its uncertainty. The uncertainty has then been adjusted to account for the uncertainty of the P- and T-violating component of the NN potential obtained within the analytical computation.

Under the assumption that EDMs are driven by P and T violation that is induced by the QCD θ-term, a relation between the EDMs of the deuteron $d^{tot}_{^2\mathrm{H}}$, the neutron d_n and the proton d_p and the calculated nuclear EDM contribution of the deuteron $d_{^2\mathrm{H}}$ can be given:

$$d^{tot}_{^2\mathrm{H}} = d_n + d_p - (5.5 \pm 3.7) \cdot 10^{-4}\,\bar{\theta}\,e\,\mathrm{fm}. \tag{5.43}$$

A cross-check of the so-extracted $\bar{\theta}$ value would be possible — still solely from data — by a measurement of the EDM of ^{3}He. Another strategy to test or falsify the $\bar{\theta}$ value would involve lattice QCD calculations and just two successful EDM measurements, namely one single-nucleon EDM, *i.e.* the one of the neutron or proton, and the deuteron EDM. If even all three of them are measured, then one could use lattice QCD for a first test correlating the proton and neutron EDM results in terms of the parameter $\bar{\theta}$ and to use formula (5.43) for an additional, orthogonal test.

If indeed the QCD θ-term would have failed these tests — either by a direct comparison of data or by the additional involvement of lattice QCD — then the following picture would emerge: in case $d_D - d_n - d_p$ is sizable *compared to what eq. (5.43) in combination with experimental or lattice data predicts*, then the dimensional analysis reveals a dominance of the $qCEDM$ and/or $4qLR$-op, feeding the coupling proportional to g_1 [4]. On the other hand, if this difference is very small, the θ-term, $qCEDM$ and $4qLR$-op are probably not at work, but one or several of the other three dimension-six P- and T-violating operators. More insight can be gained from a study of the EDM for ^{3}He. This reasoning stresses once more the need for high-precision measurements, not only of the neutron EDM but also of the EDMs of charged particles as the proton, deuteron and ^{3}He.

[4]Note that ref. [30] stated the dominance of the quark-color mechanism already under the assumption that $d_D - d_n - d_p$ itself is sizeable. The difference emerges since in ref. [30] the relative suppression between g_1^θ and g_0^θ was taken from naive dimensional analysis that predicts a negligible contribution from the g_1^θ term.

Chapter 6

The EDMs of helion and triton

After the detailed analysis of the nuclear contributions to the EDM of the deuteron presented in the preceding chapter, the focus will now shift to the analysis of nuclear contributions to the EDMs of bound states of three nucleons, namely the ^{3}He and ^{3}H nuclei[1]. The isospin selection rules which cause the EDM contribution of the potential operator eq. (5.7) to vanish in the deuteron channel are absent in the helion and triton channel and the LO contribution is now defined by eq. (5.7). As for the deuteron, the aim of this chapter is to provide an analysis of these EDMs within the framework of ChPT. Proceeding analogously to the previous chapter we begin with the analysis of the ^{3}He and ^{3}H EDMs induced by the θ-term and discuss the ^{3}He and ^{3}H EDMs induced by the effective dimension-six sources afterwards. The power counting of the single-nucleon EDM contributions and of P- and T-violating NN- and $3N$-potential and current operators are presented in section 6.2. The numerical analysis technique is employed in section 6.3 and the results are presented and discussed in section 6.4. Section 6.5 is concerned with the effective dimension-six sources. The NN and $3N$ contributions to the ^{3}He and ^{3}H EDMs are referred to as nuclear contributions below.

6.1 Single nucleon contributions

It is well known that the contribution of the EDMs of the constituent nucleons to the EDM of the nucleus largely equals the neutron EDM d_n for ^{3}He, since the spins of the protons almost cancel each other to form a system of spin 0 by the Pauli principle. The opposite is true for ^{3}H system, in which the two neutron spins are anti-aligned, such that the single nucleon contribution to the ^{3}H EDM is approximately given by the proton EDM d_p. More precisely, the total EDMs of ^{3}He and ^{3}H, denoted by $d^{tot}_{^3\mathrm{He},^3\mathrm{H}}$, equal the weighted sums of their single-nucleon

[1]The content of this chapter will be published in [129].

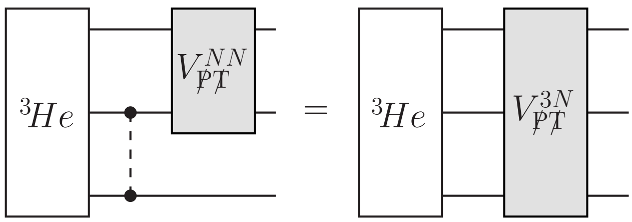

Figure 6.1: In order to compare P- and T-violating NN to $3N$ operators, a P- and T-conserving one-pion exchange is extracted from the ^{3}He (or ^{3}H) wave function for a P- and T-violating NN operator, rendering it a P- and T-violating $3N$ operator.

components (d_n and d_p) and nuclear components ($d_{^3\mathrm{He}}$ and $d_{^3\mathrm{H}}$) [30]:

$$d^{tot}_{^3\mathrm{He}} = \quad 0.88\, d_n \; - 0.047\, d_p + d_{^3\mathrm{He}}\,, \tag{6.1}$$

$$d^{tot}_{^3\mathrm{H}} = -0.050\, d_n + 0.90\, d_p \; + d_{^3\mathrm{H}}\,. \tag{6.2}$$

The subsequent sections in this chapter are dedicated to the analysis of the nuclear contributions.

6.2 Power counting

The power counting scheme for P- and T-violating NN operators presented in section 5.1 can be extended to the $3N$ system by embedding it into a power counting scheme for $3N$ operators as proposed in [116] and graphically depicted in fig. 6.1: by exploiting the Schroedinger equation $|\psi_{3N}\rangle = G_0 V|\psi_{3N}\rangle$ for a $3N$ bound state, a P- and T-conserving NN interaction can be extracted from the wave function in which the nucleon unaffected by the P- and T-violating NN interaction is involved. The resulting combination of the P- and T-conserving one-pion exchange, the free $3N$ propagator and the P- and T-violating one-pion exchange can then be considered a P and T-violating $3N$ interaction. To be more specific, let $V_{\not P\not T}(12)$ be a P- and T-violating interaction of the nucleons labelled by (1) and (2) in the $3N$ system. When $V(23)$ denotes the P- and T-conserving NN component of the $3N$ potential V of the nucleons labelled by (2) and (3), the product $V_{\not P\not T}(12)\, G_0\, V(23)$ is a $3N$ interaction, which allows for a direct comparison to other P- and T-violating $3N$ interactions.

The order estimate of an irreducible P- and T-violating NN operator has therefore to be multiplied by a factor of $m_N/(F_\pi^2 M_\pi^2)$ (a factor of m_N/M_π^2 for the free $3N$ propagator and by a factor of $1/F_\pi^2$ for the P- and T-conserving NN one-pion exchange operator extracted from the wave function) in order to obtain the order estimate of this operator in the $3N$ system.

This power counting scheme should be compared to the one of Weinberg [113], according to which a factor of $1/M_\pi^3$ is generated when an NN potential operator

Table 6.1: Power-counting scales of the P- and T-violating $3N$ potentials and (total) transition currents relevant for the three-nucleon contributions to the θ-term-induced EDMs of the ^{3}He and ^{3}H, where the equivalence $4\pi F_\pi \sim m_N$ is assumed. The power counting scales of the three-nucleon potentials and three-nucleon currents expressed in terms of g_1^θ are obtained by the replacement $g_0^\theta \to g_1^\theta m_N/M_\pi$. The dimensionless quantities g_0^θ and g_1^θ are considered to be $\mathcal{O}(1)$.

	$3N$ potential		(total) $3N$ transition current	
LO	$g_0^\theta m_N/(F_\pi^3 M_\pi^3)$	$g_1^\theta m_N^2/(F_\pi^3 M_\pi^4)$	$g_0^\theta\, e\, m_N^2/(F_\pi^3 M_\pi^5)$	$g_1^\theta\, e\, m_N^3/(F_\pi^3 M_\pi^6)$
NLO	$g_0^\theta/(F_\pi^3 M_\pi^2)$	$g_1^\theta m_N/(F_\pi^3 M_\pi^3)$	$g_0^\theta\, e\, m_N/(F_\pi^3 M_\pi^4)$	$g_1^\theta\, e\, m_N^2/(F_\pi^3 M_\pi^5)$
N^{2}LO	$g_0^\theta/(F_\pi^3 M_\pi m_N)$	$g_1^\theta/(F_\pi^3 M_\pi^2)$	$g_0^\theta\, e/(F_\pi^3 M_\pi^3)$	$g_1^\theta\, e\, m_N/(F_\pi^3 M_\pi^4)$

is embedded into a $3N$ system. The ratio of the corresponding factor in our power counting scheme, $m_N/(F_\pi^2 M_\pi^2)$, to this factor is $M_\pi m_N/F_\pi^2 \sim 4\pi M_\pi/F_\pi$, where $4\pi F_\pi \sim m_N$ has been assumed. The difference between both power counting schemes regarding an NN potential operator embedded into a $3N$ system is therefore is a factor of approximately 4π.

6.2.1 Power counting of single-nucleon operators

The $3N$ power counting of contributions from single-nucleon operators is obtained in exactly the same fashion. The power counting of the single nucleon γNN operator eq. (5.1) is explained in section 5.1. Embedding this power counting into the $3N$ power counting requires the multiplication by a factor of $(m_N/(F_\pi^2 M_\pi^2))^2$, which gives:

$$\frac{g_0^\theta\, e\, F_\pi M_\pi}{m_N^2} \times \left(\frac{m_N}{F_\pi^2 M_\pi^2}\right)^2 = g_0^\theta \frac{e}{F_\pi^3 M_\pi^3} \quad (\mathsf{N^2LO})\,. \tag{6.3}$$

This single-nucleon operator formally induces an N^{2}LO contribution here as demonstrated in the next subsection.

6.2.2 Power counting of irreducible potential operators

Due to the absence of the strict isospin selection rules imposed on NN operators in the deuteron system, the leading order (LO) contribution is now defined by the diagram class of the one-pion exchange NN potential operator induced by the g_0^θ vertex which is depicted in fig. 6.2 (a): its NN power counting is given by $g_0^\theta/(F_\pi M_\pi)$ according to tab. 5.1 in section 5.1.2. The power counting of this operator in the $3N$ system requires the multiplication of this NN power counting by the above mentioned factor $m_N/(F_\pi^2 M_\pi^2)$:

$$\frac{g_0^\theta}{F_\pi M_\pi} \times \frac{m_N}{M_\pi^2} \times \frac{1}{F_\pi^2} = g_0^\theta \frac{m_N}{F_\pi^3 M_\pi^3} \quad (\mathsf{LO})\,. \tag{6.4}$$

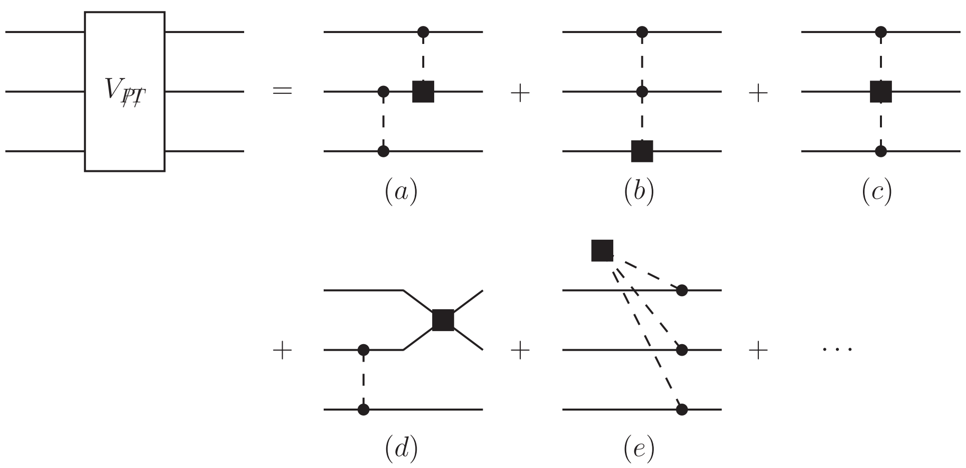

Figure 6.2: Contributions to the P- and T-violating $3N$ potential: (a) LO contributions (for a g_0^θ vertex), (b) $\mathsf{N^2LO}$ contributions (for a g_0^θ vertex), (c)-(e) $\mathsf{N^2LO}$ contributions. The diagrams (a) and (b) with g_1^θ vertices instead of a g_0^θ vertices are further suppressed by one order in magnitude. The P- and T-violating pion-nucleon vertex is depicted by a black box. A P- and T-conserving pion-nucleon vertex is depicted by a solid dot. For each class of diagrams only one representative is shown.

The power counting scales of the three leading orders are listed in tab. 6.1. Due to the suppression of g_1^θ with respect to g_0^θ by one order in our counting (see eq. 4.173 and the discussion in section 4.3), the order estimate of this diagram class induced by the g_1^θ vertex is obtained by a multiplication of the above result by a factor of M_π/m_N and is thus counted as NLO. The g_1^θ-induced one-pion exchange operator has defined the LO contribution in section 5.1 because of the isospin selection rule of the deuteron. The power counting scales of P- and T-violating NN operators in the $3N$ system can be obtained from the power counting scales of P- and T-violating operators in the NN system in section 5.1 by the multiplication by M_π/m_N. An LO P- and T-violating operator in section 5.1 is an NLO P- and T-violating operator in the $3N$ system, an NLO operator in section 5.1 is an $\mathsf{N^2LO}$ operator in the $3N$ system here and so on.

The order estimate of the Weinberg-Tomozawa vertex in the diagram class depicted in fig. 6.2 (b) is $M_\pi^2/(F_\pi^2 m_N)$. The order estimate of the diagram class of fig. 6.2 (b) with a g_0^θ vertex then reads

$$\frac{M_\pi}{F_\pi} \times \frac{1}{M_\pi^2} \times \frac{M_\pi^2}{F_\pi^2 m_N} \times \frac{1}{M_\pi^2} \times g_0^\theta = \frac{g_0^\theta}{F_\pi^3 M_\pi m_N} \quad (\mathsf{N^2LO})\,, \tag{6.5}$$

which is the order estimate of an $\mathsf{N^2LO}$ contribution. The P- and T-violating $\pi\pi NN$ vertex in the diagrams of the class depicted in in fig. 6.2 (c) comes from the terms proportional to the LECs d_{17} and d_{19} in the third-order Lagrangian in the pion-nucleon sector eq. (D.14). The LECs d_{17} and d_{19} are related to the β_1 coefficient in [42] by

$$\frac{\beta_1}{2F_\pi} N^\dagger \partial_\mu \pi_3 S^\mu N = \frac{8(-d_{17}+d_{19})M_\pi^2 \epsilon}{2F_\pi} N^\dagger \partial_\mu \pi_3 S^\mu N\,, \tag{6.6}$$

for which an upper bound of $\beta_1 = (0 \pm 9)\cdot 10^{-3}$ [30, 130, 131] exists. Expressing $(d_{17} - d_{19})$ in terms of β_1 and inserting the resulting expression into eq. (D.14), the coupling constant of the leading P- and T-violating $\pi\pi NN$ vertex becomes:

$$\frac{\beta_1(1-\epsilon^2)\bar{\theta}}{4\epsilon F_\pi^2} N^\dagger \vec{\pi}\cdot\partial_\mu \vec{\pi} S^\mu N = \frac{\beta_1 g_0^\theta}{\delta m_{np}^{str} F_\pi} N^\dagger \vec{\pi}\cdot\partial_\mu \vec{\pi} S^\mu N \equiv \frac{\bar{\beta}_1}{F_\pi} N^\dagger \vec{\pi}\cdot\partial_\mu \vec{\pi} S^\mu N\,, \tag{6.7}$$

where equation eq. (4.158) has been used. The NDA estimate of $\beta_1/\delta m_{np}^{str}$ is $1/m_N$. Although the actual value of δm_{np}^{str} is smaller than its NDA estimate, the upper bound on β_1 indicates that it might also be smaller than its NDA estimate $\epsilon M_\pi^2/m_N^2$ [132]. Furthermore, using the upper bound for β_1 and eq. (4.157), $\beta_1/\delta m_{np}^{str}$ approximately equals its NDA estimate times a factor of π. The order estimate of the diagram class depicted in fig. 6.2 (c) then reads:

$$\frac{M_\pi}{F_\pi} \times \frac{1}{M_\pi^2} \times \bar{\beta}_1 \frac{M_\pi}{F_\pi} \times \frac{1}{M_\pi^2} \times \frac{M_\pi}{F_\pi} = \frac{\bar{\beta}_1}{F_\pi^3 M_\pi} \sim \frac{g_0^\theta}{F_\pi^3 M_\pi m_N} \quad (\mathsf{N^2LO})\,, \tag{6.8}$$

This is the order estimate of an N^{2}LO diagram class. Since the above value for β_1 is only an upper bound and the uncertainty of g_1^θ which induces the LO diagram class is rather large, the digram class of fig. 6.2 (c) can safely be regarded as N^{2}LO.

The order estimate of the diagram class depicted in fig. 6.2 (d) can be obtained by the following reasoning: the P- and T-violating $4N$ vertices can be regarded to encode P- and T-violating exchanges of heavy mesons of mass m_N. Taking g_0^θ as a scale (or rather as an upper bound) for the P- and T-violating meson-nucleon coupling, M_π/F_π as a scale (upper bound) for the P- and T-conserving meson-nucleon vertex and a factor of $1/m_N^2$ for the heavy meson propagator, one arrives at an order estimate of $g_0^\theta M_\pi/(m_N^2 F_\pi)$ for the P- and T-violating $4N$ vertex. The order estimate of the diagram class ig. 6.2 (d) is then given by:

$$g_0^\theta \frac{M_\pi}{F_\pi m_N^2} \times \frac{m_N}{M_\pi^2} \times \frac{M_\pi}{F_\pi} \times \frac{1}{M_\pi^2} \times \frac{M_\pi}{F_\pi} = \frac{g_0^\theta}{F_\pi^3 M_\pi m_N} \quad (\mathsf{N^2LO})\,, \tag{6.9}$$

which is the order estimate of an N^{2}LO digram class.

According to eq. (4.177), the coupling constant Δ_3 of the P- and T-violating 3π vertex in fig. 6.2 (e) equals $m_N\Delta_3 = g_0^\theta M_\pi^2/m_N$. Inserting this expression

$$g_0^\theta \frac{M_\pi^2}{m_N} \times \left(\frac{1}{M_\pi^2}\right)^3 \times \left(\frac{M_\pi}{F_\pi}\right)^3 = \frac{g_0^\theta}{F_\pi^3 M_\pi m_N} \quad (\mathsf{N^2LO})\,, \tag{6.10}$$

which means that it is also an N^{2}LO diagram class. All other P- and T-violating irreducible potential operators with vertices from $\mathcal{L}_\pi^{(4)}$, $\mathcal{L}_{\pi N}^{(3)}$ and $\mathcal{L}_{\pi N}^{(4)}$ which are listed in appendix D yield order estimates of at least N^{2}LO.

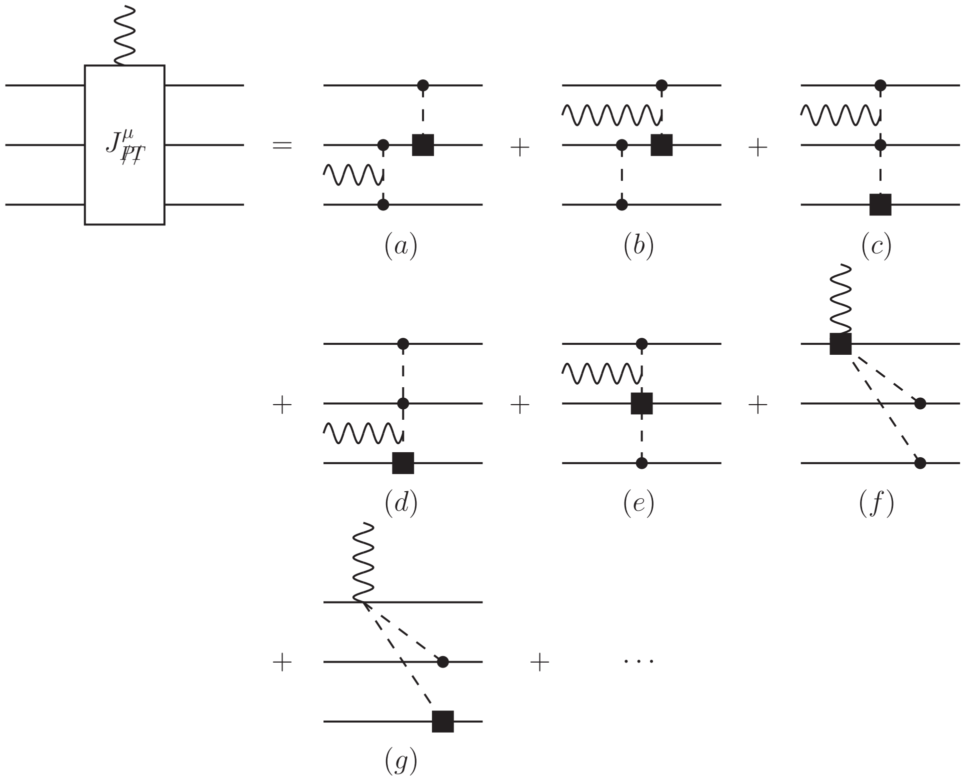

Figure 6.3: Contributions to the P- and T-violating $3N$ transition current: (a)+(b) N^{2}LO contribution (for a g_0^θ vertex) , (c)+(d) N^{4}LO contributions (for a g_0^θ vertex), (e)+(f) N^{4}LO contributions, (g) N^{2}LO contribution (for a g_0^θ vertex). Diagrams (a)-(d) and (f) with g_1^θ vertices are further suppressed by one order in magnitude. the P- and T-violating pion-nucleon vertex is depicted by a black box. A P- and T-conserving pion-nucleon vertex is depicted by a solid dot. For each class of diagrams only one representative is shown.

6.2.3 Power counting of irreducible transition current operators

In order to compare the power counting of a $3N$ potential operator to the one of a $3N$ transition current operator, the former has to be multiplied by a factor of m_N/M_π^2 accounting for an additional free three-nucleon propagator and a factor of e for the γNN coupling. The power counting scales of the P- and T-violating $3N$ transition currents from LO to N^{2}LO are listed in tab. 6.1. Various diagram classes of irreducible transition current operators are displayed in fig. 6.3.

The diagram classes of fig. 6.3 (a) and (b) have the same order estimates since they only differ by a transposition of the P- and T-violating vertex and a P- and T-conserving vertex. The order estimate of the P- and T-conserving γNN vertex is given by em_N/M_π^2, which yields the following order estimates for the diagram classes fig. 6.3 (a) and (b):

$$\frac{M_\pi}{F_\pi} \times \frac{1}{M_\pi^2} \times g_0^\theta \times \frac{m_N}{M_\pi^2} \times \frac{M_\pi}{F_\pi} \times \frac{1}{M_\pi^2} \times \frac{eM_\pi^2}{m_N} \times \frac{1}{M_\pi^2} \times \frac{M_\pi}{F_\pi} = \frac{g_0^\theta e}{F_\pi^3 M_\pi^3} \quad (\mathsf{N^2LO}), \tag{6.11}$$

which is the order estimate of an N^{2}LO diagram class. The power counting of the diagrams pictured in fig. 6.3 (c) and (d) with one Weinberg-Tomozawa vertex each is straight forward and yields N^{4}LO:

$$\frac{M_\pi}{F_\pi} \times \frac{1}{M_\pi^2} \times \frac{M_\pi^2}{F_\pi^2 m_N} \times \frac{1}{M_\pi^2} \times \frac{eM_\pi^2}{m_N} \times \frac{1}{M_\pi^2} \times g_0^\theta = \frac{g_0^\theta e}{F_\pi^3 M_\pi m_N^2} \quad (\mathsf{N^4LO}). \tag{6.12}$$

The P- and T-violating $\pi\pi NN$ vertex in fig. 6.3 (e) is same as the one in fig. 6.2 (c), which gives the following N^{4}LO order estimate:

$$\frac{M_\pi}{F_\pi} \times \frac{1}{M_\pi^2} \times \frac{eM_\pi^2}{m_N} \times \frac{1}{M_\pi^2} \times \frac{M_\pi g_0^\theta}{F_\pi m_N} \times \frac{1}{M_\pi^2} \times \frac{M_\pi}{F_\pi} = \frac{g_0^\theta e}{F_\pi^3 M_\pi m_N^2} \quad (\mathsf{N^4LO}). \tag{6.13}$$

Finally, the P- and T-violating $\gamma\pi\pi NN$ vertex in fig. 6.3 (f) originates from terms of the fouth-order pion-nucleon Lagrangian eq. (D.21). The order estimate of such a vertex is $g_0^\theta e M_\pi/(F_\pi m_N^2)$. The order estimate of the diagram class depicted in fig. 6.3 (f) is then given by:

$$\frac{g_0^\theta e M_\pi}{F_\pi m_N^2} \times \left(\frac{1}{M_\pi^2}\right)^2 \times \left(\frac{M_\pi}{F_\pi}\right)^2 = \frac{g_0^\theta e}{F_\pi^3 M_\pi m_N^2} \quad (\mathsf{N^4LO}), \tag{6.14}$$

which is the order estimate of an N^{4}LO diagram class. The order estimate of the P- and T-conserving $\gamma\pi\pi NN$ vertex in fig. 6.3 (g) is e/F_π^2. The order estimate of the entire diagram fig. 6.3 (g) is then given by:

$$\frac{e}{F_\pi^2} \times \left(\frac{1}{M_\pi^2}\right)^2 \times \frac{M_\pi}{F_\pi} \times g_0^\theta = \frac{g_0^\theta e}{F_\pi^3 M_\pi^3} \quad (\mathsf{N^2LO}). \tag{6.15}$$

This means that there is no irreducible transition current operator to be considered in this chapter. Other classes of diagrams not mentioned here are either NN diagrams which have been discussed in the previous chapter or are of irrelevant subleading orders, i.e. of an order beyond NLO. The order estimates of all vertices mentioned in this section are also listed in tab. 5.2.

6.3 Numerical analysis technique

The numerical analysis technique of the leading nuclear contributions to the EDMs of ^{3}He and ^{3}H from P- and T-violating NN potential operators is explained in this section. The technique described below is a generalization of the

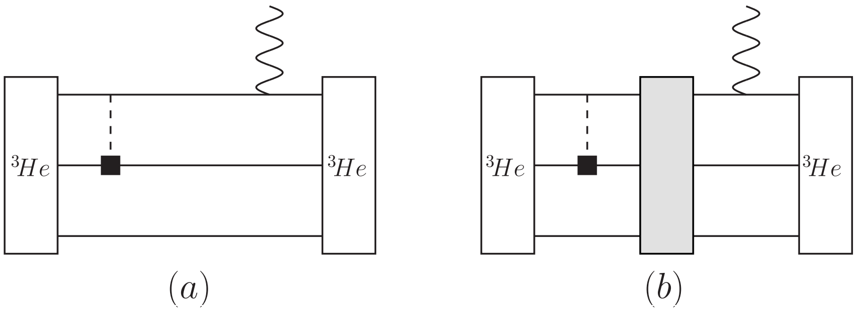

Figure 6.4: Total LO P- and T-violating ^{3}He transition current. The P- and T-violating pion-nucleon vertex is depicted by a black box. For each class of diagrams only one representative is shown. The shaded box in the center of diagram (b) denotes P- and T-conserving interactions in the intermediate state.

numerical analysis of the leading order NN contribution to the deuteron EDM presented in section 5.3 to the $3N$ system. The subsequent explanation of our numerical analysis technique is exactly the same for both $3N$ bound states. The form factor of ^{3}He (or ^{3}H) is given by the generalization of eq. (5.28) to the $3N$ system:

$$\begin{aligned} \langle \psi_{^3\mathrm{He}} | \Psi \rangle &= \langle \psi_{^3\mathrm{He}} | \mathcal{O}(\vec{q}) | \psi_{^3\mathrm{He}} \rangle \\ &+ \langle \psi_{^3\mathrm{He}} | \big(V_{\not{P}\not{T}}\, G_0 + V_{\not{P}\not{T}}\, G_0\, V\, G \big)\, \mathcal{O}(\vec{q}) | \psi_{^3\mathrm{He}} \rangle + \cdots , \end{aligned} \tag{6.16}$$

where $V_{\not{P}\not{T}}$ is either the P- and T-violating one-pion exchange NN potential operator induced by a general g_0 or g_1 vertex. Since the focus of this section is on the leading EDM contributions, the transition current operator $\mathcal{O}(\vec{q})$ can be identified with the leading order P- and T-conserving γNN coupling in heavy baryon ChPT to all nucleon lines as in section 5.3. The P- and T-violating component of the ^{3}He form factor is then given by the second matrix element on the right-hand side of eq. (6.16).

The development of the parallel program designed to run on the supercomputers *JUROPA* and *JUQUEEN* in order to numerically compute this matrix element involved a considerable programing effort. The architecture of the program requires all operators to be decomposed into their partial wave components. The partial wave decomposition of $V_{\not{P}\not{T}}$ for the considered NN potential operators in the $3N$ system is provided by eqs. (F.26) and (F.27) and the partial wave decomposition of $\mathcal{O}(\vec{q})|\psi_{^3\mathrm{He}}\rangle$ by eq. (F.28) in appendix F. The second matrix element on the right-hand side of eq. (6.16) has to be multiplied by a factor of two to account for the inverse time ordering. The completely symmetrized form for all potential and transition current operators is implied. The two matrix elements on the right-hand side of eq. (6.16) correspond either to diagrams without P- and T-conserving interactions in the intermediate state as the one depicted in fig. 6.4 (a) or to diagrams with intermediate state interactions as the one depicted in fig. 6.4 (b).

Whereas $V_{\not{P}\not{T}}$ is a pure NN potential operator, the P- and T-conserving $3N$ potential V comprises NN and $3N$ interactions. Let V_{2N}^{ij} denote the NN-interaction of nucleons (i) and (j) for $i, j = 1, 2, 3$ and $i \neq j$. The $3N$-interaction of nucleons can be decomposed into three parts with each of them being symmetric under an exchange of two nucleons:

$$V = V_{2N}^{12} + V_{3N}^{(1)} + V_{2N}^{23} + V_{3N}^{(2)} + V_{2N}^{13} + V_{3N}^{(3)}\,, \tag{6.17}$$

where the $3N$ potentials $V_{3N}^{(i)}$ are defined by

$$P_{23}\, V_{3N}^{(1)}\, P_{23} = V_{3N}^{(1)}\,, \quad P_{13}\, V_{3N}^{(2)}\, P_{13} = V_{3N}^{(2)}\,, \quad P_{12}\, V_{3N}^{(3)}\, P_{12} = V_{3N}^{(3)}\,. \tag{6.18}$$

The nucleon transposition operator P_{ij}, $i \neq j$, transposes nucleon (i) and nucleon (j) in the $3N$ system. By the means of nucleon transposition operators, the potential V can be re-expressed solely in terms of $V_{2N}^{(12)}$ and $V_{3N}^{(3)}$:

$$V = V_{2N}^{12} + V_{3N}^{(3)} + P_{12}P_{23}\,(V_{2N}^{12} + V_{3N}^{(3)})\,P_{23}P_{12} + P_{13}P_{23}\,(V_{2N}^{12} + V_{3N}^{(3)})\,P_{23}P_{13}\,. \tag{6.19}$$

Exploiting the fact that cyclic permutation operators commute with the full $3N$ propagator G and do not alter $\mathcal{O}(\vec{q})|^3\mathrm{He}\rangle$, one arrives at

$$P_{23}P_{12}\, G\, \mathcal{O}(\vec{q})|\psi_{^3\mathrm{He}}\rangle = P_{23}P_{13}\, G\, \mathcal{O}(\vec{q})|\psi_{^3\mathrm{He}}\rangle = G\, \mathcal{O}(\vec{q})|\psi_{^3\mathrm{He}}\rangle\,. \tag{6.20}$$

Inserting eq. (6.19) into eq. (6.16) the third term on the right-hand side becomes

$$\begin{aligned} V\, G\, \mathcal{O}(\vec{q})|\psi_{^3\mathrm{H}}\rangle &= (\mathbb{1} + P_{12}P_{23} + P_{13}P_{23})(V_{2N}^{12} + V_{3N}^{(3)})G\mathcal{O}(\vec{q})|\psi_{^3\mathrm{He}}\rangle \\ &\equiv (\mathbb{1} + P)(V_{2N}^{12} + V_{3N}^{(3)})G\mathcal{O}(\vec{q})|\psi_{^3\mathrm{He}}\rangle\,, \end{aligned} \tag{6.21}$$

where P is defined by $P = P_{12}P_{23} + P_{13}P_{23}$ such that $\mathbb{1} + P$ is the (cyclic) nucleon symmetrization operator. This allows us to define the Faddeev component $|U^{(3)}\rangle$ by

$$V\, G\, \mathcal{O}(\vec{q})\, |\psi_{^3\mathrm{He}}\rangle \equiv (\mathbb{1} + P)\, |U^{(3)}\rangle\,. \tag{6.22}$$

A concise introduction into Faddeev equations can be found in [125]. The Faddeev component $|U^{(3)}\rangle$ obeys the following equation:

$$\begin{aligned} |U^{(3)}\rangle &= (V_{2N}^{12} + V_{3N}^{(3)})G\mathcal{O}(\vec{q})|\psi_{^3\mathrm{He}}\rangle \\ &= (V_{2N}^{12} + V_{3N}^{(3)})G_0\mathcal{O}(\vec{q})|\psi_{^3\mathrm{He}}\rangle \\ &\quad + (V_{2N}^{12} + V_{3N}^{(3)})G_0(\mathbb{1} + P)(V_{2N}^{12} + V_{3N}^{(3)})G\mathcal{O}(\vec{q})|\psi_{^3\mathrm{He}}\rangle \\ &= (V_{2N}^{12} + V_{3N}^{(3)})G_0\mathcal{O}(\vec{q})|\psi_{^3\mathrm{He}}\rangle + (V_{2N}^{12} + V_{3N}^{(3)})G_0(\mathbb{1} + P)|U^{(3)}\rangle\,, \end{aligned} \tag{6.23}$$

where the resolvent identity eq. (5.27) has been utilized. However, this equation does not have a compact kernel. Since the term $V_{2N}^{12}G_0|U^{(3)}\rangle$ contains a δ-function for nucleon (3), the kernel is not fully connected even after a finite number of iterations. The troubling term $V_{2N}^{12}G_0|U^{(3)}\rangle$ can be re-summed independently by the application of an appropriately chosen operator to this equation. We therefore write

$$\begin{aligned}(\mathbb{1}-V_{2N}^{12}G_0)|U^{(3)}\rangle &= (V_{2N}^{12}+V_{3N}^{(3)})G_0\mathcal{O}(\vec{q})|\psi_{^3\mathrm{He}}\rangle + V_{2N}^{12}G_0P|U^{(3)}\rangle \\ &\quad + V_{3N}^{(3)}\,G_0(\mathbb{1}+P)|U^{(3)}\rangle\,,\end{aligned} \tag{6.24}$$

and exploit the identity

$$\begin{aligned}& t_{12} = V_{2N}^{12} + t_{12}G_0V_{2N}^{12} \\ \Leftrightarrow\;& (t_{12}-V_{2N}^{12}-t_{12}G_0V_{2N}^{12})G_0 = 0 \\ \Leftrightarrow\;& (\mathbb{1}+t_{12}G_0)(\mathbb{1}-V_{2N}^{12}G_0) = \mathbb{1}\,.\end{aligned} \tag{6.25}$$

By multiplication of the left-hand side and the right-hand side of eq. (6.24) by $(\mathbb{1}+t_{12}G_0)$, the Faddeev component $|U^{(3)}\rangle$ is found to obey

$$\begin{aligned}|U^{(3)}\rangle &= t_{12}G_0\mathcal{O}(\vec{q})|\psi_{^3\mathrm{He}}\rangle + (\mathbb{1}+t_{12}G_0)V_{3N}^{(3)}G_0\mathcal{O}(\vec{q})|\psi_{^3\mathrm{He}}\rangle \\ &\quad + t_{12}G_0P|U^{(3)}\rangle + (\mathbb{1}+t_{12}G_0)V_{3N}^{(3)}G_0(\mathbb{1}+P)|U^{(3)}\rangle\,,\end{aligned} \tag{6.26}$$

which has a connected kernel upon iteration and, therefore, has a well defined solution. A numerical routine which iteratively solves a Faddeev equation of the kind

$$\begin{aligned}|U^{(3)}\rangle &= t_{12}G_0|A\rangle + (\mathbb{1}+t_{12}G_0)V_{3N}^{(3)}G_0|A\rangle \\ &\quad + t_{12}G_0P|U^{(3)}\rangle + (\mathbb{1}+t_{12}G_0)V_{3N}^{(3)}G_0(\mathbb{1}+P)|U^{(3)}\rangle\,,\end{aligned} \tag{6.27}$$

for an arbitrary state $|A\rangle$ developed by David Minossi [133] has been applied in the numerical analysis of the ^{3}He and ^{3}H EDMs in this work.

6.4 EDMs of ^{3}He and ^{3}H from the θ-term

^{3}He and ^{3}H are $3N$ bound states of total angular momentum $J = 1/2$. The nuclear contributions to the EDMs of ^{3}He and ^{3}H , $d_{^3\mathrm{He}}$ and $d_{^3\mathrm{H}}$ respectively, are obtained in the same fashion as the one of the deuteron by extracting it from the P- and T-violating ^{3}He and ^{3}H form factor $F_3(q^2)$:

$$d^{tot}_{^3\mathrm{He},^3\mathrm{H}} = \lim_{q\to 0}\frac{F_3(q^2)}{2\,m_{^3\mathrm{He},^3\mathrm{H}}}\,, \tag{6.28}$$

which is defined by

$$\langle J{=}1/2, J_z{=}1/2, P'|(J^{total}_{\not{P}\not{T}})^0|J{=}1/2, J_z{=}1/2, P\rangle = -iq^3\frac{F_3(q^3)}{2\,m_{^3\mathrm{He},^3\mathrm{H}}}\,. \tag{6.29}$$

J_z in the above equation is the z-component of the total angular momentum of the nucleus, P (P') is the initial (final) four-momentum of the nucleus, q^μ is the photon four-momentum, $m_{^3\mathrm{He},^3\mathrm{H}}$ is the mass of the ^{3}He or ^{3}H nucleus and $J^{total}_{\not P \not T}$ is the total P- and T-violating transition current operator. The calculation of the EDMs of ^{3}He and ^{3}H are most efficiently performed in the Breit frame where no transfer of energy takes place and which enables us to choose $P = (0, \vec{q}/2)$ and $P' = (0, -\vec{q}/2)$. $\vec{q}$ can be chosen to point into the direction of the z-axis for further convenience: $\vec{q} = (0, 0, q)$. The EDM of the $3N$ bound system is then given by the derivative with respect to q of the P- and T-violating form factor eq. (6.16), which has been computed numerically for the considered nuclear contributions as explained in section 6.3:

$$d^{tot}_{^3\mathrm{He},^3\mathrm{H}} = \lim_{q\to 0} \frac{i}{|q|} \langle \psi_{^3\mathrm{He},^3\mathrm{H}}; J\!=\!1/2, J_z\!=\!1/2, -\vec{q}/2 | \Psi; J\!=\!1/2, J_z\!=\!1/2, \vec{q}/2 \rangle \,. \tag{6.30}$$

A set of numerical routines based on the Gauß-Legendre numerical integration method have been developed in order to compute the matrix element on the right-hand side of eq. (6.30). The numerical routines have been subjected to several tests: without the P- and T-violating one-pion exchange potentials the above matrix element reduces to the P- and T-conserving ^{3}He (or ^{3}H) form factor at leading order in ChPT. By a computation of the dependence of the form factor on the square of the photon momentum q^2, the results of [134] for ^{3}He have been confirmed. The implementation of the considered P- and T-violating potential operator induced by the g_1^θ vertex has been tested to reproduce the deuteron results when confined to the corresponding NN subsystem. Furthermore, a completely complementary Monte-Carlo based numerical implementation of the above matrix element developed by A. Nogga and S. Liebig [135] which does not account for interactions in the intermediate state provides an additional, independent cross check. Whereas our numerical implementation takes P- and T-conserving $3N$ interactions in the nuclear wave functions into account, these $3N$ interactions are not accounted for in the intermediate state[2]. $3N$ interactions in the intermediate state can be assumed to shift the results at most by a few percent (which will be demonstrated below) and can be considered irrelevant for our analysis due to the larger uncertainties of the final results (not to mention the uncertainties of g_0^θ and g_1^θ).

Two phenomenological potentials and three ChPT potentials have been utilized in our analysis for the P- and T-conserving component of the nuclear potential: the CD-Bonn potential [54] with and without $3N$ interactions (subsequently referred to as CD-Bonn TM and CD-Bonn, respectively), the Argonne v_{18} potential [56] with and without $3N$ interactions (subsequently referred to as Av_{18} UIX and Av_{18}, respectively), the N^{2}LO ChPT potential with and without $3N$

[2]The numerical routine provided by D. Minossi to solve the Faddeev type equation eq. (6.27) does not yet include $3N$ interactions.

Table 6.2: Binding energies E_{bin} of the ^{3}He and the ^{3}H nucleus with and without $3N$ interactions (3nf) in units of MeV from the Argonne v_{18} potential, the CD-Bonn potential and $\mathsf{N^2LO}$ and $\mathsf{N^3LO}$ ChPT potentials for different combinations of Spectral Function Regularization (SFR) and Lippmann-Schwinger (LS) cutoffs.

Potential	LS [MeV]	SFR [MeV]	^{3}He E_{bin} [MeV] no 3nf	^{3}He E_{bin} [MeV] with 3nf	^{3}H E_{bin} [MeV] no 3nf	^{3}H E_{bin} [MeV] with 3nf
Av_{18}	-	-	-6.920	-7.753	-7.619	-8.483
CD-Bonn	-	-	-7.262	-7.728	-7.979	-8.460
ChPT $\mathsf{N^2LO}$	450	500	-7.603	-7.725	-8.323	-8.440
ChPT $\mathsf{N^2LO}$	600	500	-7.138	-7.716	-7.845	-8.428
ChPT $\mathsf{N^2LO}$	550	600	-7.378	-7.724	-8.091	-8.428
ChPT $\mathsf{N^2LO}$	450	700	-7.670	-7.738	-8.395	-8.448
ChPT $\mathsf{N^2LO}$	600	700	-7.165	-7.746	-7.868	-8.447
ChPT $\mathsf{N^3LO}$	450	500	-6.891	–	-7.633	–
ChPT $\mathsf{N^3LO}$	600	600	-6.405	–	-7.097	–
ChPT $\mathsf{N^3LO}$	550	600	-6.579	–	-7.290	–
ChPT $\mathsf{N^3LO}$	450	700	-7.191	–	-7.924	–
ChPT $\mathsf{N^3LO}$	600	700	-6.392	–	-7.079	–

interactions [57] and the $\mathsf{N^3LO}$ ChPT potential without $3N$ interactions [57][3]. The numerical implementations of the phenomenological potentials have been provided by A. Nogga [126] and the numerical implementations of the ChPT potentials have been developed by E. Epelbaum [57]. The routines generating the wave functions of the considered nuclei from all these P- and T-conserving potentials have also been created by A. Nogga [135]. For each of these potentials, the isospin-1/2 and the less significant isospin-3/2 components of the ^{3}He and ^{3}H wave functions have been taken into account as well as electromagnetic interactions. The binding energies of the ^{3}He and ^{3}H nuclei from the considered P- and T-conserving potentials are listed in tab. 6.2. The experimental binding energies of ^{3}He and ^{3}H are given by $E_{bin} = (-7.718043 \pm 0.000002)$ MeV [136] and $E_{bin} = (-8.481798 \pm 0.000002)$ MeV [136], respectively. The differences to the binding energies from the $\mathsf{N^2LO}$ ChPT potentials amount to significantly less than 1%.

The results of our numerical analysis for the two phenomenological potentials are presented in tab. 6.3 for the g_0 and the g_1 induced P- and T-violating one-pion exchange potential operators and also for completeness for the g_2 induced P- and T-violating one-pion exchange potential operator. The g_2 vertex is irrelevant

[3]Private communication with the author: numerical implementation of the $\mathsf{N^3LO}$ ChPT potential is currently being revised.

Table 6.3: Leading order contributions to the ^{3}He and ^{3}H EDMs from the g_0 and g_1 and g_2 vertex without (d_{PW}, PW: plane wave) and with (d_{MS}, MS: multiple scattering) intermediate interactions and the total contribution $d_{^3\mathrm{He},^3\mathrm{H}}$ in units of $10^{-2} \cdot G_\pi^0\, e\,\mathrm{fm}$ with $G_\pi^0 = g_0 g_A m_N/F_\pi$, $10^{-2} \cdot G_\pi^1\, e\,\mathrm{fm}$ with $G_\pi^1 = g_1 g_A m_N/F_\pi$ and $10^{-2} \cdot G_\pi^2\, e\,\mathrm{fm}$ with $G_\pi^2 = g_2 g_A m_N/F_\pi$, respectively – calculated with the Argonne v_{18} [56] potential and the CD-Bonn potential [54] and the corresponding potentials with P- and T-conserving $3N$ interactions, Av_{18} UIX and CD-Bonn TM respectively.

nucleus	coupling	Potential	This work d_{PW}	d_{MS}	$d_{^3\mathrm{He},^3\mathrm{H}}$	[28] $d_{^3\mathrm{He},^3\mathrm{H}}$	[33] $d_{^3\mathrm{He},^3\mathrm{H}}$
^{3}He	g_0	Av_{18} UIX	−0.45	−0.12	−0.57	−1.20	−0.55
^{3}He	g_0	CD-Bonn TM	−0.56	−0.12	−0.68	−1.30	–
^{3}He	g_1	Av_{18} UIX	−1.09	−0.02	−1.11	−2.20	−1.06
^{3}He	g_1	CD-Bonn TM	−1.11	−0.03	−1.14	−2.20	–
^{3}He	g_2	Av_{18} UIX	−1.36	−0.35	−1.71	−3.40	−0.67
^{3}He	g_2	CD-Bonn TM	−1.46	−0.38	−1.83	−3.50	–
^{3}He	g_0	Av_{18}	−0.46	−0.13	−0.59	–	−0.59
^{3}He	g_0	CD-Bonn	−0.57	−0.12	−0.69	–	–
^{3}He	g_1	Av_{18}	−1.10	−0.01	−1.11	–	−1.08
^{3}He	g_1	CD-Bonn	−1.11	−0.01	−1.12	–	–
^{3}He	g_2	Av_{18}	−1.34	−0.37	−1.72	–	−0.68
^{3}He	g_2	CD-Bonn	−1.43	−0.39	−1.81	–	–
^{3}H	g_0	Av_{18} UIX	0.44	0.13	0.57	–	0.55
^{3}H	g_0	CD-Bonn TM	0.55	0.11	0.66	–	–
^{3}H	g_1	Av_{18} UIX	−1.07	−0.05	−1.11	–	−1.08
^{3}H	g_1	CD-Bonn TM	−1.09	−0.03	−1.12	–	–
^{3}H	g_2	Av_{18} UIX	1.35	0.38	1.73	–	0.69
^{3}H	g_2	CD-Bonn TM	1.44	0.36	1.80	–	–
^{3}H	g_0	Av_{18}	0.45	0.13	0.58	–	0.59
^{3}H	g_0	CD-Bonn	0.56	0.11	0.67	–	–
^{3}H	g_1	Av_{18}	−1.08	−0.04	−1.11	–	−1.10
^{3}H	g_1	CD-Bonn	−1.09	−0.01	−1.10	–	–
^{3}H	g_2	Av_{18}	1.33	0.41	1.74	–	0.70
^{3}H	g_2	CD-Bonn	1.41	0.37	1.78	–	–

for our analysis since it is not induced by any of the considered sources of P- and T-violating. The g_2 induced one-pion exchange potential operator is given by eq. (F.11) in appendix F. The results demonstrate that the impact of the $3N$

interactions in the ^{3}He and ^{3}H wave functions amounts to less than 4% of $d_{^3\mathrm{He},^3\mathrm{H}}$. Neglecting the relative sign, the results for ^{3}H deviate insignificantly from those for ^{3}He, which is a mere reflection of the fact that ^{3}He and ^{3}H are isospin partners. The difference between both phenomenological potentials manifests itself most prominently in the results for g_0. The nuclear contributions to the EDMs induced by P- and T-violating one-pion exchange potentials have been previously studied by [28] and [33] with disagreeing results. Our results are in agreement with those of [33] as far as g_0 and g_1 induced potential operators are concerned, whereas a significant discrepancy of the results for the g_2 induced potential operator exists. On the other hand our results appear to be approximately half the results of [28] for all P- and T-violating one-pion exchange potential operators.

As briefly established in section 5.3 and explained in detail in [57], the ChPT potentials require the imposition of two cutoffs: the Spectral Function Regularization cutoff (SFR) and the Lippmann-Schwinger cutoff (LS). The results of our numerical calculation from g_0, g_1 and g_2 induced P- and T-violating one-pion exchange potential operators and from ChPT potentials with different combinations of cutoffs for the P- and T-conserving component of the nuclear potential are listed in tab. 6.4 and tab. 6.5. Both sets of results obtained from the $\mathsf{N^2LO}$ and $\mathsf{N^3LO}$ ChPT potentials resemble those from the phenomenological potentials in tab. 6.3 quite accurately, where the larges deviations occur for the g_0 vertex.

The fractions of the total EDM contributions attributed to the intermediate state interactions, d_{MS}, (MS: multiple scattering), amount to almost 45% in some cases, which demonstrates that these are indeed non-negligible contributions. The relative d_{MS} contributions are significantly larger in the considered $3N$ systems than in the deuteron system, which has to be attributed to the larger number of partial wave components of the ^{3}He and ^{3}H wave functions. The set of all results for a particular P- and T-violating πNN vertex defines the uncertainty of the calculation: for g_1 and g_2 the values obtained from utilizing the phenomenological potentials lie within the range of values obtained from the $\mathsf{N^2LO}$ ChPT potential. The results for g_0 are found to be very close to but still outside the range of values obtained from the $\mathsf{N^2LO}$ ChPT potential. The range of values obtained from the $\mathsf{N^3LO}$ ChPT potential is much narrower as expected. However, the ranges of d_{PW} results for all three types of P- and T-violating πNN vertices from $\mathsf{N^2LO}$ and $\mathsf{N^3LO}$ ChPT potentials either overlap only at the fringes (as for g_0 and g_2) or do not overlap at all (as for g_1). This observation resembles the findings of section 5.3, where the range of $\mathsf{N^3LO}$ d_{MS} results was well outside the ranges of the corresponding NLO and $\mathsf{N^2LO}$ results. In a private communication with the author of [57] we have been informed that the used numerical routines for the $\mathsf{N^3LO}$ ChPT potential are currently being revised. The results from the $\mathsf{N^3LO}$ ChPT potentials are therefore displayed but disregarded in the computation of the final results and their errors.

The contributions of P- and T-conserving $3N$ interactions in the wave functions account for up to 12% of the EDM contributions $d_{^3\mathrm{He},^3\mathrm{H}}$ for the g_0 induced

P- and T-violating potential operator. This fraction is significantly less for the g_1 and g_2 induced potential operators. In general, the contributions from P- and T-conserving $3N$ interaction is much larger for P- and T-conserving ChPT potentials compared to the considered phenomenological potentials. Since P- and T-conserving interactions account for at most 45% of $d_{^3\mathrm{He},^3\mathrm{H}}$, the contributions from P- and T-conserving $3N$ interactions in the intermediate state may safely be assumed not to exceed 6% of $d_{^3\mathrm{He},^3\mathrm{H}}$. The uncertainties of our results have thus to be increased accordingly. The total contributions from P- and T-violating one-pion exchange potentials to the ^{3}He and ^{3}H EDMs are taken to be the center of the range of values defined by the $d_{^3\mathrm{He},^3\mathrm{H}}$ results from the Av_{18}, CD-Bonn and the $\mathsf{N^2LO}$ ChPT potential for all considered combinations of cutoffs. The uncertainties are defined by the maximum deviations from the centers of the ranges. The hereby obtained uncertainties are increased by contributions of P- and T-violating operators of not considered orders, i.e. $\mathsf{N^2LO}$ and beyond. The nuclear contribution to the ^{3}He EDM is then given by

$$d_{^3\mathrm{He}} = [(-0.77 \pm 0.20)\, G_\pi^0 \,+\, (-1.11 \pm 0.22)\, G_\pi^1] \cdot 10^{-2}\, e\,\mathrm{fm}\,, \tag{6.31}$$

and for the ^{3}H EDM by

$$d_{^3\mathrm{H}} = [(0.76 \pm 0.19)\, G_\pi^0 \,+\, (-1.09 \pm 0.22)\, G_\pi^1] \cdot 10^{-2}\, e\,\mathrm{fm}\,, \tag{6.32}$$

with $G_\pi^0 = g_0 g_A m_N / F_\pi$ and $G_\pi^1 = g_1 g_A m_N / F_\pi$. In the case of the θ-term, g_0^θ of eq. (4.158) and g_1^θ of eq. (4.173) can be inserted into eq. (6.31) and eq. (6.32), which gives:

$$\begin{aligned} d^\theta_{^3\mathrm{He}} &= [(1.78 \pm 0.83) + (-0.43 \pm 0.30)] \cdot 10^{-16}\, \bar\theta\, e\,\mathrm{cm} \\ &= (1.35 \pm 0.88) \cdot 10^{-16}\, \bar\theta\, \mathrm{e\,cm}\,, \end{aligned} \tag{6.33}$$

$$\begin{aligned} d^\theta_{^3\mathrm{H}} &= [(-1.74 \pm 0.80) + (-0.42 \pm 0.29)] \cdot 10^{-16}\, \bar\theta\, e\,\mathrm{cm} \\ &= (-2.16 \pm 0.85) \cdot 10^{-16}\, \bar\theta\, e\,\mathrm{cm}\,. \end{aligned} \tag{6.34}$$

These results have to be compared to the single-nucleon EDM contributions. Predictions of the proton and neutron EDM are provided by [51], which read after an adjustment of the signs:

$$d_p = -(1.1 \pm 1.1) \cdot 10^{-16}\, \bar\theta\, e\,\mathrm{cm}\,, \tag{6.35}$$
$$d_n = (2.9 \pm 0.9) \cdot 10^{-16}\, \bar\theta\, e\,\mathrm{cm}\,. \tag{6.36}$$

More recent Lattice QCD data [53] shows that the Lattice QCD input which underlies these EDM predictions understates the uncertainties. These EDM predictions are currently being revised on the basis of [53][4]. The single-nucleon

[4]Private communication with the authors of [51].

contribution to the ^{3}He EDM approximately equals the EDM of the neutron according to eq. (6.1), which has the same sign as the nuclear contribution eq. (6.33). The single-nucleon component and the nuclear component interfere constructively for the ^{3}He EDM, which is also true for the ^{3}H EDM.

In analogy to section 5.3, a tentative assessment of the short-range contributions is possible by considering heavier exchange mesons, namely the η, ρ and ω mesons. The results for the g_0, g_1 and g_2 induces one-meson exchange potentials are listed in tab. 6.6 as well as in tab. 6.7. These results agree with [33] for g_0 and g_1 induced one-meson exchange potential operators as in the pion case and deviate by a factor of two from results of [28] for g_0, g_1 and g_2 induced one-meson exchange potential operators. The results amount to less than 10% of the corresponding results for the g_0, g_1 and g_2 πNN vertices if $g_i^{\eta,\rho,\omega}\, G_{\eta,\rho,\omega} = G_\pi^i$ is assumed. Taking into consideration that the sizes of the P- and T-conserving meson-nucleon couplings are smaller than g_A (see [33] for instance), one may safely conclude that the short-range contributions are indeed in agreement with our power counting estimate of the P- and T-violating $4N$ vertex in section 6.2. The different short-range behaviors of the phenomenological potentials are also revealed by the data presented in tabs. 6.6 and 6.7: whereas the only discrepancy between the results for Av_{18} and CD-Bonn was seen for the g_0 vertex in the deuteron case, the different short-range behaviors now profoundly manifest themselves for all three types of meson-nucleon vertices.

6.5 EDMs from effective dimension-six sources

The different hierarchies of the P- and T-violating operators for the effective dimension-six sources translate into different single-nucleon and nuclear contributions to the EDMs of ^{3}He and ^{3}H. The different hierarchies of coupling constants of P- and T-violating vertices for each source of P and T violation implies that the power counting of P- and T-violating operators is also different for each source of P and T violation. The differences in the power counting of nuclear operators for each source of P and T violation with respect to the one for the θ-term and the implications on single-nucleon and nuclear contributions to the ^{3}He and ^{3}H EDMs are discussed in this section. The conclusions presented here agree with the previous findings in [30].

- *qEDM*:
  The qEDM is dominated by the single nucleon EDMs d_n and d_p, since each P- and T-violating operator without an external photon field is heavily suppressed by a factor of at least $\alpha_{em}/(4\pi)$. Therefore, the EDMs of ^{3}He and ^{3}H essentially equal their single-nucleon contributions at leading order [30]:

$$d^{tot}_{^3\mathrm{He}} \approx 0.88\, d_n - 0.047\, d_p\,, \tag{6.37}$$
$$d^{tot}_{^3\mathrm{H}} \approx -0.050\, d_n + 0.90\, d_p\,. \tag{6.38}$$

A quantitative prediction of d_n and d_p for the qEDM heavily depends on the nature of the BSM physics as well as the precise value of the associated hadronic matrix elements, which only Lattice QCD might eventually be able to deliver.

- *qCEDM*:
According to section 4.3, the g_0 and the g_1 vertex are induced at the same order by the qCEDM. The P- and T-violating one-pion exchange potential operators which they induce define the LO nuclear contributions to the EDMs of ^{3}He and ^{3}H. Other P- and T-violating hadronic operators such as the P- and T-violating γNN, 3π and $4N$ vertices yield N^{2}LO contributions. This implies a potentially significant enhancement of the nuclear contributions with respect to the single-nucleon contributions as pointed out in [30]. The quantitative assessment of g_0 and g_1 as functions of a certain parameter encoding the content of the BSM physics requires the computation of hadronic matrix elements which might only be possible within the framework of Lattice QCD. Expressed in terms of g_0 and g_1, the contributions to the EDMs of ^{3}He and ^{3}H induced by the qCEDM up to NLO are given by:

$$\begin{aligned} d^{tot}_{^3\mathrm{He}} &= 0.88\, d_n - 0.047\, d_p \\ &\quad +[(-0.77 \pm 0.20)\, G^0_\pi + (-1.11 \pm 0.22)\, G^1_\pi] \cdot 10^{-2}\, e\,\mathrm{fm}\,, \end{aligned} \tag{6.39}$$

$$\begin{aligned} d^{tot}_{^3\mathrm{H}} &= -0.050\, d_n + 0.90\, d_p \\ &\quad +[(0.76 \pm 0.19)\, G^0_\pi + (-1.09 \pm 0.22)\, G^1_\pi] \cdot 10^{-2}\, e\,\mathrm{fm}\,. \end{aligned} \tag{6.40}$$

- $4qLR$-op:
As explained in section 4.3, the isospin-violating g_1 πNN vertex as well as the P- and T-violating and isospin breaking Δ_3 3π vertex are induced at leading order by the $4qLR$-op and define the LO contributions to the EDMs of ^{3}He and ^{3}H (by the diagram classes depicted in figs. 6.2 (a) and (e)). The other P- and T-violating vertices including the g_0 vertex yield N^{2}LO contributions. This implies again a significant enhancement of the nuclear contributions compared to the single-nucleon contributions. A computation of the contribution induced by the P- and T-violating 3π vertex has not yet been completed and might ultimately provide the means to distinguish between the $4qLR$-op and the qCEDM.

- *gCEDM* and $4q$-op:
The LO EDM contributions for these two chiral-singlet operators are induced by P- and T-violating γNN and $4N$ operators with a priori unknown coefficients. Due to the Goldstone Theorem, nuclear contributions

from the g_0 and the g_1 πNN vertex are suppressed by two orders in magnitude and only give N^{2}LO contributions. Any attempt at disentangling these two sources of P and T violation requires the quantitative knowledge of the currently unknown $4N$ coupling constants for both sources, which -again- only Lattice QCD might be capable of producing. A tentative estimate of their nuclear contribution as functions of these coupling constants based on P- and T-violating exchanges of heavier mesons has been presented above. A direct calculation of the nuclear contributions from the $4N$ vertices is marred with some difficulties and is subject of an ongoing computation.

6.6 Summary

If a non-zero EDM of a nucleon or light nucleus which is significantly larger than its SM prediction is measured, further EDM measurements of other nucleons or light nuclei are required to identify the responsible source of P and T violation. Lattice QCD might eventually magnify the information extracted from the measurement of a particular nucleus and reduce the total number of necessary EDM measurements. There are several strategies to infer the responsible mechanism of the P and T violation, of which those falsifying the θ-term are the most refined due to the quantitative knowledge of g_0^θ and g_1^θ. This knowledge allows for the computation of the EDMs of ^{2}H, ^{3}He and ^{3}H induced by the θ-term as functions of $\bar{\theta}$ entirely within standard ChPT. Without any Lattice QCD input, one can measure, for instance, d_n, d_p and d_D and then extract $\bar{\theta}$ by using eq. (5.37). On the basis of eq. (6.33), the EDM of ^{3}He can then be computed and compared to a measurement. Alternatively, since the single-nucleon contributions to the ^{3}He EDM are dominated by d_n according to eq. (6.1), $\bar{\theta}$ can be inferred from the measurement of d_n and ^{3}He only, which then combined with a measurement of d_p leads to a prediction for the EDM of ^{2}H. Therefore, the measurements of the EDMs of the neutron, the proton, ^{3}He and ^{3}H are required to test the θ-term without supplementary input from, *e.g.*, Lattice QCD.

When predictions for the nucleon EDMs as functions of $\bar{\theta}$ on the basis of supplementary Lattice QCD input are available, the measurement of just one nucleon EDM would suffice to extract $\bar{\theta}$. Since the single-nucleon as well as two-nucleon contribution to the deuteron EDM from the θ-term would then be known, the prediction for the deuteron EDM can then be compared to its measurement. Alternatively, $\bar{\theta}$ can be extracted from the measurement of one nucleon and be used as the input for the testable prediction of the other nucleon. A measurement of the deuteron EDM or the ^{3}He EDM would provide an additional, orthogonal cross check. These examples illustrate that supplementary Lattice QCD input has the potential to profoundly reduce the necessary experimental effort. Unfortunately, current Lattice QCD predictions [52] for the single-nucleon EDMs are still performed for too large unphysical pion masses. A prediction of the nucleon EDMs by interpolation to the physical pion mass is given in [51]. More recent Lattice QCD data [53] indicate that the uncertainties of the data in [52] are profoundly understated and therefore also the uncertainties of the predictions of the nucleon EDMs in [51]. The EDM predictions in [51] are currently being revised on the basis of the more recent Lattice QCD input from [53][5].

The unavailability of quantitative predictions with well defined uncertainties for the EDMs induced by the effective dimension-six sources within the framework of ChPT has to be attributed to the fact that these constitute extensions of the standard QCD Lagrangian as pointed out in chapter 4. Any analysis within the effective field theory needs to be supplemented by other non-perturbative techniques – preferably Lattice QCD – to obtain quantitative predictions with well-defined uncertainties. However, such supplementary input is not likely to materialize soon. Therefore, one has at least for now to rely on NDA, which can provide order of magnitude estimates of unknown coupling constants. However, NDA might still be sufficient for a disentanglement of the effective dimension-six sources and enable one to identify the responsible source of P- and T-violating once several non-vanishing light nuclei EDMs – the more the better – have been measured [30]: if the measurements reveal that deuteron and the ^{3}He EDMs approximately equal their single-nucleon EDM contributions, the involvement of the $qEDM$ can be inferred. If the EDMs of the deuteron and helion prove to be larger than their single-nucleon contributions well outside the window of the θ-term EDM predictions, either the $qCEDM$ or the $4qLR$-op are most likely the source of the measured EDM. An assessment of the contribution from the P- and T-violating 3π vertex for the $4qLR$-op might ultimately provide a basis to distinguish between these two sources and is subject of an ongoing computation. If the EDM measurements do not fit to any of the above described patterns, the $gCEDM$ and/or the $4q$-op are probably the sources of P and T violation. Precise statements about the these two chiral-singlet effective dimension-six sources is difficult, since P- and T-violating γNN and $4N$ vertices are induced at the leading orders.

[5] Private communication with the authors of [51].

Table 6.4: Leading order contributions to the ^{3}He and ^{3}H EDMs from the g_0 and g_1 and g_2 vertex without (d_{PW}, PW: plane wave) and with (d_{MS}, MS: multiple scattering) intermediate state interactions and the total leading order nuclear EDM contributions $d_{^3\text{He},^3\text{H}}$ in units of $10^{-2} \cdot G_\pi^0\, e\,\text{fm}$ with $G_\pi^0 = g_0 g_A m_N / F_\pi$, $10^{-2} \cdot G_\pi^1\, e\,\text{fm}$ with $G_\pi^1 = g_1 g_A m_N / F_\pi$ and $10^{-2} \cdot G_\pi^2\, e\,\text{fm}$ with $G_\pi^2 = g_2 g_A m_N / F_\pi$, respectively – calculated with the N^{2}LO ChPT potential [57] without and with P- and T-conserving $3N$ interactions (3NF) for different combinations of Lippmann-Schwinger (LS) cutoffs and Spectral Function Regularization (SFR) cutoffs.

nucleus/	vertex	LS [MeV]	SFR [MeV]	without 3NF d_{PW}	without 3NF d_{MS}	without 3NF $d_{^3\text{He},^3\text{H}}$	with 3NF d_{PW}	with 3NF d_{MS}	with 3NF $d_{^3\text{He},^3\text{H}}$
^{3}He	g_0	450	500	−0.71	−0.31	−1.02	−0.68	−0.29	−0.97
^{3}He	g_0	600	500	−0.61	−0.25	−0.87	−0.56	−0.22	−0.78
^{3}He	g_0	550	600	−0.65	−0.24	−0.90	−0.60	−0.22	−0.82
^{3}He	g_0	450	700	−0.72	−0.28	−1.00	−0.69	−0.27	−0.96
^{3}He	g_0	600	700	−0.62	−0.23	−0.85	−0.56	−0.19	−0.76
^{3}He	g_1	450	500	−1.05	−0.16	−1.21	−1.08	−0.18	−1.25
^{3}He	g_1	600	500	−1.07	−0.08	−1.15	−1.06	−0.09	−1.14
^{3}He	g_1	550	600	−1.08	0.00	−1.08	−1.10	−0.01	−1.11
^{3}He	g_1	450	700	−1.06	−0.05	−1.11	−1.10	−0.08	−1.18
^{3}He	g_1	600	700	−1.10	0.15	−0.95	−1.09	0.14	−0.96
^{3}He	g_2	450	500	−1.51	−0.44	−1.95	−1.55	−0.45	−2.00
^{3}He	g_2	600	500	−1.35	−0.30	−1.65	−1.35	−0.29	−1.64
^{3}He	g_2	550	600	−1.45	−0.31	−1.76	−1.48	−0.31	−1.79
^{3}He	g_2	450	700	−1.55	−0.40	−1.95	−1.61	−0.43	−2.04
^{3}He	g_2	600	700	−1.43	−0.15	−1.58	−1.42	−0.14	−1.57
^{3}H	g_0	450	500	0.70	0.30	1.00	0.67	0.28	0.94
^{3}H	g_0	600	500	0.60	0.24	0.84	0.55	0.21	0.76
^{3}H	g_0	550	600	0.63	0.23	0.86	0.59	0.21	0.80
^{3}H	g_0	450	700	0.71	0.27	0.97	0.68	0.25	0.93
^{3}H	g_0	600	700	0.61	0.21	0.83	0.55	0.18	0.74
^{3}H	g_1	450	500	−1.03	−0.16	−1.19	−1.06	−0.17	−1.23
^{3}H	g_1	600	500	−1.05	−0.08	−1.12	−1.04	−0.08	−1.12
^{3}H	g_1	550	600	−1.05	0.00	−1.04	−1.08	−0.01	−1.09
^{3}H	g_1	450	700	−1.04	−0.05	−1.09	−1.08	−0.08	−1.16
^{3}H	g_1	600	700	−1.07	0.15	−0.93	−1.07	0.13	−0.94
^{3}H	g_2	450	500	1.49	0.42	1.91	1.54	0.43	1.97
^{3}H	g_2	600	500	1.33	0.28	1.61	1.34	0.27	1.60
^{3}H	g_2	550	600	1.42	0.28	1.70	1.47	0.29	1.76
^{3}H	g_2	450	700	1.53	0.38	1.91	1.60	0.40	2.01
^{3}H	g_2	600	700	1.41	0.13	1.54	1.41	0.12	1.53

Table 6.5: Leading order contributions to the ^{3}He and ^{3}H EDMs from the g_0 and g_1 and g_2 vertex without (d_{PW}, PW: plane wave) and with (d_{MS}, MS: multiple scattering) intermediate state interactions and the total leading order nuclear contributions $d_{^3\mathrm{He},^3\mathrm{H}}$ in units of $10^{-2} \cdot G_\pi^0\, e\,\mathrm{fm}$ with $G_\pi^0 = g_0 g_A m_N/F_\pi$, $10^{-2} \cdot G_\pi^1\, e\,\mathrm{fm}$ with $G_\pi^1 = g_1 g_A m_N/F_\pi$ and $10^{-2} \cdot G_\pi^2\, e\,\mathrm{fm}$ with $G_\pi^2 = g_2 g_A m_N/F_\pi$, respectively – calculated with the ChPT N^{3}LO [57] potential without P- and T-conserving $3N$ interactions for different combinations of Lippmann-Schwinger (LS) cutoffs and Spectral Function Regularization (SFR) cutoffs.

	LS	SFR		^{3}He			^{3}H	
vertex	[MeV]	[MeV]	d_{PW}	d_{MS}	$d_{^3\mathrm{He},^3\mathrm{H}}$	d_{PW}	d_{MS}	$d_{^3\mathrm{He},^3\mathrm{H}}$
g_0	450	500	−0.62	−0.27	−0.88	0.61	0.25	0.86
g_0	600	500	−0.53	−0.19	−0.72	0.52	0.18	0.69
g_0	550	600	−0.56	−0.19	−0.75	0.55	0.18	0.73
g_0	450	700	−0.64	−0.24	−0.88	0.63	0.23	0.85
g_0	600	700	−0.53	−0.19	−0.72	0.52	0.18	0.70
g_1	450	500	−0.91	−0.17	−1.09	−0.89	−0.17	−1.07
g_1	600	500	−0.90	−0.16	−1.07	−0.88	−0.16	−1.05
g_1	550	600	−0.91	−0.16	−1.07	−0.89	−0.16	−1.05
g_1	450	700	−0.94	−0.17	−1.11	−0.92	−0.17	−1.09
g_1	600	700	−0.92	−0.16	−1.08	−0.90	−0.16	−1.06
g_2	450	500	−1.34	−0.54	−1.87	1.33	0.52	1.85
g_2	600	500	−1.33	−0.57	−1.90	1.32	0.55	1.87
g_2	550	600	−1.33	−0.56	−1.89	1.32	0.55	1.87
g_2	450	700	−1.43	−0.56	−1.99	1.42	0.55	1.97
g_2	600	700	−1.31	−0.56	−1.87	1.30	0.54	1.85

Table 6.6: Contributions to the ^{3}He EDM from the $g_0^{\eta,\rho,\omega}$, $g_1^{\eta,\rho,\omega}$ and g_2^{ρ} ηN, ρN and ωN vertices. The results without (d_{PW}, PW: plane wave) and with (d_{MS}, MS: multiple scattering) intermediate state interactions and the total nuclear EDM contributions $d_{^3\mathrm{He},^3\mathrm{H}}$ are shown in units of $10^{-3} \cdot g_0^{\eta,\rho,\omega}\, G_{\eta,\rho,\omega}\, e\,\mathrm{fm}$, $10^{-3} \cdot g_1^{\eta,\rho,\omega}\, G_{\eta,\rho,\omega}\, e\,\mathrm{fm}$ and $10^{-3} \cdot g_2^{\rho}\, G_{\rho}\, e\,\mathrm{fm}$, where $G_{\eta,\rho,\omega}$ are the P- and T-conserving ηN, ρN and ωN coupling constants, respectively.

meson	coupling	Potential	This work d_{PW}	This work d_{MS}	This work $d_{^3\mathrm{He}}$	[27] $d_{^3\mathrm{He}}$	[33] $d_{^3\mathrm{He}}$
η	g_0	Av_{18} UIX	0.41	0.06	0.47	–	0.48
η	g_0	CD-Bonn TM	0.68	0.05	0.73	–	–
ρ	g_0	Av_{18} UIX	0.32	−0.04	0.27	0.60	0.27
ρ	g_0	CD-Bonn TM	0.69	−0.09	0.60	1.20	–
ω	g_0	Av_{18} UIX	−0.20	0.01	−0.19	−0.50	−0.19
ω	g_0	CD-Bonn TM	−0.38	0.04	−0.34	−0.80	–
η	g_1	Av_{18} UIX	−1.42	0.40	−1.02	–	−0.97
η	g_1	CD-Bonn TM	−1.59	0.46	−1.13	–	–
ρ	g_1	Av_{18} UIX	−0.70	0.28	−0.42	−0.90	−0.40
ρ	g_1	CD-Bonn TM	−0.86	0.35	−0.51	−1.10	–
ω	g_1	Av_{18} UIX	0.90	−0.32	0.57	1.1	0.52
ω	g_1	CD-Bonn TM	1.10	−0.42	0.68	1.1	–
ρ	g_2	Av_{18} UIX	0.94	−0.12	0.82	1.50	0.31
ρ	g_2	CD-Bonn TM	1.30	−0.24	1.06	1.90	–
η	g_0	Av_{18}	0.47	0.09	0.56	–	0.57
η	g_0	CD-Bonn	0.74	0.08	0.83	–	–
ρ	g_0	Av_{18}	0.32	−0.05	0.27	–	0.30
ρ	g_0	CD-Bonn	0.70	−0.09	0.61	–	–
ω	g_0	Av_{18}	−0.22	0.01	−0.21	–	−0.22
ω	g_0	CD-Bonn	−0.41	0.02	−0.39	–	–
η	g_1	Av_{18}	−1.49	0.39	−1.10	–	−1.07
η	g_1	CD-Bonn	−1.66	0.45	−1.22	–	–
ρ	g_1	Av_{18}	−0.74	0.28	−0.45	–	−0.44
ρ	g_1	CD-Bonn	−0.89	0.35	−0.55	–	–
ω	g_1	Av_{18}	0.89	−0.33	0.56	–	0.52
ω	g_1	CD-Bonn	1.09	−0.43	0.67	–	–
ρ	g_2	Av_{18}	0.90	−0.11	0.79	–	0.30
ρ	g_2	CD-Bonn	1.25	−0.23	1.02	–	–

Table 6.7: Contributions to the ^{3}H EDM from the $g_0^{\eta,\rho,\omega}$, $g_1^{\eta,\rho,\omega}$ and g_2^{ρ} ηN, ρN and ωN vertices. The results without (d_{PW}, PW: plane wave) and with (d_{MS}, MS: multiple scattering) intermediate state interactions and the total nuclear EDM contributions $d_{^3\mathrm{He},^3\mathrm{H}}$ are shown in units of $10^{-3} \cdot g_0^{\eta,\rho,\omega}\, G_{\eta,\rho,\omega}\, e\,\mathrm{fm}$, $10^{-3} \cdot g_1^{\eta,\rho,\omega}\, G_{\eta,\rho,\omega}\, e\,\mathrm{fm}$ and $10^{-3} \cdot g_2^{\rho}\, G_{\rho}\, e\,\mathrm{fm}$, where $G_{\eta,\rho,\omega}$ are the P- and T-conserving ηN, ρN and ωN coupling constants, respectively.

meson	coupling	Potential	This work d_{PW}	This work d_{MS}	This work $d_{^3\mathrm{H}}$	[27] $d_{^3\mathrm{H}}$	[33] $d_{^3\mathrm{H}}$
η	g_0	Av_{18} UIX	−0.40	−0.06	−0.46	–	−0.48
η	g_0	CD-Bonn TM	−0.67	−0.03	−0.70	–	–
ρ	g_0	Av_{18} UIX	−0.31	0.04	−0.28	–	−0.27
ρ	g_0	CD-Bonn TM	−0.68	0.09	−0.59	–	–
ω	g_0	Av_{18} UIX	0.19	−0.01	0.18	–	0.19
ω	g_0	CD-Bonn TM	0.37	−0.04	0.33	–	–
η	g_1	Av_{18} UIX	−1.39	0.37	−1.01	–	−0.97
η	g_1	CD-Bonn TM	−1.56	0.46	−1.10	–	–
ρ	g_1	Av_{18} UIX	−0.69	0.27	−0.42	–	−0.40
ρ	g_1	CD-Bonn TM	−0.84	0.35	−0.49	–	–
ω	g_1	Av_{18} UIX	0.88	−0.30	0.58	–	0.53
ω	g_1	CD-Bonn TM	1.09	−0.41	0.68	–	–
ρ	g_2	Av_{18} UIX	−0.94	0.11	−0.84	–	−0.32
ρ	g_2	CD-Bonn TM	−1.30	0.25	−1.05	–	–
η	g_0	Av_{18}	−0.45	−0.10	−0.55	–	−0.57
η	g_0	CD-Bonn	−0.73	−0.06	−0.79	–	–
ρ	g_0	Av_{18}	−0.32	0.05	−0.27	–	−0.30
ρ	g_0	CD-Bonn	−0.69	0.09	−0.61	–	–
ω	g_0	Av_{18}	0.22	0.00	0.21	–	0.22
ω	g_0	CD-Bonn	0.40	−0.03	0.37	–	–
η	g_1	Av_{18}	−1.46	0.37	−1.10	–	−1.08
η	g_1	CD-Bonn	−1.62	0.45	−1.18	–	–
ρ	g_1	Av_{18}	−0.72	0.27	−0.45	–	−0.44
ρ	g_1	CD-Bonn	−0.87	0.34	−0.53	–	–
ω	g_1	Av_{18}	0.88	−0.31	0.57	–	0.54
ω	g_1	CD-Bonn	1.08	−0.42	0.66	–	–
ρ	g_2	Av_{18}	−0.90	0.09	−0.81	–	−0.32
ρ	g_2	CD-Bonn	−1.25	−0.24	−1.01	–	–

Chapter 7

Conclusions and outlook

This thesis provides a thorough analysis of the EDMs of the deuteron, helion and triton. The existence of non-vanishing EDMs of nuclei with a non-degenerate ground state implies the violation of the parity and the time-reversal symmetries in nuclear interactions. There are several sources of P and T violation: the θ-term of QCD is the only source of P and T violation within the SM beyond the complex phase of the CKM matrix. Depending on the size of the physical parameter $\bar{\theta}$, the θ-term is capable of inducing EDMs of light nuclei $\gtrsim 10^{-29}\,\mathrm{e\,cm}$, which is the envisioned accuracy of EDM measurements proposed by the Storage Ring EDM collaboration and the JEDI collaboration [24]. Other sources of significant P and T violation arise in BSM theories such as supersymmetry, multi-Higgs scenarios, etc. All potential sources of significant P and T violation would manifest themselves as EDMs of light nuclei. Since each source gives rise to a specific hierarchy of EDMs of light nuclei, a disentanglement of the sources of P and T violation on the basis of EDM measurements of several light nuclei is feasible. These hierarchies of light nuclei EDMs have been derived in this thesis and improve upon the results of previous studies [27–29, 33] as described below.

In order to derive the hierarchies of the EDMs of light nuclei for each source of P and T violation, hadronic observables at energies below the scale $\Lambda_{\mathrm{QCD}} \sim 200$ MeV have to be determined. This entails that the connection between operators at high energies $\sim \Lambda_{\mathrm{BSM}}$ with BSM degrees of freedom and operators at low energies $\lesssim \Lambda_{\mathrm{QCD}}$ has to be established. This has been accomplished by employing a two-step effective field theory approach as in [30, 49]: in the first step, high-energy BSM operators are evolved to the energy scale $\Lambda_{\mathrm{had}} \gtrsim 1$ GeV as proposed and performed in [10, 35–38, 40]. By integrating out all degrees of freedom with masses above Λ_{had} from P- and T-violating operators, the authors compiled the complete set of leading effective operators at the energy scale of Λ_{had}. This list of effective dimension-six operators consists of the so called quark EDM ($qEDM$), the quark-chromo EDM ($qCEDM$), the four-quark left-right operator ($4qLR$-op), the gluon-chromo EDM ($gCEDM$) and the four-quark operator ($4q$-op). They are graphically depicted in fig. 1.1. These effective, non-renormalizable dimension-six operators at the energy scale Λ_{had} and the dimension-four QCD θ-term were the starting point of the analysis presented in this thesis.

The second step involved the employment of ChPT, the low-energy effective field theory of QCD, in order to complete the connection to hadronic operators at the energy scale Λ_{QCD}. The QCD θ-term is a genuine element of the QCD Lagrangian and allows for a treatment entirely within standard ChPT. Another recent study of the θ-term induced effective Lagrangian in the Weinberg formulation of two-flavor ChPT is presented in [42]. This thesis provides a thorough derivation of the induced effective Lagrangian within the Gasser-Leutwyler formulation of two-flavor ChPT in chapter 4 and quantitative predictions of the coupling constants of the most important P- and T-violating vertices for the first time. These coupling constants have proven to be functions of either the quark mass induced component of the neutron-proton mass difference or the strong component of the square of the mass difference between charged and neutral pions. By resorting to the latest results for these two quantities, the coupling constants of the leading P- and T-violating isospin-0 and isospin-1 pion-nucleon vertices have been found to be the following functions of $\bar{\theta}$:

$$g_0^\theta = (-0.018 \pm 0.007)\bar{\theta}\,, \quad g_1^\theta = (0.003 \pm 0.002)\bar{\theta}\,. \tag{7.1}$$

The inclusion of effective P- and T-violating dimension-six operators constitutes an amendment of the standard QCD Lagrangian and implies that the treatment of the effective dimension-six operators at energies below Λ_{QCD} is beyond the realm of standard ChPT. The standard ChPT Lagrangian has to be amended accordingly as pointed out in [30, 39] by new, additional terms with unknown coefficients (LECs). The derivation of the amended ChPT Lagrangians induced by the effective dimension-six operators in the Gasser-Leutwyler formulation of two-flavor ChPT is presented in chapter 4 of this thesis. Since the new LECs are not quantitatively known, the coupling constants of the leading P- and T-violating vertices can not be computed explicitly as functions of parameters which encode specific BSM physics. Other non-perturbative techniques are required to assess the sizes of these coupling constants, among which Lattice QCD has the highest predictive capacity. Lattice QCD results are, however, not likely to materialize any time soon and one has – at least for now – to resort to *Naive Dimensional Analysis* (NDA) in order to obtain order of magnitude estimates. In contrast to the θ-term analysis, neither the signs nor the center values of the coupling constants of leading P-and T-violating vertices can be inferred from NDA. These order of magnitude estimates might still be sufficient to determine the hierarchies of coupling constants of leading P- and T-violating vertices for each source of P and T violation [39]. The leading coupling constants of the P- and T-violating isospin-0 and isospin-1 pion-nucleon vertices, g_0 and g_1 respectively, are estimated to be larger than the θ-term predictions and of the same order for the $qCEDM$, for instance. The coupling constants induced by other effective dimension-six operators exhibit different hierarchies. These different hierarchies were found to translate into different hierarchies of light nuclei EDMs, as described in chapters 5 and 6.

The isospin selection rules of the deuteron render it a rather selective system in which the EDM contributions of most P- and T-violating operators vanish. The selective nature of the deuteron and the quantitative knowledge of g_0^θ and g_1^θ allowed the θ-term induced deuteron EDM to be computed up to next-to-next-to-leading order. Whereas previous studies of the deuteron EDM in [25–27, 29–33] focused on the leading order EDM contribution (according to the counting in this thesis), a detailed analysis of next-to-next-to-leading order nuclear contributions and a quantitative prediction with a well-defined uncertainty of the NN contribution to the deuteron EDM as a function of $\bar{\theta}$ is provided – for the first time – in chapter 5. The uncertainty of the result accounts for the uncertainty of the P- and T-violating component as well as the P- and T-conserving component of the nuclear potential. The θ-term induced deuteron EDM result is given by

$$d^{tot}_{^2\mathrm{H}} = d_n + d_p + (-0.54 \pm 0.37) \cdot 10^{-16}\,\bar{\theta}\,e\,\mathrm{cm}\,, \tag{7.2}$$

where d_n and d_p denote the EDMs of the neutron and proton, respectively.

When a single non-zero EDM of the deuteron, proton or neutron is measured, additional information is required to identify (or rather falsify) the source of P and T violation. The strict isospin selection rules of the deuteron are absent from helion and triton systems and a measurement of the EDM of one of them would provide necessary additional information. The analysis of the nuclear contributions to the helion and triton EDMs induced by the θ-term up to next-to-leading order with quantitative predictions and well-defined uncertainties is presented in chapter 6 of this thesis. The results for the EDMs of the helion and the triton induced by the θ-term as functions of $\bar{\theta}$ are given by

$$d^{tot}_{^3\mathrm{He}} = 0.880\,d_n + 0.047\,d_p + (1.35 \pm 0.88\,) \cdot 10^{-16}\,\bar{\theta}\,e\,\mathrm{cm}\,, \tag{7.3}$$
$$d^{tot}_{^3\mathrm{H}} = -0.050\,d_n + 0.900\,d_p + (-2.16 \pm 0.85\,) \cdot 10^{-16}\,\bar{\theta}\,e\,\mathrm{cm}\,. \tag{7.4}$$

Effective field theory predictions for the EDMs of the neutron d_n and of the proton d_p have limited predictive capacity due to unknown counter terms at leading order as explained in the introduction. Supplementary input from, *e.g.*, Lattice QCD is required to quantify these counter terms. The currently available Lattice QCD predictions for the single-nucleon EDMs are at too large unphysical pion masses [52]. By an interpolation to physical pion masses, the authors of [51] found

$$d_p = -(1.1 \pm 1.1) \cdot 10^{-16}\,\bar{\theta}\,e\,\mathrm{cm}\,, \tag{7.5}$$
$$d_n = (2.9 \pm 0.9) \cdot 10^{-16}\,\bar{\theta}\,e\,\mathrm{cm}\,. \tag{7.6}$$

More recent Lattice QCD data [53] indicates that the uncertainty of the Lattice QCD data in [52] that underlies [51] is profoundly understated. A revision of the single-nucleon EDM predictions in [51] on the basis of [53] with most likely significantly larger uncertainties is in the pipeline[1]. According to eqs. (7.3)-(7.6), the single-nucleon and nuclear contributions to the helion and triton EDMs would interfere constructively.

Based on these accurate predictions for the nuclear contributions to the EDMs of light nuclei induced by the θ-term, several schemes of testing the θ-term are proposed at the end of chapter 6, which involve the measurements of several light nuclei. The measurement of the EDM of the radioactive triton is only possible in very few laboratories (with military research divisions) around the world. The triton EDM is therefore highly unlikely to be measured and can be disregarded.

1. Let the non-vanishing EDMs of the proton, the neutron and deuteron be measured. The parameter $\bar{\theta}$ can then be calculated by using eq. (7.2) and be inserted into eq. (7.3) to obtain a prediction for the helion EDM. A measurement of the helion EDM can then falsify a significant involvement of the θ-term.

2. Since the single-nucleon contribution to the helion EDM approximately equals the neutron EDM, the measurements of the neutron EDM and the helion EDM would suffice to extract $\bar{\theta}$ by utilizing eq. (7.3). A comparison of the θ-term prediction for the deuteron EDM on the basis of eq. (7.2) to a measurement of the deuteron EDM and the proton EDM can then rule out the θ-term.

3. Supplementary Lattice QCD input to quantify the unknown leading order counter terms in the single-nucleon EDM calculation is capable of reducing the necessary experimental effort. A measurement of one of the single-nucleon EDMs would then be sufficient to extract $\bar{\theta}$ and to compute the other nucleon EDM which has not been measured. By using eq. (7.2) or eq. (7.3), testable predictions for the deuteron or helion EDM can be obtained.

4. On the basis of Lattice QCD input, the $\bar{\theta}$ value obtained from the measurement of one single-nucleon EDM can be taken as input for the a prediction of the other nucleon EDM. A measurement of the other nucleon EDM would provide a test of the θ-term involving only nucleon EDM measurements. Measurements of the EDMs of the deuteron and/or the helion would then provide an additional, orthogonal test of the θ-term.

If these θ-term tests fail, the source of P and T violation might be one (or several) effective dimension-six operators. Chapter 6 provides predictions for the nuclear contributions to the helion and triton EDMs induced by the effective

[1] Private communication with the authors of [51].

dimension-six operators as functions of the coupling constants g_0 and g_1, which deviate from those of [30] by a factor of two and agree with those of [33]. The NDA estimates of these coupling constants yield different patterns of enhancements of nuclear EDM contributions, which has also been pointed out in [30]:

- $qCEDM$:
  The πNN coupling constants g_0 and g_1, which are both induced at leading order, are potentially larger than their θ-term counterparts. This would imply a significant enhancement of the nuclear EDM contributions to the EDMs of the deuteron, helion and triton with respect to their single-nucleon contributions. If the measurements of the EDMs of light nuclei reveal such nuclear enhancements beyond the θ-term predictions, the $qCEDM$ (or the $4qLR$-op, see below) is most likely the source of P and T violation.

- $4qLR$-op:
  The leading P- and T-violating vertices induced by the $4qLR$-op are the isospin-1 pion-nucleon vertex with coupling constant g_1 and the three-pion vertex with coupling constant Δ_3. The coupling constant of the P- and T-violating isospin-0 pion-nucleon vertex, g_0, is suppressed with respect to g_1 and Δ_3. Since the leading nuclear contribution to the deuteron EDM is defined by the g_1 vertex, the nuclear contribution to the deuteron is expected to be relatively larger for the $4qLR$-op than for other effective dimension-six sources. Furthermore, the Δ_3 induced leading order nuclear contribution to the helion EDM might be sizable and provide another means of disentanglement from the $qCEDM$.

- $qEDM$:
  Since all coupling constants of P- and T-violating vertices without the photon field are suppressed by at least a factor of $\alpha_{em}/(4\pi)$, the EDMs of the deuteron, the helion and the triton are approximately equal to their single-nucleon EDM contributions. If EDM measurements confirm such a scenario, the $qEDM$ is likely to be the source of P and T violation.

- $gCEDM$ and $4q$-op:
  If the θ-term, the $qCEDM$ and the $4qLR$-op are excluded, the $gCEDM$ and the $4q$-op can also be the sources of P and T violation. These two effective dimension-six sources are difficult to disentangle without Lattice QCD input, since they induce P- and T-violating $4N$ and γNN vertices at leading orders. Coupling constants of vertices involving pions are significantly suppressed by a factor of M_π^2/m_N^2 according to Goldstone's theorem. Therefore, the EDMs of the deuteron, the helion and the triton can be estimated to roughly equal their single-nucleon EDM contributions. In this case, a disentanglement from the $qEDM$ which induces a smillar pattern might prove to be difficult.

The measurements of non-zero EDMs of light nuclei would therefore provide valuable information on new physics coming from the θ-term and BSM theories. The identification of a hierarchy among EDMs of light nuclei would falsify particular effective dimension-six sources and therefore certain BSM theories that dominantly contribute to one of the four types, *e.g.* left-right symmetric models [137].

The analysis of EDMs of light nuclei can be further refined: the $4qLR$-op induces a leading order nuclear EDM contribution which involves the P- and T-violating 3π Δ_3 vertex. The inclusion of such $3N$ diagrams into our program is subject of an ongoing effort. The computation of the EDM contributions from P- and T-violating short-range $4N$ operators is another unresolved issue. Due to the model dependence of the short-range components of the P- and T-conserving nuclear potentials, this computation is marred with difficulties which we soon expect to settle. Ultimate improvement of the results presented in this thesis might come from Lattice QCD[2] . The quantitative knowledge of yet unknown coupling constants and counter terms would allow us to overcome the reliance on NDA and to obtain accurate quantitative predictions for the EDMs of light nuclei which are induced by the effective dimension-six sources.

[2] Note that the πNN coupling constant g_0^θ can be extracted from a Lattice QCD computation of the Schiff moment of the nucleon [50].

Appendix A

Ward identities

The aim of this appendix is to explain how the set of Ward identities of a quantum field theory can be encoded in the generating functional by introducing external source fields for composite operators as demonstrated by Gasser and Leutwyler in [43, 44, 60], for instance. The presentation below is based on reference [60, 78]. Consider a quantum field theory with degrees of freedom $\{\phi^i\}$ and a set of currents $\{J_j^\mu\}$. Let the classical action S be invariant under infinitesimal local transformations of a Lie group G, which is parametrized by local coordinates $\{\epsilon^k(x)\}$. The action of the quantum field theory is assumed to be the sum of the classical action S and an action S_J which is comprised of all source terms η^i for the degrees of freedom and f_j^μ for the currents J_j^μ:

$$S[\{\phi^i\};\{J_\mu^j\}] = S[\{\phi^i\}] + S_J[\{\eta^i\},\{f_j^\mu\}]\,. \tag{A.1}$$

The extension of the classical Lagrangian S_J is given by

$$S_J[\{\eta^i(x)\},\{f_j^\mu(x)\}] := \int d^4x \left(\sum_i \eta^i(x)\phi_i(x) + \sum_j f_j^\mu(x) J_\mu^j\right)\,. \tag{A.2}$$

Whereas S is invariant under G transformations of $\{\phi^i\}$, S_J is in general not invariant under G because the external source fields $\{\eta^i\}$ and $\{f_\mu^j\}$ transform a priori trivially under G. Since Green functions do in general not depend on particular gauge transformations, the generating functional

$$\exp(iZ[\{\eta^i(x)\},\{f_j^\mu(x)\}]) = \int \{\mathcal{D}\phi^i\} \exp\left(S[\{\phi^i(x)\}] + S_Q[\{\eta^i(x)\},\{f_j^\mu(x)\}]\right) \tag{A.3}$$

has to be invariant under local G transformations. Let us assume that the functional integration measure is invariant under G and that the source fields $\{\eta^i(x)\}$ and $\{f_\mu^j\}$ transform in such a way that the complete action S is invariant under G. The source fields transform complementary to the degrees of freedom $\{\phi^i(x)\}$ of the theory and the currents $\{J_\mu^j\}$, respectively. Since the currents are constructed from the degrees of freedom of the theory, i.e. $J^j_\mu = J^i_\mu(\{\phi^i\})$, their transformation properties are induced by those of $\{\phi^i\}$. Each source field $\eta^i(x)$ or $f^j_\mu(x)$ then transforms in general as a basis state of a particular representation $D_{(i)}$ or $D_{(j)}$. We may in general assume that one source field for each basis state of such representations exists and label the set of source fields $\{f^{j,l}_\mu\}$, where $l = 1, ..., \dim(D_{(j)})$. Let the structure constants of the corresponding Lie algebras be defined by

$$[t^{(j)}_l, t^{(j)}_m] = \sum_n i c_{lmn} t^{(j)}_n \,, \tag{A.4}$$

where $t^{(j)}_l$ are the generators of the representation $D_{(j)}$. The source fields $\{f^{j,l}_\mu(x)\}$ then transform under local G transformations by (no summation over k)

$$F^{(j)}(\epsilon^k(x), f^{j,l}_\mu(x)) = D_{(j)}(\epsilon^k(x)) f^{j,l}_\mu(x) D^{-1}_{(j)}(\epsilon^k(x)) - i\partial_\mu D_{(j)}(\epsilon^k(x)) D^{-1}_{(j)}(\epsilon^k(x))\,, \tag{A.5}$$

which amounts to the infinitesimal transformation

$$\delta f^{j,l}_\mu(x) = \partial_\mu \epsilon^l(x) + c^{(j)}_{lmn} f^{j,m}_\mu \epsilon^n(x)\,. \tag{A.6}$$

Note that the pure gauge term $-i\partial_\mu D_{(j)}(\epsilon^k(x)) D^{-1}_{(j)}(\epsilon^k(x))$ may not exist for all source fields. Similar expressions hold for the source fields of the degrees of freedom $\{\eta^i\}$.

For the generating functional whose functional integration measure transforms trivially under G (i.e. in the absence of anomalies), one then finds:

$$\begin{aligned}
\exp(iZ[\{\eta^i(x)\}, \{f^{j,l}_\mu(x)\}]) &= \int \mathcal{D}\{\phi^i\} \exp\left(S[\{\phi^i\}; \{\eta^i\}, \{f^{j,l}_\mu\}]\right) \\
&= \int \mathcal{D}\{\phi^i\} \exp\left(S[\{(\phi^i)'\}; \{(\eta^i)'\}, \{(f^{j,l}_\mu)'\}]\right) \\
&= \int \mathcal{D}\{(\phi^i)'\} \exp\left(S[\{(\phi^i)'\}; \{(\eta^i)'\}, \{(f^{j,l}_\mu)'\}]\right) \\
&= \int \mathcal{D}\{\phi^i\} \exp\left(S[\{\phi^i\}; \{(\eta^i)'\}, \{(f^{j,l}_\mu)'\}]\right) .
\end{aligned} \tag{A.7}$$

Eq. (A.7) demonstrates that the generating functional

$$W[\{\eta^i\}, \{f^{j,l}_\mu\}] := \exp(iZ[\{\eta^i(x)\}, \{f^{j,l}_\mu(x)\}])\,, \tag{A.8}$$

is invariant under G transformations of the source fields $\{\eta^i\}$ and $\{f^{j,l}_\mu\}$:

$$W[\{\eta^i\}, \{f^{j,l}_\mu\}] = W[\{(\eta^i)'\}, \{(f^{j,l}_\mu)'\}]\,. \tag{A.9}$$

Therefore, in the absence of gauge anomalies, Ward identities can be derived from the invariance of the generating functional under local G transformations applied to the source fields while the degrees of freedom remain unaffected by the G transformations:

$$\int d^4x\, \epsilon^k(x) \left[\sum_i a_i \frac{\delta}{\delta \eta^i(x)} + \sum_{j,l} \mathcal{O}_k^{(j)l,\mu} \frac{\delta}{\delta f_\mu^{j,l}(x)} \right] W[\{\eta^i\}, \{f_\mu^{(j),l}\}] = 0\,, \quad \text{(A.10)}$$

where $a_i \in \mathbb{C}$ and the coefficients $\mathcal{O}_k^{(j)l,\mu}$ denote in general operators. This relation generates the set of Ward identities obeyed by the Green functions of the theory. The completely G invariant generating functional W therefore encodes all Ward identities.

Appendix B

Quark multilinears

The quark multilinears considered in section 4.2 of this theses are quark bilinears and quark quadrilinears. A chiral $SU(2)_L \times SU(2)_R$ transformation of the left-handed and right-handed quark fields in quark multilinears induces a transformation in the space of quark mutlilinears. It will be shown in this appendix that a quark multilinear in general admits a decomposition into quark mutlilinears which transform as basis states of particular irreducible representations of $O(4)$, for which $SU(2)_L{\times}SU(2)_R$ is the double covering group. In order to provide a systematic study of quark bilinears and quadrilinears the connection between the representation theory of $O(4)$ and quark multilinears is explained and the set of all quark bilinears and quark multilinears which transform as basis states of irreducible representations of $O(4)$ is compiled.

We will explain that the relationship between quark multilinears and the representation theory of $SO(4)$ is established by the set of $SU(2)_L \times SU(2)_R$ group actions on (symmetric) tensor products of elements of the quaternion algebra $\mathbb{H}_4$. There is a one-to-one correspondence between the quaternion algebra $\mathbb{H}_4$ and the real vector space of matrices spanned by the set $\{\mathbb{1}, i\tau_1, i\tau_2, i\tau_3\}$ with τ_i being the Pauli matrices. A group action F of a group G and a space X is defined as the group homomorphism of G into the group of homeomorphic maps from X onto itself:

$$\begin{aligned} &F : G \times X \to X\,, \quad (g, x) \mapsto F_g(x)\,, \\ &F_{g_1} \circ F_{g_2}(x) = F_{g_1 \cdot g_2}(x) \quad \forall g_1, g_2 \in G\,, \forall x \in X\,. \end{aligned} \tag{B.1}$$

The connection between $SU(2)_L \times SU(2)_R$ group actions on $\mathbb{H}_4$ and quark multilinears can be illustrated by the following example. The quark bilinear $-\bar{q}\gamma^\mu\tau_3 q$ can be re-expressed in terms of left- and right-handed quark fields:

$$i\bar{q}\gamma^\mu(i\tau_3)q = i\bar{q}_L\gamma^\mu(i\tau_3)q_L + i\bar{q}_R\gamma^\mu(i\tau_3)q_R\,. \tag{B.2}$$

The Dirac matrix γ^μ can therefore be considered to define a group action on $(i\tau_k) \in \mathbb{H}_4$:

$$(i\tau_k) + (i\tau_k) \mapsto L^\dagger(i\tau_k)L + R^\dagger(i\tau_k)R\,, \quad (L, R) \in SU(2)_L{\times}SU(2)_R\,. \tag{B.3}$$

This appendix is therefore organized as follows: the algebra of quaternions $\mathbb{H}_4$ is introduced in the first section of this appendix. The second section is concerned with the investigation of $SU(2)_L \times SU(2)_R$ group actions on $\mathbb{H}_4$ and the representation theory of $SO(4)$. The third section of this appendix explains the connection between the representation theory of $O(4)$ and group actions on (tensor products of) $\mathbb{H}_4$, from which the set of all quark bilinears and quark quadrilinears which transform as basis states of irreducible representations of $O(4)$ is derived.

B.1 Quaternions

The quaternion algebra $\mathbb{H}_4$ is a four dimensional, non-commutative, associative algebra over the real numbers (a detailed explanation of the quaternion algebra can be found in *e.g.* [138–140]). $\mathbb{H}_4$ is generated by $\{1, i, j, k\}$ where i, j and k obey

$$i^2 = j^2 = k^2 = ijk = -1 \tag{B.4}$$

For a general element $q \in \mathbb{H}_4$, the conjugate $q^* \in \mathbb{H}_4$ is defined by

$$q = a + bi + cj + dk \quad \rightarrow \quad q^* = a - bi - cj - dk\,. \tag{B.5}$$

The quaternion algebra $\mathbb{H}_4$ is isomorphic to the associative algebra generated by $\{\mathbb{1}, i\tau_1, i\tau_2, i\tau_3\}$, where τ_i denote Pauli matrices. The norm of a quaternion $q \in \mathbb{H}_4$ is defined by

$$||q|| = \sqrt{q^* q} = \sqrt{a^2 + b^2 + c^2 + d^2}\,. \tag{B.6}$$

Exploiting the isomorphism to the associative algebra generated by the set $\{\mathbb{1}, i\sigma_1, i\sigma_2, i\sigma_3\}$, the norm of a quaternion can be expressed in terms of the determinant of a complex 2×2 matrix:

$$\det \begin{pmatrix} a + ib & id + c \\ id - c & a - ib \end{pmatrix} = a^2 + b^2 + c^2 + d^2\,. \tag{B.7}$$

This proves that the group of quaternions of norm equal to one –called unit quaternions– is isomorphic to $SU(2)$:

$$\{q \in \mathbb{H}_4 |\ ||q|| = 1\} \simeq SU(2)\,. \tag{B.8}$$

Let M be the isomorphism

$$M : a + ib + jc + kd \mapsto \begin{pmatrix} a + ib & id + c \\ id - c & a - ib \end{pmatrix}\,, \tag{B.9}$$

and F be the group action of $SU(2)_L \times SU(2)_R$ on $\mathbb{H}_4$ defined by:

$$F :\ SU(2)_L \times SU(2)_R \times \mathbb{H}_4 \rightarrow \mathbb{H}_4\,, \quad q \mapsto L\, M(q)\, R^\dagger\,. \tag{B.10}$$

Since F preserves the norm for all $q \in \mathbb{H}_4$, this group action is an automorphism of $SU(2)$ if restricted to unit quaternions. For all $g \in SU(2)$ the negative $-g$ is also an element of $SU(2)$, which implies that F is not injective on $SU(2)_L \times SU(2)_R$ since the pairs (L, R), $(-L, -R) \in SU(2)_L \times SU(2)_R$ map onto the same homeomorphism of $\mathbb{H}_4$ onto $\mathbb{H}_4$.

B.2 The representation theory of $SO(4)$

The connection between the group $SU(2)_L \times SU(2)_R$ and the Lie group $SO(4)$ is drawn by the well-known Cayley-Klein decomposition of $SO(4)$ matrices (a detailed explanation of this connection between the quaternion algebra and $SO(4)$ is given in *e.g.* [138–143]). Let N denote the isomorphism between $\mathbb{R}^4$ and $\mathbb{H}_4$:

$$N : \mathbb{R}^4 \to \mathbb{H}_4\,, \quad (a, b, c, d) \mapsto a + ib + jc + kd\,. \tag{B.11}$$

An $SO(4)$ rotation matrix A can be re-expressed as (Cayley-Klein)

$$A \in SO(4)\,, x \in \mathbb{R}^4 :\; A\,x = (M \circ N)^{-1}(L\,M \circ N(x)\,R^\dagger)\,, \quad L, R \in SU(2)_{L,R}\,, \tag{B.12}$$

which demonstrates that the group action F of eq. (B.10) defines a 2-1 homomorphism $SU(2)_L \times SU(2)_R \to SO(4)$, since $(L, R) \in SU(2)_L \times SU(2)_R$ and $(-L, -R) \in SU(2)_L \times SU(2)_R$ map onto the same element of SO(4).

Let $D_{(j_1,j_2)}$ be a representation of $SU(2)_L \times SU(2)_R$ of dimension $(2j_1{+}1)(2j_2{+}1)$ for integers or half integers j_1, j_2. In order for $D_{(j_1,j_2)}$ to be also a representation of $SO(4)$, it has to obey:

$$D_{(j_1,j_2)}(L, R) = D_{(j_1,j_2)}(-L, -R)\,, \quad \forall\,(L, R) \in SU(2)_L \times SU(2)_R\,, \tag{B.13}$$

which requires $j_1 + j_2$ to equal integer values. In general, multiple tensor products of (fundamental) two-dimensional representations of $SU(2)_L \times SU(2)_R$,

$$\begin{aligned}
&\underbrace{D_{(1/2,0)} \otimes \cdots \otimes D_{(1/2,0)}}_{m-\text{times}} \otimes \underbrace{D_{(0,1/2)} \otimes \cdots \otimes D_{(0,1/2)}}_{n-\text{times}} : \\
&SU(2)_L \times SU(2)_R \times \underbrace{\mathbb{C}^2 \otimes \cdots \otimes \mathbb{C}^2}_{m-\text{times}} \otimes \underbrace{\mathbb{C}^2 \otimes \cdots \otimes \mathbb{C}^2}_{n-\text{times}} \\
&\to \underbrace{\mathbb{C}^2 \otimes \cdots \otimes \mathbb{C}^2}_{m-\text{times}} \otimes \underbrace{\mathbb{C}^2 \otimes \cdots \otimes \mathbb{C}^2}_{n-\text{times}}\,,
\end{aligned} \tag{B.14}$$

are (not necessarily irreducible) representations of $SO(4)$ if $m + n$ is even. Let us consider the set of such tensor products of rank two (i.e. $m + n = 1$). The group actions corresponding to irreducible representations of $SO(4)$ of rank 1 can be defined by

$$\begin{aligned}
&\dim = 4 && D_{(1/2,1/2)} && : M(q) \mapsto LM(q)R^\dagger\,, && \text{(B.15)}\\
&\dim = 4 && D_{(1/2,1/2)} && : RM(q)L^\dagger\,, && \text{(B.16)}\\
&\dim = 3 && D_{(1,0)} && : M(q) \mapsto LM(q)L^\dagger\,, && \text{(B.17)}\\
&\dim = 3 && D_{(0,1)} && : M(q) \mapsto RM(q)R^\dagger\,, && \text{(B.18)}\\
&\dim = 1 && D_{(0,0)} && : M(1) = \mathbb{1} \mapsto LM(1)L^\dagger\,, && \text{(B.19)}\\
&\dim = 1 && D_{(0,0)} && : M(1) = \mathbb{1} \mapsto RM(1)R^\dagger\,, && \text{(B.20)}
\end{aligned}$$

for $q \in \mathbb{H}_4$ and $(L, R) \in SU(2)_L \times SU(2)_R$. Note that the group action on $\mathbb{H}_4$ corresponding to a particular irreducible representation of $SO(4)$ (and $SU(2)_L \times SU(2)_R$) is not necessarily unique. All group actions defined in eqs. (B.15)-(B.20) are formally different group actions.

Group actions F on the tensor product space of multiple copies of $\mathbb{H}_4$,

$$F : SU(2)_L \times SU(2)_R \times (\mathbb{H}_4 \otimes \cdots \otimes \mathbb{H}_4) \to (\mathbb{H}_4 \otimes \cdots \otimes \mathbb{H}_4)\,, \qquad \text{(B.21)}$$

can constitute higher dimensional irreducible representations of $SO(4)$. Let the notation $(i\tau_j)_L$ and $(i\tau_j)_R$, $j = 1, 2, 3$, imply the following definitions of $SU(2)_L \times SU(2)_R$ group actions on a subspace of $\mathbb{H}_4$:

$$\begin{aligned}
&\dim = 3 : && (i\tau_j)_L \mapsto (Li\tau_j L^\dagger)_L\,, && \text{(B.22)}\\
&\dim = 3 : && (i\tau_j)_R \mapsto (Ri\tau_j R^\dagger)_R\,. && \text{(B.23)}
\end{aligned}$$

The group actions on $\mathbb{H}_4 \otimes \mathbb{H}_4$ – subsequently referred to as the (rank 2) tensor product of two elementary (rank 1) $SU(2)_L \times SU(2)_R$ group actions – corresponding to tensor products of the representations $D_{(1,0)}$ and $D_{(0,1)}$ are then given by (the '$\otimes$' is omitted for convenience below, *e.g.* $(i\tau_j)_{L,R}(i\tau_k)_{L,R}$ is meant to imply $(i\tau_j)_{L,R} \otimes (i\tau_k)_{L,R}$)

$$\begin{aligned}
&(0,1) \otimes (0,1) : && (i\tau_j)_R (i\tau_k)_R \mapsto (Ri\tau_j R^\dagger)_R (Ri\tau_k R^\dagger)_R\,, && \text{(B.24)}\\
&(1,0) \otimes (1,0) : && (i\tau_j)_L (i\tau_k)_L \mapsto (Li\tau_j L^\dagger)_L (Li\tau_k L^\dagger)_L\,, && \text{(B.25)}\\
&(1,0) \otimes (0,1) : && (i\tau_j)_L (i\tau_k)_R \mapsto (Li\tau_j L^\dagger)_L (Ri\tau_k R^\dagger)_R\,, && \text{(B.26)}
\end{aligned}$$

which do a priori not constitute irreducible representations of $SO(4)$ and may decompose into direct sums of irreducible representation of $SO(4)$. The basis states of the lowest-dimensional irreducible representations are obtained by identifying linear combinations of the basis vectors $(i\tau_j)_{L/R}(i\tau_k)_{L/R}$ with well defined properties under exchanges of j and k (summation of identical indices implied):

$$\begin{aligned}
&\dim = 1: && (0,0) && : && (i\tau_m)_L(i\tau_m)_L\,, && \text{(B.27)}\\
&\dim = 1: && (0,0) && : && (i\tau_m)_R(i\tau_m)_R\,, && \text{(B.28)}\\
&\dim = 3: && (1,0) && : && (i\tau_j)_L(i\tau_k)_L - (i\tau_k)_L(i\tau_j)_L\,, && \text{(B.29)}\\
&\dim = 3: && (0,1) && : && (i\tau_j)_R(i\tau_k)_R - (i\tau_k)_R(i\tau_j)_R\,, && \text{(B.30)}\\
&\dim = 5: && (2,0) && : && (i\tau_j)_L(i\tau_k)_L + (i\tau_k)_L(i\tau_j)_L - 2(i\tau_m)_L(i\tau_m)_L\,, && \text{(B.31)}\\
&\dim = 5: && (0,2) && : && (i\tau_j)_R(i\tau_k)_R + (i\tau_k)_R(i\tau_j)_R - 2(i\tau_m)_R(i\tau_m)_R\,, && \text{(B.32)}\\
&\dim = 9: && (1,1) && : && (i\tau_j)_L(i\tau_k)_R\,, && \text{(B.33)}\\
&\dim = 9: && (1,1) && : && (i\tau_j)_R(i\tau_k)_L\,. && \text{(B.34)}
\end{aligned}$$

In order to explore the $SU(2)_L{\times}SU(2)_R$ group actions on $\mathbb{H}_4{\otimes}\mathbb{H}_4$ corresponding to the tensor product of representations $D_{(1/2,1/2)} \otimes D_{(1/2,1/2)}$, the quantities (t_α) and $(t^\dagger_\alpha)$ are introduced to imply the group actions on $\mathbb{H}_4$ defined by

$$\dim = 4: \qquad (t_\alpha) \mapsto (L t_\alpha R^\dagger)\,, \tag{B.35}$$

$$\dim = 4: \qquad (t^\dagger_\alpha) \mapsto (R t^\dagger_\alpha L^\dagger)\,, \tag{B.36}$$

with

$$t_0 = \mathbb{1}\,, \quad t_1 = i\tau_1\,, \quad t_2 = i\tau_2\,, \quad t_3 = i\tau_3\,. \tag{B.37}$$

For $g_{\alpha\beta} = \mathrm{diag}(1,-1,-1,-1)$[1], the basis states of the lowest-dimensional irreducible representations of $SO(4)$ expressed in terms of tensor products of the four-dimensional group action eq. (B.35) are given by:

$$\begin{aligned}
&\dim = 1 && (0,0) && : (t_\alpha)(t_\beta)\, g_{\alpha\beta}\,, && \text{(B.38)}\\
&\dim = 3+3 && (1,0)\oplus(0,1) && : (t_\alpha)(t_\beta) - (t_\beta)(t_\alpha)\,, && \text{(B.39)}\\
&\dim = 9 && (1,1) && : (t_\alpha)(t_\beta) + (t_\beta)(t_\alpha) - 2(t_\alpha)(t_\beta)\, g_{\alpha\beta}\,. && \text{(B.40)}
\end{aligned}$$

By replacing $(t_{\alpha,\beta})$ by $(t^\dagger_{\alpha,\beta})$ the lowest-dimensional irreducible representations of $SO(4)$ expressed in terms of tensor products of the group action defined in eq. (B.36) are obtained.

B.3 The representation theory of $O(4)$

The well-known connection between the quaternion algebra $\mathbb{H}_4$ and the Lie group $O(4)$ is the following [140, 142–144]: the group $O(4) = SO(4) \times \mathbb{Z}_2$ consists of two copies of $SO(4)$ and is thus not connected. The parity transformation P defined as the spacial inversion of three components of a general real four-vector,

$$P : \mathbb{R}^4 \to \mathbb{R}^4\,, \quad (x_1, x_2, x_3, x_4) \mapsto (x_1, -x_2, -x_3, -x_4)\,, \tag{B.41}$$

[1] We do not distinguish between covariance and contravariance here.

transforms an element of one connected component into an element of the other connected component. By exploiting the isomorphism N of eq. (B.11) between $\mathbb{R}^4$ and $\mathbb{H}_4$, the parity transformation P is found to correspond to the following $\mathbb{Z}_2$ group action on $\mathbb{H}_4$:

$$\tilde{P} = NPN^{-1} : \mathbb{Z}_2 \times \mathbb{H}_4 \to \mathbb{H}_4 , \quad \mathbb{1} , i\tau_1 , i\tau_2 , i\tau_3 \mapsto \mathbb{1} , -i\tau_1 , -i\tau_2 , -i\tau_3 , \tag{B.42}$$

i.e. to be equivalent to the conjugation of quaternions (or to hermitian conjugation of $\mathbb{1}$ and $i\tau_{1,2,3}$). The composition of the parity transformation with an $SO(4)$ matrix A then amounts to an exchange of the left and right unit quaternion in the Cayley-Klein 2-1 isomorphism of eq. (B.12):

$$\begin{aligned} P\,A\,x &= (M \circ N)^{-1}([L\,M \circ N(x)\,R^\dagger]^\dagger) \\ &= (M \circ N)^{-1}(R\,[M \circ N(x)]^\dagger\,L^\dagger) = (M \circ N)^{-1}(R\,M \circ N(Px)\,L^\dagger) \,. \end{aligned} \tag{B.43}$$

Let $D_{(j,j)}$ be a representation of $O(4)$ and $v_1 \otimes v_2$ and element of the base space of $D_{(j,j)}$. Eq. (B.43) demonstrates that the representation of the element P has to obey

$$\begin{aligned} D_{(j,j)}(P)\,D_{(j,j)}(L,R)\,v_1 \otimes v_2 &= D_{(j,j)}(P)\,(D_{(j)}(L)\,v_1 \otimes D_{(j)}(R)\,v_2) \\ &= D_{(j,j)}(R,L)\,D_{(j,j)}(P) v_1 \otimes v_2 \,. \end{aligned} \tag{B.44}$$

Therefore, a representation $D_{(j_1,j_2)}$ of $SO(4)$ is also a representation of $O(4)$ if and only if it is symmetric under an exchange of the indices j_1 and j_2. For arbitrary j_1 and j_2, the irreducible representation $D_{(j_1,j_2)}$ of $SO(4)$ induces the symmetrized representation $D_{(j_1,j_2)\oplus(j_2,j_1)}$ of $O(4)$, which is irreducible if $j_1 \neq j_2$ and decomposes into two irreducible representation of equal dimensions if $j_1 = j_2$. This observation implies that irreducible representations $D_{(j_1,j_2)}$ of $SO(4)$ with $j_1 \neq j_2$ induce exactly one irreducible $O(4)$ representation, whereas irreducible representations $D_{(j,j)}$ of $SO(4)$ induce two separate representations of $O(4)$.

For arbitrary half integers or integers j_1, j_2 with $j_1 + j_2 \in \mathbb{N}$, the generalization of eq. (B.44) reads:

$$D_{(j_1,j_2)\oplus(j_2,j_1)}(P) D_{(j_1,j_2)\oplus(j_2,j_1)}(L,R) = D_{(j_1,j_2)\oplus(j_2,j_1)}(R,L) D_{(j_1,j_2)\oplus(j_2,j_1)}(P) \,. \tag{B.45}$$

The action of $D_{(j_1,j_2)\oplus(j_2,j_1)}(P)$ on an element of the base space $v_1 \otimes v_2 \oplus v_3 \otimes v_4$ is required to be

$$D_{(j_1,j_2)\oplus(j_2,j_1)}(P)(v_1 \otimes v_2 \oplus v_3 \otimes v_4) = v_4 \otimes v_3 \oplus v_2 \otimes v_1 \,, \tag{B.46}$$

which can be proven by the following brief computation:

$$\begin{aligned}
& D_{(j_1,j_2)\oplus(j_2,j_1)}(L,R)\,(v_1\otimes v_2\oplus v_3\otimes v_4) \\
= \;& [D_{(j_1,j_2)\oplus(j_2,j_1)}(P)]^2 D_{(j_1,j_2)\oplus(j_2,j_1)}(L,R)\,(v_1\otimes v_2\oplus v_3\otimes v_4) \\
= \;& D_{(j_1,j_2)\oplus(j_2,j_1)}(P) D_{(j_1,j_2)\oplus(j_2,j_1)}(R,L) D_{(j_1,j_2)\oplus(j_2,j_1)}(P)\,(v_1\otimes v_2\oplus v_3\otimes v_4) \\
= \;& D_{(j_1,j_2)\oplus(j_2,j_1)}(P) D_{(j_1,j_2)\oplus(j_2,j_1)}(R,L)\,(v_4\otimes v_3\oplus v_2\otimes v_1) \\
= \;& D_{(j_1,j_2)\oplus(j_2,j_1)}(P)\,(D_{(j_1)}(R)v_4\otimes D_{(j_2)}(L)v_3\oplus D_{(j_2)}(R)v_2\otimes D_{(j_1)}(L)v_1) \\
= \;& D_{(j_1)}(L)v_1\otimes D_{(j_2)}(R)v_2\oplus D_{(j_2)}(L)v_3\otimes D_{(j_1)}(R)v_4) \\
= \;& D_{(j_1,j_2)\oplus(j_2,j_1)}(L,R)\,(v_1\otimes v_2\oplus v_3\otimes v_4)\,.
\end{aligned} \tag{B.47}$$

Due to

$$[D_{(j_1,j_2)\oplus(j_2,j_1)}(P)]^2 = \mathbb{1}\,, \tag{B.48}$$

$D_{(j_1,j_2)\oplus(j_2,j_1)}(P)$ must have eigenvalues ± 1 and the basis states of the irreducible representations have definite parity, $p = \pm 1$. It is convenient to refer to the two irreducible representations of $O(4)$ in $D_{(j,j)\oplus(j,j)}$ by $D_{(j,j)^\pm}$.

B.3.1 Representations of $O(4)$ and quaternions

Utilizing the notation introduced by eq. (B.22), eq. (B.23), eq. (B.35) and eq. (B.36) and defining

$$(0,0) \quad \dim = 1: \qquad (\mathbb{1})_L \mapsto (L\mathbb{1}L^\dagger)_R = (\mathbb{1})_L\,, \tag{B.49}$$

$$(0,0) \quad \dim = 1: \qquad (\mathbb{1})_R \mapsto (R\mathbb{1}R^\dagger)_R = (\mathbb{1})_R\,, \tag{B.50}$$

the group actions of $SU(2)_L \times SU(2)_R$ on $\mathbb{H}_4$ which correspond to the lowest-dimensional irreducible representations of $O(4)$ are given by:

$$(0,0)^\pm \qquad \dim = 1 \quad : \quad (\mathbb{1})_L \pm (\mathbb{1})_R\,, \tag{B.51}$$

$$(1/2,1/2)^\pm \qquad \dim = 4+4: \quad (t_0) \pm (t_0^\dagger)\,, (t_i) \mp (t_i^\dagger)\,, \tag{B.52}$$

$$(1,0)\oplus(0,1) \qquad \dim = 6 \quad : \quad (i\tau_j)_L + (i\tau_j)_R\,, (i\tau_j)_L - (i\tau_j)_R\,. \tag{B.53}$$

For convenience, the tensor products $(i\tau_j)_{L,R}\otimes(i\tau_k)_{L,R}$ and $(t_\alpha^{(\dagger)})\otimes(t_\beta^{(\dagger)})$ are denoted by $(i\tau_j)_{L,R}(i\tau_k)_{L,R}$ and $(t_\alpha^{(\dagger)})(t_\beta^{(\dagger)})$, respectively, in this subsection. The basis states of the lowest-dimensional irreducible representations of $O(4)$ expressed in terms of tensor products of $(i\tau_j)$ read (which can also be proven by a direct computation):

$$
\begin{aligned}
&(0,0)^{\pm} &&: (i\tau_m)_R(i\tau_m)_R \pm (i\tau_m)_L(i\tau_m)_L\,, && \text{(B.54)}\\
&(1,0)\oplus(0,1) &&: (\delta^{jl}\delta^{km}-\delta^{jm}\delta^{kl})[(i\tau_l)_L(i\tau_m)_L \pm (i\tau_l)_R(i\tau_m)_R]\,, && \text{(B.55)}\\
&(2,0)\oplus(0,2) &&: (\delta^{jl}\delta^{km}+\delta^{jm}\delta^{kl}-2\delta^{jk}\delta^{lm})[(i\tau_k)_L(i\tau_l)_L \pm (i\tau_k)_R(i\tau_l)_R]\,, && \text{(B.56)}\\
&(1,1)^{+} &&: (i\tau_j)_L(i\tau_k)_R - (i\tau_j)_R(i\tau_k)_L - (j\leftrightarrow k)\,, && \text{(B.57)}\\
& && \ \ (i\tau_j)_L(i\tau_k)_R + (i\tau_j)_R(i\tau_k)_L + (j\leftrightarrow k)\,, && \text{(B.58)}\\
&(1,1)^{-} &&: (i\tau_j)_L(i\tau_k)_R - (i\tau_j)_R(i\tau_k)_L + (j\leftrightarrow k)\,, && \text{(B.59)}\\
& && \ \ (i\tau_j)_L(i\tau_k)_R + (i\tau_j)_R(i\tau_k)_L - (j\leftrightarrow k)\,. && \text{(B.60)}
\end{aligned}
$$

The tensor product of two six-dimensional representations of $O(4)$ decomposes into:

$$
\begin{aligned}
& [(1,0)\oplus(0,1)]\otimes[(1,0)\oplus(0,1)]\\
= \; & [(2,0)\oplus(0,2)]\oplus(1,1)^{+}\oplus(1,1)^{-}\oplus[(1,0)\oplus(0,1)]\oplus(0,0)^{+}\oplus(0,0)^{-}\,,
\end{aligned}
\tag{B.61}
$$

i.e. into one 10-dimensional, two 9-dimensional, one 6-dimensional and two one-dimensional irreducible representations of $O(4)$, whose basis states with their implied group actions are given by eq. (B.54) and eqs. (B.55)-(B.60).

The other relevant tensor products of irreducible representations of $O(4)$ decompose into

$$
\begin{aligned}
(1/2,1/2)^{\pm}\otimes(1/2,1/2)^{\pm} &= (1,1)^{+}\oplus[(1,0)\oplus(0,1)]\oplus(0,0)^{+}\,, && \text{(B.62)}\\
(1/2,1/2)^{\pm}\otimes(1/2,1/2)^{\mp} &= (1,1)^{-}\oplus[(1,0)\oplus(0,1)]\oplus(0,0)^{-}\,. && \text{(B.63)}
\end{aligned}
$$

Utilizing the notation for group actions defined by eq. (B.35) and eq. (B.36), the basis states with implied group actions of the lowest-dimensional irreducible representations of $O(4)$ expressed in terms of tensor products of (t_α) and $(t^\dagger_\alpha)$ are given by:

$$
\begin{aligned}
&(0,0)^{\pm} && \dim = 1 &&: [(t_\alpha)(t_\beta) \pm (t^\dagger_\alpha)(t^\dagger_\beta)]g_{\alpha\beta}\,, && \text{(B.64)}\\
&(1,0)\oplus(0,1) && \dim = 6 &&: [(t_\alpha)(t_\beta) \pm (t^\dagger_\alpha)(t^\dagger_\beta)] - [(t_\beta)(t_\alpha) \pm (t^\dagger_\beta)(t^\dagger_\alpha)]\,, && \text{(B.65)}\\
&(1,1)^{\pm} && \dim = 9+9 &&: (g_{\alpha\rho}g_{\beta\sigma}+g_{\beta\rho}g_{\alpha\sigma}-2g_{\alpha\beta}g_{\rho\sigma})[(t_\rho)(t_\sigma) \pm (t^\dagger_\rho)(t^\dagger_\sigma)]\,. && \text{(B.66)}
\end{aligned}
$$

Note that the different relative signs in eq. (B.65) define two identical (Fierz-equivalent) sets of tensors (which are given explicitly by eqs. (B.67)-(B.68) and eqs. (B.71)-(B.72), respectively). The basis states of the $(1,1)^{+}$ and $(1,1)^{-}$ representations are given by eq. (B.69)-(B.70) and eq. (B.73)-(B.74) below, respectively. The basis states of the irreducible representations of $O(4)$ in the decompositions of specific tensor products of four-dimensional irreducible representations of $O(4)$

read:
$(1/2,1/2)^{\pm}\otimes(1/2,1/2)^{\pm}$: $i,j=1,2,3,\ i\neq j$

$$\begin{aligned}
&(1,0)\oplus(0,1) && \dim=6: && (t_i)(t_j)+(t_i^\dagger)(t_j^\dagger)-(i\leftrightarrow j)\,, && \text{(B.67)}\\
& && && (t_0)(t_i)-(t_0^\dagger)(t_i^\dagger)-(0\leftrightarrow i)\,, && \text{(B.68)}\\
&(1,1)^+ && \dim=9: && (t_i)(t_j)+(t_i^\dagger)(t_j^\dagger)+(i\leftrightarrow j)\,, && \text{(B.69)}\\
& && && (t_0)(t_i)-(t_0^\dagger)(t_i^\dagger)+(0\leftrightarrow i)\,, && \text{(B.70)}
\end{aligned}$$

$(1/2,1/2)^{\pm}\otimes(1/2,1/2)^{\mp}$: $i,j=1,2,3,\ i\neq j$

$$\begin{aligned}
&(1,0)\oplus(0,1) && \dim=6: && (t_i)(t_j)-(t_i^\dagger)(t_j^\dagger)-(i\leftrightarrow j)\,, && \text{(B.71)}\\
& && && (t_0)(t_i)+(t_0^\dagger)(t_i^\dagger)-(0\leftrightarrow i)\,, && \text{(B.72)}\\
&(1,1)^- && \dim=9: && (t_i)(t_j)-(t_i^\dagger)(t_j^\dagger)+(i\leftrightarrow j)\,, && \text{(B.73)}\\
& && && (t_0)(t_i)+(t_0^\dagger)(t_i^\dagger)+(0\leftrightarrow i)\,, && \text{(B.74)}
\end{aligned}$$

where only the six "off-diagonal" ($\alpha\neq\beta$) basis states for the $(1,1)^{\pm}$ representations are shown.

The "off-diagonal" basis states of the $(1,1)^{\pm}$ representations in terms of tensor products of (t_α) and $(t_\beta^\dagger)$ are given by ($i,j=1,2,3$ and $i\neq j$):

$$\begin{aligned}
&(1,1)^+ && \dim=9: && (t_0)(t_i^\dagger)-(t_0^\dagger)(t_i)+(t_i^\dagger)(t_0)-(t_i)(t_0^\dagger)\,, && \text{(B.75)}\\
& && && (t_i)(t_j^\dagger)+(t_i^\dagger)(t_j)+(t_j^\dagger)(t_i)+(t_j)(t_i^\dagger)\,, && \text{(B.76)}\\
&(1,1)^- && \dim=9: && (t_0)(t_i^\dagger)+(t_0^\dagger)(t_i)+(t_i^\dagger)(t_0)+(t_i)(t_0^\dagger)\,, && \text{(B.77)}\\
& && && (t_i)(t_j^\dagger)-(t_i^\dagger)(t_j)+(t_j^\dagger)(t_i)-(t_j)(t_i^\dagger)\,. && \text{(B.78)}
\end{aligned}$$

The basis states of the $(1,1)^+$ representation in eqs. (B.75)-(B.76) are identical (Fierz-equivalent) to the basis states given in eqs. (B.57)-(B.58) since they define exactly the same $SU(2)_L\times SU(2)_R$ tensors. Phrased differently, representations of $O(4)$ allow for different expressions in terms of group actions on (multiple) tensor products of copies of $\mathbb{H}_4$. In fact, the existence of Fierz identities is a direct consequence of this statement. By the means of a Fierz-type projection [145] a connection between them can be drawn: let

$$(X_s\otimes X_t')_{ijkl},\ (Y_u\otimes Y_v')_{ijkl}\,,\quad X_s,X_t',Y_u,Y_v'\in\mathbb{C}^2\otimes\mathbb{C}^2\,, \tag{B.79}$$

be two bases of the same space which can be expressed as a tensor product of two spaces in more than one way. A scalar product B is defined by

$$B(X_s\otimes X_t',Y_u\otimes Y_v')=\sum_{ijkl}(X_s\otimes X_t')_{ijkl}(Y_u\otimes Y_v')^\dagger_{ijkl}\,. \tag{B.80}$$

For instance, two different expressions of the basis states of the irreducible (1,0) $SO(4)$ representation are given by

$$(\tau_s)_R = (\mathbb{1})_R(\tau_s)_R\,, \quad i\epsilon^{s'tu}(\tau_t)_R(\tau_u)_R\,. \tag{B.81}$$

The scalar product eq. (B.80) of basis states from two different expressions in terms of tensor products yields:

$$[(\mathbb{1})_R]_{ij}[(\tau_s)_R]_{kl}[(\tau_t)_R]_{ij}[(\tau_u)_R]_{kl}\epsilon^{s'tu}/4 = 0\,, \tag{B.82}$$

$$[(\mathbb{1})_R]_{kl}[(\tau_s)_R]_{ij}[(\tau_t)_R]_{ij}[(\tau_u)_R]_{kl}\epsilon^{s'tu}/4 = 0\,, \tag{B.83}$$

$$[(\mathbb{1})_R]_{li}[(\tau_s)_R]_{jk}[(\tau_t)_R]_{ij}[(\tau_u)_R]_{kl}\epsilon^{s'tu}/4 = -\delta_{ss'}\,, \tag{B.84}$$

$$[(\mathbb{1})_R]_{jk}[(\tau_s)_R]_{li}[(\tau_t)_R]_{ij}[(\tau_u)_R]_{kl}\epsilon^{s'tu}/4 = \delta_{ss'}\,. \tag{B.85}$$

B.3.2 $O(4)$ representations and quark multilinears

So far only the regular tensor product of basis states of $SO(4)$ representations with implied $SU(2)_L \times SU(2)_R$ group actions have been considered. However, quark mutlilinears with more than two quarks constitute symmetric tensor products of basis states with implied $SU(2)_L \times SU(2)_R$ group actions, since a general quark multilinear is the commutative product of multiple quark bilinears. The symmetric tensor product, denoted by '$\odot$', is defined for n vectors v_i by

$$v_1 \odot \cdots \odot v_n = \sum_\sigma \frac{1}{n!} v_{\sigma(1)} \otimes \cdots \otimes v_{\sigma(n)}\,, \tag{B.86}$$

where the sum is over all permutations $\sigma(1), \cdots, \sigma(n)$ of the index set $\{1, \cdots, n\}$. The symmetric tensor product of two irreducible representations of dimension d yields a representation of dimension $D = d + (d-1) + \cdots + 1$.

The interest of this thesis is in the decompositions of the symmetric tensor products of the lowest-dimensional irreducible representations of $O(4)$. The symmetric tensor product of the two 6-dimensional irreducible representations yields a reducible representation of dimension 21 which decomposes into the irreducible representations

$$[(1,0)\oplus(0,1)]\odot[(1,0)\oplus(0,1)] = (1,1)^+\oplus(2,0)\oplus(0,2)\oplus(0,0)^+\oplus(0,0)^-\,, \tag{B.87}$$

where the basis states of the irreducible representations $(1,1)^+$, $(2,0) \oplus (0,2)$ and $(0,0)^\pm$ are given by eq. (B.54), eq. (B.56), eq. (B.57) and eq. (B.58) with $(i\tau_j)_L(i\tau_k)_R = (i\tau_k)_R(i\tau_j)_L$. Note that the basis states of the $(1,1)^-$ can not be expressed in terms of symmetric tensor products of $(i\tau_i)_{L,R}$. The symmetric tensor product of two identical 4-dimensional irreducible representations yields a 10-dimensional reducible representation which decomposes into

$$(1/2,1/2)^\pm \odot (1/2,1/2)^\pm = (1,1)^+ \oplus (0,0)^+\,. \tag{B.88}$$

The basis state of the base states of $(0,0)^+$ and $(1,1)^+$ are defined by eq. (B.64), eqs. (B.69)-(B.70) and eqs. (B.75)-(B.76) with $(t_\alpha^{(\dagger)})(t_\beta^{(\dagger)}) = (t_\beta^{(\dagger)})(t_\alpha^{(\dagger)})$. The decomposition of the symmetric tensor product of two different 4-dimensional irreducible representations reads:

$$(1/2,1/2)^\pm \odot (1/2,1/2)^\mp = (1,1)^- \oplus (0,0)^- \,, \tag{B.89}$$

where the basis states of the of $(0,0)^-$ and $(1,1)^-$ are defined by eq. (B.64), eqs. (B.73)-(B.74) and eqs. (B.77)-(B.78) with $(t_\alpha^{(\dagger)})(t_\beta^{(\dagger)}) = (t_\beta^{(\dagger)})(t_\alpha^{(\dagger)})$.

When the quark field is defined to be the $SU(2)$ flavor doublet of the two lightest quark flavors (u,d), the space of quark bilinears is given by the symmetric tensor product of the Clifford algebra of Dirac matrices $(\mathcal{A}_D)$ and the algebra of the isospin Pauli matrices $(\mathcal{A}_I)$:

$$\mathcal{A}_D = \{\mathbb{1}, \gamma^\mu, \gamma^\mu\gamma_5, \gamma_5, \sigma^{\mu\nu}\}, \quad \mathcal{A}_I = \{i\mathbb{1}, \tau_1, \tau_2, \tau_3\} \,. \tag{B.90}$$

Whereas the matrices in $\mathcal{A}_D$ define the chiralities of the quark fields in a quark bilinear, the isospin matrices in $\mathcal{A}_I$ determine the quark flavors in a quark bilinear. Since quark bilinears are hermitian, they have to be eigenstates of the parity transformation $P : (L,R) \mapsto (R,L)$ which converts a right-handed quark field into a left-handed quark field and vice versa. This is also true for quark quadrilinears and quark multilinears in general which demonstrates the connection of quark multilinears to the representation theory of $O(4)$: a matrix in $\mathcal{A}_D$ defines a particular $SU(2)_L \times SU(2)_R$ group action on the isospin algebra $\mathcal{A}_I$, which can be identified with the quaternion algebra $\mathbb{H}_4$ (the above defined basis of the $\mathcal{A}_I$ is obtained from the standard basis of $\mathbb{H}_4$ by multiplication of each element by $-i$). The set $\mathcal{A}_D$ therefore corresponds to all possible $SU(2)_L \times SU(2)_R \times \mathbb{Z}_2$ group actions on $\mathcal{A}_I \sim \mathbb{H}_4$, where $\mathbb{Z}_2$ denotes the group of parity transformations. This is however not a one-to-one correspondence, since two different matrices in $\mathcal{A}_D$ can in general define the same $SU(2)_L \times SU(2)_R \times \mathbb{Z}_2$ group action, *e.g.* $\mathbb{1}$ and $\sigma^{\mu\nu}$. To illustrate this statement, consider the quark bilinear

$$i\bar{q}\tau_k\gamma_5 q = i\bar{q}_L\tau_k q_R - i\bar{q}_R\tau_k q_L \,. \tag{B.91}$$

The Dirac matrix γ_5 defines the $SU(2)_L \times SU(2)_R$ group action on the element $i\tau_k$ of $\mathbb{H}_4$ which is associated with a basis state of the $(1/2,1/2)^+$ representation (see eq. (B.52).

One has to emphasize the subtle difference between the parity transformation in relativistic quantum field theory and the parity group action on $\mathbb{H}_4$: the parity operation on $\mathbb{H}_4$ amounts to a combination of the exchange of the elements of $SU(2)_L$ and $SU(2)_R$ and the hermitian conjugation of the basis elements such that all states of a particular irreducible representation have the same parity eigenvalue. In the field theory case, the requirement of hermiticity causes quark bilinears which transform under $SU(2)_L \times SU(2)_R \times \mathbb{Z}_2$ as basis states of a particular $O(4)$ representation to have in general different parity eigenvalues.

Based on the findings of this appendix, the list of all quark quadrilinears which transform as basis states of particular irreducible $O(4)$ representations can be compiled. The set of P- and/or T-violating quark quadrilinears, the irreducible $O(4)$ representation to which they belong (first column) and the number of P- and/or T-violating quark quadrilinears each representation contains (second column) is given by (summation over k implied, no summation over i'):

$$
\begin{array}{llcll}
(0,0)^- & 1\,\not{P}\ \text{-state} & : & \bar{q}\gamma_\mu\tau_k q\bar{q}\gamma^\mu\gamma_5\tau_k q\,, & \text{(B.92)}\\
(1,1)^+ & 3\,\not{P}\not{T}\ \text{-states} & : & \epsilon^{kij}\bar{q}\gamma_\mu\tau_i q\bar{q}\gamma^\mu\gamma_5\tau_j q\,, & \text{(B.93)}\\
(2,0)\oplus(0,2) & 5\,\not{P}\ \text{-states} & : & (\delta_{ik}\delta_{jl}+\delta_{jk}\delta_{il}-2\delta_{ij}\delta_{kl})\bar{q}\gamma_\mu\tau_i q\bar{q}\gamma^\mu\gamma_5\tau_j q\,, & \text{(B.94)}\\
(0,0)^- & 1\,\not{P}\not{T}\ \text{-state} & : & \bar{q}q\bar{q}i\gamma_5 q-\bar{q}\tau_k q\bar{q}i\gamma_5\tau_k q\,, & \text{(B.95)}\\
(1,1)^+ & 3\,\not{P}\not{T}\ \text{-states} & : & \bar{q}q\bar{q}i\gamma_5\tau_i q\pm\bar{q}\tau_i q\bar{q}i\gamma_5 q\,, & \text{(B.96)}\\
(1,1)^- & 6\,\not{P}\not{T}\ \text{-states} & : & \bar{q}\tau_i q\bar{q}i\gamma_5\tau_j q\pm\bar{q}\tau_j q\bar{q}i\gamma_5\tau_i q\quad i\neq j\,, & \text{(B.97)}\\
 & & & \bar{q}\tau_{i'}q\bar{q}i\gamma_5\tau_{i'}q+\bar{q}q\bar{q}i\gamma_5 q\,. & \text{(B.98)}
\end{array}
$$

Note that the different relative signs in eq. (B.96) and eq. (B.97) define two different sets of tensors which transform as the same respective basis states of the same representation.

This derivation of quark multilinears presented in this appendix immediately reveals Fierz identities among quark multilinears. A Fierz identity between two quark multilinears exists when they transform as the same basis state of the same irreducible representation and as identical tensors. This is the case for

$$\bar{q}q\bar{q}i\gamma_5\tau_k q-\bar{q}\tau_k q\bar{q}i\gamma_5 q \quad \text{and} \quad \epsilon^{kij}\bar{q}\gamma_\mu\tau_i q\bar{q}\gamma^\mu\gamma_5\tau_j q\,, \tag{B.99}$$

for instance, which transform as the same basis state of the $(1,1)^+$ representation and as identical tensors.

Appendix C

The Weinberg formulation of $SU(2)$ ChPT

The aim of this appendix is to demonstrate the connection between the two equivalent formulations of $SU(2)$ ChPT, by Gasser and Leutwyler [43] and by Weinberg [41], respectively. The equivalence of these two formulations is based on the observation made in appendix B: a chiral $SU(2)_L \times SU(2)_R$ transformation of the quark fields in a quark bilinear induces a vector or tensor $SO(4)$ rotation on the set of quark bilinears. The chiral $SU(2)_L \times SU(2)_R$ transformation of the quark fields and the induced $SO(4)$ transformation are just two sides of the same coin. The relationship between quark fields in a quark bilinears and the vector space of quark bilinears is resemblant of the relationship between vector spaces and their dual vector spaces. The same is true for quark multilinears in general.

In order establish the relationship between the two formulations of $SU(2)$ ChPT, the derivation of the transformation properties of the Goldstone boson fields has to be revisited. Let $v_0 \in \mathcal{B}$ be the ground state in the field space $\mathcal{B}$ (i.e. the state without Goldstone bosons) and let $F : G \times \mathcal{B} \to \mathcal{B}$ be a group action of the group G on this space, with the ground state v_0 invariant under $H \subset G$:

$$F_{g_1 g_2}(v) = F_{g_1}(F_{g_2}(v)) \quad \forall v \in \mathcal{B}\,, \quad v_0 \mapsto F_h(v_0) = v_0 \quad \forall h \in H\,. \tag{C.1}$$

F defines a one-to-one map from the set of left cosets G/H onto $\mathcal{B}$:

$$F : G \times \mathcal{B} \to G/H \times \mathcal{B} \to \mathcal{B}\,, \quad F|_{G/H \times \{v_0\}} : G/H \times \{v_0\} \leftrightarrow \mathcal{B}\,. \tag{C.2}$$

Since $H \subset G$ is a subgroup of G, any product $g_1 \cdot g_2$, $g_1, g_2 \in G$, equals $g' \cdot h$ for some $h \in H$ and $g' \in G$ and the group action thus obeys

$$F_{g_1 \cdot g_2} = F_{g' \circ h}\,, \tag{C.3}$$

for all $g_1, g_2 \in G$ and suitable $g' \in G$, $h \in H$. Let $\{\pi^i\}$ be the set of Goldstone boson fields, which are essentially the parameters of G/H, whose elements act on the ground state v_0. According to eq. (C.3), the Goldstone boson fields transform under G by

$$F_g \circ F_{g(\{\pi^i\})}(v_0) = F_{g'(\{\pi^i\},g)} \circ F_{h(\{\pi^i\},g)}(v_0) = F_{g'(\{\pi^i\},g)}(v_0)\,, \tag{C.4}$$

where g' and h depend on g and $g(\{\pi^i\})$.

Eq. (C.4) is the starting point for both formulations of $SU(2)$ ChPT. Both formulations are discussed in the exponential parametrization [88, 89] first. The realization of the $SU(2)_L \times SU(2)_R$ group action on the ground state v_0 chosen by Gasser and Leutwyler [43] is defined by an axial rotation of the ground state $v_0 = \mathbb{1}$:

$$F_{g(\{\pi^i\})}(v_0) = u(\vec{\pi})\,\mathbb{1}\,u(\vec{\pi}) = U(\vec{\pi})\,, \quad u, U \in SU(2)\,, \tag{C.5}$$

where $U = u^2$ is the standard U matrix (the group action F for a general $g=(L,R)$ is given by $\mathbb{1} \mapsto R\mathbb{1}L^\dagger$). The matrix $U = \exp(i\vec{\pi}\cdot\vec{\tau})$ is essentially an axial $SU(2)_A$ rotation of the ground state $v_0 = \mathbb{1}$ parametrized by the Goldstone boson fields $\{\pi^i\}$. For this definition of F (the Gasser-Leutwyler realization) the transformation law eq. (C.4) reads:

$$\begin{aligned} F_g \circ F_{g(\{\pi^i\})}(v_0) = Ru(\vec{\pi})\mathbb{1}u(\vec{\pi})L^\dagger &= u(\vec{\pi}\,')V\mathbb{1}V^\dagger u(\vec{\pi}\,') \qquad = U(\vec{\pi}\,') \\ &= F_{g'(\{\pi\},g)} \circ F_{h(\{\pi^i\},g)}(v_0) = F_{g'(\{\pi^i\},g)}(v_0)\,, \end{aligned} \tag{C.6}$$

for $V \in SU(2)_V = H$.

The other realization of the group action employed by Weinberg utilizes the induced $SO(4)$ transformation: since the Goldstone bosons map bijectively onto $G/H = SU(2)_L{\times}SU(2)_R/SU(2)_V$ where $SU(2)_V$ is the diagonal vector subgroup $\{(V,V)|V \in SU(2)\}$, the elements $\{\mathbb{1},\mathbb{1}\}$ and $\{-\mathbb{1},-\mathbb{1}\}$ are in the same left coset. The spontaneous symmetry breaking pattern $SU(2)_L{\times}SU(2)_R \to SU(2)_V$ is then equivalent to $SO(4) \to SO(3)$ because of

$$SU(2)/\{\mathbb{1},-\mathbb{1}\} = \mathbb{R}P^3 = SO(3)\,, \tag{C.7}$$

where $\mathbb{R}P^3$ is the real projective 3-space. Let the group action F on G now be explicitly defined by the $SO(4)$ rotations $g \in SO(4)$ and $h \in SO(3) \subset SO(4)$ which act on the ground state denoted by the real four-vector v_0. The Goldstone boson fields map bijectively onto $SO(4)/SO(3)$ and can be represented by an $SO(4)$ matrix U_4 (the Goldstone bosons parametrize the $\mathbb{S}^3 \sim SO(4)/SO(3)$ manifold). The generators of $SO(4)$ are readily obtained from the group action of $SU(2)_L \times SU(2)_R$ on $\mathbb{H}_4$ eq. (B.12) and read:

$$(T^k)_{i4} = -(T^k)_{4i} = -i\delta_{ki}, \quad (T^k)_{ij} = (T^k)_{44} = 0\,, \tag{C.8}$$

$$(H^l)_{ij} = -i\epsilon_{ijl}, \qquad (H^l)_{i4} = (H^l)_{4i} = (H^l)_{44} = 0\,, \tag{C.9}$$

where H^k are the generators of $H\subset G$. A possible parametrization of the $SO(4)$ matrix U_4 corresponding to an axial transformation of the ground state (i.e. parameterizing $SO(4)/SO(3)$) is then given by:

$$U_4 = \exp\left[i \begin{pmatrix} 0 & 0 & 0 & -i\pi_1/F_\pi \\ 0 & 0 & 0 & -i\pi_2/F_\pi \\ 0 & 0 & 0 & -i\pi_3/F_\pi \\ i\pi_1/F_\pi & i\pi_2/F_\pi & i\pi_3/F_\pi & 0 \end{pmatrix} \right] . \tag{C.10}$$

The four vector $v_0 = (0,0,0,n)$, $n \in \mathbb{R}$, represents a ground state which is invariant under H. The transformation law eq. (C.4) of the Goldstone bosons then reads:

$$\begin{aligned} F^*_g \circ F^*_{g(\{\pi^i\})}(v_0) = g\, U_4(\vec{\pi})\, v_0 = U_4(\vec{\pi}\,')\, h(\vec{\pi}, g)\, v_0 \qquad &= U_4(\vec{\pi}')v_0 \\ = F^*_{g'(\{\pi^i\},g)} \circ F^*_{h(\{\pi^i\},g)}(v_0) &= F^*_{g'(\{\pi\},g)}(v_0)\,, \end{aligned} \tag{C.11}$$

where $g \in G$ and $h \in H \subset G$ are $SO(4)$ matrices. The F in eq. (C.4) has been replaced by F^* here since the Weinberg realization of the group action can be regarded as the group action induced by the Gasser-Leutwyler realization of F in the same manner as a map of the quark fields in a quark bilinear induces a map on the vector space of quark bilinears.

Whereas in the Gasser-Leutwyler formulation the leading kinetic term, for instance, in the effective Lagrangian is given by

$$c_{GL}\langle \partial_\mu U \partial^\mu U^\dagger \rangle = c_{GL} 2(\partial_\mu \vec{\pi})(\partial^\mu \vec{\pi}) + \cdots\,, \tag{C.12}$$

the leading kinetic term in the effective Lagrangian in the Weinberg formulation would read (see section 19.5 of [41])

$$2c_W(\partial_\mu U_4 v_0)^T(\partial_\mu U_4 v_0) = 2c_W n(\partial_\mu \vec{\pi})(\partial^\mu \vec{\pi}) + \cdots\,, \tag{C.13}$$

for some real constants c_{GL} and c_W. The connection between both realizations of the group action is established by the 2-1 homomorphism of $SU(2)_L \times SU(2)_R$ onto $SO(4)$ eq. (B.12).

There is another more convenient parametrization for the Weinberg realization of the group action which is based on the standard stereographic projection of the 3-sphere $\mathbb{S}^3$ (the north pole is taken to lie on the fourth axis, $\pi^2 = \pi_1^2 + \pi_2^2 + \pi_3^2$):

$$\left(\frac{2\pi_1/F_0}{1+\pi^2/F_0}, \frac{2\pi_2/F_0}{1+\pi^2/F_0}, \frac{2\pi_3/F_0}{1+\pi^2/F_0}, \frac{1-(\pi_1^2+\pi_2^2+\pi_3^2)/F_0}{1+\pi^2/F_0} \right)\,, \qquad F_0 = 2F_\pi\,. \tag{C.14}$$

This parametrization can be expressed as an (axial) $SO(4)$ rotation given by the matrix

$$U_4 = \begin{pmatrix} 1-\frac{2\pi_1^2/F_0^2}{1+\pi^2/F_0^2} & -\frac{2\pi_1\pi_2/F_0^2}{1+\pi^2/F_0^2} & -\frac{2\pi_1\pi_3/F_0^2}{1+\pi^2/F_0^2} & \frac{2\pi_1/F_0}{1+\pi^2/F_0^2} \\ -\frac{2\pi_2\pi_1/F_0^2}{1+\pi^2/F_0^2} & 1-\frac{2\pi_2^2/F_0^2}{1+\pi^2/F_0^2} & -\frac{2\pi_2\pi_3/F_0^2}{1+\pi^2/F_0^2} & \frac{2\pi_2/F_0}{1+\pi^2/F_0^2} \\ -\frac{2\pi_3\pi_1/F_0^2}{1+\pi^2/F_0^2} & -\frac{2\pi_3\pi_2/F_0^2}{1+\pi^2/F_0^2} & 1-\frac{2\pi_3^2/F_0^2}{1+\pi^2/F_0^2} & \frac{2\pi_3/F_0}{1+\pi^2/F_0^2} \\ -\frac{2\pi_1/F_0}{1+\pi^2/F_0^2} & -\frac{2\pi_2/F_0}{1+\pi^2/F_0^2} & -\frac{2\pi_3/F_0}{1+\pi^2/F_0^2} & \frac{1-\pi^2/F_0^2}{1+\pi^2/F_0^2} \end{pmatrix}\,, \tag{C.15}$$

which acts on the north pole $(0,0,0,n)$. This is the preferred parametrization in the Weinberg formulation of $SU(2)$ ChPT.

It has been demonstrated in appendix B that quark multilinears can be regarded as basis states of irreducible representations of $O(4)$. In general, a chiral symmetry breaking quark structure $\mathcal{S}_q$ (i.e. a quark multilinear) exhibits the same transformation properties under G as a corresponding structure $\mathcal{S}_{\text{eff}}$ in the effective Lagrangian:

$$\begin{aligned} \mathcal{S}_q[\{q_i\}] &\mapsto \mathcal{S}_q[F_g^q(\{q_i\})] = F_g^*(\mathcal{S}_q[\{q_i\}])\,, \\ \mathcal{S}_{\text{eff}}[F_{g(\{\pi^i\})}, v_0] &\mapsto \mathcal{S}_{\text{eff}}[F_g \circ F_{g(\{\pi^i\})}, v_0] = F_g^* \circ F_{g(\{\pi^i\})}^*(\mathcal{S}_{\text{eff}}[F_e, v_0])\,, \end{aligned} \tag{C.16}$$

where F^q is the group action on the quark fields, F is the corresponding group action in the effective theory (on the ground state or on the Goldstone boson fields) and F^* is the induced map on the (vector-)space of chiral structures, which is identical for quark structures and chiral structures in the effective field theory. The group action F is in general a group action on an element of the set $\{\mathbb{1}, \tau_1, \tau_2, \tau_3\}$. The equation in the second line of eq. (C.16) reveals the two equivalent methods of constructing chiral symmetry breaking structures in the effective field theory Lagrangian. In the Gasser-Leutwyler formulation, a chiral symmetry breaking term in the effective Lagrangian can be constructed from the Goldstone boson matrix U and its hermitian conjugate to transform under $SU(2)_L \times SU(2)_R$ (or equivalently $O(4)$) identically to the corresponding quark multilinear. As an example one may consider the isospin violating component of the quark mass matrix and its leading counter part in the pion-sector effective Lagrangian, which read in the Gasser-Leutwyler formulation:

$$\mathcal{S}[\{q_i\}] = \bar{q}_L \tau_3 q_R + \bar{q}_R \tau_3 q_L \qquad \mapsto \mathcal{S}[F_g^q(\{q_i\})] = \bar{q}_L L^\dagger \tau_3 R q_R + \bar{q}_R R^\dagger \tau_3 L q_L\,, \tag{C.17}$$

$$\mathcal{S}_{\text{eff}}[F_{g(\{\pi^i\})}, v_0] = \langle U\tau_3 + U^\dagger \tau_3 \rangle \mapsto \mathcal{S}_{\text{eff}}[F_g \circ F_{g(\{\pi^i\})}, v_0] = \langle RUL^\dagger \tau_3 + LU^\dagger R^\dagger \tau_3 \rangle\,. \tag{C.18}$$

In the Weinberg formulation of $SU(2)$ ChPT, a term without Goldstone bosons is constructed which exhibits the same transformation properties under $O(4)$ (or equivalently $SU(2)_L \times SU(2)_R$) as its corresponding quark multilinear. The Goldstone bosons are then introduced by an axial $SO(4)$ rotation (i.e. expressible in terms of U_4 of eq. (C.10) or eq. (C.15)) which is paramterized by the Goldstone boson fields:

$$\mathcal{S}_{\text{eff}}[F_e, v_0] \mapsto F_{g(\{\pi^i\})}^*(\mathcal{S}_{\text{eff}}[F_e, v_0])\,. \tag{C.19}$$

We demonstrate the Weinberg procedure of constructing chiral symmetry breaking terms in the pion and pion-nucleon sector effective Lagrangian for the quark bilinears in the 4-dimensional $(1/2,1/2)^+$ representation of $O(4)$. The fourth component of a vector in this representation transforms as the isospin conserving component of quark mass term, i.e. it transforms as a scalar under $H\subset G$. The other components of a vector in this representation transform as a P- and T-violating three-vector under $H\subset G$. The application of U_4 of eq. (C.10) to the four vectors in the pion sector and the pion nucleon sector with the correct transformation properties yields:

$$\begin{aligned} (U_4(0,0,0,1)^T)_4 &= (\vec{\pi}/F_\pi,(1-\vec{\pi}^2/(2F_\pi^2)))+\cdots\,, && \text{(C.20)} \\ (U_4(0,0,0,N^\dagger N)^T)_4 &= (\vec{\pi}/F_\pi,(1-\vec{\pi}^2/(2F_\pi^2)))N^\dagger N+\cdots\,, && \text{(C.21)} \end{aligned}$$

which is identical to the expressions obtained within the Gasser-Leutwyler formulation. The list of further structures in the Weinberg formulation with their corresponding structures in the Gasser-Leutwyler formulation reads:

$$\begin{aligned} & N^\dagger N && \leftrightarrow \quad N^\dagger N\,, \\ & (U_4(0,0,0,N^\dagger N)^T)_4 && \leftrightarrow \quad \langle\chi_+\rangle N^\dagger N\,, \\ & (U_4(N^\dagger\vec{\tau}N,0)^T)_3 && \leftrightarrow \quad N^\dagger\hat{\chi}N=N^\dagger(\chi_+-\langle\chi_+\rangle)N\,, \\ & eF_{\mu\nu}\left(((U_4)_{ik}(U_4)_{jl}-(U_4)_{jk}(U_4)_{il})N^\dagger T_{kl}N\right)_{34} && \leftrightarrow \quad N^\dagger\hat{f}^+_{\mu\nu}N=N^\dagger(f^+_{\mu\nu}-\langle f^+_{\mu\nu}\rangle)N\,, \end{aligned}$$

where the antisymmetric matrix T is given by

$$T=\begin{pmatrix} 0 & 0 & 0 & \tau_1 \\ 0 & 0 & 0 & \tau_2 \\ 0 & 0 & 0 & \tau_3 \\ -\tau_1 & -\tau_2 & -\tau_3 & 0 \end{pmatrix}\,. \qquad \text{(C.22)}$$

Higher terms in the effective Lagrangian are tensor products of these representations. They can be obtained in exactly the same manner by constructing tensors without Goldstone bosons and with the correct transformation properties under $O(4)$ transformations. Whereas in the Gasser-Leutwyler formulation such structures in the pion sector and pion-nucleon sector are easily obtained by composition of fundamental building blocks, the construction of higher order structures in the Weinberg formulation proves to be increasingly tedious. Furthermore, the simple extension of $SU(2)$ ChPT to $SU(3)$ ChPT in the Gasser-Leutwyler formulation is not possible for the Weinberg formulation of $SU(2)$ ChPT.

Appendix D

The effective Lagrangian from the θ-term

Based on the findings of section 4.2, this appendix provides the complete list of P- and T-violating terms in the pion sector Lagrangian $\mathcal{L}_\pi$ and in the pion-nucleon sector Lagrangian $\mathcal{L}_{\pi N}$ up to $\mathcal{O}(p^4)$ which are induced by the θ-term. The Lagrangians listed below are the Lagrangians prior to the selection of the correct ground state and represent the most general set of independent P- and T-violating terms. The complete list of P- and T-violating terms in the pion-nucleon sector induced by the θ-term up to $\mathcal{O}(p^4)$ is already implicitly contained in [91]. The lists of pion-nucleon terms found below are thus compilations of the P- and T-violating terms relevant for our analysis from [91].

The P- and T-violating terms in the effective Lagrangian from the θ-term are essentially those with insertions of the source field χ, i.e. terms proportional to p_0 and p_3 and powers thereof. As explained in section 4.2, the $qCEDM$ and $4qLR$-op require the introduction of new source fields. The P- and T-violating terms in the effective Lagrangian induced by these two sources of P and T violation can be obtained by a duplication of $\chi_\pm$ structures. The eigenvalues of fundamental building blocks and external fields and combinations thereof under P and T transformations utilized to compile the lists in this appendix are given in appendix I.

The following notation is adopted below: the quantities $\bar{s}_0$, $\bar{s}_3$, $\bar{p}_0$ and $\bar{p}_3$ denote $2Bs_0$, $2Bs_3$, $2Bp_0$ and $2Bp_3$, respectively. Furthermore, a Lagrangian $\bar{\mathcal{L}}$ consists of all terms in the corresponding Lagrangian $\mathcal{L}$ in standard ChPT which contain P- and T-violating terms relevant for our analysis. The additional superscripts 0 and 3 indicate that the Lagrangian $\bar{\mathcal{L}}$ contains only terms proportional to $\bar{p}_0$ and $\bar{p}_3$, respectively.

The only external field relevant for the analysis of EDMs is the electromagnetic field and the left- and right-handed source fields are therefore set to

$$r_\mu \to -\frac{e}{2}\tau_3 A_\mu, \quad l_\mu \to -\frac{e}{2}\tau_3 A_\mu\,, \quad v_\mu^{(s)} \to -\frac{e}{2}A_\mu. \tag{D.1}$$

The P- and T-violating terms provided below constitute the complete set of independent P- and T-violating terms before the correct ground state within QCD and ChPT in the presence of P and T violation has been selected. The ground-state selection procedure results in a mixing of source fields as demonstrated in section 4.3. Furthermore, in order to obtain terms in an arbitrary parametrization, the matrix U in the exponential parametrization has to be replaced by the matrix U of eq. (4.73).

D.1 The P- and T-violating Lagrangian in the pion sector

The leading order P- and T-violating terms in the pion sector Lagrangian are contained in the mass term of the chiral Lagrangian of [43]:

$$\mathcal{L}_\pi^{(2)} = \frac{F_\pi}{4}\langle \chi U^\dagger + U\chi^\dagger\rangle\,, \tag{D.2}$$

which gives rise to a leading order term (the wiggled arrow indicates that only the leading P- and T-violating terms in the chiral structure are displayed)

$$\frac{F_\pi}{4}\langle \chi U^\dagger + U\chi^\dagger\rangle \rightsquigarrow \bar{p}_3\, F_\pi\, \frac{\pi_3}{F_\pi}\left(1-\frac{\pi^2}{6F_\pi^2}\right). \tag{D.3}$$

Within the selection procedure of the correct ground state the tadpole term is removed, which reinstates the stability of the vacuum. The next-to-leading order pion sector Lagrangian of [43, 78],

$$\mathcal{L}_\pi^{(4)} = +\frac{l_3}{16}\langle \chi U^\dagger + U\chi^\dagger\rangle^2 - \frac{l_7}{16}\langle \chi U^\dagger - U\chi^\dagger\rangle^2 + \cdots\,, \tag{D.4}$$

yields the P- and T-violating terms

$$\frac{l_3}{16}\langle \chi U^\dagger + U\chi^\dagger\rangle^2 \;\rightsquigarrow\; 2l_3\,\bar{s}_0\,\bar{p}_3\frac{\pi_3}{F_\pi}\left(1-\frac{2\pi^2}{3F_\pi^2}\right), \tag{D.5}$$

$$-\frac{l_7}{16}\langle \chi U^\dagger - U\chi^\dagger\rangle^2 \;\rightsquigarrow\; -2l_7\,\bar{p}_0\,\bar{s}_3\,\frac{\pi_3}{F_\pi}\left(1-\frac{2\pi^2}{3F_\pi^2}\right), \tag{D.6}$$

which give rise to yet another pion-tadpole terms which are eliminated by the ground state selection procedure.

D.2 The P- and T-violating Lagrangian in the pion-nucleon sector

The complete pion-nucleon Lagrangian up to $\mathcal{O}(p^4)$ is presented in [91], which implicitly contains all P- and T-violating terms up to $\mathcal{O}(p^4)$. The additional fundamental building blocks in the pion-nucleon sector which contain derivatives of the pion fields and photon fields are the connection Γ_μ, the axial vector u_μ and the symmetric tensor $h_{\mu\nu}$. The building blocks Γ_μ and u_μ are defined by eq. (4.43) and eq. (4.44), respectively. The building block $h_{\mu\nu}$ is defined by

$$h_{\mu\nu} = [\mathcal{D}_\mu, u_\nu] + [\mathcal{D}_\nu, u_\mu] \,. \tag{D.7}$$

The expansions of these building blocks in powers of pion fields for the electromagnetic field as the sole external field read:

$$\begin{aligned} u_\mu = \quad & -\frac{1}{F_\pi}\partial_\mu\vec{\pi}\cdot\vec{\tau} + \frac{1}{6F_\pi^3}(\pi^2\,\partial_\mu\vec{\pi}\cdot\vec{\tau} - \vec{\tau}\cdot\vec{\pi}\,\vec{\pi}\cdot\partial_\mu\vec{\pi}) \\ & +eA_\mu\frac{(\vec{\pi}\times\vec{\tau})_3}{F_\pi}\left(1-\frac{\pi^2}{6F_\pi^2}\right) + \cdots\,, \end{aligned} \tag{D.8}$$

$$\Gamma_\mu = \quad i\frac{(\vec{\pi}\times\partial_\mu\vec{\pi})\cdot\vec{\tau}}{4F_\pi^2} + \frac{ieA_\mu}{2}\left(\tau_3 - \frac{(\pi^2\tau_3 - \vec{\pi}\cdot\vec{\tau}\,\pi_3)}{2F_\pi^2}\right) + \cdots\,, \tag{D.9}$$

$$\begin{aligned} h_{\mu\nu} = \quad & -2\frac{\partial_\mu\partial_\nu\vec{\pi}\cdot\vec{\tau}}{F_\pi} + 2e\frac{A_\mu(\partial_\nu\vec{\pi}\times\vec{\pi})_3 + A_\nu(\partial_\mu\vec{\pi}\times\vec{\pi})_3}{F_\pi} \\ & +2e^2A_\mu A_\nu\frac{\pi_1\tau_1+\pi_2\tau_2}{F_\pi} + \cdots\,. \end{aligned} \tag{D.10}$$

The leading order P- and T-violating terms in the pion-nucleon sector emerge from the $\mathcal{O}(p^2)$ ChPT pion-nucleon sector Lagrangian given by

$$\bar{\mathcal{L}}_{\pi N}^{(2)} := c_1\langle\chi_+\rangle N^\dagger N + c_5 N^\dagger\hat{\chi}_+ N\,, \tag{D.11}$$

which leads to the leading order P- and T-violating pion-nucleon terms

$$c_1\langle\chi_+\rangle N^\dagger N \ \rightsquigarrow\ 4\,c_1\,\bar{p}_3\,\frac{\pi_3}{F_\pi}\left(1-\frac{\pi^2}{6F_\pi^2}\right)N^\dagger N\,, \tag{D.12}$$

$$c_5 N^\dagger\hat{\chi}_+ N \ \rightsquigarrow\ 2\,c_5\,\bar{p}_0\,N^\dagger\frac{\vec{\pi}\cdot\vec{\tau}}{F_\pi}\left(1-\frac{\pi^2}{6F_\pi^2}\right)N\,. \tag{D.13}$$

Further P- and T-violating terms are contained in the $\mathcal{O}(p^3)$ pion-nucleon sector Lagrangian $\mathcal{L}_{\pi N}^{(3)}$:

$$\bar{\mathcal{L}}_{\pi N}^{(3)0} = d_{17}N^\dagger\langle S\cdot u\,\hat{\chi}_+\rangle N + d_{19}N^\dagger[S\cdot\mathcal{D},\langle i\chi_-\rangle]N\,, \tag{D.14}$$

$$\bar{\mathcal{L}}_{\pi N}^{(3)3} = d_5 N^\dagger[\hat{\chi}_-, v\cdot u]N + d_{16}\langle\chi_+\rangle N^\dagger S\cdot uN + d_{18}N^\dagger[S\cdot\mathcal{D}, i\hat{\chi}_-]N\,, \tag{D.15}$$

$\bar{\mathcal{L}}_{\pi N}^{(3)0}$ and $\bar{\mathcal{L}}_{\pi N}^{(3)3}$ are the sums of all structures in $\mathcal{L}_{\pi N}^{(3)}$ which contain terms proportional to $\bar{p}_0$ and $\bar{p}_3$, respectively. The operators with pions in $\bar{\mathcal{L}}_{\pi N}^{(3)0}$ in-between

$N^\dagger$ and N give

$$\begin{aligned}\langle S\cdot u\hat{\chi}_+\rangle &\rightsquigarrow -4\bar{p}_0 S^\mu \frac{\vec{\pi}\cdot\partial_\mu\vec{\pi}}{F_\pi^2}\,, &\text{(D.16)}\\ [S\cdot\mathcal{D},\langle i\chi_-\rangle] &\rightsquigarrow 4\bar{p}_0 S^\mu \frac{\vec{\pi}\cdot\partial_\mu\vec{\pi}}{F_\pi^2}\,, &\text{(D.17)}\end{aligned}$$

whereas the operators with pions in $\bar{\mathcal{L}}_{\pi N}^{(3)3}$ yield

$$\begin{aligned}[\hat{\chi}_-, v\cdot u] &\rightsquigarrow 4\bar{p}_3\frac{(\partial_0\vec{\pi}\times\vec{\tau})_3}{F_\pi}\left(1-\frac{\pi^2}{6F_\pi^2}\right)+2\bar{p}_3\frac{(\vec{\pi}\times\vec{\tau})_3\,\vec{\pi}\cdot\partial_0\vec{\pi}}{3F_\pi^2}\\ &\quad -2\bar{p}_3\frac{(\vec{\pi}\times\partial_0\vec{\pi})\cdot\vec{\tau}\pi_3}{F_\pi^3}+4\bar{p}_3 eA_0\frac{\pi_1\tau_1+\pi_2\tau_2}{F_\pi}\left(1-\frac{\pi^2}{6F_\pi^2}\right)\\ &\quad -2\bar{p}_3 eA_0\frac{(\pi^2\pi_3\tau_3-\vec{\pi}\cdot\vec{\tau}\pi_3^2)}{F_\pi^3}\,, &\text{(D.18)}\\ S\cdot u\langle\chi_+\rangle &\rightsquigarrow -4\bar{p}_3 S^\mu\frac{\partial_\mu\vec{\pi}\cdot\vec{\tau}\pi_3}{F_\pi^2}+4\bar{p}_3 eS^\mu A_\mu\frac{(\vec{\pi}\times\vec{\tau})_3\pi_3}{F_\pi^2}\,, &\text{(D.19)}\\ [S\cdot\mathcal{D}, i\hat{\chi}_-] &\rightsquigarrow 2\bar{p}_3 S^\mu\frac{\partial_\mu\vec{\pi}\cdot\vec{\tau}\pi_3}{F_\pi^2}-2\bar{p}_3 eS^\mu A_\mu\frac{(\vec{\pi}\times\vec{\tau})_3\pi_3}{F_\pi^2}\,. &\text{(D.20)}\end{aligned}$$

The list of all terms containing the source field χ in the $\mathcal{O}(p^4)$ pion-nucleon sector Lagrangian $\mathcal{L}_{\pi N}^{(4)}$ is fairly extensive. By resorting to the same notation as above, all structures in $\mathcal{L}_{\pi N}^{(4)}$ which give terms proportional to $\bar{p}_0$ and $\bar{p}_3$ are combined into $\bar{\mathcal{L}}_{\pi N}^{(4)0}$ and $\bar{\mathcal{L}}_{\pi N}^{(4)3}$, respectively. All structures in $\mathcal{L}_{\pi N}^{(4)}$ which yield terms simultaneously proportional to $\bar{p}_0$ as well as $\bar{p}_3$ are combined into $\bar{\mathcal{L}}_{\pi N}^{(4)03}$.

Those terms proportional to $\bar{p}_0$ are included in the Lagrangian

$$\begin{aligned}\bar{\mathcal{L}}_{\pi N}^{(4)0} &= N^\dagger\big(e_{23}\hat{\chi}_+\langle u\cdot u\rangle+e_{24}\hat{\chi}_+\langle(v\cdot u)^2\rangle+e_{25}u_\mu\langle\hat{\chi}_+u^\mu\rangle+e_{26}v\cdot u\langle\hat{\chi}_+u^\mu\rangle\\ &\quad +e_{27}[S^\mu,S^\nu]\langle\hat{\chi}_+[u_\mu,u_\nu]\rangle+e_{28}iS^\mu v^\nu[\hat{\chi}_+,h_{\mu\nu}]+e_{29}iS^\mu[[\mathcal{D}_\mu,\hat{\chi}_+],v\cdot u]\\ &\quad +e_{30}[\mathcal{D}_\mu,[\mathcal{D}^\mu,\hat{\chi}_+]]+e_{31}\langle\chi_-\rangle[S\cdot u,v\cdot u]+e_{32}v^\mu v^\nu\langle i\chi_-\rangle h_{\mu\nu}\\ &\quad +e_{33}u_\mu[\mathcal{D}^\mu,\langle i\chi_-\rangle]+e_{40}\langle\hat{\chi}_+\hat{\chi}_+\rangle+e_{107}i[S^\mu,S^\nu]\langle f_{\mu\nu}^+\rangle\hat{\chi}_+\\ &\quad +e_{108}i[S^\mu,S^\nu]\langle\hat{f}_{\mu\nu}^+\hat{\chi}_+\rangle+e_{109}iS^\mu v^\nu[f_{\mu\nu}^-,\hat{\chi}_+]+e_{110}iS^\mu v^\nu\langle f_{\mu\nu}^+\rangle\langle\chi_-\rangle\\ &\quad +e_{111}iS^\mu v^\nu\hat{f}_{\mu\nu}^+\langle\chi_-\rangle\big)N\,, &\text{(D.21)}\end{aligned}$$

whose expansion in powers of pion fields yield the following terms:

$$\hat{\chi}_+\langle u\cdot u\rangle$$
$$\rightsquigarrow\quad 4\bar{p}_0\frac{\vec{\pi}\cdot\vec{\tau}}{F_\pi}\left(\frac{\partial_\mu\vec{\pi}\cdot\partial^\mu\vec{\pi}}{F_\pi^2}+e^2A^\mu A_\mu\frac{\pi^2}{F_\pi^2}-2eA^\mu\frac{(\vec{\pi}\times\partial_\mu\vec{\pi})_3}{F_\pi^2}\right), \tag{D.22}$$

$$\hat{\chi}_+\langle(v\cdot u)^2\rangle$$
$$\rightsquigarrow\quad 4\bar{p}_0\frac{\vec{\pi}\cdot\vec{\tau}}{F_\pi}\left(\frac{(\partial_0\vec{\pi})^2}{F_\pi^2}+e^2A_0^2\frac{\pi^2}{F_\pi^2}-2eA_0\frac{(\vec{\pi}\times\partial_0\vec{\pi})_3}{F_\pi^2}\right), \tag{D.23}$$

$$u_\mu\langle\hat{\chi}_+u^\mu\rangle$$
$$\rightsquigarrow\quad 4\bar{p}_0\left(\frac{(\partial_\mu\vec{\pi}\cdot\vec{\tau})\,(\partial^\mu\vec{\pi}\cdot\vec{\pi})}{F_\pi^3}-e\frac{(\vec{\pi}\times\vec{\tau})_3\cdot\vec{\pi}A^\mu(\partial_\mu\vec{\pi})}{F_\pi^3}\right), \tag{D.24}$$

$$v\cdot u\langle\hat{\chi}_+v\cdot u\rangle$$
$$\rightsquigarrow\quad 4\bar{p}_0\left(\frac{(\partial_0\vec{\pi}\cdot\vec{\tau})\,(\partial^0\vec{\pi}\cdot\vec{\pi})}{F_\pi^3}-e\frac{(\vec{\pi}\times\vec{\tau})_3\cdot\vec{\pi}A0(\partial_0\vec{\pi})}{F_\pi^3}\right), \tag{D.25}$$

$$[S^\mu,S^\nu]\langle\hat{\chi}_+[u_\mu,u_\nu]\rangle$$
$$\rightsquigarrow\quad 8i\bar{p}_0[S^\mu,S^\nu]\left(\frac{\vec{\pi}\cdot(\partial_\mu\vec{\pi}\times\partial_\nu\vec{\pi})}{F_\pi^3}+e\frac{\pi_3(A_\nu\vec{\pi}\cdot\partial_\mu\vec{\pi}-A_\mu\vec{\pi}\cdot\partial_\nu\vec{\pi})}{F_\pi^3}\right.$$
$$\left.+e\frac{\pi^2(A_\nu\partial_\mu\pi_3-A_\mu\partial_\nu\pi_3)}{F_\pi^3}\right), \tag{D.26}$$

$$iS^\mu v^\nu[\hat{\chi}_+,h_{\mu\nu}]$$
$$\rightsquigarrow\quad 8\bar{p}_0S^\mu v^\nu\left(\frac{(\vec{\pi}\times\partial_\mu\partial_\nu\vec{\pi})\cdot\vec{\tau}}{F_\pi^2}-e\frac{A_\mu(\vec{\pi}\cdot\partial_\nu\vec{\pi}\tau_3-\partial_\nu\vec{\pi}\cdot\vec{\tau}\pi_3)}{F_\pi^2}\right.$$
$$\left.-e\frac{A_\nu(\vec{\pi}\cdot\partial_\mu\vec{\pi}\tau_3-\partial_\mu\vec{\pi}\cdot\vec{\tau}\pi_3)}{F_\pi^2}-e^2A_\mu A_\nu\frac{(\vec{\pi}\times\vec{\tau})_i(\delta_{i1}\pi_1+\delta_{i2}\pi_2)}{F_\pi^2}\right), \tag{D.27}$$

$$iS^\mu[[\mathcal{D}_\mu,\hat{\chi}_+],v\cdot u]$$
$$\rightsquigarrow\quad 4\bar{p}_0S^\mu\left(i\frac{(\partial_\mu\vec{\pi}\times\partial_0\vec{\pi})\cdot\tau}{F_\pi^3}+eA_0\frac{\partial_\mu\vec{\pi}\cdot\vec{\pi}\tau_3-\vec{\pi}\cdot\vec{\tau}\partial_\mu\pi_3}{F_\pi^3}\right.$$
$$\left.-eA_\mu\frac{\partial_0\vec{\pi}\cdot\vec{\pi}\tau_3-\vec{\pi}\cdot\vec{\tau}\partial_0\pi_3}{F_\pi^3}\right), \tag{D.28}$$

$$[\mathcal{D}_\mu,[\mathcal{D}^\mu,\hat{\chi}_+]]$$
$$\rightsquigarrow\quad 2\bar{p}_0\left(\partial_\mu\partial^\mu\frac{\vec{\pi}\cdot\vec{\tau}}{F_\pi}-eA_\mu\frac{(\partial^\mu\vec{\pi}\times\vec{\tau})_3}{F_\pi}-2e\partial^\mu A_\mu\frac{(\vec{\pi}\times\vec{\tau})_3}{F_\pi}\right.$$
$$\left.+e^2A_\mu A^\mu\frac{(\pi_1+\pi_2)}{F_\pi}\right), \tag{D.29}$$

$$
\begin{aligned}
&\langle\chi_-\rangle[S\cdot u, v\cdot u] \\
&\rightsquigarrow \quad -8\bar{p}_0 S^\mu v^\nu \Bigg(\frac{(\partial_\mu\vec{\pi}\times\partial_\nu\vec{\pi})\cdot\vec{\tau}}{F_\pi^2} + e\frac{(A_\nu\vec{\pi}\cdot\partial_\mu\vec{\pi} - A_\mu\vec{\pi}\cdot\partial_\nu\vec{\pi})\tau_3}{F_\pi^2} \\
&\qquad -e\frac{(A_\nu\partial_\mu\pi_3 - A_\mu\partial_\nu\pi_3)\vec{\pi}\cdot\vec{\tau}}{F_\pi^2}\Bigg), \qquad \text{(D.30)}
\end{aligned}
$$

$$
\begin{aligned}
&iv^\mu v^\nu\langle\chi_-\rangle h_{\mu\nu} \\
&\rightsquigarrow \quad 8\bar{p}_0 v^\mu v^\nu \left(\frac{\partial_\mu\partial_\nu\vec{\pi}\cdot\vec{\tau}}{F_\pi} - e\frac{A_\mu(\partial_\nu\vec{\pi}\times\vec{\tau})_3 + A_\nu(\partial_\mu\vec{\pi}\times\vec{\tau})_3}{F_\pi}\right), \qquad \text{(D.31)}
\end{aligned}
$$

$$
\begin{aligned}
&iu_\mu[\mathcal{D}^\mu, \langle\chi_-\rangle] \\
&\rightsquigarrow \quad 4\bar{p}_0\left(\frac{\partial_\mu\vec{\pi}\cdot\vec{\tau}\vec{\pi}\cdot\partial\mu\vec{\pi}}{F_\pi^3} - eA_\mu\frac{(\vec{\pi}\times\vec{\tau})_3\vec{\pi}\cdot\partial^\mu\vec{\pi}}{F_\pi^3}\right), \qquad \text{(D.32)}
\end{aligned}
$$

and

$$
\begin{aligned}
\langle\hat{\chi}_+\hat{\chi}_+\rangle &\rightsquigarrow 16\bar{s}_3\bar{p}_0\frac{\pi_3}{F_\pi}\left(1-\frac{2\pi^2}{3F_\pi^2}\right), && \text{(D.33)}\\
i[S^\mu,S^\nu]\langle f^+_{\mu\nu}\rangle\hat{\chi}_+ &\rightsquigarrow -i4\bar{p}_0 e[S^\mu,S^\nu]F_{\mu\nu}\frac{\vec{\pi}\cdot\vec{\tau}}{F_\pi}\left(1-\frac{\pi^2}{6F_\pi^2}\right), && \text{(D.34)}\\
i[S^\mu,S^\nu]\langle \hat{f}^+_{\mu\nu}\hat{\chi}_+\rangle &\rightsquigarrow -i4\bar{p}_0 e[S^\mu,S^\nu]F_{\mu\nu}\frac{\pi_3}{F_\pi}\left(1-\frac{\pi^2}{6F_\pi^2}\right), && \text{(D.35)}\\
iS^\mu v^\nu[\hat{f}^-_{\mu\nu},\hat{\chi}_+] &\rightsquigarrow -4\bar{p}_0 e S^\mu v^\nu F_{\mu\nu}\frac{\pi_3\vec{\pi}\cdot\vec{\tau}-\pi^2\tau_3}{F_\pi^2}, && \text{(D.36)}\\
S^\mu v^\nu\langle f^+_{\mu\nu}\rangle\langle i\chi_-\rangle &\rightsquigarrow 8\bar{p}_0 e S^\mu v^\nu F_{\mu\nu}\left(1-\frac{\pi^2}{2F_\pi^2}\right), && \text{(D.37)}\\
S^\mu v^\nu \hat{f}^+_{\mu\nu}\langle i\chi_-\rangle &\rightsquigarrow 4\bar{p}_0 e S^\mu v^\nu F_{\mu\nu}\left(\tau_3+\frac{\vec{\pi}\cdot\vec{\tau}\pi_3-2\pi^2\tau_3}{2F_\pi^2}\right). && \text{(D.38)}
\end{aligned}
$$

Terms proportional to $\bar{p}_3$ are contained in the Lagrangian

$$
\begin{aligned}
\bar{\mathcal{L}}^{(4)3}_{\pi N} = \; & N^\dagger\big(e_{19}\langle\chi_+\rangle\langle u\cdot u\rangle + e_{20}\langle\chi_+\rangle\langle(v\cdot u)^2\rangle + e_{21}[S^\mu,S^\nu]\langle\chi_+\rangle[u_\mu,u_\nu] \\
& + e_{22}[\mathcal{D}_\mu,[\mathcal{D}^\mu,\langle\chi_+\rangle]] + e_{34}\langle\hat{\chi}_-[S\cdot u, v\cdot u]\rangle + e_{35}v^\mu v^\nu\langle\hat{\chi}_- h_{\mu\nu}\rangle \\
& + e_{36}i\langle u_\mu[\mathcal{D}^\mu,\hat{\chi}_-]\rangle + e_{37}i[S^\mu,S^\nu][u_\mu,[\mathcal{D}_\nu,\hat{\chi}_-]] + e_{38}\langle\chi_+\rangle\langle\chi_+\rangle \\
& + e_{105}i[S^\mu,S^\nu]\langle f^+_{\mu\nu}\rangle\langle\chi_+\rangle + e_{106}i[S^\mu,S^\nu]\hat{f}^+_{\mu\nu}\langle\chi_+\rangle + e_{112}iS^\mu v^\nu\langle f^+_{\mu\nu}\rangle\hat{\chi}_- \\
& + e_{113}iS^\mu v^\nu\langle\hat{f}^+_{\mu\nu}\hat{\chi}_-\rangle + e_{114}i[S^\mu,S^\nu][f^-_{\mu\nu},\hat{\chi}_-]\big)N, \qquad \text{(D.39)}
\end{aligned}
$$

whose expansion in powers of pion fields gives the P- and T-violating terms

$$\begin{aligned}
&\langle\chi_+\rangle\langle u\cdot u\rangle \\
&\rightsquigarrow\ 8\bar{p}_3\left(\frac{\pi_3\partial_\mu\vec{\pi}\cdot\partial^\mu\vec{\pi}}{F_\pi^3}+e^2A^\mu A_\mu\frac{\pi^2\pi_3}{F_\pi^3}-2ieA^\mu\frac{(\vec{\pi}\times\partial_\mu\vec{\pi})_3\pi_3}{F_\pi^3}\right),
\end{aligned} \tag{D.40}$$

$$\begin{aligned}
&\langle\chi_+\rangle\langle(v\cdot u)^2\rangle \\
&\rightsquigarrow\ 8\bar{p}_3\left(\frac{\pi_3(\partial_0\vec{\pi})^2}{F_\pi^3}+e^2A_0^2\frac{\pi^2\pi_3}{F_\pi^2}-2ieA_0\frac{(\vec{\pi}\times\partial_0\vec{\pi})_3\pi_3}{F_\pi^2}\right),
\end{aligned} \tag{D.41}$$

$$\begin{aligned}
&[S^\mu,S^\nu][u_\mu,u_\nu]\langle\chi_+\rangle \\
&\rightsquigarrow\ 8i\bar{p}_3[S^\mu,S^\nu]\left(\frac{(\partial_\mu\vec{\pi}\times\partial_\nu\vec{\pi})\cdot\vec{\tau}\pi_3}{F_\pi^3}+e\frac{(A_\mu\vec{\pi}\cdot\partial_\nu\vec{\pi}-A_\nu\vec{\pi}\cdot\partial_\mu\vec{\pi})\pi_3\tau_3}{F_\pi^3}\right. \\
&\qquad\left.-e\frac{(A_\mu\partial_\nu\pi_3-A_\nu\partial_\nu\pi_3)\vec{\pi}\cdot\vec{\tau}\tau_3}{F_\pi^3}\right),
\end{aligned} \tag{D.42}$$

$$\begin{aligned}
&[\mathcal{D}_\mu,[\mathcal{D}^\mu,\langle\chi_+\rangle] \\
&\rightsquigarrow\ 4\bar{p}_3\partial_\mu\partial^\mu\left[\frac{\pi_3}{F_\pi}\left(1-\frac{\pi^2}{6F_\pi^2}\right)\right],
\end{aligned} \tag{D.43}$$

$$\begin{aligned}
&\langle\hat{\chi}_-[S\cdot u,v\cdot u]\rangle \\
&\rightsquigarrow\ -8\bar{p}_3S^\mu v^\nu\left(\frac{(\partial_\mu\vec{\pi}\times\partial_\nu\vec{\pi})_3}{F_\pi^2}+e\frac{(A_\nu\vec{\pi}\cdot\partial_\mu\vec{\pi}-A_\mu\vec{\pi}\cdot\partial_\nu\vec{\pi})}{F_\pi^2}\right. \\
&\qquad\left.-e\frac{(A_\nu\partial_\mu\pi_3-A_\mu\partial_\nu\pi_3)\pi_3}{F_\pi^2}\right),
\end{aligned} \tag{D.44}$$

$$\begin{aligned}
&iv^\mu v^\nu\langle\hat{\chi}_-h_{\mu\nu}\rangle \\
&\rightsquigarrow\ 8\bar{p}_3v^\mu v^\nu\frac{\partial_\mu\partial_\nu\pi_3}{F_\pi},
\end{aligned} \tag{D.45}$$

$$\begin{aligned}
&i\langle u_\mu[\mathcal{D}^\mu,\hat{\chi}_-]\rangle \\
&\rightsquigarrow\ -4\bar{p}_3\left(\frac{\partial_\mu\vec{\pi}\cdot\partial^\mu\vec{\pi}\,\pi_3}{F_\pi^3}-eA_\mu\frac{(\vec{\pi}\times\partial^\mu\vec{\pi})_3\pi_3}{F_\pi^3}+eA_\mu A^\mu\frac{(\pi_1^2+\pi_2^2)\pi_3}{F_\pi^2}\right),
\end{aligned} \tag{D.46}$$

$$\begin{aligned}
&i[S^\mu,S^\nu][u_\mu,[\mathcal{D}_\nu,\hat{\chi}_-]] \\
&\rightsquigarrow\ -i4\bar{p}_3[S^\mu,S^\nu]\left(\frac{(\partial_\mu\vec{\pi}\times\partial_\nu\vec{\pi})\cdot\vec{\tau}\pi_3}{F_\pi^3}-2eA_\nu\frac{\partial_\mu\vec{\pi}\cdot\vec{\pi}\tau_3-\partial_\mu\pi_3\vec{\pi}\cdot\vec{\tau}}{F_\pi^3}\right),
\end{aligned} \tag{D.47}$$

and

$$\langle\chi_+\rangle\langle\chi_+\rangle \rightsquigarrow 32\bar{s}_0\bar{p}_3\frac{\pi_3}{F_\pi}\left(1-\frac{2\pi^2}{3F_\pi^2}\right) \tag{D.48}$$

$$i[S^\mu,S^\nu]\langle f^+_{\mu\nu}\rangle\langle\chi_+\rangle \rightsquigarrow -i8\bar{p}_3 e[S^\mu,S^\nu]F_{\mu\nu}\frac{\pi_3}{F_\pi}\left(1-\frac{\pi^2}{6F_\pi^2}\right), \tag{D.49}$$

$$i[S^\mu,S^\nu]\hat{f}^+_{\mu\nu}\langle\chi_+\rangle \rightsquigarrow -i4\bar{p}_3 e[S^\mu,S^\nu]F_{\mu\nu}\left(\frac{\pi_3\tau_3}{F_\pi}+\frac{3\pi^2\vec{\pi}\cdot\vec{\tau}-4\pi^2\pi_3\tau_3}{6F_\pi^3}\right), \tag{D.50}$$

$$S^\mu v^\nu\langle f^+_{\mu\nu}\rangle i\hat{\chi}_- \rightsquigarrow 4\bar{p}_3 eS^\mu v^\nu F_{\mu\nu}\left(\tau_3-\frac{\vec{\tau}\cdot\vec{\pi}\pi_3}{2F_\pi^2}\right), \tag{D.51}$$

$$S^\mu v^\nu\langle \hat{f}^+_{\mu\nu} i\hat{\chi}_-\rangle \rightsquigarrow 4\bar{p}_3 eS^\mu v^\nu F_{\mu\nu}\left(1-\frac{\pi^2}{2F_\pi^2}\right), \tag{D.52}$$

$$[S^\mu,S^\nu][f^-_{\mu\nu},i\hat{\chi}_-] \rightsquigarrow 4i\bar{p}_3 e[S^\mu,S^\nu]F_{\mu\nu}\left(\frac{\pi_1\tau_1+\pi_2\tau_2}{F_\pi}+\frac{\pi^2\pi_3\tau_3-\pi_3^2\vec{\pi}\cdot\vec{\tau}}{2F_\pi^3}\right). \tag{D.53}$$

Finally, terms proportional to $\bar{p}_0$ to $\bar{p}_3$ are included in the Lagrangian

$$\bar{\mathcal{L}}^{(4)03}_{\pi N} = N^\dagger\big(e_{39}\hat{\chi}_+\langle\chi_+\rangle + e_{41}\hat{\chi}_-\langle\chi_-\rangle\big)N\,. \tag{D.54}$$

The expansion in powers of pion fields of the terms in this Lagrangian yields at leading orders

$$\hat{\chi}_+\langle\chi_+\rangle \rightsquigarrow 8\bar{s}_0\bar{p}_0\frac{\vec{\pi}\cdot\vec{\tau}}{F_\pi}\left(1-\frac{2\pi^2}{3F_\pi^2}\right)+8\bar{s}_3\bar{p}_3\frac{\pi_3}{F_\pi}\left(\tau_3-\frac{\vec{\pi}\cdot\vec{\tau}\pi_3}{2F_\pi^2}-\frac{\pi^2\tau_3}{6F_\pi^2}\right), \tag{D.55}$$

$$\hat{\chi}_-\langle\chi_-\rangle \rightsquigarrow 8\bar{s}_0\bar{p}_0\frac{\vec{\pi}\cdot\vec{\tau}}{F_\pi}\left(1-\frac{2\pi^2}{3F_\pi^2}\right)+8\bar{s}_3\bar{p}_3\frac{\pi_3}{F_\pi}\left(\tau_3-\frac{\vec{\pi}\cdot\vec{\tau}\pi_3}{2F_\pi^2}-\frac{\pi^2\tau_3}{6F_\pi^2}\right). \tag{D.56}$$

Only a fraction of the P- and T-violating terms presented above are relevant for computation of the EDMs of light nuclei. The power counting of of a particular EDM contribution from each of the above vertices has to be discussed separately. However, terms containing two photon fields generate highly suppressed contributions, since one photon has to be integrated out giving a loop factor of $\alpha_{em}/(4\pi)$.

Appendix E

Fundamental integrals

This appendix provides the list of some master integrals in the analytic computation of the nuclear contributions to the deuteron EDM in section 5.2. As usual, divergences are absorbed into the quantity

$$L := \frac{\mu^{4-d}}{16\pi^2}\left\{\frac{1}{d-4} + \frac{1}{2}[\gamma_E - 1 - \ln(4\pi)]\right\}, \tag{E.1}$$

where the scale μ is introduced in dimensional regularization and $\gamma_E = 0.577215...$ is the Euler-Mascheroni constant. The integrals below are calculated for

$$M_\pi^2 + z(z-1)k^2 - z^2(k\cdot v)^2 > 0\,, \quad k\cdot v = 0 + \cdots\,. \tag{E.2}$$

Expression proportional to v^μ, $v^\mu v^\nu$, etc. are disregarded since they would vanish upon contraction with S_μ, $S_\mu S_\nu$, etc. The zero-components of nucleon momenta are also disregarded since they are considered to yield subleading contributions. Furthermore, the definition $\xi := |\vec{k}|^2/(4M_\pi^2)$ will be utilized below. The integrals I_{00}, I_{10} , I_{12} already appear in [58]. The solution of the integral I_{11} has already been presented in [78].

1:

$$\begin{aligned} I_{00} &= \int \frac{d^4l}{(2\pi)^4}\frac{1}{[v\cdot l + i\epsilon][l^2 - M_\pi^2 + i\epsilon][(l+k)^2 - M_\pi^2 + i\epsilon]} \\ &= -i\frac{1}{8\pi}\frac{\operatorname{arccot}(2M_\pi/|\vec{k}|)}{|\vec{k}|} + \cdots\,, \end{aligned} \tag{E.3}$$

2:

$$\begin{aligned} I_{10} &= \int \frac{d^4l}{(2\pi)^4}\frac{1}{[v\cdot l + i\epsilon]^2[l^2 - M_\pi^2 + i\epsilon][(l+k)^2 - M_\pi^2 + i\epsilon]} \\ &= \frac{i}{8\pi^2}\int_0^1 dz \frac{1}{[M_\pi^2 + z(z-1)k^2 - i\epsilon]} && \text{(E.4)} \\ &= -\frac{1}{4\pi^2}\ln\left(\frac{\sqrt{1+\xi}+\sqrt{\xi}}{\sqrt{1+\xi}-\sqrt{\xi}}\right)\frac{1}{4M_\pi^2\sqrt{\xi}\sqrt{1+\xi}} + \cdots\,, && \text{(E.5)} \end{aligned}$$

3:

$$
\begin{aligned}
I_{11} &= \int \frac{d^d l}{(2\pi)^4} \frac{\mu^{4-d}}{[l^2 - M_\pi^2 + i\epsilon][(l+k)^2 - M_\pi^2 + i\epsilon]} \\
&= -i2L + i\frac{1}{16\pi^2}\left[\ln\left(\frac{\mu^2}{M_\pi^2}\right) - 1\right] - \frac{i}{16\pi^2}\int_0^1 dz \ln\left(\frac{z(z-1)k^2}{M_\pi^2} + 1 - i\epsilon\right) \\
&= -i2L + i\frac{1}{16\pi^2}\left[\ln\left(\frac{\mu^2}{M_\pi^2}\right) - 1\right] \\
&\quad -\frac{i}{16\pi^2}\left(\frac{\sqrt{1+\xi}}{\sqrt{\xi}}\ln\left(\frac{\sqrt{1+\xi}+\sqrt{\xi}}{\sqrt{1+\xi}-\sqrt{\xi}}\right) - 2\right) + \cdots\,, \qquad \text{(E.6)}
\end{aligned}
$$

4:

$$
\begin{aligned}
I_{12} &= \int \frac{d^d l}{(2\pi)^4} \frac{-i\mu^{4-d}}{[v\cdot l + i\epsilon]^2[l^2 - M_\pi^2 + i\epsilon]} \\
&= 4L - \frac{1}{8\pi^2}\left[\ln\left(\frac{\mu^2}{M_\pi^2}\right) - 1\right] + \cdots\,, \qquad \text{(E.7)}
\end{aligned}
$$

5:

$$
\begin{aligned}
I_{20} &= \int \frac{d^4 l}{(2\pi)^4} \frac{i}{[v\cdot l + i\epsilon]^3[l^2 - M_\pi^2 + i\epsilon][(l+k)^2 - M_\pi^2 + i\epsilon]} \\
&= \frac{1}{32\pi}\int_0^1 dz \frac{1}{[z(z-1)k^2 + M_\pi^2 - i\epsilon]^{3/2}} \qquad \text{(E.8)} \\
&= \frac{1}{8\pi}\frac{1}{M_\pi^3(1+\xi)} + \cdots\,, \qquad \text{(E.9)}
\end{aligned}
$$

6:

$$
\begin{aligned}
I_{21} &= \int \frac{d^4 l}{(2\pi)^4} \frac{1}{[v\cdot l + i\epsilon]^3[l^2 - M_\pi^2 + i\epsilon]} \\
&= \frac{i}{16\pi}\frac{1}{M_\pi}\,. \qquad \text{(E.10)}
\end{aligned}
$$

These scalar integrals emerge also in the solutions of the following tensorial integrals:
1:

$$
\begin{aligned}
&\int \frac{d^4 l}{(2\pi)^4} \frac{l^\mu}{[v\cdot l + i\epsilon]^2[l^2 - M_\pi^2 + i\epsilon][(l+k)^2 - M_\pi^2 + i\epsilon]}\,, \\
&= C_1^{(1)} k^\mu + \cdots\,, \qquad \text{(E.11)} \\
C_1^{(1)} &= -\frac{I_{10}}{2}\,, \qquad \text{(E.12)}
\end{aligned}
$$

2:

$$\int \frac{d^4l}{(2\pi)^4} \frac{l^\mu l^\nu}{[v\cdot l+i\epsilon]^2[l^2-M_\pi^2+i\epsilon][(l+k)^2-M_\pi^2+i\epsilon]}$$

$$= C_1^{(2)} k^\mu k^\nu + C_2^{(2)} k^2 g^{\mu\nu} + \cdots\,, \tag{E.13}$$

$$C_1^{(2)} = \frac{1}{2k^2}\left[\frac{iI_{12}}{2} - \left(1-\frac{3k^2}{4M_\pi^2}\right)M_\pi^2 I_{10} + I_{11}\right]\,, \tag{E.14}$$

$$C_2^{(2)} = \frac{1}{2k^2}\left[\frac{iI_{12}}{2} + \left(1-\frac{k^2}{4M_\pi^2}\right)M_\pi^2 I_{10} - I_{11}\right]\,, \tag{E.15}$$

3:

$$\int \frac{d^4l}{(2\pi)^4} \frac{l^\mu l^\nu l^\rho}{[v\cdot l+i\epsilon]^2[l^2-M_\pi^2+i\epsilon][(l+k)^2-M_\pi^2+i\epsilon]}$$

$$= C_1^{(3)} k^\mu k^\nu k^\rho + C_2^{(3)}(k^\mu g^{\nu\rho} + k^\nu g^{\mu\rho} + k^\rho g^{\mu\nu}) + \cdots\,, \tag{E.16}$$

$$C_1^{(3)} = \frac{1}{k^2}\left[-\frac{3iI_{12}}{8} + \left(1-\frac{5}{3}\frac{k^2}{4M_\pi^2}\right)\frac{3}{4}M_\pi^2 I_{10} - \frac{3I_{11}}{4}\right]\,, \tag{E.17}$$

$$C_2^{(3)} = \left[-\frac{iI_{12}}{8} - \left(1-\frac{k^2}{4M_\pi^2}\right)\frac{3}{12}M_\pi^2 I_{10} + \frac{3I_{11}}{12}\right]\,, \tag{E.18}$$

4:

$$\int \frac{d^4l}{(2\pi)^4} \frac{l^\mu}{[v\cdot l+i\epsilon]^3[l^2-M_\pi^2+i\epsilon][(l+k)^2-M_\pi^2+i\epsilon]}$$

$$= D_1^{(1)} k^\mu + \cdots\,, \tag{E.19}$$

$$D_1^{(1)} = i\frac{I_{20}}{2}\,, \tag{E.20}$$

5:

$$\int \frac{d^4l}{(2\pi)^4} \frac{l^\mu l^\nu}{[v\cdot l+i\epsilon]^3[l^2-M_\pi^2+i\epsilon][(l+k)^2-M_\pi^2+i\epsilon]}$$

$$= D_1^{(2)} k^\mu k^\nu + D_2^{(2)} k^2 g^{\mu\nu} \cdots\,, \tag{E.21}$$

$$D_1^{(2)} = \frac{1}{2k^2}\left[\frac{I_{21}}{2} + \left(1-\frac{3k^2}{4M_\pi^2}\right)M_\pi^2 iI_{20} + iI_{00}\right]\,, \tag{E.22}$$

$$D_2^{(2)} = \frac{1}{2k^2}\left[\frac{I_{21}}{2} - \left(1-\frac{k^2}{4M_\pi^2}\right)M_\pi^2 iI_{20} - iI_{00}\right]\,. \tag{E.23}$$

Appendix F

NN- and $3N$-Operators

This appendix is concerned with the matrix elements of the P- and T-violating potential operators and the leading order current operator in systems consisting of two and three nucleons, which are used in the numerical computation of the EDMs of the ^{2}H-, ^{3}He- and ^{3}H-nucleus. The conventions for reduced matrix elements, $9j$-symbols and spherical harmonics and Jacobi coordinates are those adopted in [146].

F.1 NN Operators

The two-nucleon (NN) system is defined by the total momentum and the relative momentum of the two nucleons,

$$\vec{P} = \vec{k}_1 + \vec{k}_2 \,, \tag{F.1}$$

$$\vec{p} = \frac{1}{2}(\vec{k}_1 - \vec{k}_2) \,, \tag{F.2}$$

the total spin s with its z-component m_s and the total isospin i with its z-component m_i. The NN system may equally be defined in terms of angular momentum eigenfunctions with quantum number l, which couples with the total spin s to a total angular momentum j and its z-component m. A state in this basis is defined by the absolute value of the relative momentum of the two nucleons, the total momentum of the NN system and the set of quantum numbers $\{l, s, j, m, i, m_i\}$.

An NN interaction such as the one-pion exchange conserves in general the total momentum of the NN system, the total angular momentum j and its third component m of the NN system and the isospin z-component m_i of the NN system, whereas all other quantum numbers as well as the absolute value of the relative momentum may be subject to change. The matrix element in the above defined basis of the spin-changing and isospin-conserving potential operator (equivalent to eq. (5.7))

$$\tilde{V}_\pi^{(0)} = i\frac{G_\pi^{(0)}}{2m_N}\frac{(\vec{p}-\vec{p}')\cdot(\vec{\sigma}_{(1)}-\vec{\sigma}_{(2)})}{(\vec{p}-\vec{p}')^2+M_\pi^2}\vec{\tau}_{(1)}\cdot\vec{\tau}_{(2)}\,, \tag{F.3}$$

where $G_\pi^{(0)}$ is defined by $G_\pi^{(0)} = g_0 m_N g_A/F_\pi$, proves to be after a lengthy computation:

$$\begin{aligned}
&\langle p';(l's')j',m';i',m_i'|\tilde{V}_\pi^{(0)}|p;(ls)j,m;i,m_i\rangle = \\
&+i\frac{G_\pi^{(0)}}{m_N}\sum_{\lambda_1+\lambda_2=1}\sum_{k=0}^{\infty}324\sqrt{2}(-1)^{k+l'}\pi g_k(p,p')(p')^{\lambda_1}(-p)^{\lambda_2}(2k+1)^{3/2} \\
&\times\sqrt{\frac{(2\lambda_1+1)(2\lambda_2+1)}{(2\lambda_1+1)!(2\lambda_2+1)!}}\sqrt{(2s+1)(2s'+1)(2j+1)(2i+1)} \\
&\times C(k,0,\lambda_1,0,l',0)C(k,0,\lambda_2,0,l,0)C(j,m,0,0,j',m')C(i,m_i,0,0,i',m_i') \\
&\times\begin{Bmatrix} k & k & 0 \\ \lambda_1 & \lambda_2 & 1 \\ l' & l & 1\end{Bmatrix}\begin{Bmatrix} l' & l & 1 \\ s' & s & 1 \\ j' & j & 0\end{Bmatrix}\left(\begin{Bmatrix} 1/2 & 1/2 & 1 \\ 1/2 & 1/2 & 0 \\ s' & s & 1\end{Bmatrix} - \begin{Bmatrix} 1/2 & 1/2 & 0 \\ 1/2 & 1/2 & 1 \\ s' & s & 1\end{Bmatrix}\right) \\
&\times\begin{Bmatrix} 1/2 & 1/2 & 1 \\ 1/2 & 1/2 & 1 \\ i' & i & 0\end{Bmatrix}.
\end{aligned} \tag{F.4}$$

Here p and p' denote the absolute values of the relative momenta of the initial and final NN system. The function $g_k(p,p')$ is the projection of the denominator of the pion propagator onto the Legendre polynomial $P_k(\cos\theta)$ with the normalization

$$\int_{-1}^{+1} d\cos\theta P_i(\cos\theta)P_j(\cos\theta) = \frac{2\delta_{ij}}{2i+1}\,, \tag{F.5}$$

which is given by

$$g_k(p,p') := \int_{-1}^{+1} d\cos\theta\frac{P_k(\cos\theta)}{p^2+p'^2-2\,pp'\cos\theta+M_\pi^2}\,. \tag{F.6}$$

The functions $C(j_1,m_1,j_2,m_2,j,m)$ denote Clebsch-Gordan coefficients for two particles with angular momentum quantum numbers (j_1,m_1) and (j_2,m_2) coupling to a total angular momentum (j,m). The 9j-symbols in eq. (F.4) are defined by

$$\begin{aligned}
&\sqrt{(2j_{12}+1)(2j_{34}+1)(2j_{13}+1)(2j_{24}+1)}\begin{Bmatrix} j_1 & j_2 & j_{12} \\ j_3 & j_4 & j_{34} \\ j_{13} & j_{24} & j\end{Bmatrix} \\
= \;& \langle((j_1j_2)j_{12},(j_3j_4)j_{34})j|((j_1j_3)j_{13}(j_2j_4)j_{24})j\rangle\,.
\end{aligned} \tag{F.7}$$

In the derivation of eq. (F.4), the identity

$$\begin{aligned}&\langle (l's')j'||\{A^a \otimes B^b\}^c||(ls)j\rangle \\ = \quad &\sqrt{(2l'+1)(2s'+1)(2j+1)(2c+1)} \begin{Bmatrix} l' & l & a \\ s' & s & b \\ j' & j & c \end{Bmatrix} \langle l'||A^a||l\rangle\langle s'||B^b||s\rangle \,,\end{aligned} \tag{F.8}$$

has been exploited, which relates the reduced matrix element of a tensor product of two spherical tensors A and B of ranks a and b, respectively, to yield a spherical tensor of rank c to the reduced matrix elements of the single tensors A and B.

The matrix element of the isospin-1 potential operator (equivalent to eq. (5.8))

$$\tilde{V}_\pi^{(1)} = i\frac{G_\pi^{(1)}}{4m_N}\frac{(\vec{p}-\vec{p}\,')^i}{(\vec{p}-\vec{p}\,')^2+M_\pi^2}\left[(\sigma^i_{(1)}+\sigma^i_{(2)})(\tau^3_{(1)}-\tau^3_{(2)})+(\sigma^i_{(1)}-\sigma^i_{(2)})(\tau^3_{(1)}+\tau^3_{(2)})\right] \,, \tag{F.9}$$

$G_\pi^{(1)} = g_1 m_N g_A/F_\pi$, which is comprised of two components that either conserve the total spin and change the total isospin or change the total spin and conserve the total isospin of the NN system, reads

$$\begin{aligned}&\langle p';(l's')j',m';i',m_i'|\tilde{V}_\pi^{(1)}|p;(ls)j,m;i,m_i\rangle = \\ &-i\frac{G_\pi^{(1)}}{m_N}\sum_{\lambda_1+\lambda_2=1}\sum_{k=0}^{\infty} 54\sqrt{6}(-1)^{k+l'}\pi g_k(p,p')(p')^{\lambda_1}(-p)^{\lambda_2}(2k+1)^{3/2} \\ &\times\sqrt{\frac{(2\lambda_1+1)(2\lambda_2+1)}{(2\lambda_1+1)!(2\lambda_2+1)!}}\sqrt{(2s+1)(2s'+1)(2j+1)(2i+1)} \\ &\times C(k,0,\lambda_1,0,l',0)C(k,0,\lambda_2,0,l,0)C(j,m,0,0,j',m')C(i,m_i,1,0,i',m_i') \\ &\times\begin{Bmatrix} k & k & 0 \\ \lambda_1 & \lambda_2 & 1 \\ l' & l & 1 \end{Bmatrix}\begin{Bmatrix} l' & l & 1 \\ s' & s & 1 \\ j' & j & 0 \end{Bmatrix} \\ &\times\Bigg[\left(\begin{Bmatrix} 1/2 & 1/2 & 1 \\ 1/2 & 1/2 & 0 \\ s' & s & 1 \end{Bmatrix}+\begin{Bmatrix} 1/2 & 1/2 & 0 \\ 1/2 & 1/2 & 1 \\ s' & s & 1 \end{Bmatrix}\right)\left(\begin{Bmatrix} 1/2 & 1/2 & 1 \\ 1/2 & 1/2 & 0 \\ i' & i & 1 \end{Bmatrix}-\begin{Bmatrix} 1/2 & 1/2 & 0 \\ 1/2 & 1/2 & 1 \\ i' & i & 1 \end{Bmatrix}\right) \\ &+\left(\begin{Bmatrix} 1/2 & 1/2 & 1 \\ 1/2 & 1/2 & 0 \\ s' & s & 1 \end{Bmatrix}-\begin{Bmatrix} 1/2 & 1/2 & 0 \\ 1/2 & 1/2 & 1 \\ s' & s & 1 \end{Bmatrix}\right)\left(\begin{Bmatrix} 1/2 & 1/2 & 1 \\ 1/2 & 1/2 & 0 \\ i' & i & 1 \end{Bmatrix}+\begin{Bmatrix} 1/2 & 1/2 & 0 \\ 1/2 & 1/2 & 1 \\ i' & i & 1 \end{Bmatrix}\right)\Bigg] \,,\end{aligned} \tag{F.10}$$

The matrix element of the isospin-2 potential operator

$$\tilde{V}_\pi^{(2)} = i\frac{G_\pi^{(2)}}{2m_N}\frac{(\vec{p}-\vec{p}\,')\cdot(\vec{\sigma}_{(1)}-\vec{\sigma}_{(2)})}{(\vec{p}-\vec{p}\,')^2+M_\pi^2}(3\tau^3_{(1)}\tau^3_{(2)}-\vec{\tau}_{(1)}\cdot\vec{\tau}_{(2)}) \,, \tag{F.11}$$

with $G_\pi^{(2)} = g_2 m_N g_A / F_\pi$ is given by

$$
\begin{aligned}
&\langle p';(l's')j',m';i',m_i'|\tilde{V}_\pi^{(2)}|p;(ls)j,m;i,m_i\rangle = \\
&-i\frac{G_\pi^{(1)}}{m_N}\sum_{\lambda_1+\lambda_2=1}\sum_{k=0}^{\infty}648\sqrt{5}(-1)^{k+l'}\pi g_k(p,p')(p')^{\lambda_1}(-p)^{\lambda_2}(2k+1)^{3/2} \\
&\times\sqrt{\frac{(2\lambda_1+1)(2\lambda_2+1)}{(2\lambda_1+1)!(2\lambda_2+1)!}}\sqrt{(2s+1)(2s'+1)(2j+1)(2i+1)} \\
&\times C(k,0,\lambda_1,0,l',0)C(k,0,\lambda_2,0,l,0)C(j,m,0,0,j',m')C(i,m_i,2,0,i',m_i') \\
&\times\begin{Bmatrix} k & k & 0 \\ \lambda_1 & \lambda_2 & 1 \\ l' & l & 1 \end{Bmatrix}\begin{Bmatrix} l' & l & 1 \\ s' & s & 1 \\ j' & j & 0 \end{Bmatrix}\left(\begin{Bmatrix} 1/2 & 1/2 & 1 \\ 1/2 & 1/2 & 0 \\ s' & s & 1 \end{Bmatrix} - \begin{Bmatrix} 1/2 & 1/2 & 0 \\ 1/2 & 1/2 & 1 \\ s' & s & 1 \end{Bmatrix}\right) \\
&\times\begin{Bmatrix} 1/2 & 1/2 & 1 \\ 1/2 & 1/2 & 1 \\ i' & i & 2 \end{Bmatrix}. \qquad \text{(F.12)}
\end{aligned}
$$

So far only one-pion exchange operators have been considered. The potential operators for heavier mesons, the η, ρ and ω mesons, are apart from the P- and T-conserving and P- and T-violating πNN coupling constants identical up to relative and overall signs. Let g_i^η, g_i^ρ, g_i^ω be the P- and T-violating meson-nucleon coupling constants and $g_{\eta N}$, $g_{\rho N}$, $g_{\omega N}$ the P- and T-conserving meson-nucleon coupling constants with $i = 0, 1, 2$. Furthermore, we define $G_m^{(i)} := g_i^m m_N g_{mN}/F_\pi$ for $i = 0, 1, 2$ and $m = \eta, \rho, \omega$. The leading one-meson exchange potential operators induced by such P- and T-violating meson-nucleon vertices are then given by (see [33] for instance)

$$\tilde{V}_\eta^{(0)} = i\frac{G_\eta^{(0)}}{2m_N}\frac{(\vec{p}-\vec{p}\,')\cdot(\vec{\sigma}_{(1)}-\vec{\sigma}_{(2)})}{(\vec{p}-\vec{p}\,')^2+M_\eta^2}, \qquad \text{(F.13)}$$

$$\tilde{V}_\rho^{(0)} = -i\frac{G_\rho^{(0)}}{2m_N}\frac{(\vec{p}-\vec{p}\,')\cdot(\vec{\sigma}_{(1)}-\vec{\sigma}_{(2)})}{(\vec{p}-\vec{p}\,')^2+M_\rho^2}\vec{\tau}_{(1)}\cdot\vec{\tau_{(2)}}, \qquad \text{(F.14)}$$

$$\tilde{V}_\omega^{(0)} = -i\frac{G_\omega^{(0)}}{2m_N}\frac{(\vec{p}-\vec{p}\,')\cdot(\vec{\sigma}_{(1)}-\vec{\sigma}_{(2)})}{(\vec{p}-\vec{p}\,')^2+M_\omega^2}, \qquad \text{(F.15)}$$

for g_0-type ηNN-, ρNN- and ωNN vertices,

$$\tilde{V}_\eta^{(1)} = i\frac{G_\eta^{(1)}}{4m_N}\frac{(\vec{p}\,'-\vec{p})^i}{(\vec{p}-\vec{p}\,')^2+M_\eta^2}\left[(\sigma^i_{(1)}+\sigma^i_{(2)})(\tau^3_{(1)}-\tau^3_{(2)})-(\sigma^i_{(1)}-\sigma^i_{(2)})(\tau^3_{(1)}+\tau^3_{(2)})\right] , \tag{F.16}$$

$$\tilde{V}_\rho^{(1)} = i\frac{G_\rho^{(1)}}{4m_N}\frac{(\vec{p}\,'-\vec{p})^i}{(\vec{p}-\vec{p}\,')^2+M_\rho^2}\left[(\sigma^i_{(1)}+\sigma^i_{(2)})(\tau^3_{(1)}-\tau^3_{(2)})-(\sigma^i_{(1)}-\sigma^i_{(2)})(\tau^3_{(1)}+\tau^3_{(2)})\right] , \tag{F.17}$$

$$\tilde{V}_\omega^{(1)} = -i\frac{G_\omega^{(1)}}{4m_N}\frac{(\vec{p}\,'-\vec{p})^i}{(\vec{p}-\vec{p}\,')^2+M_\omega^2}\left[(\sigma^i_{(1)}+\sigma^i_{(2)})(\tau^3_{(1)}-\tau^3_{(2)})+(\sigma^i_{(1)}-\sigma^i_{(2)})(\tau^3_{(1)}+\tau^3_{(2)})\right] , \tag{F.18}$$

for g_1-type ηNN-, ρNN- and ωNN- and

$$\tilde{V}_\rho^{(2)} = -i\frac{G_\rho^{(2)}}{2m_N}\frac{(\vec{p}-\vec{p}\,')\cdot(\vec{\sigma}_{(1)}-\vec{\sigma}_{(2)})}{(\vec{p}-\vec{p}\,')^2+M_\rho^2}(3\tau^3_{(1)}\tau^3_{(2)}-\vec{\tau}_{(1)}\cdot\vec{\tau}_{(2)}) , \tag{F.19}$$

for the g_2-type ρNN vertex. The partial wave decompositions of these potential operators can be readily obtained from the decompositions of one-pion exchange potential operators with the same type of P- and T-violating πNN vertex.

The operator $\mathcal{O}(q)$ describing the emission of a photon by one nucleon in the NN system shifts the momentum of this nucleon by the photon four-momentum q. Since all EDM calculations are performed in the Breit-frame where $q=(0,\vec{q})$, this operator is a function of the photon three-momentum $\mathcal{O}(\vec{q})$. We assume that the vector $\vec{q}$ points into the direction of the z-axis, i.e. $\vec{q}=q\,\vec{e}_z$, and consider the photon-nucleon coupling at leading order in heavy baryon ChPT, $ie(\mathbb{1}+\tau^3)/2$. Let $\Psi_{^2\mathrm{H}}$ denote the deuteron wave function and $\vec{P}_{in}$ the total momentum of the incoming deuteron state. When the photon couples to one specific nucleon, the transition matrix element of $\mathcal{O}(q)=\mathcal{O}(\vec{q})$ from the sum over all deuteron states with total momentum $\vec{P}_{in}$ to an outgoing NN state defined by the total momentum $\vec{P}^o$, relative momentum p^o and the set of NN quantum numbers

$\{l^o, s^o, j^o, m^o, i^o, m_i^o\}$ proves to be

$$
\begin{aligned}
&\langle p^o, \vec{P}^o; (l^o s^o) j^o, m^o; i^o, m_i^o | \mathcal{O}(\vec{q}) | \Psi_{^2\mathrm{H}}, \vec{P}_{in} \rangle = \\
&ie\pi \sum_{\alpha^I} \sum_{m_l^o=-min(l^I,l^o)}^{min(l^I,l^o)} \sum_{m_s^I} (-1)^{m_l^o} \delta^{(3)}(\vec{P}_{in} - \vec{P}^o - \vec{q})\, \delta_{s^I s^o} \\
&\times C(l^o, m_l^o, s^I, m_s^I, j^o, m^o)\, C(l^I, m_l^I, s^I, m_s^I, j^I, m^I) \\
&\times \left(\int_{-1}^{+1} d\cos\theta\, Y_{l^o,-m_l^o}(\cos\theta, 0) Y_{l^I,m_l^I}(\cos\theta', 0) \Psi_{^2\mathrm{H}}^{\alpha^I}(p') \right) \\
&\times \left(\delta_{i^I i^o} \delta_{m_i^I m_i^o} + 6\sqrt{2i^I+1}\, C(i^I, m_i^I, 1, 0, i^o, m_i^o) \begin{Bmatrix} 1/2 & 1/2 & 1 \\ 1/2 & 1/2 & 1 \\ i^o & i^I & 1 \end{Bmatrix} \right) ,
\end{aligned}
\tag{F.20}
$$

where the angle θ' and the momentum p' are defined by

$$
\cos\theta' := \frac{p^o \cos\theta + 2q/3}{\sqrt{(p^o)^2 + 4\, q\, p^o \cos\theta/3 + 4\, q^2/3}} , \tag{F.21}
$$

$$
p' := \sqrt{(p^o)^2 + 4\, q\, p^o \cos\theta/3 + 4\, q^2/9} . \tag{F.22}
$$

The first summation in eq. (F.20) is over all sets of quantum numbers $\alpha^I = \{l^I, s^I, j^I, m^I, i^I, m_i^I\}$. The application of the transposition operator to the system consisting of the two nucleons labelled by (1) and (2) in order to account for the photon coupling to nucleon (2) simply yields a factor of two.

F.2 $3N$ Operators

The three-nucleon ($3N$) system is most conveniently described by the Jacobi momenta

$$
\vec{p}_{12} = \frac{1}{2}(\vec{k}_1 - \vec{k}_2) , \tag{F.23}
$$

$$
\vec{p}_3 = \frac{2}{3}\vec{k}_3 - \frac{1}{3}(\vec{k}_1 + \vec{k}_2) , \tag{F.24}
$$

$$
\vec{P} = \vec{k}_1 + \vec{k}_2 + \vec{k}_3 , \tag{F.25}
$$

where $\vec{k}_1$, $\vec{k}_2$ and $\vec{k}_3$ are the three-momenta of the three nucleons in the $3N$ system which may be labelled by (1), (2) and (3); $\vec{p}_{12}$ is the relative momentum of nucleons (1) and (2), $\vec{p}_3$ is the relative momentum of the subsystem consisting of nucleons (1) and (2) and the subsystem of nucleon (3) and $\vec{P}$ is the total momentum of the $3N$ system. Alternatively, the $3N$ system can be defined by the absolute values of the relative momenta $\vec{p}_{12}$ and $\vec{p}_3$, the total momentum $\vec{P}$ and the set of quantum numbers $\{l_{12}, s_{12}, j_{12}, l_3, s_3, J, M, i_{12}, i_3, i, m_i\}$. Here l_{12} and s_{12} denote the angular momentum and total spin of the subsystem consisting of nucleons (1) and (2), which couple to a total angular momentum j_{12}. The angular momentum of nucleon (3), l_3, with respect to the nucleon subsystem comprised of the nucleons (1) and (2) and the spin of nucleon (3), s_3, couple to a total angular momentum j_3. These total angular momenta then couple to the total angular momentum J of the $3N$ system with its z-component M. The isospin of the NN subsystem i_{12} couples with the isospin of nucleon (3), i_3, to the total isospin i of the $3N$ system with the z-component m_i.

The matrix elements in this basis of the NN potential operators eq. (F.3), eq. (F.9) and eq. (F.11) are obtained by embedding the NN system in the most convenient way into the $3N$ system. Let the potential operators only affect the NN subsystem of nucleons (1) and (2). The momentum and spin space matrix elements of these potential operators are expressed in terms of the above NN system matrix elements by

$$\begin{aligned}
&\langle p'_{12}, p'_3; ((l'_{12}s'_{12})j'_{12}(l'_3s'_3)j'_3)J', M'|\tilde{V}_m^{(i)}(12)|p_{12}, p_3; ((l_{12}s_{12})j_{12}(l_3s_3)j_3)J, M\rangle \\
&= \sum_{m_{12}=-l_{12}}^{l_{12}} \sum_{m'_{12}=-l'_{12}}^{l'_{12}} \sum_{m_3=-l_3}^{l_3} C(j'_{12}, m'_{12}, j'_3, m_3, J', M')\, C(j_{12}, m_{12}, j_3, m_3, J, M) \\
&\quad \times \langle p'_{12}; (l'_{12}s'_{12})j'_{12}m'_{12}|\tilde{V}_m^{(i)}(12)|p_{12}; (l_{12}s_{12})j_{12}m_{12}\rangle \frac{\delta(p_3 - p'_3)}{(p'_3)^2} \delta_{l_3l'_3}\delta_{j_3j'_3}\delta_{m_3m'_3}\,,
\end{aligned} \tag{F.26}$$

whereas the isospin space matrix elements are given by

$$\begin{aligned}
&\langle (i'_{12}i'_3)i', m'_i|\tilde{V}_m^{(i)}(12)|(i_{12}i_3)i, m_i\rangle \\
&= \sum_{m_{i12}=-i_{12}}^{i_{12}} \sum_{m'_{i12}=-i'_{12}}^{i'_{12}} \sum_{m_{i3}=-i_3}^{i_3} C(i'_{12}, m'_{i12}, i'_3, m_{i3}, i', m'_i)\, C(i_{12}, m_{i12}, i_3, m_{i3}, i, m_i) \\
&\quad \times \langle i'_{12}, m'_{i12}|\tilde{V}_m^{(i)}(12)|i_{12}, m_{i12}\rangle\, \delta_{i_3i'_3}\delta_{m_{i3}m'_{i3}}\,.
\end{aligned} \tag{F.27}$$

The complete matrix elements for the $3N$ system are then obtained by summing over all permutations of the three nucleons.

The operator $\mathcal{O}(\vec{q})$ shifts the (three-)momentum of one of the nucleons of the $3N$ system by $\vec{q}$. We first consider the case when the photon couples to nucleon (3). Let $\Psi_{^3\mathrm{He}}$ denote the ^{3}He wave function, $\vec{P}_{in}$ its total momentum and $\vec{q} = q\vec{e}_z$ the photon momentum in the Breit-frame. The transition matrix element of the operator $\mathcal{O}(\vec{q})$ from sum over all ^{3}He states to an outgoing state defined by p^o_{12}, p^o_3, $\vec{P}^o$ and the set of $3N$ quantum numbers

$\{l_{12}^o, s_{12}^o, j_{12}^o, l_3^o, s_3^o, j_3^o, J^o, M^o, i_{12}^o, i_3^o, i^o, m_i^o\}$ is given by

$$\langle p_{12}^o, p_3^o, \vec{P}^o; ((l_{12}^o s_{12}^o) j_{12}^o (l_3^o s_3^o) j_3^o) J^o, M^o; (i_{12}^o i_3^o) i^o, m_i^o | \mathcal{O}(\vec{q}) | \Psi_{^3He}, \vec{P}_{in} \rangle =$$

$$\begin{aligned}
& ie\pi \sum_{\alpha^I} \delta^{(3)}(\vec{P}_{in} - \vec{P}^o - \vec{q})\, \delta_{s_{12}^I s_{12}^o} \delta_{l_{12}^I l_{12}^o} \delta_{i_{12}^I i_{12}^o} \\
& \times \sum_{l^o} \sum_{l^I} \sum_{s^o} \sum_{m_{12}^o=-l_{12}^o}^{l_{l12}^o} \sum_{m_3^o=-min(l_3^o,l_3^I)}^{min(l_3^o,l_3^I)} (-1)^{m_3^o} \\
& \times C(l_{12}^o, m_{12}^o, l_3^o, m_3^o, l^o, m_{12}^o - m_3^o)\, C(l^o, m_{12}^o + m_3^o, s^o, M^o - m_{12}^o - m_3^o, J^o, M^o) \\
& \times C(l_{12}^o, m_{12}^o, l_3^I, m_3^o, l^I, m_{12}^o - m_3^o)\, C(l^I, m_{12}^o + m_3^o, s^o, M^I - m_{12}^o - m_3^o, J^I, M^I) \\
& \times \begin{Bmatrix} l_{12}^o & s_{12}^o & j_{12}^o \\ l_3^o & s_3^o & j_3^o \\ l^o & s^o & J^o \end{Bmatrix} \begin{Bmatrix} l_{12}^o & s_{12}^o & j_{12}^I \\ l_3^I & s_3^o & j_3^I \\ l^I & s^o & J^I \end{Bmatrix} \\
& \times \sqrt{(2l^I+1)(2l^o+1)(2j_{12}^I+1)(2j_{12}^o+1)(2j_3^I+1)(2j_3^o+1)}\,(2s^o+1) \\
& \times \left(\int_{-1}^{+1} d\cos\theta Y_{l_3^o,-m_3^o}(\cos\theta, 0) Y_{l_3^I,m_3^o}(\cos\theta', 0) \Psi_{^2\mathrm{H}}^{\alpha^I}(p') \right) \\
& \times \left(\delta_{I^o I^I}\, \delta_{I_3^o I_3^I}\, \delta_{i_{12}^o i_{12}^I} + \sqrt{18(2i_{12}^o+1)(2I^I+1)} C(i^I, m_i^I, 1, 0, i^o, m_i^o) \begin{Bmatrix} i_{12}^o & i_{12}^o & 0 \\ 1/2 & 1/2 & 1 \\ i^o & i^I & 1 \end{Bmatrix} \right),
\end{aligned} \tag{F.28}$$

where the angle θ' and the momentum p' are defined by

$$\cos\theta' := \frac{p_3^o \cos\theta + 2q/3}{\sqrt{(p_3^o)^2 + 4\, q\, p_3^o \cos\theta/3 + 4\, q^2/3}}\,, \tag{F.29}$$

$$p' := \sqrt{(p_3^o)^2 + 4\, q\, p_3^o \cos\theta/3 + 4\, q^2/9}\,. \tag{F.30}$$

The first sum is over all sets of $3N$ quantum numbers

$$\alpha^I = \{l_{12}^I, s_{12}^I, j_{12}^I, l_3^I, s_3^I, j_3^I, J^I, M^I, i_{12}^I, i_3^I, i^I, m_i^I\}\,. \tag{F.31}$$

In order to obtain the full $3N$ matrix element taking into account the couplings of the photon to all three nucleons, the sum over all permutations of the nucleons (1), (2) and (3) has to be computed.

Appendix G

Alternative derivations of g_0^θ and g_1^θ

This appendix has been published in [101].

G.1 An update of the derivation of Lebedev *et al.*

This part of the appendix contains an update of the derivation of the P- and T-violating πNN coupling constants g_0^θ and g_1^θ in [26]. In addition to the usual parametrization of the θ-term-induced isospin-conserving and CP-violating πNN coupling

$$g_0^\theta = \frac{m_* \bar{\theta}}{F_\pi} \langle N|\bar{u}u - \bar{d}d|N\rangle \tag{G.1}$$

the authors of ref. [26] introduced — via the π^0–η mixing[1] — the isospin-breaking counter part

$$g_1^\theta = \frac{m_* \bar{\theta}}{F_\pi} \frac{\sqrt{3}(m_d - m_u)}{4(m_s - \hat{m})} \frac{1}{\sqrt{3}} \langle N|\bar{u}u + \bar{d}d - 2\bar{s}s|N\rangle \ . \tag{G.2}$$

This is an alternative derivation of the result for g_1^θ eq. (4.173) obtained from the ground state selection procedure, discussed in section 4.3, because the l_7 coefficient of the fourth-order Lagrangian effectively summarizes the π^0–η mixing by the quark-mass dependent shift to the pion-mass-squared $(\delta M_\pi^2)^{\rm str}$.

Inserting the strong-interaction contribution to the neutron-proton mass difference $(m_u - m_d)\langle N|\bar{u}u - \bar{d}d|N\rangle = \delta m_{np}^{\rm str}$ and utilizing the parameter ϵ as defined

[1] Actually, via the π^0–η_8 mixing. For consistency, we replaced here their π^0-η mixing angle by the customary one of chiral perturbation theory [111] — note the explicit $\hat{m}$ subtraction in the denominator.

Table G.1: The value of g_0^θ, g_1^θ, and the ratio g_1^θ/g_0^θ predicted from eqs. (G.9) and (G.10) with (i) the original SU(3) parameters b_D and b_F of ref. [58], with (ii) the alternative set of parameters based on eqs. (G.13) and (G.14), (iii) in the case that $b_D + b_F$ of (i) are replaced by c_5 of eq. (G.12). The listed uncertainties do not contain systematical SU(3) errors.

		g_0^θ $[\bar\theta]$	g_1^θ $[\bar\theta]$	g_1^θ/g_0^θ
(i)	b_D & b_F from [58]	-0.026 ± 0.002	0.00092 ± 0.00017	-0.036 ± 0.007
(ii)	b_D & b_F alternative	-0.023 ± 0.005	0.00088 ± 0.00016	-0.038 ± 0.011
(iii)	$b_D + b_F \to c_5$	-0.018 ± 0.007	0.00092 ± 0.00017	-0.051 ± 0.022

at the end of sect. 2.2, we derive (4.158) again:

$$g_0^\theta = \frac{\delta m_{np}^{\rm str}(1-\epsilon^2)}{4F_\pi\epsilon}\,\bar\theta\,.$$

Similarly, starting now from eq. (G.2), we get

$$g_1^\theta = -\frac{\bar\theta}{8F_\pi}\,(1-\epsilon^2)\,\epsilon\,\frac{M_\pi^2}{M_K^2-M_\pi^2}\,\hat m\langle N|\bar uu+\bar dd-2\bar ss|N\rangle \tag{G.3}$$

with $M_\pi^2 = 2B\hat m + \mathcal{O}(\mathcal{M}^2)$ and $M_K^2 = B(m_s+\hat m) + \mathcal{O}(\mathcal{M}^2)$ for the square of the pion and kaon mass, respectively, where here $\mathcal{M}$ is the quark mass matrix for three light flavors. According to refs. [105, 147] we have $\hat m\langle N|\bar uu+\bar dd-2\bar ss|N\rangle = \hat m\langle N|\bar uu+\bar dd|N\rangle(1-y)$ with $\sigma_{\pi N} \equiv \sigma_{\pi N}(0) = \hat m\langle p|\bar uu+\bar dd|p\rangle$ and $y \equiv 2\langle p|\bar ss|p\rangle/\langle p|\bar uu+\bar dd|p\rangle$, where $|p\rangle$ denotes here the proton state. The final result is therefore

$$g_1^\theta = -\frac{\bar\theta}{8F_\pi}\,(1-\epsilon^2)\,\epsilon\,\frac{M_\pi^2}{M_K^2-M_\pi^2}\,\sigma_{\pi N}(1-y)\,. \tag{G.4}$$

Inserting $\delta m_{np}^{\rm str} = (2.6\pm0.5)\,\text{MeV}$ from ref. [94], $F_\pi = 92.2\,\text{MeV}$, and the $\overline{MS}$ quark masses at 2 GeV from [34], we get

$$g_0^\theta \approx (-0.018\pm0.007)\,\bar\theta \tag{G.5}$$

and

$$g_1^\theta \approx (0.0012\pm0.0004)\,\bar\theta \tag{G.6}$$

with $\sigma_{\pi N}(0) = 45\,\text{MeV}$ and $y = 0.21\pm0.20$ from [147] as additional input.

Thus we find

$$\frac{g_1^\theta}{g_0^\theta} = -\frac{\epsilon^2}{2}\,\frac{M_\pi^2}{M_K^2-M_\pi^2}\,\frac{\sigma_{\pi N}(0)(1-y)}{\delta m_{np}^{\rm str}} \approx -0.07\pm0.04 \tag{G.7}$$

as the ratio of the isospin-breaking *versus* the isospin-conserving CP-violating πNN coupling constants which are induced by the θ-term. If we rather applied the values $\sigma_{\pi N}(0) = 59(7)\,\mathrm{MeV}$ and $y \approx 0$ from refs. [148, 149] (for an update of this work see ref. [150]), we would get

$$g_1^\theta \approx (0.0021 \pm 0.0004)\,\bar\theta \qquad \text{and} \qquad \frac{g_1^\theta}{g_0^\theta} \approx -0.11 \pm 0.05 \tag{G.8}$$

as values for g_1^θ and the ratio instead. In summary, the ratios listed in (G.7) and (G.8) are compatible with the estimate (4.174).

G.2 Derivation via SU(3) chiral perturbation theory

In SU(3) ChPT the D-type and F-type CP-violating $\pi^0 NN$ coupling constants are (see *e.g.* the U(3) ChPT calculation of ref. [151])

$$g^D_{\pi^0 NN} = \frac{4B\bar\theta m_*}{F_\pi} b_D \qquad \text{and} \qquad g^F_{\pi^0 NN} = \frac{4B\bar\theta m_*}{F_\pi} b_F\,,$$

respectively, whereas

$$g^D_{\eta NN} = \frac{-4B\bar\theta m_*}{F_\pi}\frac{b_D}{\sqrt3} \qquad \text{and} \qquad g^F_{\eta NN} = \frac{4B\bar\theta m_*}{F_\pi}\sqrt3 b_F$$

are the corresponding ηNN (actually $\eta_8 NN$) counter parts. Here $4B\,b_D$ and $4B\,b_F$ are the coefficients of the anticommutator (D-type) and commutator (F-type) term of the quark mass matrix with the baryon matrix. Therefore, the SU(3) counter parts of eqs. (4.158) and (G.4) are [2]

$$g_0^\theta = \frac{4B\bar\theta m_*(b_D+b_F)}{F_\pi} = \bar\theta\frac{M_\pi^2}{F_\pi}(1-\epsilon^2)(b_D+b_F), \tag{G.9}$$

$$\begin{aligned} g_1^\theta &= \frac{4B\bar\theta m_*}{F_\pi}\,\frac{3b_F-b_D}{\sqrt3}\,\frac{\sqrt3}{4}\,\frac{m_d-m_u}{m_s-\hat m} \\ &= \bar\theta\frac{M_\pi^2}{F_\pi}(1-\epsilon^2)\,(3b_F-b_D)\,\frac{\epsilon\,M_\pi^2}{4(M_K^2-M_\pi^2)}\,, \end{aligned} \tag{G.10}$$

where $(\sqrt3/4)(m_d-m_u)/(m_s-\hat m)$ is the π^0-η (actually π^0-η_8) mixing angle. Thus, in this case we get the ratio

$$\frac{g_1^\theta}{g_0^\theta} = \frac{\epsilon\,M_\pi^2}{4(M_K^2-M_\pi^2)}\,\frac{3b_F-b_D}{b_D+b_F}\,. \tag{G.11}$$

[2] The proportionality of g_1^θ to $3b_F-b_D$ may come at first sight as a surprise. The strange-quark content of the nucleon, however, is proportional to $b_0+b_D-b_F$ to leading order in the chiral expansion, such that g_1^θ for small or vanishing y is factually proportional to $2b_0+b_D+b_F$ which in turn is proportional to $2c_1$. For more details see *e.g.* refs. [152, 153].

If the values $b_F = -0.209\,\mathrm{GeV}^{-1}$ and $b_D = 0.066\,\mathrm{GeV}^{-1}$ of ref. [58] are inserted, we get the first row of table G.1. However, there is a mismatch by a factor 1.5 approximately between the SU(3) octet quantity

$$b_D + b_F = -\frac{m_\Xi - m_\Sigma}{4(M_K^2 - M_\pi^2)} \approx (-0.143 \pm 0.004)\,\mathrm{GeV}^{-1}$$

used in [45, 48, 117] and the SU(2) low-energy coefficient (LEC)

$$c_5 = \frac{\delta m_{np}^{\mathrm{str}}}{4M_\pi^2 \epsilon} \approx (-0.097 \pm 0.034)\,\mathrm{GeV}^{-1}\,, \tag{G.12}$$

although according to SU(3) ChPT both quantities should agree to leading order, see eq. (27) of ref. [152][3].

Moreover, an alternative procedure to parametrize the above sum is

$$\begin{aligned} b_D + b_F &= \frac{\delta m_{np}^{\mathrm{str}}}{4(M_{K^+}^2 - (M_{\pi^+}^2 - M_{\pi^0}^2) - M_{K^0}^2)} \\ &\approx (-0.126 \pm 0.024)\,\mathrm{GeV}^{-1}\,, \end{aligned} \tag{G.13}$$

where the electromagnetic mass shifts are removed (via the Dashen theorem [100] in the denominator) and where the prediction falls in-between the original one and the c_5 value. Using an analogous parametrization for b_F, we get

$$b_F = \frac{m_{\Sigma^-} - m_{\Sigma^+}}{8(M_{K^+}^2 - (M_{\pi^+}^2 - M_{\pi^0}^2) - M_{K^0}^2)} \approx -0.196\,\mathrm{GeV}^{-1} \tag{G.14}$$

and $b_D = +(0.069 \pm 0.024)\,\mathrm{GeV}^{-1}$ from (G.13) instead of the above listed values from [58], such that the values in the second row of table G.1 are generated instead. The result for $3b_F - b_D$ is approximately the same in both parametrizations, namely $-0.69\,\mathrm{GeV}^{-1}$ in the original one [58] and $-0.66\,\mathrm{GeV}^{-1}$ in the modified one.

Finally, replacing $b_D + b_F$ of [58] by c_5 of eq. (G.12), we get the values in the third row of table G.1.

Only the last SU(3) value of the ratio g_1^θ/g_0^θ is in the range of our estimate (4.174), but all three are compatible with the estimate of (G.7). The quoted numbers of table G.1, however, do not contain a systematical error connected with an SU(3) ChPT calculation. For standard quantities such an uncertainty is certainly of the order of 50 %. For the quantity c_5 this uncertainty should be rather 100 %—200 %, see *e.g.* footnote 3. Taking these SU(3) errors into account, the estimates of table G.1 are compatible with the range quoted in (4.174).

---

[3] In fact, the latter equation which is based on eq. (5.7) of ref. [153] predicts that the NLO correction to c_5 is much larger than c_5 (or $b_D + b_F$) itself, namely $\Delta c_5 = 0.49\,\mathrm{GeV}^{-1}$. This quantity is of similar size as $\Delta c_1 = +0.2\,\mathrm{GeV}^{-1}$.

Appendix H

Trace technology

The aim of this appendix is to present an efficient technique to calculate spin matrix elements of composite particles, which has been pointed out by Christoph Hanhart. Let us consider a composite system which consists of two spin-1/2 particles. The spin space of particle (n) is spanned by

$$|v^1_{(n)}\rangle = \begin{pmatrix}1\\0\end{pmatrix}, \quad |v^2_{(n)}\rangle = \begin{pmatrix}0\\1\end{pmatrix}, \tag{H.0.1}$$

i.e. $(|v^i_n\rangle)_k = \delta_{ik}$. An arbitrary state of the composite two-particle system can be described by a matrix A:

$$|\psi\rangle = A_{ij}\,|v^i_{(1)}\rangle\,|v^j_{(2)}\rangle\,. \tag{H.0.2}$$

Another state can be defined in the same fashion by a matrix B.

Consider a matrix $M_{(1)}$ acting on particle (1) and a matrix $N_{(2)}$ acting on particle (2). The multiplication of *e.g.* the matrix $M_{(1)}$ with the vector $|v^i_{(n)}\rangle$ returns column i of the matrix $M_{(1)}$: $(M_{(1)}|v^i_{(n)}\rangle)_k = (M_{(1)})_{ki}$. If both matrices act on the composite state defined by the matrix A, the resulting state is given by

$$(A)_{ij}\,(M_{(1)}|v^i_{(1)}\rangle)_k\,(N_{(2)}|v^j_{(2)}\rangle)_l = (M_{(1)})_{ki}\,(A)_{ij}\,(N_{(2)})_{lj}\,. \tag{H.0.3}$$

The projection on the hermetian conjugate of the state defined by B then yields

$$\begin{aligned}\langle v^k_{(1)}|\langle v^l_{(2)}|(B^*)_{kl}M_{(1)}N_{(2)}(A)_{ij}|v^i_{(1)}\rangle|v^j_{(2)}\rangle &= (B^*)_{kl}\,(M_{(1)})_{ki}\,(A)_{ij}\,(N_{(2)})_{lj}\\ &= \mathrm{Tr}\left[(B^*N_{(2)})^T M_{(1)}A\right]\\ &= \mathrm{Tr}\left[N^T_{(2)}B^\dagger M_{(1)}A\right]\,,\end{aligned} \tag{H.0.4}$$

where the T denotes the transposed matrix.

Spin-0 and spin-1 composite states, for instance, are expressible in terms of Pauli σ-matrices by

$$|0,0\rangle = \frac{1}{\sqrt{2}}(\sigma^2)_{ij}|v^i_{(1)}\rangle\,|v^j_{(2)}\rangle\,, \tag{H.0.5}$$

$$|1,k\rangle = \frac{1}{\sqrt{2}}(\sigma^k\sigma^2)_{ij}|v^i_{(1)}\rangle\,|v^j_{(2)}\rangle\,, \tag{H.0.6}$$

for $k = 1, 2, 3$, which are just the regular Cartesian representations of the spin-0 and spin-1 states. Spin matrix elements of spin operators involving composite states are thus expressible as traces of products of σ-matrices. By utilizing the identity

$$\sigma^2(\sigma^i)^T\sigma^2 = -\sigma^i\,, \tag{H.0.7}$$

matrix elements of arbitrary spin operators in systems consisting of two spin-1/2 particles are easily obtained.

As an example one may consider the matrix element $\langle 1, t|(\sigma^k_{(1)} + \sigma^k_{(2)})|1, s\rangle$, which gives:

$$\begin{aligned}
& \frac{1}{2}\langle v^i_{(1)}|\langle v^j_{(2)}|(\sigma^t\sigma^2)^*_{ij}(\sigma^k_{(1)} + \sigma^k_{(2)})(\sigma^s\sigma^2)_{lm}|v^l_{(1)}\rangle|v^m_{(2)}\rangle \\
= \; & \frac{1}{2}\mathrm{Tr}[\sigma^2\sigma^t\sigma^k_{(1)}\sigma^s\sigma^2] + \frac{1}{2}\mathrm{Tr}[(\sigma^k_{(2)})^T\sigma^2\sigma^t\sigma^s\sigma^2] \\
= \; & \frac{1}{2}\mathrm{Tr}[\sigma^t\sigma^k_{(1)}\sigma^s] - \frac{1}{2}\mathrm{Tr}[\sigma^k_{(2)}\sigma^t\sigma^s] \\
= \; & i\epsilon^{tks} - i\epsilon^{kts} = 2i\epsilon^{stk}\,.
\end{aligned}$$

Appendix I

P and T transformations

This appendix provides the eigenvalues of operators under P- and T-transformations, which are utilized in the derivation of the P- and T-violating Lagrangians.

I.1 Elementary observables

The behavior under P, T-transformations of the spatial four-vector x^μ, the derivative $\partial_\mu = \frac{\partial}{\partial x^\mu}$, the momentum p_μ, the four-velocity v_μ , the orbital angular momentum $\vec{l} = \vec{x} \times \vec{p}$, the spin $\frac{1}{2}\vec{\sigma}$, and the total angular momentum $\vec{J}$ is given by

$$\begin{array}{ccccccc}
x^\mu & \stackrel{P}{\longleftrightarrow} & +x_\mu & \text{and} & x^\mu & \stackrel{T}{\longleftrightarrow} & -x_\mu\,, \\
\partial_\mu & \stackrel{P}{\longleftrightarrow} & +\partial^\mu & \text{and} & \partial_\mu & \stackrel{T}{\longleftrightarrow} & -\partial^\mu\,, \\
i\partial_\mu & \stackrel{P}{\longleftrightarrow} & +i\partial^\mu & \text{and} & i\partial_\mu & \stackrel{T}{\longleftrightarrow} & +i\partial^\mu\,, \\
p_\mu & \stackrel{P}{\longleftrightarrow} & +p^\mu & \text{and} & p_\mu & \stackrel{T}{\longleftrightarrow} & +p^\mu\,, \\
v_\mu & \stackrel{P}{\longleftrightarrow} & +v^\mu & \text{and} & v_\mu & \stackrel{T}{\longleftrightarrow} & +v^\mu\,, \\
\vec{l} & \stackrel{P}{\longleftrightarrow} & +\vec{l} & \text{and} & \vec{l} & \stackrel{T}{\longleftrightarrow} & -\vec{l}, \\
\frac{1}{2}\vec{\sigma} & \stackrel{P}{\longleftrightarrow} & +\frac{1}{2}\vec{\sigma} & \text{and} & \frac{1}{2}\vec{\sigma} & \stackrel{T}{\longleftrightarrow} & -\frac{1}{2}\vec{\sigma}\,, \\
\vec{J} & \stackrel{P}{\longleftrightarrow} & +\vec{J} & \text{and} & \vec{J} & \stackrel{T}{\longleftrightarrow} & -\vec{J}\,.
\end{array}$$

I.2 The external fields

The corresponding behavior of the external fields (the vector field v_μ, the axial-vector field a_μ, the scalar field s, the pseudoscalar field p, the electric four-vector A_μ) can *e.g.* be found – in the isoscalar case – in [154], Chap. 3-4-4; see also the table in appendix I.8. In detail:[1]

$$
\begin{array}{rclcrcl}
v_\mu & \stackrel{P}{\longleftrightarrow} & +v^\mu & \text{and} & v_\mu & \stackrel{T}{\longleftrightarrow} & +(v^\mu)^*\,, \\
a_\mu & \stackrel{P}{\longleftrightarrow} & -a^\mu & \text{and} & a_\mu & \stackrel{T}{\longleftrightarrow} & +(a^\mu)^*\,, \\
s & \stackrel{P}{\longleftrightarrow} & +s & \text{and} & s & \stackrel{T}{\longleftrightarrow} & +s^*\,, \\
p & \stackrel{P}{\longleftrightarrow} & -p & \text{and} & p & \stackrel{T}{\longleftrightarrow} & -p^*\,, \\
A_\mu & \stackrel{P}{\longleftrightarrow} & +A^\mu & \text{and} & A_\mu & \stackrel{T}{\longleftrightarrow} & +A^\mu\,, \\
i\mathcal{D}_\mu & \stackrel{P}{\longleftrightarrow} & +i\mathcal{D}^\mu & \text{and} & i\mathcal{D}_\mu & \stackrel{T}{\longleftrightarrow} & +i\mathcal{D}^\mu\,, \\
i\mathcal{D}_{\mu\perp} & \stackrel{P}{\longleftrightarrow} & +i\mathcal{D}^\mu_\perp & \text{and} & i\mathcal{D}_{\mu\perp} & \stackrel{T}{\longleftrightarrow} & +i\mathcal{D}^\mu_\perp\,,
\end{array}
$$

where $\mathcal{D}_\mu = \partial_\mu + \Gamma_\mu - iv^{(s)}_\mu$ is the covariant derivative acting on nucleons and $\mathcal{D}^\mu_\perp = \mathcal{D}^\mu - v^\mu\,(v\cdot\mathcal{D})$.

I.3 The pion field and composite quantities

The behavior of the pion (Goldstone boson) field $\pi = \vec{\tau}\cdot\vec{\pi}$ follows from the one of p of App. I.2. The matrix $u \equiv \exp(i\pi/F_0)$, $\chi = s + ip$, the electromagnetic field strength tensor $F_{\mu\nu} = \partial_\mu A_\nu - \partial_\nu A_\mu$, the electric field $\vec{E}$, the magnetic field $\vec{B}$, $\partial_\mu\pi$ and $[\pi, \partial_\mu\pi]$ transform therefore according to App.I.1 and App. I.2 as follows:[2]

$$
\begin{array}{rclcrcl}
\pi & \stackrel{P}{\longleftrightarrow} & -\pi & \text{and} & \pi & \stackrel{T}{\longleftrightarrow} & -\pi^*\,, \\
u & \stackrel{P}{\longleftrightarrow} & u^\dagger & \text{and} & u & \stackrel{T}{\longleftrightarrow} & u^*\,, \\
U & \stackrel{P}{\longleftrightarrow} & U^\dagger & \text{and} & U & \stackrel{T}{\longleftrightarrow} & U^*\,, \\
\chi & \stackrel{P}{\longleftrightarrow} & \chi^\dagger & \text{and} & \chi & \stackrel{T}{\longleftrightarrow} & \chi^*\,, \\
F_{\mu\nu} & \stackrel{P}{\longleftrightarrow} & +F^{\mu\nu} & \text{and} & F_{\mu\nu} & \stackrel{T}{\longleftrightarrow} & -F^{\mu\nu}\,, \\
\vec{E} & \stackrel{P}{\longleftrightarrow} & -\vec{E} & \text{and} & \vec{E} & \stackrel{T}{\longleftrightarrow} & +\vec{E}\,, \\
\vec{B} & \stackrel{P}{\longleftrightarrow} & +\vec{B} & \text{and} & \vec{B} & \stackrel{T}{\longleftrightarrow} & -\vec{B}\,, \\
\partial_\mu\pi & \stackrel{P}{\longleftrightarrow} & -\partial^\mu\pi & \text{and} & \partial_\mu\pi & \stackrel{T}{\longleftrightarrow} & +\partial^\mu\pi^*\,, \\
[\pi,\partial_\mu\pi] & \stackrel{P}{\longleftrightarrow} & +[\pi,\partial^\mu\pi] & \text{and} & [\pi,\partial_\mu\pi] & \stackrel{T}{\longleftrightarrow} & -[\pi,\partial^\mu\pi]^*\,.
\end{array}
$$

[1] Of course, here and in the following the omitted arguments of the fields transform as

$$(\vec{x},t) \stackrel{P}{\longleftrightarrow} (-\vec{x},t) \quad \text{and} \quad (\vec{x},t) \stackrel{T}{\longleftrightarrow} (\vec{x},-t).$$

Note that the anti-unitary time-reversal operator T can be written as the product $T = UK$ where K complex conjugates everything to its right ($KiK^{-1} = K^{-1}iK = -i$), such that U is an unitary operator, see *e.g.* [155]. Thus A^* is the complex conjugate of a non-Dirac matrix A (here an isospin matrix, in general a flavor matrix). Remember $\tau_i^* = \tau_i^T$. Thus if A contains only the unity and τ_3 (or the unity, λ_3 and λ_8) as flavor matrices, the complex conjugation can be dropped.

Note that $x^\mu, s, p, v_\mu, a_\mu \stackrel{PCT}{\longleftrightarrow} -x^\mu, s, p, -v_\mu, -a_\mu$, see *e.g.* Ref. [154].

[2] Remember that $\pi \stackrel{C}{\longleftrightarrow} \pi^T$ and $U \stackrel{C}{\longleftrightarrow} U^T$, such that $\pi \stackrel{PCT}{\longleftrightarrow} \pi^\dagger = \pi$ and $U \stackrel{PCT}{\longleftrightarrow} U$.

I.4 Bilinears of relativistic nuclear spinors

Compare with Sec. 3-4-4 of Ref. [154] and with App. I.2.

$$
\begin{array}{rclcrcl}
\bar{n}n & \overset{P}{\longleftrightarrow} & +\bar{n}n & \text{and} & \bar{n}n & \overset{T}{\longleftrightarrow} & +\bar{n}n\,, \\
\bar{n}i\gamma_5 n & \overset{P}{\longleftrightarrow} & -\bar{n}i\gamma_5 n & \text{and} & \bar{n}i\gamma_5 n & \overset{T}{\longleftrightarrow} & -\bar{n}i\gamma_5 n\,, \\
\bar{n}\gamma^\mu n & \overset{P}{\longleftrightarrow} & +\bar{n}\gamma_\mu n & \text{and} & \bar{n}\gamma^\mu n & \overset{T}{\longleftrightarrow} & +\bar{n}\gamma_\mu n\,, \\
\bar{n}\gamma^\mu\gamma_5 n & \overset{P}{\longleftrightarrow} & -\bar{n}\gamma_\mu\gamma_5 n & \text{and} & \bar{n}\gamma^\mu\gamma_5 n & \overset{T}{\longleftrightarrow} & +\bar{n}\gamma_\mu\gamma_5 n\,, \\
\bar{n}\sigma^{\mu\nu} n & \overset{P}{\longleftrightarrow} & +\bar{n}\sigma_{\mu\nu} n & \text{and} & \bar{n}\sigma^{\mu\nu} n & \overset{T}{\longleftrightarrow} & -\bar{n}\sigma_{\mu\nu} n\,, \\
\bar{n}\sigma^{\mu\nu}\gamma_5 n & \overset{P}{\longleftrightarrow} & -\bar{n}\sigma_{\mu\nu}\gamma_5 n & \text{and} & \bar{n}\sigma^{\mu\nu}\gamma_5 n & \overset{T}{\longleftrightarrow} & -\bar{n}\sigma_{\mu\nu}\gamma_5 n\,, \\
\bar{n}\sigma^{\mu\nu}i\gamma_5 n & \overset{P}{\longleftrightarrow} & -\bar{n}\sigma_{\mu\nu}i\gamma_5 n & \text{and} & \bar{n}\sigma^{\mu\nu}\gamma_5 n & \overset{T}{\longleftrightarrow} & -\bar{n}\sigma_{\mu\nu}\gamma_5 n\,, \\
\bar{n}i\sigma^{\mu\nu}q_\nu n & \overset{P}{\longleftrightarrow} & +\bar{n}i\sigma_{\mu\nu}q^\nu n & \text{and} & \bar{n}i\sigma^{\mu\nu}q_\nu n & \overset{T}{\longleftrightarrow} & +\bar{n}i\sigma_{\mu\nu}q^\nu n\,, \\
\bar{n}\sigma^{\mu\nu}q_\nu\gamma_5 n & \overset{P}{\longleftrightarrow} & -\bar{n}\sigma_{\mu\nu}q^\nu\gamma_5 n & \text{and} & \bar{n}\sigma^{\mu\nu}q_\nu\gamma_5 n & \overset{T}{\longleftrightarrow} & -\bar{n}\sigma_{\mu\nu}q^\nu\gamma_5 n\,.
\end{array}
$$

I.5 Bilinears of heavy-baryon nuclear spinors

Compare with Sec. 5.5.3 of Ref. [78] and App. I.4. Note that to leading order

$$
\begin{array}{rcl}
N^\dagger i\gamma_5 N & = & 0\,, \\
N^\dagger\gamma^\mu N & = & v^\mu N^\dagger N\,, \\
N^\dagger\gamma^\mu\gamma_5 N & = & 2N^\dagger S^\mu N\,, \\
N^\dagger\sigma^{\mu\nu} N & = & 2\epsilon^{\mu\nu\rho\sigma}N^\dagger v_\rho S_\sigma N\,, \\
N^\dagger\sigma^{\mu\nu}\gamma_5 N & = & 2i\left(v^\mu N^\dagger S^\nu N - v^\nu N^\dagger S^\mu N\right)\,,
\end{array}
$$

where $S^\mu = \frac{i}{2}\sigma^{\mu\nu}v_\nu\gamma_5$. Note that $S^\mu = (0, \frac{1}{2}\vec{\sigma})$ if $v^\mu = (1, \vec{0})$. In summary, we have

$$
\begin{array}{rclcrcl}
N^\dagger N & \overset{P}{\longleftrightarrow} & +N^\dagger N & \text{and} & N^\dagger N & \overset{T}{\longleftrightarrow} & +N^\dagger N\,, \\
N^\dagger S^\mu N & \overset{P}{\longleftrightarrow} & -N^\dagger S_\mu N & \text{and} & N^\dagger S^\mu N & \overset{T}{\longleftrightarrow} & +N^\dagger S_\mu N\,.
\end{array}
$$

Note that the latter is consistent with the angular momentum behavior given in App. I.1.

I.6 The conventional building blocks

The combinations of hermitian conventional building blocks transform as scalars:

$$
\begin{array}{rclcrcl}
\chi_+ & \overset{P}{\longleftrightarrow} & +\chi_+ & \text{and} & \chi_+ & \overset{T}{\longleftrightarrow} & +\chi_+^*\,, \\
\widehat{\chi}_+ & \overset{P}{\longleftrightarrow} & +\widehat{\chi}_+ & \text{and} & \widehat{\chi}_+ & \overset{T}{\longleftrightarrow} & +\widehat{\chi}_+^*\,, \\
N^\dagger N & \overset{P}{\longleftrightarrow} & +N^\dagger N & \text{and} & N^\dagger N & \overset{T}{\longleftrightarrow} & +N^\dagger N\,;
\end{array}
$$

pseudoscalars:

$$
\begin{array}{lcl}
i\chi_- & \stackrel{P}{\longleftrightarrow} & -i\chi_- \quad \text{and} \quad i\chi_- \stackrel{T}{\longleftrightarrow} -i\chi_-^* \,, \\
i\widehat{\chi}_- & \stackrel{P}{\longleftrightarrow} & -i\widehat{\chi}_- \quad \text{and} \quad i\widehat{\chi}_- \stackrel{T}{\longleftrightarrow} -i\widehat{\chi}_-^* \,,
\end{array}
$$

vectors:

$$
\begin{array}{rclcrcl}
i\Gamma_\mu & \stackrel{P}{\longleftrightarrow} & +i\Gamma^\mu & \text{and} & i\Gamma_\mu & \stackrel{T}{\longleftrightarrow} & +\left(i\Gamma^\mu\right)^* \,, \\
N^\dagger v^\mu N & \stackrel{P}{\longleftrightarrow} & +N^\dagger v_\mu N & \text{and} & N^\dagger v^\mu N & \stackrel{T}{\longleftrightarrow} & +N^\dagger v_\mu N \,;
\end{array}
$$

axial-vectors:

$$
\begin{array}{rclcrcl}
u_\mu & \stackrel{P}{\longleftrightarrow} & -u^\mu & \text{and} & u_\mu & \stackrel{T}{\longleftrightarrow} & +(u^\mu)^* \,, \\
N^\dagger S^\mu N & \stackrel{P}{\longleftrightarrow} & -N^\dagger S_\mu N & \text{and} & N^\dagger S^\mu N & \stackrel{T}{\longleftrightarrow} & +N^\dagger S_\mu N \,;
\end{array}
$$

antisymmetric tensors:

$$
\begin{array}{rcl}
F_{\mu\nu} & \stackrel{P}{\longleftrightarrow} & +F^{\mu\nu} \,, \\
F_{\mu\nu} & \stackrel{T}{\longleftrightarrow} & -F^{\mu\nu} \,, \\
f^+_{\mu\nu} & \stackrel{P}{\longleftrightarrow} & +f^{+\,\mu\nu} \,, \\
f^+_{\mu\nu} & \stackrel{T}{\longleftrightarrow} & -\left(f^{+\,\mu\nu}\right)^* \,, \\
i[u_\mu, u_\nu] & \stackrel{P}{\longleftrightarrow} & +i[u^\mu, u^\nu] \,, \\
i[u_\mu, u_\nu] & \stackrel{T}{\longleftrightarrow} & \left(i[u^\mu, u^\nu]\right)^* \,, \\
\epsilon^{\mu\nu\rho\sigma} N^\dagger v_\rho S_\sigma N & \stackrel{P}{\longleftrightarrow} & +\epsilon_{\mu\nu\rho\sigma} N^\dagger v^\rho S^\sigma N \,, \\
\epsilon^{\mu\nu\rho\sigma} N^\dagger v_\rho S_\sigma N & \stackrel{T}{\longleftrightarrow} & -\epsilon_{\mu\nu\rho\sigma} N^\dagger v^\rho S^\sigma N \,;
\end{array}
$$

antisymmetric dual tensors:

$$
\begin{array}{rcl}
\widetilde{F}_{\mu\nu} & \stackrel{P}{\longleftrightarrow} & -\widetilde{F}^{\mu\nu} \,, \\
\widetilde{F}_{\mu\nu} & \stackrel{T}{\longleftrightarrow} & +\widetilde{F}^{\mu\nu} \,, \\
\epsilon_{\mu\nu\rho\sigma} i[u^\rho, u^\sigma] & \stackrel{P}{\longleftrightarrow} & -\epsilon^{\mu\nu\rho\sigma} i[u_\rho, u_\sigma] \,, \\
\epsilon_{\mu\nu\rho\sigma} i[u^\rho, u^\sigma] & \stackrel{T}{\longleftrightarrow} & -\epsilon^{\mu\nu\rho\sigma} (i[u_\rho, u_\sigma])^* \,, \\
f^-_{\mu\nu} & \stackrel{P}{\longleftrightarrow} & -f^{-\,\mu\nu} \,, \\
f^-_{\mu\nu} & \stackrel{T}{\longleftrightarrow} & +\left(f^{-\,\mu\nu}\right)^* \,, \\
N^\dagger [v^\mu, S^\nu] N & \stackrel{P}{\longleftrightarrow} & -N^\dagger [v_\mu, S_\nu] N \,, \\
N^\dagger [v^\mu, S^\nu] N & \stackrel{T}{\longleftrightarrow} & +N^\dagger [v_\mu, S_\nu] N \,;
\end{array}
$$

symmetric tensors:

$$
\begin{array}{rclcrcl}
\{u_\mu, u_\nu\} & \stackrel{P}{\longleftrightarrow} & +\{u^\mu, u^\nu\} & \text{and} & \{u_\mu, u_\nu\} & \stackrel{T}{\longleftrightarrow} & +\{u^\mu, u^\nu\}^* \\
N^\dagger v^\mu v^\nu N & \stackrel{P}{\longleftrightarrow} & +N^\dagger v^\mu v^\nu N & \text{and} & N^\dagger v^\mu v^\nu N & \stackrel{T}{\longleftrightarrow} & +N^\dagger v^\mu v^\nu N \,;
\end{array}
$$

symmetric 'dual' tensors:

$$
\begin{aligned}
h_{\mu\nu} &\stackrel{P}{\longleftrightarrow} -h^{\mu\nu}\,, \\
h_{\mu\nu} &\stackrel{T}{\longleftrightarrow} -\left(h^{\mu\nu}\right)^*\,, \\
N^\dagger i\{v^\mu, S^\nu\}N &\stackrel{P}{\longleftrightarrow} -N^\dagger i\{v_\mu, S_\nu\}N\,, \\
N^\dagger i\{v^\mu, S^\nu]N &\stackrel{T}{\longleftrightarrow} -N^\dagger i\{v_\mu, S_\nu\}N\,.
\end{aligned}
$$

I.7 Some composites

$$
\begin{aligned}
N^\dagger i\mathcal{D}_\mu N &\stackrel{P}{\longleftrightarrow} +N^\dagger i\mathcal{D}^\mu N\,, \\
N^\dagger i\mathcal{D}_\mu N &\stackrel{T}{\longleftrightarrow} N^\dagger i\mathcal{D}^\mu N\,, \\
N^\dagger iv\cdot\Gamma N &\stackrel{P}{\longleftrightarrow} +N^\dagger iv\cdot\Gamma N\,, \\
N^\dagger iv\cdot\Gamma N &\stackrel{T}{\longleftrightarrow} N^\dagger iv\cdot\Gamma N\,, \\
N^\dagger S^\mu u_\mu N &\stackrel{P}{\longleftrightarrow} +N^\dagger S_\mu u^\mu N\,, \\
N^\dagger S^\mu u_\mu N &\stackrel{T}{\longleftrightarrow} +N^\dagger S_\mu u^\mu N\,, \\
N^\dagger A N &\stackrel{P}{\longleftrightarrow} +N^\dagger A N\,, \\
N^\dagger A N &\stackrel{T}{\longleftrightarrow} +N^\dagger A N\,, \\
N^\dagger i[S^\mu, S^\nu]B_{\mu\nu}N &\stackrel{P}{\longleftrightarrow} +N^\dagger i[S^\mu, S^\nu]B_{\mu\nu}N\,, \\
N^\dagger i[S^\mu, S^\nu]B_{\mu\nu}N &\stackrel{T}{\longleftrightarrow} +N^\dagger i[S^\mu, S^\nu]B_{\mu\nu}N\,, \\
N^\dagger \epsilon^{\mu\nu\rho\sigma}C_{\mu\nu\rho\sigma}N &\stackrel{P}{\longleftrightarrow} +N^\dagger \epsilon^{\mu\nu\rho\sigma}C_{\mu\nu\rho\sigma}N\,, \\
N^\dagger \epsilon^{\mu\nu\rho\sigma}C_{\mu\nu\rho\sigma}N &\stackrel{T}{\longleftrightarrow} +N^\dagger \epsilon^{\mu\nu\rho\sigma}C_{\mu\nu\rho\sigma}N\,,
\end{aligned}
$$

with

$$
A = (v\cdot\mathcal{D})^2,\ D^2,\ \{S\cdot i\mathcal{D}, v\cdot u\}\,,\ (v\cdot u)^2,\ u\cdot u,\ \langle\chi_+\rangle,\ \widehat{\chi}_+;
$$

$$
B_{\mu\nu} = iu_\mu u_\nu,\ f^+_{\mu\nu},\ v^{(s)}_{\mu\nu};
$$

$$
C_{\mu\nu\sigma\rho} \equiv v_\mu S_\nu B_{\rho\sigma}.
$$

I.8 Table of discrete symmetry transformations

Qu.	P	C	T	PT	PCT	Qu.†
S	S	S^T	S^*	S^*	S	S
P	-P	P^T	-P^*	P^*	P	P
V_μ	V^μ	-$\mathrm{V}_\mu^\mathsf{T}$	$\mathrm{V}^{\mu *}$	V_μ^*	-V_μ	V_μ
A_μ	-A^μ	$\mathrm{A}_\mu^\mathsf{T}$	$\mathrm{A}^{\mu *}$	-A_μ^*	-A_μ	A_μ
$\mathrm{T}_{\mu\nu}$	$\mathrm{T}^{\mu\nu}$	-$\mathrm{T}_{\mu\nu}^\mathsf{T}$	-$\mathrm{T}^{\mu\nu *}$	-$\mathrm{T}_{\mu\nu}^*$	$\mathrm{T}_{\mu\nu}$	$\mathrm{T}_{\mu\nu}$
$\widetilde{\mathrm{T}}_{\mu\nu}$	-$\widetilde{\mathrm{T}}^{\mu\nu}$	-$\widetilde{\mathrm{T}}_{\mu\nu}^\mathsf{T}$	$\widetilde{\mathrm{T}}^{\mu\nu *}$	-$\widetilde{\mathrm{T}}_{\mu\nu}^*$	$\widetilde{\mathrm{T}}_{\mu\nu}$	$\widetilde{\mathrm{T}}_{\mu\nu}$
$\mathrm{H}_{\mu\nu}$	$\mathrm{H}^{\mu\nu}$	$\mathrm{H}_{\mu\nu}^\mathsf{T}$	$\mathrm{H}^{\mu\nu *}$	$\mathrm{H}_{\mu\nu}^*$	$\mathrm{H}_{\mu\nu}$	$\mathrm{H}_{\mu\nu}$
$\widetilde{\mathrm{H}}_{\mu\nu}$	-$\widetilde{\mathrm{H}}^{\mu\nu}$	$\widetilde{\mathrm{H}}_{\mu\nu}^\mathsf{T}$	-$\widetilde{\mathrm{H}}^{\mu\nu *}$	$\widetilde{\mathrm{H}}_{\mu\nu}^*$	$\widetilde{\mathrm{H}}_{\mu\nu}$	$\widetilde{\mathrm{H}}_{\mu\nu}$

Table I.1: Discrete symmetry transformation of the following quantities: scalar field S, pseudo-scalar field P, vector field V_μ, axial-vector field A_μ, antisymmetric tensor field $\mathrm{T}_{\mu\nu}$ and its dual $\widetilde{\mathrm{T}}_{\mu\nu}$, symmetric tensor field $\mathrm{H}_{\mu\nu}$ and its 'dual' $\widetilde{\mathrm{H}}_{\mu\nu}$. The last column shows that all quantities are (defined to be) hermitian. With the exception of the (axial) vector fields, all other quantities have the eigenvalue +1 under the combined PCT transformation.

Bibliography

[1] WMAP, C. Bennett *et al.*, Astrophys.J.Suppl. **208**, 20 (2013), arXiv:1212.5225.

[2] A. Riotto and M. Trodden, Ann.Rev.Nucl.Part.Sci. **49**, 35 (1999), hep-ph/9901362.

[3] A. Sakharov, Pisma Zh.Eksp.Teor.Fiz. **5**, 32 (1967).

[4] A. Dolgov and Y. Zeldovich, Rev.Mod.Phys. **53**, 1 (1981).

[5] M. Pospelov and A. Ritz, Annals Phys. **318**, 119 (2005), hep-ph/0504231.

[6] J. Smith, E. Purcell, and N. Ramsey, Phys.Rev. **108**, 120 (1957).

[7] T. Mannel and N. Uraltsev, Phys.Rev. **D85**, 096002 (2012), 1202.6270.

[8] T. Mannel and N. Uraltsev, JHEP **1303**, 064 (2013), 1205.0233.

[9] G. 't Hooft, Phys.Rev.Lett. **37**, 8 (1976).

[10] M. Ramsey-Musolf and S. Su, Phys.Rept. **456**, 1 (2008), hep-ph/0612057.

[11] S. Weinberg, Phys.Rev.Lett. **63**, 2333 (1989).

[12] J. L. Feng, K. T. Matchev, and Y. Shadmi, eConf **C010630**, P307 (2001), hep-ph/0110157.

[13] V. Dzuba and V. Flambaum, Int.J.Mod.Phys. **E21**, 1230010 (2012), arXiv:1209.2200.

[14] C. Baker *et al.*, Phys.Rev.Lett. **97**, 131801 (2006), hep-ex/0602020.

[15] W. Griffith *et al.*, Phys.Rev.Lett. **102**, 101601 (2009).

[16] J. Hudson *et al.*, Nature **473**, 493 (2011).

[17] D. Kara *et al.*, New J.Phys. **14**, 103051 (2012), arXiv:1208.4507.

[18] ACME Collaboration, J. Baron *et al.*, (2013), arXiv:1310.7534.

[19] EDM Collaboration, Y. Semertzidis *et al.*, AIP Conf.Proc. **698**, 200 (2004), hep-ex/0308063.

[20] Y. F. Orlov, W. M. Morse, and Y. K. Semertzidis, Phys.Rev.Lett. **96**, 214802 (2006), hep-ex/0605022.

[21] D. Anastassopoulos *et al.*, Search for a permanent electric dipole moment of the deuteron nucleus at the 10^{-29} e cm level, AGS Proposal, April 2008, available from http://www.bnl.gov/edm/ (2014).

[22] A. Lehrach, B. Lorentz, W. Morse, N. Nikolaev, and F. Rathmann, (2012), arXiv:1201.5773.

[23] R. Engels *et al.*, COSY proposal #216, May 2012, available from http://www2.fz-juelich.de/ikp/jedi/documents/proposals.shtml (2012).

[24] J. Pretz, Hyperfine Interact. **214**, 111 (2013), arXiv:1301.2937.

[25] I. Khriplovich and R. Korkin, Nucl.Phys. **A665**, 365 (2000), nucl-th/9904081.

[26] O. Lebedev, K. A. Olive, M. Pospelov, and A. Ritz, Phys.Rev. **D70**, 016003 (2004), hep-ph/0402023.

[27] C.-P. Liu and R. Timmermans, Phys.Rev. **C70**, 055501 (2004), nucl-th/0408060.

[28] I. Stetcu, C.-P. Liu, J. L. Friar, A. Hayes, and P. Navratil, Phys.Lett. **B665**, 168 (2008), arXiv:0804.3815.

[29] J. de Vries, E. Mereghetti, R. Timmermans, and U. van Kolck, Phys.Rev.Lett. **107**, 091804 (2011), arXiv:1102.4068.

[30] J. de Vries *et al.*, Phys.Rev. **C84**, 065501 (2011), arXiv:1109.3604.

[31] I. Afnan and B. Gibson, Phys.Rev. **C82**, 064002 (2010), arXiv:1011.4968.

[32] B. Gibson and I. Afnan, AIP Conf.Proc. **1441**, 579 (2012).

[33] Y.-H. Song, R. Lazauskas, and V. Gudkov, Phys.Rev. **C87**, 015501 (2013), arXiv:1211.3762.

[34] Particle Data Group, J. Beringer *et al.*, Phys.Rev. **D86**, 010001 (2012).

[35] W. Buchmüller and D. Wyler, Nucl.Phys. **B268**, 621 (1986).

[36] A. De Rujula, M. Gavela, O. Pene, and F. Vegas, Nucl.Phys. **B357**, 311 (1991).

[37] B. Grzadkowski, M. Iskrzynski, M. Misiak, and J. Rosiek, JHEP **1010**, 085 (2010), arXiv:1008.4884.

[38] J. Ng and S. Tulin, Phys.Rev. **D85**, 033001 (2012), arXiv:1111.0649.

[39] J. de Vries, E. Mereghetti, R. Timmermans, and U. van Kolck, Annals Phys. **338**, 50 (2013), arXiv:1212.0990.

[40] W. Dekens and J. de Vries, JHEP **1305**, 149 (2013), arXiv:1303.3156.

[41] S. Weinberg, *The Quantum Theory of Fields. Vol. 2: Modern Applications* (Cambridge University Press, 1996).

[42] E. Mereghetti, W. Hockings, and U. van Kolck, Annals Phys. **325**, 2363 (2010), arXiv:1002.2391.

[43] J. Gasser and H. Leutwyler, Annals Phys. **158**, 142 (1984).

[44] J. Gasser and H. Leutwyler, Nucl.Phys. **B250**, 465 (1985).

[45] R. Crewther, P. Di Vecchia, G. Veneziano, and E. Witten, Phys.Lett. **B88**, 123 (1979).

[46] A. Pich and E. de Rafael, Nucl.Phys. **B367**, 313 (1991).

[47] W. Hockings and U. van Kolck, Phys.Lett. **B605**, 273 (2005), nucl-th/0508012.

[48] K. Ottnad, B. Kubis, U.-G. Meißner, and F.-K. Guo, Phys.Lett. **B687**, 42 (2010), arXiv:0911.3981.

[49] J. de Vries, R. Timmermans, E. Mereghetti, and U. van Kolck, Phys.Lett. **B695**, 268 (2011), arXiv:1006.2304.

[50] E. Mereghetti, J. de Vries, W. Hockings, C. Maekawa, and U. van Kolck, Phys.Lett. **B696**, 97 (2011), arXiv:1010.4078.

[51] F.-K. Guo and U.-G. Meißner, JHEP **1212**, 097 (2012), arXiv:1210.5887.

[52] E. Shintani, T. Blum, and T. Izubuchi, PoS **ConfinementX**, 330 (2012).

[53] E. Shintani, Talk given at the *International Workshop XLII on Gross Properties of Nuclei and Nuclear Excitations* in Hirschegg (2014).

[54] R. Machleidt, Phys.Rev. **C63**, 024001 (2001), nucl-th/0006014.

[55] J. Haidenbauer and W. Plessas, Phys.Rev. **C30**, 1822 (1984).

[56] R. B. Wiringa, V. Stoks, and R. Schiavilla, Phys.Rev. **C51**, 38 (1995), nucl-th/9408016.

[57] E. Epelbaum, Phys.Lett. **B639**, 456 (2006), nucl-th/0511025.

[58] V. Bernard, N. Kaiser, and U.-G. Meißner, Int.J.Mod.Phys. **E4**, 193 (1995), hep-ph/9501384.

[59] K. Fujikawa, Phys.Rev.Lett. **42**, 1195 (1979).

[60] H. Leutwyler, Annals Phys. **235**, 165 (1994), hep-ph/9311274.

[61] A. Belavin, A. M. Polyakov, A. Schwartz, and Y. Tyupkin, Phys.Lett. **B59**, 85 (1975).

[62] R. Bott, Bull.Soc.Math.Fr. **84**, 251 (1956).

[63] V. Baluni, Phys.Rev. **D19**, 2227 (1979).

[64] T. Cheng and L. Li, *Gauge Theory of Elementary Particle Physics* (Oxford University Press, 1984).

[65] E. Shabalin, Sov.J.Nucl.Phys. **28**, 75 (1978).

[66] A. Czarnecki and B. Krause, Phys.Rev.Lett. **78**, 4339 (1997), hep-ph/9704355.

[67] M. Gavela *et al.*, Phys.Lett. **B109**, 215 (1982).

[68] K. Hagiwara, R. Peccei, D. Zeppenfeld, and K. Hikasa, Nucl.Phys. **B282**, 253 (1987).

[69] Y. Nambu, Phys.Rev.Lett. **4**, 380 (1960).

[70] J. Goldstone, A. Salam, and S. Weinberg, Phys.Rev. **127**, 965 (1962).

[71] H. Leutwyler, Chiral Effective Lagrangians, 1991.

[72] S. Weinberg, Phys.Rev.Lett. **18**, 188 (1967).

[73] S. Weinberg, Phys.Rev.Lett. **18**, 507 (1967).

[74] S. Weinberg, Phys.Rev. **166**, 1568 (1968).

[75] L.-F. Li and H. Pagels, Phys.Rev.Lett. **26**, 1204 (1971).

[76] M. Gell-Mann, R. Oakes, and B. Renner, Phys.Rev. **175**, 2195 (1968).

[77] S. Weinberg, Physica **A96**, 327 (1979).

[78] S. Scherer, Adv.Nucl.Phys. **27**, 277 (2003), hep-ph/0210398.

[79] B. Kubis, (2007), hep-ph/0703274.

[80] J. Wess and B. Zumino, Phys.Lett. **B37**, 95 (1971).

[81] E. Witten, Nucl.Phys. **B223**, 422 (1983).

[82] K.-C. Chou, H.-Y. Guo, K. Wu, and X.-C. Song, Phys.Lett. **B134**, 67 (1984).

[83] N. K. Pak and P. Rossi, Nucl.Phys. **B250**, 279 (1985).

[84] J. Manes, Nucl.Phys. **B250**, 369 (1985).

[85] J. Bijnens, C. Bruno, and E. de Rafael, Nucl.Phys. **B390**, 501 (1993), hep-ph/9206236.

[86] J. Gasser, M. Sainio, and A. Svarc, Nucl.Phys. **B307**, 779 (1988).

[87] N. Fettes, U.-G. Meißner, and S. Steininger, Nucl.Phys. **A640**, 199 (1998), hep-ph/9803266.

[88] S. R. Coleman, J. Wess, and B. Zumino, Phys.Rev. **177**, 2239 (1969).

[89] J. Callan, Curtis G., S. R. Coleman, J. Wess, and B. Zumino, Phys.Rev. **177**, 2247 (1969).

[90] H. Georgi, *Weak Interactions and Modern Particle Theory* (Benjamin/Cummings Pub. Co., 1984).

[91] N. Fettes, U.-G. Meißner, M. Mojžiš, and S. Steininger, Annals Phys. **283**, 273 (2000), hep-ph/0001308.

[92] E. E. Jenkins and A. V. Manohar, Baryon Chiral Perturbation Theory, 1991.

[93] V. Bernard, N. Kaiser, J. Kambor, and U.-G. Meißner, Nucl.Phys. **B388**, 315 (1992).

[94] A. Walker-Loud, C. E. Carlson, and G. A. Miller, Phys.Rev.Lett. **108**, 232301 (2012), arXiv:1203.0254.

[95] V. Baru *et al.*, Nucl.Phys. **A872**, 69 (2011), arXiv:1107.5509.

[96] T. Becher and H. Leutwyler, JHEP **0106**, 017 (2001), hep-ph/0103263.

[97] J. Gasser, M. Ivanov, E. Lipartia, M. Mojžiš, and A. Rusetsky, Eur.Phys.J. **C26**, 13 (2002), hep-ph/0206068.

[98] P. Büttiker and U.-G. Meißner, Nucl.Phys. **A668**, 97 (2000), hep-ph/9908247.

[99] C. Hanhart and A. Wirzba, Phys.Lett. **B650**, 354 (2007), nucl-th/0703012.

[100] R. F. Dashen, Phys.Rev. **D3**, 1879 (1971).

[101] J. Bsaisou, C. Hanhart, S. Liebig, U.-G. Meißner, A. Nogga, and A. Wirzba, Eur.Phys.J. **A49**, 31 (2013), arXiv:1209.6306.

[102] B. Borasoy, Phys.Rev. **D61**, 114017 (2000), hep-ph/0004011.

[103] M. Cini, S. Fubini, and A. Stanghellini, Phys.Rev. **114**, 1633 (1959).

[104] W. Cottingham, Annals Phys. **25**, 424 (1963).

[105] J. Gasser and H. Leutwyler, Phys.Rept. **87**, 77 (1982).

[106] S. R. Beane, K. Orginos, and M. J. Savage, Nucl.Phys. **B768**, 38 (2007), hep-lat/0605014.

[107] A. Filin, V. Baru, E. Epelbaum, J. Haidenbauer, C. Hanhart, A. Kudryavstev, and U.-G. Meißner, Phys.Lett. **B681**, 423 (2009), arXiv:0907.4671.

[108] V. Baru, C. Hanhart, M. Hoferichter, B. Kubis, A. Nogga, and D. Phillips, Nucl.Phys. **A872**, 69 (2011), arXiv:1107.5509.

[109] T. Becher and H. Leutwyler, JHEP **0106**, 017 (2001), hep-ph/0103263.

[110] J. Gasser, M. Ivanov, E. Lipartia, M. Mojžiš, and A. Rusetsky, Eur.Phys.J. **C26**, 13 (2002), hep-ph/0206068.

[111] J. Gasser and H. Leutwyler, Nucl.Phys. **B250**, 539 (1985).

[112] A. Gasparyan, J. Haidenbauer, C. Hanhart, and J. Speth, Phys.Rev. **C68**, 045207 (2003), nucl-th/0307072.

[113] S. Weinberg, Phys.Lett. **B295**, 114 (1992), hep-ph/9209257.

[114] E. Epelbaum, H.-W. Hammer, and U.-G. Meißner, Rev.Mod.Phys. **81**, 1773 (2009), 0811.1338.

[115] S. Liebig, V. Baru, F. Ballout, C. Hanhart, and A. Nogga, Eur.Phys.J. **A47**, 69 (2011), arXiv:1003.3826.

[116] V. Baru, C. Hanhart, and A. Nogga, in preparation (2014).

[117] A. Pich and E. de Rafael, Nucl.Phys. **B367**, 313 (1991).

[118] U. van Kolck, M. Rentmeester, J. L. Friar, J. T. Goldman, and J. de Swart, Phys.Rev.Lett. **80**, 4386 (1998), nucl-th/9710067.

[119] C. Maekawa, E. Mereghetti, J. de Vries, and U. van Kolck, Nucl.Phys. **A872**, 117 (2011), arXiv:1106.6119.

[120] V. Stoks, R. Klomp, C. Terheggen, and J. de Swart, Phys.Rev. **C49**, 2950 (1994), nucl-th/9406039.

[121] N. Kaiser, R. Brockmann, and W. Weise, Nucl.Phys. **A625**, 758 (1997), nucl-th/9706045.

[122] N. Kaiser, Phys.Rev. **C62**, 024001 (2000), nucl-th/9912054.

[123] S.-L. Zhu, C. Maekawa, B. Holstein, M. Ramsey-Musolf, and U. van Kolck, Nucl.Phys. **A748**, 435 (2005), nucl-th/0407087.

[124] V. Bernard, Prog.Part.Nucl.Phys. **60**, 82 (2008), arXiv:0706.0312.

[125] W. Glöckle, H. Witala, D. Huber, H. Kamada, and J. Golak, Phys.Rept. **274**, 107 (1996).

[126] A. Nogga, private communication (2013).

[127] A. Nogga and C. Hanhart, Phys.Lett. **B634**, 210 (2006), nucl-th/0511011.

[128] E. Epelbaum, W. Glöckle, and U.-G. Meißner, Nucl.Phys. **A747**, 362 (2005), nucl-th/0405048.

[129] J. Bsaisou, C. Hanhart, S. Liebig, U.-G. Meißner, D. Minossi, A. Nogga, and A. Wirzba, in preperation (2014).

[130] U. van Kolck, M. Rentmeester, J. L. Friar, J. T. Goldman, and J. de Swart, Phys.Rev.Lett. **80**, 4386 (1998), nucl-th/9710067.

[131] N. Kaiser, Phys.Rev. **C73**, 044001 (2006), nucl-th/0601099.

[132] A. Nogga *et al.*, Phys.Lett. **B639**, 465 (2006), nucl-th/0602003.

[133] D. Minossi, PhD thesis, University of Bonn, in preparation (2014).

[134] J. Carlson and R. Schiavilla, Rev.Mod.Phys. **70**, 743 (1998).

[135] S. Liebig, V. Baru, F. Ballout, C. Hanhart, and A. Nogga, Eur.Phys.J. **A47**, 69 (2011), arXiv:1003.3826.

[136] J. Purcell, J. Kelley, E. Kwan, C. Sheu, and H. Weller, Nucl.Phys. **A848**, 1 (2010).

[137] W. Bernreuther, W. Dekens, J. de Vries, C. Hanhart, U.-G. Meißner, A. Wirzba, and J. Bsaisou, in preperation (2014).

[138] T. Yam, *Hamilton's Quaternions, Handbook of Algebra Vol. 3, 429-454* (North-Holland, 2003).

[139] J. Stillwell, *Naive Lie Theory* (Springer, 2008).

[140] A. Beardon, *Algebra and Geometry* (Cambridge University Press, 2005).

[141] M. Lorente and P. D. Kramer, (2003), gr-qc/0402050.

[142] H. Coxeter, The American Mathematically Monthly **53**, 136 (1946).

[143] W. Fulton and J. Harris, *Representation Theory* (Springer, 2004).

[144] M. Hamermesh, *Group Theory and its Application to Physical Problems* (Dover Publications, 1989).

[145] J. F. Nieves and P. B. Pal, Am.J.Phys. **72**, 1100 (2004), hep-ph/0306087.

[146] W. Glöckle, *The Quantum Mechanical Few-Body Problem* (Springer, 1983).

[147] B. Borasoy and U.-G. Meißner, Annals Phys. **254**, 192 (1997), hep-ph/9607432.

[148] J. Alarcon, J. Martin Camalich, and J. Oller, Phys.Rev. **D85**, 051503 (2012), arXiv:1110.3797.

[149] J. Martin Camalich, J. Alarcon, and J. Oller, Prog.Part.Nucl.Phys. **67**, 327 (2012), arXiv:1111.4934.

[150] J. Alarcon, L. Geng, J. Martin Camalich, and J. Oller, (2012), arXiv:1209.2870.

[151] K. Ottnad, Diploma thesis, University of Bonn, unpublished (2009).

[152] M. Mai, P. C. Bruns, B. Kubis, and U.-G. Meißner, Phys.Rev. **D80**, 094006 (2009), arXiv:0905.2810.

[153] M. Frink and U.-G. Meißner, JHEP **0407**, 028 (2004), hep-lat/0404018.

[154] C. Itzykson and J. Zuber, *Quantum Field Theory* (McGraw-Hill, 1980).

[155] A. Zee, *Quantum Field Theory in a Nutshell* (Princeton Univ. Press, 2003).

Danksagung

Mein vornehmlichster Dank gebührt meinem Betreuer, PD Dr. Andreas Wirzba, für seine hervorragende Betreuung und Unterstützung, seinen Rat und seine stete Bereitschaft, mir in unseren vielen Gesprächen sein tiefgründiges physikalisches Verständnis und seine wissenschaftliche Gründlichkeit zu vermitteln.

Meine vornehmlichste Dankbarkeit möchte ich ebenso Prof. Dr. Ulf-G. Meißner ausdrücken, für die Ermöglichung meines Promotionsstudiums, seine umfangreiche Unterstützung, seinen Rat und sein Interesse an meiner Arbeit, das mir immer ein Ansporn war.

Mein ganz besonderer Dank gilt ebenso Prof. Dr. Christoph Hanhart und Dr. Andreas Nogga für ihre ständige Unterstützung und ihre wertvollen Ratschläge. Das Erlernen der Feinheiten der parallelen Programmierung, der Benutzung von Großrechnern im Allgemeinen und des Umgang mit den Großrechnern des Forschungszentrums Jülich, Juropa und Juqueen, im Besonderen habe ich als große Bereicherung empfunden.

Ich danke ebenfalls außerordentlich Dr. Jordy de Vries für unsere vielen anregenden Diskussionen und das sorgfältige Korrekturlesen meiner Dissertation. Bei David Minossi und Dr. Susanna Liebig möchte ich mich ebenso für unsere Zusammenarbeit herzlich bedanken. Auch bei Dr. Timo Lähde und Prof. Dr. Thomas Luu bedanke ich mich herzlich für die Durchsicht meiner Arbeit und unsere zahlreichen gewinnbringenden Gespräche.

Außerden möchte ich mich bei Prof. Dr. Werner Bernreuther, Prof. Dr. Evgeny Epelbaum, Dr. Feng-Kun Guo, Dr. Johann Haidenbauer, Prof. Dr. Siegfried Krewald und Prof. Dr. Nikolai N. Nikolaev für ihren Rat und unseren Austausch bedanken.

Darüber hinaus gebührt Melanie Comuth-Werner, Dr. Greta Guidoboni, Prof. Dr. Andreas Lehrach, Prof. Dr. William Morse, Prof. Dr. Jörg Pretz, PD Dr. Frank Rathmann, Gisela Roes, Prof. Dr. Edward Stephenson, Prof. Dr. Hans Ströher mein besonderer Dank.

Auch danke ich Dr. Emanuele Mereghetti, Prof. Dr. Cheng-Pang Liu, Prof. Dr. Micheal Ramsey-Musolf, Prof. Dr. Rob Timmermans and Prof. Dr. Bira van Kolck für unsere Diskussionen.